Archaeological marine carbonates in northern Hokkaido, Japan:
Methodology, chronology and palaeothermometry

Tansy Branscombe

Brasenose College

D.Phil. Archaeological Science

University of Oxford, 2022



Abstract

The site of Hamanaka 2, Rebun Island (Hokkaido), contains an archaeological record including well-preserved faunal remains, including clam shells and cod otoliths, from hunter-gatherer groups across the Epi-Jomon to Historical Ainu periods. As demonstrated by sclerochronologists worldwide, incremental stable isotope analysis of marine carbonates can provide an archaeologically-relevant and directly-datable proxy record of oceanic palaeotemperature, which is especially important for coastal sites such as Hamanaka 2. Despite this, marine carbonates from the site have not yet been used for this purpose, partly due to concerns over a variable regional marine reservoir effect. This, in combination with the possibility of 'old' shells being incorporated into younger stratigraphic units, means that any climatic information gained can be difficult to associate conclusively with the stratigraphic unit from which it was excavated. This thesis aims to address the methodological and interpretational obstacles relating to the archaeological use of this material at Hamanaka 2, and considers the local palaeotemperature record these materials can provide and their implications.

The first paper examines the candidacy of the Sakhalin surf clam as a sub-annual temperature record, using stable isotope analysis of modern shells to compare carbonate-derived temperature estimates with observed water temperature. The results confirm that, as with most large, slow-growing marine bivalves, this species is a reliable recorder or water temperature, although seasonal extremes are likely to be dampened in the shell isotopic record. The second paper focuses on the complications arising from high resolution incremental sampling of marine carbonates, specifically the issue of contamination from embedding resin, and the relative merits of hand drilling versus micromilling. Comparison between two series of directly comparable samples shows that embedding may produce implausibly high $\delta^{13}C$ values in the embedded, micromilled samples. This is interpreted as evidence of the contamination effect of resin on $\delta^{13}C$, whilst $\delta^{18}O$ appears unaffected. The results indicate that hand drilling fast-growing species can provide a sub-annual

palaeotemperature record comparable to micromilling, minimising sampling time and maximising sample size.

The final paper addresses the main archaeological questions of the thesis. It assesses the palaeotemperature record of shells and otoliths from Hamanaka 2 over the Epi-Jomon-Final Okhotsk period in the context of new radiocarbon dates, which are paired with existing terrestrial dates. This allows calculation of new marine reservoir corrections, useful not only for this site but all others in the region which contain similar marine evidence. The integration of marine material into Bayesian chronological modelling at Hamanaka 2 constrains the timing of the Final Okhotsk period more tightly compared to previous models, showing a revised end date of 1107-958 cal BP. $\delta^{18}O$ results show no clear temperature trend across the study period, although the single Early Okhotsk otolith sampled is consistent with the existing suggestion that this period saw a short-lived period of cooler temperatures. Overall, stable isotope analysis and radiocarbon dating combine to show the potential of marine carbonate material from Hamanaka 2 as a climatic and chronological record.

Preface & Acknowledgements

This thesis is the result of almost five years' work, condensed into the format of three research articles bookended by an introduction, summary and conclusion. The 'integrated' article-based thesis, as opposed to a traditional monograph, certainly had many benefits. It allowed me to focus closely on specific research questions, especially discrete methodological issues which – while relevant to other researchers in the field – do not fit so easily into a narrative text. It also allowed me to gain useful critique from journal editors and peer reviewers throughout the process, which has undoubtedly improved the quality of the research overall, and for which I am very grateful. Beyond this though, the 'integrated' approach does have downsides. Foremost among them, in my opinion, is that the discussion in the thesis is necessarily concise and outward-looking, and that the more reflective and narrative aspects of the traditional thesis are much harder to maintain. This section is therefore intended to fill some of these gaps, outlining some of the key obstacles and decisions that informed the progression of the research, and of course thanking various important people and institutions who assisted along the way.

At the outset of my DPhil, the project (of course) looked rather different. I originally intended to continue on a similar path as my MPhil research, which used stable oxygen isotope analysis from the growth edge of archaeological shells to estimate their seasonal of collection. This has the advantage of providing not only a proxy for sea surface temperatures, but also a direct insight into the resource collection habits and seasonal scheduling of archaeological groups. The majority of the first year of this DPhil was spent familiarising myself with the literature on seasonal scheduling during northern Japanese prehistory and planning a research trip to collect material from Hamanaka 2 during the summer of 2018. It would have been useful to begin preparing lab protocols and testing the precision of the departmental carbonate mass spectrometer during this year alongside this, but unfortunately it coincided with major refurbishments and building works in the department which meant the labs were not accessible during this time.

The most major change in research direction occurred during the second year of the project, once I had collected archaeological shell specimens from Japan and took them to the Penryn campus of the University of Exeter to receive training from members of their Sclerochronology Research Group. Once able to section these shells and analyse them microscopically for the first time, it became clear that the growth pattern of the surf clam species in question was not going to be suited to season of collection analysis. Although the first 8-10 years of life showed rapid shell deposition and thick shell increments suited to sub-annual stable isotope analysis, in subsequent years the growth edge showed slow and minimal growth, meaning that growth increments were too thin to reliably sample from the final season of growth. This necessitated a pivot to the earlier years of growth and a more methodological and palaeoenvironmental focus. Moreover, the relatively small number of shells available, and their restriction to certain layers of the site, led to the inclusion of otoliths as an additional experimental source of marine carbonate evidence. Isotopic results from the otoliths proved difficult to compare to that of the clams, as Pacific cod are more mobile and occupy a deeper-water ocean habitat.

Once the labs in Oxford reopened and I was able to run standards on the carbonate mass spectrometer at the Oxford Research Laboratory for Archaeology and the History of Art, it became evident that the precision offered by the instrument would not be sufficient for subannual or seasonal palaeothermometry. Instead, I obtained a NERC Facilities Grant (Appendix 1) to undertake stable isotope analysis (and eventually the majority of the micromilling) at the Stable Isotope Facility at the British Geological Survey, Keyworth. This not only granted access to their high-precision instruments, but also meant I was able to benefit from the enormous expertise of the laboratory staff. Finally, the labs in Oxford closed once again between March and September 2020, as the coronavirus pandemic unfolded. This of course had an enormous impact on the work I had planned, meaning that scheduled time on the electron probe microanalyzer and the possibility of another sample collection trip to Japan had to be abandoned altogether. All subsequent lab work was

significantly delayed. This combination of factors is what ultimately led to the thesis as it is currently presented.

Throughout this process, there have been a whole host of wonderful people and institutions who have supported me. My primary funding came from the Clarendon Fund. It would not have been possible for me to undertake a DPhil without this scholarship, and for that I am very grateful. Nevertheless, I firmly believe that this scholarship has serious catching-up to do in terms of student welfare, and I hope that in the near future it will concede the need to fund post-graduate researchers in a way that more fairly recognises their research contribution to the university, and will begin to provide essential benefits such as funded sick leave. While UKRI has now recognised this necessity, it is disappointing that a university such as Oxford, where more than 50% of students report that their experience at the university has negatively impacted their mental health[1], has not yet made this step.

A number of other institutions have funded various aspects of this research. NEIFSC project grant [IP-1944-1119] facilitated the stable isotope analysis, and NEIFSC project grant [IP-2278-0320] provided funding for the radiocarbon dating (Appendix 1). Further fieldwork and research funding was generously granted by the Sasakawa Fund, the Oxford University Travel Grant, Hokkaido University, the British Geological Survey, the Meyerstein Fund, and the Brasenose College Graduate Research Grant and Student Support Fund.

A number of academics have also been extremely generous with their time and energy in supporting me through this project, both academically and personally. First of all, I would like to thank my supervisors Julia Lee-Thorp and Rick Schulting, whose guidance, expertise and belief has been essential, especially over the past two years of pandemic living. I would also like to particularly thank and credit Professor Melanie Leng, director of the NEIF Stable Isotope Facility, for her generous help during the lab work and data analysis undertaken. She had a key role in encouraging the genesis of

[1] OUSU Report on Student Welfare, Mental Health, and Support (June 2016)

the second paper of this thesis, as a potential resolution for some of the issues noticed in the stable isotope results. I am grateful as well to the Sclerochronology Research Group at the University of Exeter, who so kindly welcomed me into their lab to provide training. In particular, thanks go to Stella Alexandroff, Alejandro Román-González, Paul Butler and James Scourse. Equally, thanks are owed to researchers and members of staff at the University of Oxford department of Earth Sciences, the University of Hokkaido, the British Geological Survey, and of course the University of Oxford School of Archaeology. Gratitude is also owed to a number of other individuals for their help and support: Peter Ditchfield, Victoria Smith, Christopher Day, Hamish Couper, Jonathon Wells, Dave Peat, Emma Loftus, Catherin West, Jamie Cameron, Dave Chivall, Lorena Becerra-Valdiva, Hilary Sloane, Yu Hirasawa, Taena Uemura, Tomonari Takahashi, Takumi Tsutaya, Takao Sato, and Hirofumi Kato. Finally, thank you to all anonymous peer reviewers who commented on drafts of these articles during journal submission.

On a personal and level, I would like to give a special thank you to my incredible friends and family, without whom I would definitely have given up a hundred times over. Thanks to the BAR team, who have been an excellent motivator over the last few months. To Emese Végh, Rebecca Smith and Marjolein Bosch – you are incredible people, scientists, and friends, and I am so lucky to have you to inspire me. Thank you to my bridesmaids – Cat, Claire, Indigo, Isabelle, Lydia and Sarah – who have put up with my joint PhD- and wedding-woes admirably. An extra special shout-out to Indi, who has had to suffer me her entire life and is still the best sister ever, even though I pushed her into a ditch that one time. Thank you to the whole Stuart family for making me feel so warmly welcomed since well before the DPhil. Thank you to my parents – I am so grateful that I have always had your love and support.

To Gwyn, who gives me a reason to get out of bed every (other) morning.

To Chris, who has always been my greatest cheerleader and confidante, and an all-round incomparable life-partner. Without your personal-chef-ing, tea-making, dog-walking, tear-wiping and hand-holding, none of this work would ever have existed.

Table of Contents

Abstract ..... **i**

Preface and Acknowledgements ..... **iii**

Introduction **1**

The Late Holocene Archaeology of Northern Japan 3

Hamanaka 2, Rebun Island, Hokkaido 8

Research Design 14

Sample Selection and Collection 16

Species of Interest 21

Spisula sachalinensis (Sakhalin surf clam) 23

Gadus macrocephalus (Pacific cod) 24

Research Questions 27

Climate and Environment in Japan 31

Modern Japan 31

Palaeoclimatic Reconstructions 35

Archaeometric Methods 40

Stable Isotope Palaeothermometry 41

Radiocarbon Dating 48

Paper 1: The potential of marine bivalve *Spisula* sachalinensis as a marine temperature record ... **51**

Abstract 51

Introduction 51

Growth and ecology 52

Materials and methods 53

Results 54

Discussion 54

How well does $\delta^{18}O_{shell}$ data match modern SST records? 54

Interpretation of $\delta^{13}C_{shell}$ results 55

Potential confounding factors to $\delta^{18}O_{shell}$ interpretation 55

Implications for palaeothermometry 60

Conclusion 61

References 61

Paper 2: Micromilling Vs Hand Drilling in Stable Isotope Analyses of Incremental Carbonates: the Potential for δ13C Contamination by Embedding Resin **63**

Abstract 63

Introduction 64
Methods 65
Results and Discussion 66
Conclusions 69
References 70
Paper 3: Stable Isotope Palaeothermometry and Radiocarbon Chronology of Marine Carbonates from Hamanaka 2, Rebun Island (Japan) **72**
Abstract 72
Introduction 73
Materials and methods 76
Results 79
Discussion 83
New ΔR values 83
An updated chronological model for Hamanaka 2 86
$\delta^{13}C$ results 87
$\delta^{18}O$ results 88
Conclusions 91
Acknowledgements 93
Figures 94
Bibliography 101
Appendix 1: OxCal code 106
Appendix 2: full radiocarbon results 119
Appendix 3: combined dates 121
Discussion and Conclusion **122**
Future Research Directions 129
Sample Size 129
Trace Element Analysis 131
Stable Isotope Analysis 132
Radiocarbon Dating 132
Conclusion 133
Bibliography **136**
Appendix 1: Successful external grant applications **156**
Appendix 2: Photographs of sampled shells and otoliths **168**
Appendix 3: Full $\delta^{18}O$ and $\delta^{13}C$ results **173**
Appendix 4: Electron microprobe analysis **180**

Appendix 5: Bayesian models for paired shell radiocarbon dates **182**

Co-authorship Statements **184**

List of Figures

Introduction

Figure 1 Overview of the cultural divergence between Honshu (l) and Hokkaido (r) between the Jomon and Imperial periods 4

Figure 2 Hamanaka 2 at the beginning of the 2018 field season 7

Figure 3 Map of Hokkaido showing the location of Hamanaka 2 and major regional oceanographic currents. Image reproduced from Müller et al. (2016) 8

Figure 4 Map of Hamanaka showing the location of different excavation sites. Reproduced from Hirasawa (2018) 9

Figure 5 Map showing the distribution of archaeological sites on Hamanaka 2. Reproduced from Hirasawa (2018) 10

Figure 6 Stratigraphic profile for Hamanaka 2 (modified from Muller et al. 2016), showing the location of selected samples, existing chronology and key climatic events 15

Figure 7 Spisula sachalinensis shells with cm scale. Image via iNaturalist.ca, (c) Kim, Hyun-Tae (CC BY-NC-SA) 19

Figure 8 Native distribution of S. sachalinensis. (AquaMaps 2019) 23

Figure 9 Native distribution of Gadus macrocephalus. (AquaMaps 2019) 25

Figure 10 Pair of sagittal otoliths from G. macrocephalus (Pacific cod) with 2 mm scale. Image from: Alaska Fisheries Science Center Quarterly Report, April 2015 25

Figure 11 Koppen-Geiger climate map of Japan. Edited from image by Ali Zifan via Wikimedia Commons 30

Figure 12 Northern Japanese biomes and currents. Reproduced from Leipe et al. (2013) 31

Figure 13 Bathymetric map of Japan showing major ocean currents. Bathymetric data from NOAA (National Oceanic and Atmospheric Administration) 34

Figure 14 Multi-proxy climate reconstructions from Lake Toyoni over the past 1000 years.). Image reproduced from McColl (2016). 37

Figure 15 Holocene palaeoenvironmental proxies. Image reproduced from Brookes et al. (2016). 38

Paper 1

Figure 1 Schematic illustration of Spisula sachalinensis showing section along the axis of maximum growth 52

Figure 2 Map showing the location of Tomakomai within northern Honshu, and the surrounding ocean currents 52

Figure 3 Image of sectioned Spisula sachalinensis valves showing completed micromill sampling and the location of growth lines 53

Figure 4 Graph plotting oxygen and carbon stable isotope results. Peaks and troughs in $\delta^{18}O_{shell}$ marked with arrows 58
Figure 5 Temperature estimation based on $\delta^{18}O_{shell}$ results, overlain on average annual SST range for Tomakomai 59

Paper 2

Figure 1 Illustration of Spisula sachalinensis showing section along the axis of maximum growth 65
Figure 2 Plots showing the $\delta^{13}C$ and $\delta^{18}O$ results for shells II_1 and VIII_3 for both the micromilled samples (a) and the hand drilled samples (b) 66
Figure 3 Scan of sampled sections for shells II_1 and VIII_3 showing the corresponding micromilled and hand drilled regions 67
Figure 4 Plot showing (a) $\delta^{13}C$ results from hand drilled and micromilled samples, and (b) $\delta^{18}O$ results from hand drilled and micromilled samples 68

Paper 3

Figure 1 Map of Hokkaido showing the location of Hamanaka II, and the major oceanographic currents influencing the region. Image reproduced from Müller et al. 2016 94
Figure 2 Stratigraphic profile for Hamanaka II (modified from Müller et al. 2016), showing locations of proposed samples, existing chronology, and key climatic events 95
Figure 3 illustration showing the way in which Spisula sachalinensis shells were sectioned from umbo to shell edge, along the axis of maximum growth 96
Figure 4 Results plot of radiocarbon sequence for Hamanaka 2, including 73 dates over 14 phases 97
Figure 5 Scatter graphs showing $\delta^{13}C$ and $\delta^{18}O$ results for shells from the Final-/Epi-Jomon, Towada 2, Motochi 1 and Motochi 2 units at Hamanaka 2 99
Figure 6 Boxplots showing SST range. Top: SST by specimen, black circles show the mid-range point ((minSST+maxSST)/2) 100

List of tables

Introduction

Table 1 Summary of existing radiocarbon dates for previous excavations at Hamanaka 2 12
Table 2 Chronological model from Junno et al. (2021). Conventional chronologies from Deryugin, 2008; Ono, 2008; Tashiro, 2017; Hirasawa and Kato, 2019 16
Table 3 Descriptions and criteria for selected Koppen-Geiger identifiers, as per Peel et al. (2007) 32

Paper 1

Table 1 Summary of average monthly observed SST (◦C) for the Tomakomai coast for the period of 1992–2002 53

Table 2 Stable isotope data from shells TBMOD1 and TBMOD2 alongside $\delta^{18}O_{shell}$-derived sea surface temperature (SST) 54

Paper 2

Table 1 Summary of stable isotope results from shells II_1 and VIII_3 66

Paper 3

Table 1 List of ^{14}C dates from marine samples at Hamanaka II obtained in this project 79

Table 2 Estimations of age for each ^{14}C-dated S. sachalinensis specimen 80

Table 3 Summary results of shell and otolith $\delta^{18}O$ analysis 81

Table 4 Summary of SST estimations by period, as calculated using $\delta^{18}O$ 82

Table 5 ΔR values from Miyata et al. (2016), updated using the Marine20 radiocarbon curve 84

Table 6 New ΔR values calculated using the marine ^{14}C results from this thesis 84

Introduction

This thesis deals with marine carbonate material from the archaeological site of Hamanaka 2, Rebun Island. The project began with primarily archaeological research questions concerning late Holocene environmental change, human-environment interactions and seasonal behaviours. As it progressed, it became increasingly clear that methodological questions were going to be equally important to address, and that these were often a prerequisite for approaching the archaeological topics of interest. In this chapter, I will introduce the main topics relevant to the subsequent papers.

Firstly, the archaeology of northern Japan will be introduced, as well as the specific research history of Hamanaka 2. After this, the modern and palaeoenvironmental context of northern Japan will be summarised. This leads on to discussion of the specific questions this project will address, which will draw on aspects of all the aforementioned topics. This introduction will highlight gaps in the current knowledge, as well as the particular techniques that this thesis will employ. Modern climate and environment is of course always of interest when investigating ancient conditions, but this context is also especially relevant for the first paper, which presents a modern validation study for the use of the main bivalve species discussed as an ocean temperature proxy record. The palaeoenvironmental context is then key to understanding the archaeological research questions which investigate the (inter)dependence of cultural and environmental change.

This introduction will also discuss stable isotope analysis and review its use as a tool for palaeotemperature reconstructions. This is one of two main archaeometric techniques underpinning the thesis, and is also the main topic of the first two papers, both of which explore different methodological questions on the technique and its application to the species of interest. Lastly, radiocarbon dating will be introduced, which is the second archaeometric technique used in this research. This is a key element of the final paper in this thesis, providing essential chronological

context for the stable isotope palaeothermometry and for the chronology of northern Japanese archaeology more generally.

Before beginning, it is important to highlight a significant limitation of this review. Despite the wealth of scientific literature produced in Japan every year (Pearson 1992), only a fraction of this is readily accessible to non-Japanese speakers. This is not only due to the fact that most Japanese publications are of course written in Japanese, but also because these publications are often difficult to find and access. Journal or article titles written in Japanese characters can have multiple possible English translations, and are not immediately searchable in reference software. This in turn affects the ease with which physical copies of Japanese volumes can be found.

Where possible, Japanese and other foreign language texts have been accessed with the help of English summaries, translated sections, or their discussion in other literature. However, this issue is difficult to fully overcome. For this reason, the following sections, particularly those dealing specifically with Japanese climate and archaeology, should be read with the understanding that they constitute a review fundamentally biased towards English-language discourse. This is inescapably an incomplete view, but can at least be considered representative of the literature widely accessible in the international arena.

This thesis project was undertaken in collaboration with Japanese archaeologists from the University of Hokkaido, whose guidance was used to ensure that there were no ethical issues in the retrieval of materials and subsequent analyses. The archaeological excavations at Hamanaka 2 are currently run by the Hokkaido University Centre for Ainu and Indigenous Studies, whose team is sensitive to the ethical issues that can surround indigenous archaeology. There is no modern Ainu population living on Rebun Island, but the field school does run significant outreach to involve the local community, including welcoming visitors to site, inviting local school children for workshops, and an ethnographic project amongst the local community which is running alongside the archaeological excavations (Gomes and Kondo 2020).

The Late Holocene Archaeology of Northern Japan

The Japanese archaeological record is extremely rich and varied, and benefits from an 'incredible' abundance of governmentally organised salvage excavations (Shinya and Son 2017). A recent meta-analysis of site distribution used data from more than 12,000 archaeological sites in Hokkaido alone (Nakazawa 2011 p. 234; Abe et al. 2016). Edward S. Morse is widely considered to have undertaken the first systematic archaeological excavation in Japan in the 1870s (W. Edwards 2005), recognising the presence of prehistoric shell middens at Ōmori, Tokyo. Since then, interest in prehistoric archaeology has moved on from antiquarian collections towards academic investigation. Governmental recognition for archaeological finds was cemented by the 1950 "Protection of Cultural Properties" act (W. Edwards 2005; Nakazawa 2011). This enforces the protection and preservation of archaeological material, and requires archaeological investigation in the case of any development on either public or privately owned land.

Japanese prehistory does not follow the ternary systems well known from Europe and Africa (Tomii 2014). Instead, it sees a shorter Palaeolithic period followed by the Jomon, broadly characterised by the development of early ceramic technology. After this point, there is significant geographical variability in Japanese cultural history. Farming communities and later imperial politicisation emerged in Honshu and the south islands, while hunter-gatherer-fisher economy persisted in Hokkaido, eventually also incorporating elements of rice, wheat and millet cultivation during the Ainu period (Weber, Jordan, and Kato 2013). Figure 1 illustrates this cultural divergence, and shows the series of hunter-gatherer cultures in Hokkaido until its colonisation by the Japanese state in the late 19th century (Ohnuki-Tierney 1976; Hudson 2014; Seaton 2017).

As seen in Figure 1, during the period of state formation in Honshu, the Jomon period in Hokkaido was followed by the Epi-Jomon (also known as the Zoku-Jomon). The Jomon and Epi-Jomon are both examples of 'complex' hunter-gatherer society (Arnold 1996; Sassaman 2004; Junko Habu 2008; Takeshi 2014), with increasing social differentiation, seasonal sedentism and formal cemeteries (Kodama 2003; Pearson 2007; Weber, Jordan, and Kato 2013; Takeshi 2014). Although predominantly following a hunter-gatherer subsistence model, evidence has also been found for

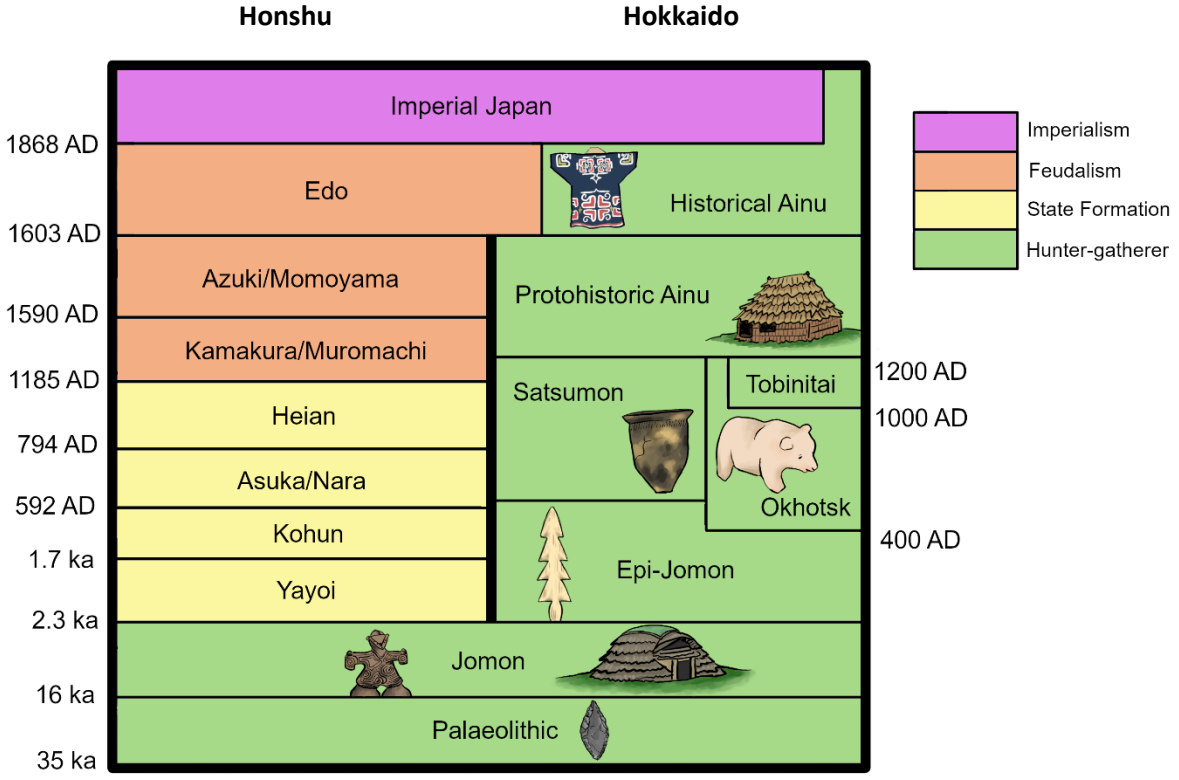


Figure 1: Overview of the cultural divergence between Honshu (l) and Hokkaido (r) between the Jomon and Imperial periods

plant cultivation and food production (e.g. Y.-I. Sato, Yamanaka, and Takahashi 2003; Crawford 2008). Although the extent to which 'complexity' is actually uncommon in hunter-gatherer society is debatable (Arnold 1996; Petersen and Meiklejohn 2007), it is traits such as these which help fuel significant and sustained academic interest in the Jomon period.

In northern and eastern Hokkaido, the Epi-Jomon period was followed by the Okhotsk (Figure 1). This culture is not unique to Hokkaido, with origins in the Amur basin and arriving to Hokkaido via nearby Sakhalin in the fourth and fifth centuries AD (Yamaura 1998). This cultural package can be seen along the north and northeast coasts of Hokkaido, as well as on the northern islands of Rebun

and Rishiri (Müller et al. 2016), from the sixth century until the thirteenth century AD (Matsumura et al. 2006; Weber, Jordan, and Kato 2013).

Although the groups are genetically distinct, in terms of diet and mobility the Okhotsk was partially a continuation of Epi-Jomon activities (T. Sato et al. 2007; T. Sato et al. 2009; T. Sato et al. 2010). Based on artefactual similarities, the development of the Okhotsk on Sakhalin was likely heavily influenced by contact with the concurrent Epi-Jomon in Hokkaido (Kikuchi 1978; Yamaura 1998). Notably, the Okhotsk is known for its coastal fishing niche, with isotopic results confirming the high contribution of marine protein to human diet in this period (Naito et al., 2010). The Okhotsk is particularly known for specialised sea mammal hunting (Yamaura 1998; Abe et al. 2016; Müller et al. 2016). This is reminiscent of the development and importance of sea mammal hunting for some Epi-Jomon groups in southern Hokkaido (Nishimoto 1984; Yamaura 1998).

Differences between the Epi-Jomon and Okhotsk can be seen in the scale and intensity of human activity. Compared to preceding cultures, the Okhotsk shows more intensive use of coastal and terrestrial resources, as well as larger 'village' settlements, and increasing social stratification (Befu and Chard 1964; Lebedintsev et al. 1998; Hudson 1999; Amano and Vasilevski 2002; Weber, Jordan, and Kato 2013). Another significant difference is the arrival of domesticated pigs, although this practice did not spread as far as the eastern Hokkaido Okhotsk (Yamaura 1998). Owing to the mixed economy, including marine hunting, cereal cultivation and pig husbandry, Leipe et al. (2017) characterises the Okhotsk as 'epitomis(ing) the complexity and diversity of the middle ground economy'.

Satsumon culture developed from the Epi-Jomon during the seventh century AD in the SW of Hokkaido, and persisted alongside the Okhotsk until the 13th century AD (Okada 1998; Matsumura et al. 2006; Weber, Jordan, and Kato 2013). The Satsumon moved away from maritime adaptations, instead focusing subsistence activities on terrestrial hunting and freshwater salmon fishing (Okada 1998). Southern influences from Honshu also played a significant role in the formation of the

Satsumon culture, leading to the introduction of cereal cultivation to southern Hokkaido as a supplement to foraging (Crawford and Yoshizaki 1987; Crawford and Takamiya 1990; Ōnishi 2014). Leipe et al. (2017) suggests that the naked barley of the Okhotsk originated in continental Russia, while Satsumon hulled barley came from Kofun farmers in neighbouring Honshu. This distinction illustrates the separate cultural trajectories of north and south Hokkaido during the Satsumon/Okhotsk period.

While the Satsumon and Okhotsk periods remained distinct neighbours for several hundred years, it is thought that the end of the Okhotsk period occurs concurrently with expansion of the Satsumon into northern Hokkaido territories (Hudson 2014; Smale 2014). Okhotsk culture retreated to coastal fringes from c. 1000 AD, and most of Hokkaido shifted from Okhotsk-style marine fishing to riverine salmon fishing (Hudson 1999). This resulted in the development of the Tobinitai cultural group, thought to represent an Okhotsk/Satsumon 'hybrid culture' (Hudson, 1999; Smale, 2014), and ancestral to the subsequent Ainu (Omoto and Saitou 1997; Tajima et al. 2004; Jeong, Nakagome, and Di Rienzo 2016).

Formative Ainu deposits in Hokkaido date from the start of the thirteenth century AD, with the appearance of the Classic Ainu from 1600 AD (Matsumura et al. 2006). These periods are sometimes grouped as the 'Historic Ainu' or 'Ainu culture period' (Weber, Jordan, and Kato 2013; Hudson 2014), as opposed to the 'Modern Ainu' which is considered to be the continuation of the culture following Japanese colonisation in 1869. The Historic Ainu is in many ways similar to the SW Hokkaido Satsumon, with formalised cemeteries, and a mixed hunter-gatherer-fisher economy which also incorporated elements of rice, wheat and millet farming (Weber, Jordan, and Kato 2013). However, the Ainu culture is not purely a development from the Satsumon. Instead, authors such as Smale (2014) and Hudson (Hudson 1999; Hudson 2014) suggest that the Ainu more likely originated from interaction between the Okhotsk and Satsumon, for example via the aforementioned Tobinitai.

Behaviourally, Hudson (2014) emphasises the complexity of Ainu culture, noting their sedentism, social stratification, plant cultivation, trade networks and maritime navigation. This classes the Ainu as non-traditional foragers. Differences between ethnographic Ainu mobility and that of other modern hunter-gatherer groups is illustrated by Kelly (1983), who records the Ainu as having only 2 residential moves per year, compared to the average of 17 among his sample of 32 cultures. The Ainu are also highly diverse in terms of the environments and ecological niches occupied. The Classic Ainu ranges from the Kurils to northern Honshu, spanning arctic to temperate latitudes, which in turn comprise a variety of faunal suites (Ohnuki-Tierney 1976). Due to this geographic breadth, Ainu ecology must have been similarly diverse, for example Crawford and Bleed (1998) discuss the importance of diversity in Ainu scheduling activities in order to deal with differences in snowfall across Hokkaido.



Figure 2: Hamanaka 2 at the beginning of the 2018 field season

Hamanaka 2, Rebun Island, Hokkaido

The archaeological material used in this thesis comes from the site of Hamanaka 2, Rebun Island (Figure 2). Rebun Island is the northernmost island of the Japanese archipelago, located in the Sea of Japan off the far northwest coast of Hokkaido (Figure 3). Much of the island shows steep topography, with cliffs and rocky shore along the east and west coasts especially (Hirasawa and Kato 2019). The island is well-known for its unusual 'Alpine' flora (Tatewaki 1973; Tatewaki and Tohyama 1975; Yamaki 2015) which has earned it the name 'Floating Flower Island'. Due to its remoteness, it

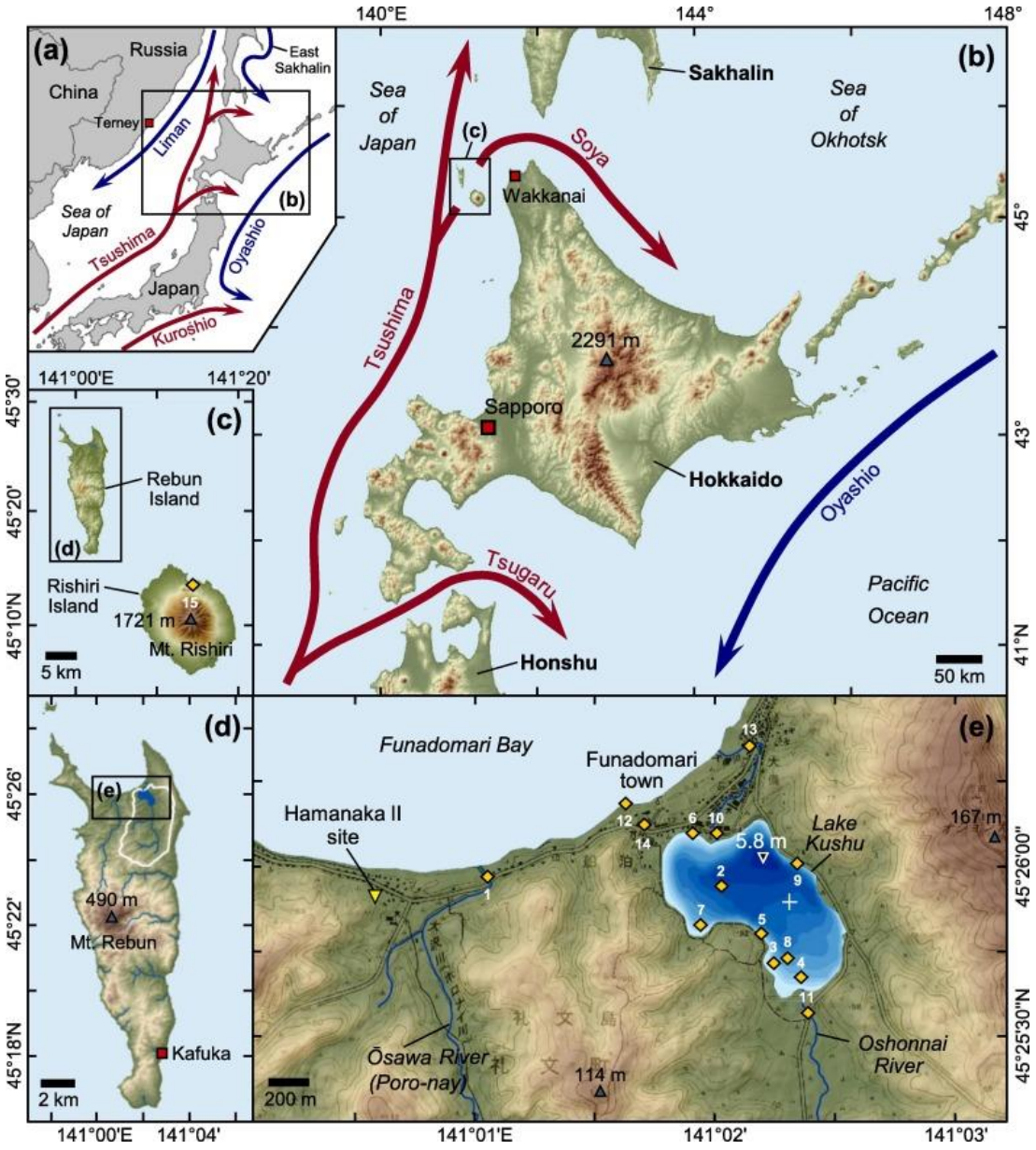


Figure 3: Map of Hokkaido showing the location of Hamanaka 2 and major regional oceanographic currents. Image reproduced from Müller et al. (2016)

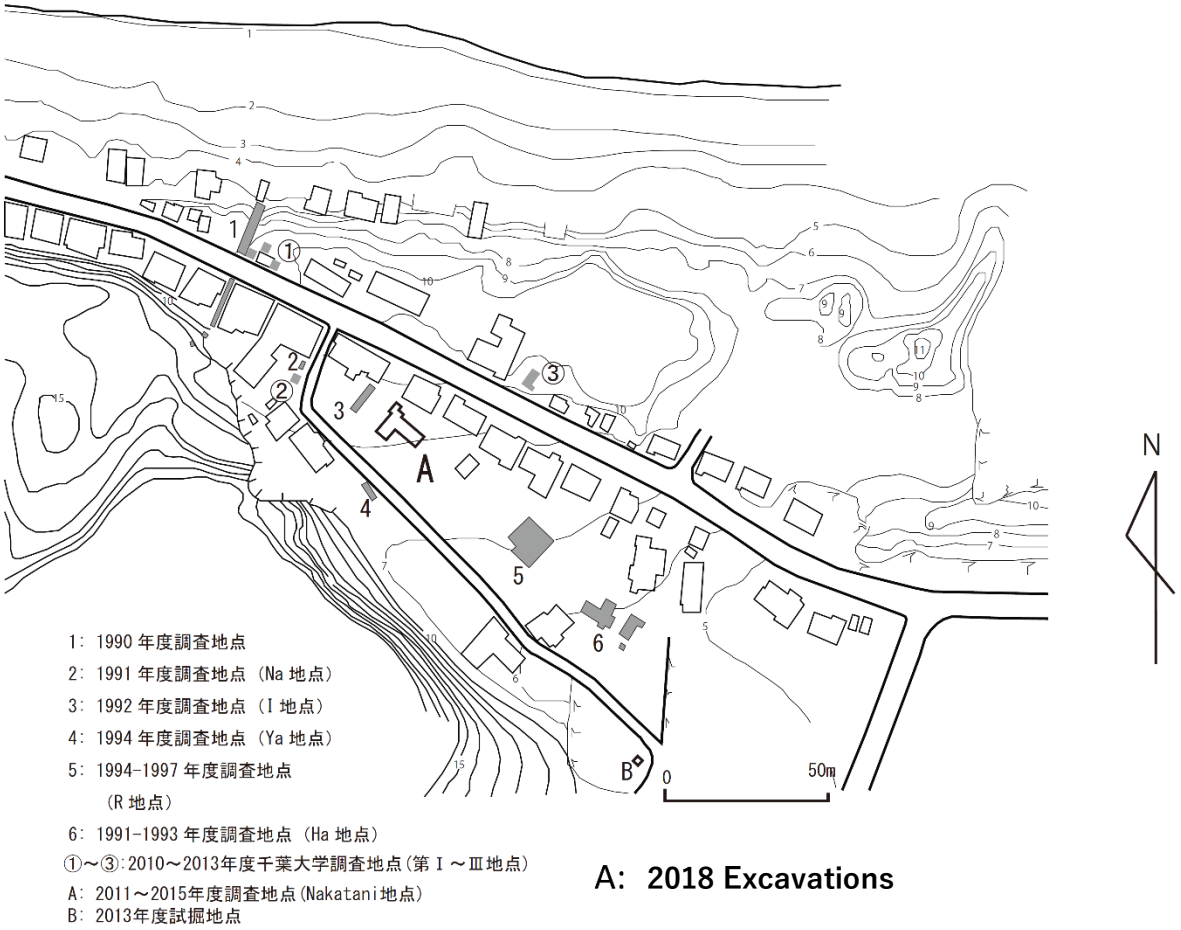


Figure 4: Map of Hamanaka showing the location of different excavation sites. Reproduced from Hirasawa (2018)

lacks many of the larger mammal species present in the rest of Hokkaido, with no bears, deer or foxes (Hirasawa and Kato 2019). This means that aquatic fauna – fish, shellfish and sea mammals – have become especially important dietary sources both for its modern and ancient populations. In the past, domesticated pigs and dogs have also been important resources (T. Sakaguchi 2007a; Leipe et al. 2017; Junno et al. 2021).

The island is rich in archaeology (Figure 4, 5), with evidence of occupation from the Late Jomon to the Historic Ainu and a long history of excavation. Hamanaka 2 is located on the island's northern coast, in an area of sand dunes next to the large, shallow and sheltered Funadomari Bay (T. Sakaguchi 2007b). Lake Kushu, which provided the sediment cores discussed below, is ~1.5 km to the east.

Hamanaka 2 has produced evidence from the late Jomon period onwards, although it is thought that remains dating to the Middle Jomon might still be confirmed from as-yet unexcavated strata (Hirasawa 2018). The site's sand dune location has led to good preservation of faunal remains (Hirasawa 2018; Hirasawa and Kato 2020). With its sheltered position next to Funadomari bay and within easy walking distance to freshwater lake Kushu and the Osawa river, the Hamanaka sand dunes provide a base with especially easy access to aquatic resources. It is unsurprising then, that the local area remains occupied and that the site overlaps significantly with the modern Hamanaka village.

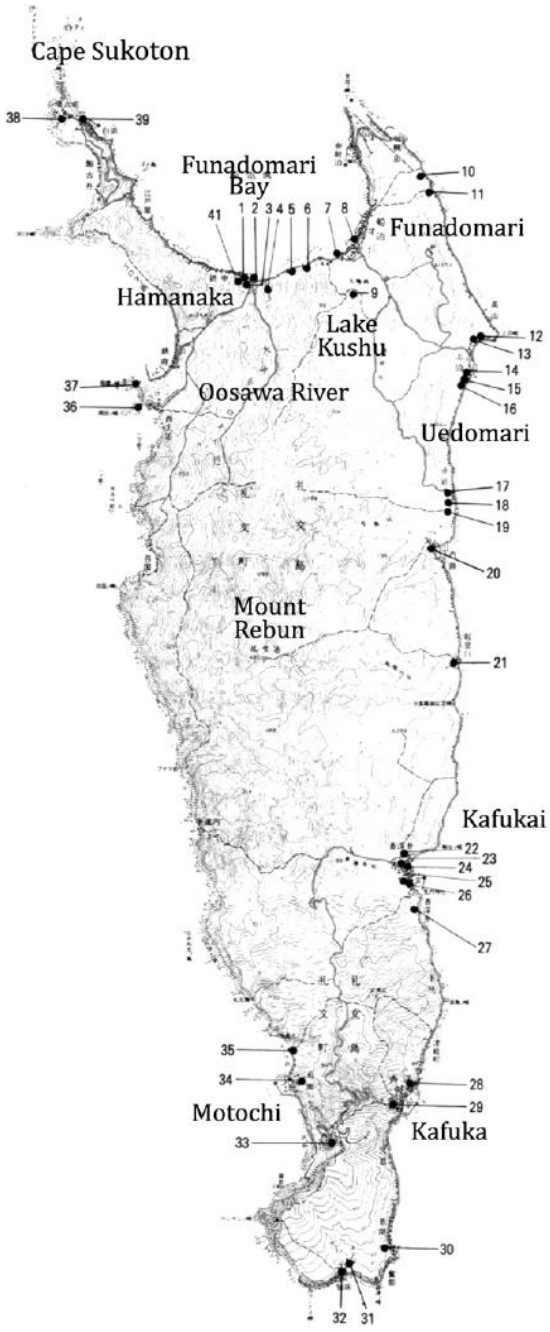


Figure 5: Map showing the distribution of archaeological sites on Hamanaka 2. Reproduced from Hirasawa (2018)

The first academic excavations at Hamanaka were led by researchers from Hokkaido University in 1949. Since 1990, various excavations and surveys have taken place focusing on different regions of the site, as shown in Figure 4, following the discovery of significant and well-stratified prehistoric remains during drainage repair works (Hirasawa and Kato 2019). Excavations from 2011-2017 formed part of the Baikal-Hokkaido Archaeology Project, jointly run by the Universities of Hokkaido and Alberta, which aimed 'to reconstruct and explain patterns and processes of culture change' by comparing archaeological evidence from prehistoric Cis-Baikal

and Hokkaido (Weber, Jordan, and Kato 2013 p. 4). From 2018 to 2023, excavations are funded by the Japan Society for the Promotion of Science as part of a 'Core-to-Core' project led by Professor Hirofumi Kato from the Hokkaido University Center for Ainu and Indigenous Studies. This significant research history has produced a host of published data, including e.g. ceramic analysis (Sakaguchi 2007b), stable isotope analysis (Naito et al. 2010a; Tsutaya et al. 2021), radiocarbon dating (Miyata et al. 2016; Junno et al. 2021), osteology/palaeopathology (Ishida et al. 1994; Okamoto et al. 2016), residue analysis (Miyata et al. 2009) and palaeobotany (Müller et al. 2016; Leipe et al. 2017). This breadth of research, along with sediment core research from lake Kushu, provides an excellent basis for this thesis.

A number of pre-existing radiocarbon dates are available for the site, summarised in Table 1. Being marine-focused hunter-gatherers, occupants of the site are thought to have consumed a diet containing a significant proportion of marine input (Okamoto et al. 2016). This is confirmed through stable carbon and nitrogen isotope values from Okhotsk human remains at the site, which show an estimated 94% dietary contribution of marine protein (Naito et al. 2010b). This means that human remains from the site, as well as many of the animal remains where habitat or diet is aquatic, will be affected by a marine reservoir effect when radiocarbon dated. Miyata et al. (2016) provide an estimate of the local marine reservoir effects for the Late Jomon period at Hamanaka 2, by comparing dates from charred wood, molluscs, sea birds, sea lions and charred material from pot sherds. They produce ΔR values varying from 30±58 ^{14}C yr (from mollusc shells) to 304±70 ^{14}C yr (from charred residues), illustrating how the reservoir effect varies depending on the unique aquatic diet/habitat of the sampled material.

The most recent chronology from Hamanaka 2 uses Bayesian modelling to constrain the dating of each occupation phase (Junno et al. 2021). Researchers combined terrestrial seed and charcoal dates from previous studies (Müller et al. 2016; Leipe et al. 2017; Leipe et al. 2018) with new dates on seeds from throughout the stratigraphic sequence. Results of their model are summarised in

Table 2. The chronology suggests that after the initial period of occupation during the Late- to Epi-Jomon, there was a period of inactivity for ~750 years between ~250 BCE and ~500 CE. Evidence from the Jomon layers suggests a focus on seasonal (late spring/early summer) food procession of pinnipeds and sea birds (Sakaguchi 2007b; Sakaguchi 2007a). While food processing remains a key site activity from the Okhotsk onwards, after this point evidence of fishing and shellfishing increases which indicates that occupation extended beyond the spring/summer season and that marine resources were a key cold-season resource (Sakaguchi 2007a; Junno et al. 2021), potentially requiring well-developed seafaring technology (Eda, Koike, and Higuchi 2016). From the Okhotsk period onwards human burials also form part of the assemblage, along with zooarchaeological evidence of animal rituals/worship, continuing into the Historical Ainu (Sakaguchi 2007a; Smale 2014; Junno et al. 2021). Excavations in the Ainu layers have uncovered abalone shell midden deposits which show small-scale and potentially ritualised processing of this species (Hirasawa and Kato 2020; H. Kato 2020).

Table 1: Summary of existing radiocarbon dates for previous excavations at Hamanaka 2

Layer	Lab No.	Date (^{14}C yr)	+/-	Material	Cultural Attribution	Ref
V	PLD-6305	3805	20	Charred material on pot	Late Jomon	Miyata et al. 2009
V	PLD-6306	3815	20	Charred material on pot	Late Jomon	Miyata et al. 2009
V	PLD-6453	3730	35	Charred material on pot	Late Jomon	Miyata et al. 2009
V	PLD-6454	3715	35	Charred material on pot	Late Jomon	Miyata et al. 2009
V	PLD-6455	3840	35	Charred material on pot	Late Jomon	Miyata et al. 2009
V	PLD-6456	2980	35	Wood	Late Jomon	Miyata et al. 2009
V	PLD-6457	3035	35	Wood	Late Jomon	Miyata et al. 2009
V	PLD-8847	3550	25	Shell	Late Jomon	Miyata et al. 2016
V	PLD-8848	3550	25	Shell	Late Jomon	Miyata et al. 2016
V	PLD-8849	3715	25	Shell	Late Jomon	Miyata et al. 2016
V	PLD-8850	3470	25	Shell	Late Jomon	Miyata et al. 2016

V	PLD-8851	3500	25	Shell	Late Jomon	Miyata et al. 2016
V	PLD-10582	3735	30	Sea lion	Late Jomon	Miyata et al. 2016
V	PLD-10583	3635	30	Alcidae	Late Jomon	Miyata et al. 2016
IIIb	Poz-60766	1305	30	Seed	Okhotsk	Müller et al. 2016
IIIb	Poz-60767	1265	30	Seed	Okhotsk	Müller et al. 2016
IIIb	Poz-60768	1215	30	Seed	Okhotsk	Müller et al. 2016
I	Poz-60760	165	30	Seed	Historical Ainu	Müller et al. 2016
I	Poz-60761	115	30	Seed	Historical Ainu	Müller et al. 2016
I	Poz-60762	210	30	Wood	Historical Ainu	Müller et al. 2016
IIIa	Poz-84277	1215	30	Seed	Okhotsk	Leipe et al. 2017
IIIa	Poz-84278	1170	30	Seed	Okhotsk	Leipe et al. 2017
IIIb	Poz-81340	1220	30	Seed	Okhotsk	Leipe et al. 2017
IIIb	Poz-81341	1215	30	Seed	Okhotsk	Leipe et al. 2017
IIIb	Poz-81342	1180	30	Seed	Okhotsk	Leipe et al. 2017
IIIc	Poz-84280	1285	30	Seed	Okhotsk	Leipe et al. 2017
IIIc	Poz-84281	1275	30	Seed	Okhotsk	Leipe et al. 2017
IIId	Poz-84282	1295	30	Seed	Okhotsk	Leipe et al. 2017
IIId	Poz-84283	1335	30	Seed	Okhotsk	Leipe et al. 2017
IIId	Poz-84284	1475	30	Seed	Okhotsk	Leipe et al. 2017
IIId	Poz-84285	1275	30	Seed	Okhotsk	Leipe et al. 2017
IIIe	Poz-84286	1350	30	Seed	Okhotsk	Leipe et al. 2017
IIIe	Poz-84287	1520	30	Seed	Okhotsk	Leipe et al. 2017
N/A	Tka-16063	1689	20	Human remains	Okhotsk	Okamoto et al. 2016
IIIc	Nuta2-21213	1320	40	Seed	Okhotsk	Junno et al. 2021
IIIe	Nuta2-21216	1154	45	Seed	Okhotsk	Junno et al. 2021
IV	Poz-102824	1535	30	Seed	Okhotsk	Junno et al. 2021
V	Poz-102853	1540	30	Seed	Okhotsk	Junno et al. 2021

V	Poz-102825	1550	30	Seed	Okhotsk	Junno et al. 2021
VII	Nuta2-21214	2176	43	Seed	Epi-Jomon	Junno et al. 2021
I	Poz-73796	120	30	Seed	Historical Ainu	Leipe et al. 2018
I	Poz-91168	80	30	Seed	Historical Ainu	Leipe et al. 2018
I	Poz-91169	1175	30	Seed	Historical Ainu	Leipe et al. 2018
IIa	Poz-73797	215	30	Seed	Satsumon	Leipe et al. 2018
IIa	Poz-91167	1245	30	Seed	Satsumon	Leipe et al. 2018
IIb	Poz-73798	210	30	Seed	Unidentified	Leipe et al. 2018
IIc	Poz-91165	130	30	Seed	Okhotsk	Leipe et al. 2018
IIc	Poz-73799	1165	30	Seed	Okhotsk	Leipe et al. 2018
IIIa	Poz-73801	170	30	Seed	Okhotsk	Leipe et al. 2018
IIIc	Poz-73802	1455	30	Seed	Okhotsk	Leipe et al. 2018
VII	Poz-91170	1555	30	Seed	Epi-Jomon	Leipe et al. 2018
VII	Poz-91177	2115	30	Seed	Epi-Jomon	Leipe et al. 2018
VII	Poz-91175	2170	30	Seed	Epi-Jomon	Leipe et al. 2018
VII	Poz-73803	2195	30	Seed	Epi-Jomon	Leipe et al. 2018
VII	Poz-73804	2200	35	Seed	Epi-Jomon	Leipe et al. 2018
VII	Poz-73805	2220	30	Seed	Epi-Jomon	Leipe et al. 2018
VII	Poz-73806	2220	30	Seed	Epi-Jomon	Leipe et al. 2018
VII	Poz-91171	2220	30	Seed	Epi-Jomon	Leipe et al. 2018
VIII	Poz-91179	2200	30	Seed	Final Jomon/Epi-Jomon	Leipe et al. 2018
VIII	Poz-91178	2240	30	Seed	Final Jomon/Epi-Jomon	Leipe et al. 2018

Research Design

The following section describes the direction this thesis will take, and will be followed by a discussion of the broader climatic and scientific context drawn upon in the rest of the thesis. Firstly

the sample collection for this project will be discussed, as well as some limitations of this thesis, and the two main species of interest. For *S. sachalinensis*, there will be significant discussion of its growth and ecological niche in Paper 1, therefore for the avoidance of unnecessary repetition this will only be briefly considered here. Lastly, the main research questions tackled by the three central research papers will be introduced.

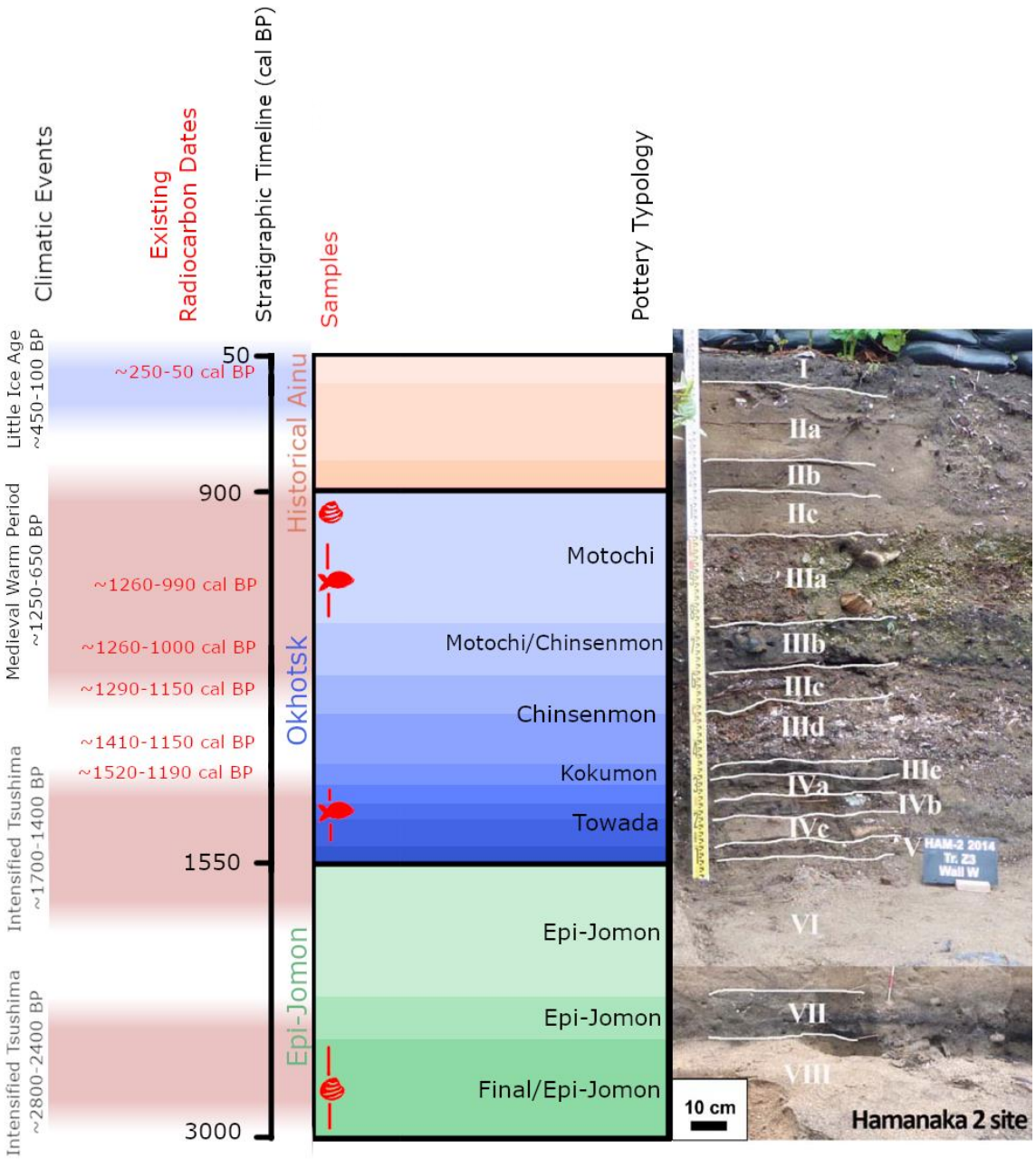


Figure 6: Stratigraphic profile for Hamanaka 2 (modified from Muller et al. 2016), showing the location of selected samples, existing chronology and key climatic events. Towada (layer IV) samples did not have enough stratigraphic information to identify a sublayer

Sample Selection and Collection

As already discussed, Japanese prehistoric archaeology has a long history of shell midden research (Oikawa 1995; Junko Habu et al. 2011; W. Edwards 2005) as well as significant climatic contrast between seasons, which is a prerequisite in order to gain subannual information for marine carbonate proxy records. Hamanaka 2 specifically was chosen as it not only benefits from a large body of previous research, but also as a site with ongoing fieldwork and pre-existing research connections to the archaeology department at the University of Oxford. This allowed personal involvement with the fieldwork happening at Hamanaka 2 as well as meaning that this thesis could build on the research of earlier projects and the established relationship that the Hokkaido University project has with the local community of Rebun Island as well as the indigenous Ainu community of Hokkaido more broadly. Palynological evidence from sediment cores at nearby Lake Kushu are also a useful local record against which new palaeoenvironmental proxies can be compared.

The archaeological samples used in this thesis (see Appendix 2) were collected during the 2018 and 2019 fieldwork seasons at Hamanaka 2. A five-week fieldtrip to Japan from July 2018 allowed for sample collection from Hamanaka 2, as well as involvement in excavations at the site during the entirety of the regular field season. This trip also included travel to the University of Hokkaido to

Table 2: Chronological model from Junno et al. (2021). Conventional chronologies from Deryugin, 2008; Ono, 2008; Tashiro, 2017; Hirasawa and Kato, 2019

Culture period	Typology	Unit	Inferred site activities	Conventional chronology	Modeled phase boundaries (mean values)	Modeled phase boundaries (2-σ range)
Historical Ainu		I	Shell midden Animal rituals	1550–1900 CE	1797–1853 CE	1750–1933 CE
Satsumon		IIa		1100–1200 CE	1773–1797 CE	1737–1852 CE
Unidentified cultural component		IIb			1744–1773 CE	1697–1800 CE
Final Okhotsk	Motochi Phase 2	IIc	Shell midden	800–900 CE	1710–1744 CE	1669–1788 CE
	Motochi Phase 1	IIIa	Animal rituals		817–1710 CE	772–1761 CE
Late Okhotsk	Chinsenmon	IIIb	Human burials	650–800 CE	749–817 CE	687–878 CE
		IIIc			712–749 CE	671–797 CE
		IIId				
Middle Okhotsk	Kokumon/Enoura B	IIIe		550–650 CE	678–712 CE	645–765 CE
		IIIf			573–678 CE	513–751 CE
Early Okhotsk	Towada Phase 2	IV	Stone working	400–550 CE	538–573 CE	445–637 CE
	Towada Phase 1	V	Food processing Animal rituals Human burials		489–538 CE	373–588 CE
Sand layer (no findings)		VI	Natural formation		258 BCE–489 CE	356 BCE–570 CE
Epi-Jomon	Unclassified Epi-Jomon pottery	VII	Stone working	350 BCE– 350 CE	276–258 BCE	362–177 BCE
Final Jomon/ Epi- Jomon	Hamanaka-Omagari, Nusamai	VIII	Food processing Animal rituals	350–1050 BCE	299–276 BCE	391–202 BCE

assess collections from Hamanaka 2 that were stored at the Centre for Ainu & Indigenous Studies (CAIS). A further two weeks in Japan in both Sapporo and Rebun Island complete the sample selection in 2019. This second trip included the collection of modern shell samples in Sapporo.

Archaeological sample collection was organised in discussion with Professor Hirofumi Kato at the University of Hokkaido, and was supported by various members of the 2018 and 2019 fieldwork teams at Hamanaka 2. Export of the archaeological and modern samples was done in communication with the Hokkaido University team, local Sapporo contacts, Oxford University and DEFRA, to ensure that all required permissions were obtained. The main requirement for this was the thorough cleaning of the modern shells from organic matter prior to export to meet DEFRA guidelines on the importing of organic materials into the UK, as well as confirming with the Japanese authorities (via Japanese colleagues) that for export purposes the 'archaeological' material was not considered a 'buried cultural property' as they were not human-made artefacts.

Initially the intention of this project had been to collect shells from throughout the site chronology to use them as a palaeoenvironmental proxy across the period from the Late Jomon to the Historical Ainu (c. 4000-80 cal. BP). On arrival at CAIS in 2018 and reviewed the samples stored from previous fieldwork seasons, it became clear that in previous years molluscs had not been routinely recorded or retained. The exception to this was an assemblage of Ainu abalone shells, which were considered evidence of ritual processing (Hirasawa and Kato 2020; H. Kato 2020). This meant that sampling was limited to the material excavated during the 2018/19 seasons, alongside any additional material stored by the field school on Rebun Island. The total accessible mollusc assemblage included 92 shells, of which 22 were the large bivalve species *Spisula sachalinensis* (Schrenk 1862), 68 were the smaller bivalve species *Glycymeris vestita*, and 2 were of the gastropod species *Neptunea arthritica*. This should not be taken as an exhaustive list of the mollusc species found at Hamanaka 2, as other smaller species or those found in smaller numbers continue to be discarded while the research team had no active interest in studying these species. This means that this thesis does not

contain discussion on the overall mollusc assemblage from Hamanaka 2, as consistent zooarchaeological recording of the species present/absent is not available from which to draw conclusions. Based on the results of this thesis, feedback was passed to the field team at Hamanaka 2 that in future seasons it would be useful to collect marine carbonate material (in particular larger molluscs and otoliths) as a valuable future resource for paleoenvironmental and dating material.

Although *G. vestita* were the more abundant species, they are also the smaller of the two bivalve species and are the main species that make up the substrate at nearby Funadomari bay. Due to this considerable local abundance of *G. vestita* shells, it is considered highly likely that at least some of the examples excavated from Hamanaka 2 are present due to natural inclusion into the sediment via strong winds/tides or movement by sea birds (Erlandson and Moss 2001; López, Penchaszadeh, and Marcomini 2008; Kimura, Yokoyama, and Hirano 2011). Furthermore, due to the small size of the species and lack of modern interest in the species as a human food source, it is also unlikely that they were collected live for dietary purposes. If they were collected by humans, it seems more likely that they were collected for decorative use, potentially due to the regular occurrence of perforations on the shell surface (Matsutaro 1970). This means that *G. vestita* shells could significantly predate the stratigraphic units in which they were found, and are therefore not good candidates for archaeologically-relevant stable isotope palaeothermometry.

By contrast, *S. sachalinensis* is a commercially important dietary resource in modern Japan, commonly found in archaeological sites in the northwest Pacific (e.g. Vladimir and Gorbunov 2004; Nikitin, Sayenko, and Lutaenko 2016; Nishimoto 1985; Amano and Vasilevski 2002) with the suggestion that they represent dietary use by coastal hunter-gatherers (Nikitin, Sayenko, and Lutaenko 2016). As this decreases the chance that the shells predate their stratigraphic unit, *Spisula sachalinensis* was chosen as the main mollusc species of interest for this thesis. Shells were visually examined for signs of predation or edge rounding in order to exclude any that evidence of non-anthropogenic deposition or having been collected from a beach context.

The *S. sachalinensis* assemblage available from Hamanaka 2 covers layer VIII (Final/Epi-Jomon), layer IIc (Final Okhotsk), and layer I (mixed topsoil/Historical Ainu) (Hirasawa 2018). Although layer I has produced some Historical Ainu evidence from Hamanaka 2, my experience excavating this layer during the 2018 field season suggested that this layer had been disturbed by modern construction activities and so it was excluded from analysis in this project. In order to augment my sample size, Professor Takao Sato, University of Keio, whose team had undertaken previous zooarchaeological research on the Hamanaka 2 material provided additional material. They confirmed that they had some Okhotsk mollusc and otolith remains which could use to complement the original selection. Unfortunately, none of the available material was *S. sachalinensis*, so otoliths of the species *Macrocephalus gadus* (Pacific cod) were chosen as an additional species of interest to provide extra samples from the Early and Final Okhotsk periods. Figure 6 shows the stratigraphic units which provided mollusc and otolith specimens for the thesis alongside the previously known radiometric and typological chronology for the site.



Figure 7: Spisula sachalinensis shells with cm scale. Image via iNaturalist.ca, (c) Kim, Hyun-Tae (CC BY-NC-SA)

The palaeoceanographic information recorded by otoliths is more complicated than that of molluscs due to the increased mobility of the species, but there is some previous literature available for the species *G. macrocephalus* which suggests that the species can be successfully used in palaeothermometry (Uzawa 1992; West, Wischniowski, and Johnston 2012; Helser, Kastelle, McKay, et al. 2018). Unlike with molluscs though, the possible migration patterns of the species should be considered, as cod can show varying migration patterns between different stocks (Moss 2011).

Via stable oxygen isotope analysis, the carbonate remains of both *S. sachalinensis* and *G. vestita,* can provide a palaeothermometric record for the Rebun Island region. On a broad regional scale, such palaeothermometry is relevant to the climatic history of Hokkaido, which compared to the southern Japanese Islands shows relatively few historical climate records due to its unique cultural history (Mikami 2008; Zaiki, Grossman, and Mikami 2012; Takarabe 2017). This has led researchers to utilise a variety of palaeoenvironmental techniques to infer the climate-history of Hokkaido, for example tree ring width data and palaeobotanical analysis, to build up a picture of Holocene climate in the regional and the extent to which it showed agreement with southern Japan and global climate trends (Buckley and Kobayashi 1990; Igarashi 2013; Müller et al. 2016). On a more explicitly archaeology level, Weber et al. (2013) lay out a foundation for the use of palaeoclimatic information when interpreting the lifeways of Holocene hunter-gatherers. They outline the role that Holocene climatic shifts may have played in the development of the cultural sequence in Hokkaido, although with the caveat that it is difficult to empirically link climate change to cultural change in the archaeological record. Within the framework of human behavioural ecology and cultural transmission theory, they suggest that there is scope to better-integrate high resolution palaeoclimatic data with hunter-gatherer ecology, without disregarding the key anthropogenic factors such as invention and decision. The high-resolution palaeothermometry provided by marine carbonate stable oxygen isotope analysis fits into this framework well, by providing an empirical climate record which can be directly connected to human ecology through the use of shell midden samples.

Before moving on, it is important to highlight some key methodological limitations of this thesis. Firstly, species-specific sclerochronological and taphonomic studies are beyond its scope due to limited time and resources. No high resolution microscopic sclerochronological analysis will be performed, meaning that growth lines are not being consistently analysed and measured under the microscope, so statistical analysis of the width of growth lines as a possible palaeoclimatic record (e.g. Marali and Schöne 2015) is not considered. As outlined by Hausmann et al. (2019), this

sacrifices some accuracy in the identification of annual and non-annual growth lines for the sake of expedience. Likewise, although specimens will be checked macroscopically for signs of taphonomic degradation such as charring or rolled/smoothed edges, a full taphonomic analysis will not be undertaken, and there will be no microscopic assessment to check for less obvious taphonomic damage. Full taphonomic analysis of the specimens used in this project could be undertaken in future, which may provide useful further information to contextualise the conclusions reached in this thesis.

Small sample size is a further limitation of this thesis, which was unfortunately unavoidable due to the lack of consistent collection of mollusc remains from Hamanaka 2 prior to the 2018 field season. As adjusted collection methods – in which large, likely dietary, species of molluscs are retained during excavation – have been recommended to the fieldwork as a result of this thesis, it is hoped that in future excavation seasons the available sample size will be increased and that there may then be scope to expand this project by the addition of further samples. The last limitation to highlight is the lack of in-situ environmental data for Rebun Island. Due to this lack of in-situ data, this project relies on local annual averages for the ocean surrounding Rebun island as measured by satellite infra-red measurements and buoy and ship measurements. These provide information on annual temperature trends in the modern region, but do not give specific data for Hamanaka Bay. In future, in-situ seawater measurements from Hamanaka Bay could provide better baseline measures of sea surface temperature, salinity and $\delta^{18}O$ to contextualise archaeological data. In particular, local salinity and seawater $\delta^{18}O$ measurements would be useful to gain an improved understanding of the freshwater input to Hamanaka Bay, and whether this is expected to significantly influence the $\delta^{18}O$ range expected for locally-collected molluscs.

Species of Interest

The archaeological material used in this thesis come from two species: the marine bivalve *Spisula sachalinensis*, and the Pacific Cod *Gadus macrocephalus*. Calcium carbonate structures are targeted

for analysis, using the shell of *S. sachalinensis*, and the sagittal otolith of *G. macrocephalus*. These are both incrementally-grown structures, and before we discuss these species in more details it is useful to outline how these structures grow and introduce how the growth lines and increments within these structures are formed.

In molluscs, shell material is composed of mostly inorganic calcium carbonate (aragonite and/or calcite), along with organic matrices (Suzuki and Nagasawa 2013). In the 1970s, Richard Lutz and colleagues proposed the first cohesive theory for the incremental formation of shell growth lines (Lutz and Rhoads 1977; Lutz and Rhoads 1980). They suggested that during aerobic respiration in molluscs shells – i.e. while a bivalve species is open at high tide – calcium carbonate (relatively) rich in organics is deposited as an increment of shell growth. By contrast, while a valve is closed (at low tide), conditions become increasingly anaerobic and, in order to neutralise acids produced as a by-product of anaerobic respiration, a period of decalcification occurs. This frees organic material back into the shell's mantle and pallial fluids, which is subsequently reincorporated into the shell structure once aerobic respiration resumes. This process results in circadian cycles of microstructural shell growth which relate to lunar and solar cycles (Lutz and Rhoads 1977). Beyond these microstructural rhythms, there is also annual periodicity in shell growth, with alternating growth lines and increments (Jones 1980). The structural composition of these layers of shell growth varies by species, with the timing of the annual changes between growth increment and growth line formation being triggered by the spawning season or a shift to unfavourable environmental conditions such as temperature extremes or low pH (Jones 1980; Schöne 2008; Butler et al. 2013; Córdova-Rodríguez et al. 2022).

Otoliths, like marine mollusc shells, are incrementally-growth structures composed largely of calcium carbonate. Otoliths are usually precipitated as aragonite, although calcite and vaterite can be present in particular species or conditions, for example in the case of sturgeon or paddlefish (Wood et al. 2022). In the case of otoliths, their function as mechano-receptors mean that growth is

regulated by the anatomy and mechanics of the inner-ear, in which they are situated (Morales-Nin 2000). As with mollusc shell, otoliths form alternating layers of calcium carbonate crystal structures and associated organic matrices on a circadian rhythm (Morales-Nin 2000). Microstructural increments in otoliths are formed due to daily changes in the protein content of the macula, which is the source of protein precipitated in otolith carbonate (Gauldie and Nelson 1988; Morales-Nin 2000). Beyond daily rhythms, otoliths form growth lines (checks) in response to environmental or life history changes, for example migration in the water column, new habitats, spawning, or deteriorated environmental conditions (Pannella 1971; Karakiri and von Westernhagen 1989; Katayama 2018; Jessop 2021). External conditions such as temperature, salinity and pH also effect the growth rate, meaning that as in molluscs, measurements of increment width over the life history of an individual can serve as a useful proxy for environmental conditions (Vieira et al. 2020).

Spisula sachalinensis (Sakhalin surf clam)

Spisula sachalinensis (Schrenk 1862, Figure 7) is a large marine bivalve which inhabits shallow coastal waters around the Northwest Pacific, including northern Japan, the Russian Far East and Korea (Figure 8). The species is also known as Ubagai and Hokkigai in Japanese, and its synonymised names include: *Mactra sachalinensis, Pseudocardium sachalinense, Mactra dunkeri, Mactra lühdorfii, Mactra sybyllae,* and *Trigonella straminea* (MolluscaBase 2022). In the Ainu language the species is known as 'poksey' or 'tutterep' (Martineau 2012). The species is commercially important in modern Japan, with its distinct pink muscle served as a popular seafood dish. As such, it has been the subject of numerous studies in Japan concerning its nutrition, growth and spawning (Golikov and Scarlato 1970; K. Sasaki 1981; Lee, Chang, and Park 1996; Sakurai, Seto, and Nakao 1996; e.g. S. Sasaki and Ohta 1999), but

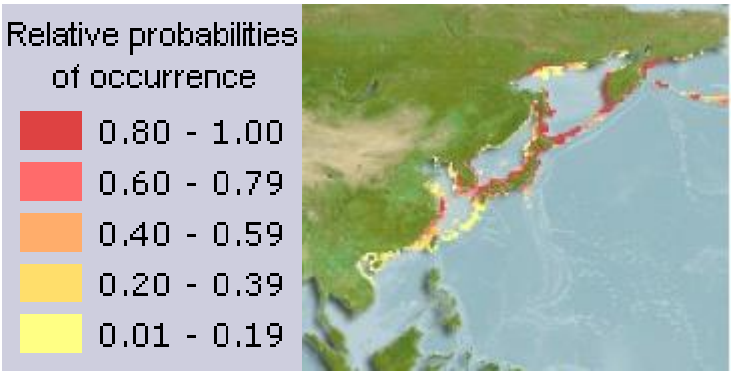


Figure 8: Native distribution of S. sachalinensis. *(AquaMaps 2019)*

relatively little previous research pertaining to its potential as a palaeothermometer (Khim, Woo, and Je 2000; Mann et al. 2013).

The shells of *S. sachalinensis* are fully aragonitic ($CaCO_3$), and are composed of alternating layers of nacreous and prismatic growth, in which chemical composition is the same but aragonite crystals are differently oriented (Y. Kato and Hamai 1975). In the nacreous layer aragonite is formed in 'plates', while the prismatic layer is comprised of larger aragonite 'prisms' (Heuer et al. 2001). Nacreous layers of shell growth represent periods of slow/ceased growth, which can be triggered by seasonal peaks/troughs in SST (sea surface temperature), predation attempts, storm disturbances and the species' reproductive cycle (Yamamoto 1947; Y. Kato and Hamai 1975; K. Sasaki 1981). An outer protein layer – the periostracum – is formed around the calcareous shell (Y. Kato and Hamai 1975), although in archaeological shells this outer layer is usually worn off via post-depositional taphonomic processes.

S. sachalinensis lives in sandy substrates at a depth range of 1-15 m (Golikov and Scarlato 1970; K. Sasaki 1989; S. Sasaki and Ohta 1999). Shells can reach a maximum length of up to ~10 cm, with the majority of fast growth occurring in the first eight of life, after which annual shell deposition is negligible (K. Sasaki 1981). In Hokkaido the species spawns in spring/early summer, with rapid shell growth during this period (Y. Kato and Hamai 1975). Kato and Hamai (1975) assert that shell growth shows good fitness with Gompertz' (1825) growth model.

Gadus macrocephalus (Pacific cod)

The Pacific cod is a cold water demersal/benthic fish (Spies and Weingartner 2007; West, Wischniowski, and Johnston 2012), which lives throughout the northern Pacific continental shelf (Figure 9). This species grows up to a maximum recorded length of 122 cm, and lives a maximum of 25 years (Chen 2014), although ages up to 13 years are more common (Spies and Weingartner 2007). It is predominantly a vertically migratory species, coming to shore seasonally for feeding

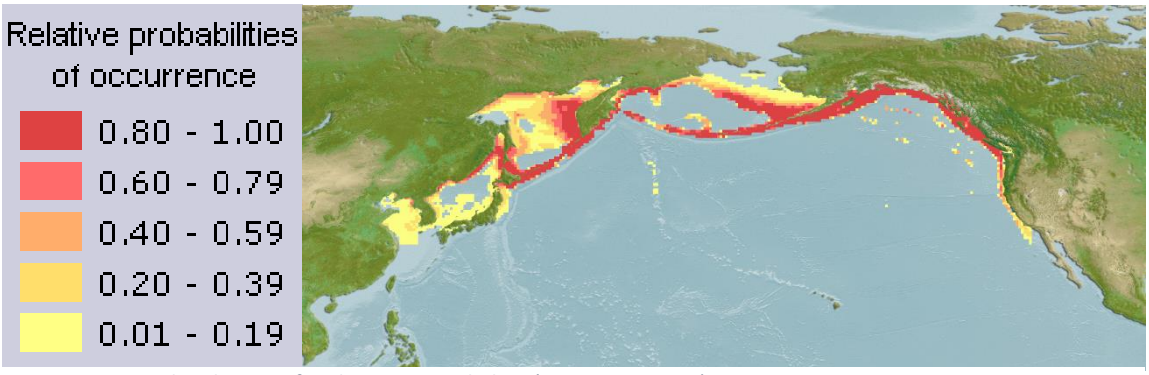


Figure 9: Native distribution of Gadus macrocephalus. *(AquaMaps 2019)*

during the warm season (Savin 2008; Savin and Kalchugin 2011; West, Wischniowski, and Johnston 2012). Their depth ranges between 25-500 m (West, Wischniowski, and Johnston 2012). The majority of individuals reach sexual maturity by four years, and spawning happens in deeper waters during the cold season in water temperatures between 0-12 °C (Spies and Weingartner 2007; West, Wischniowski, and Johnston 2012; Chen 2014). In Hokkaido and the surrounding waters, this is usually between December and March (Mishima 1984). In the warmer season the fish move into shallower coastal waters to feed, and are opportunistic feeders with a diet including smaller fish, crustaceans and small cephalopods (Yamamura, Watanabe, and Shimazaki 1993).

Otoliths are small incrementally grown carbonate structures which grow in the inner ear of fish. In total a fish will have three pairs of otoliths, although the sagittal is by far the largest and is therefore used preferentially for research purposes. It is also much more common for sagittal otoliths to be recovered from archaeological (or palaeontological) contexts due to their larger size. Pacific cod produce sagittal otoliths (Figure 10) of up to ~2 cm in length, providing enough

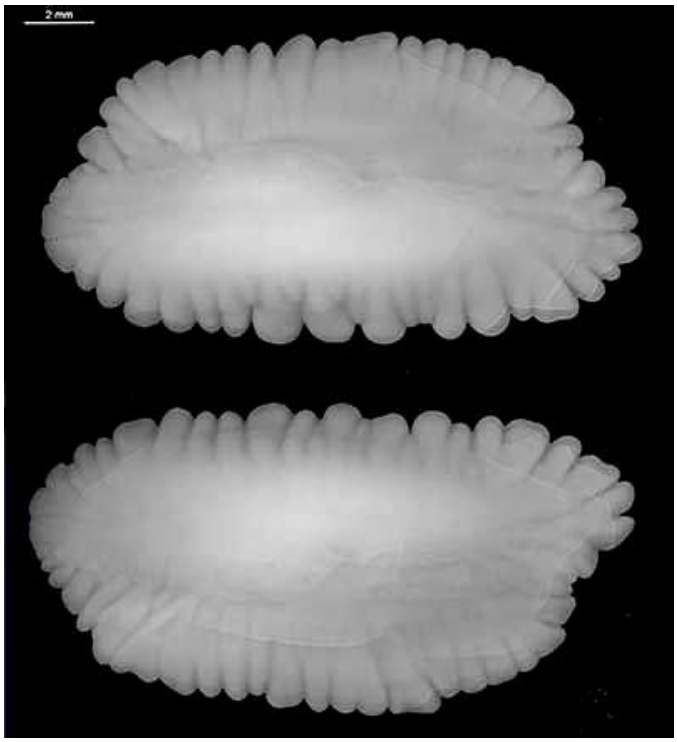


Figure 10: Pair of sagittal otoliths from G. macrocephalus *(Pacific cod) with 2 mm scale. Image from: Alaska Fisheries Science Center Quarterly Report, April 2015*

material for incremental milling across a transect to target life history changes. Like molluscs, otoliths are composed of calcium carbonate. They are typicially c. 95 wt% aragonite, 4 wt% organic matter and <1 wt% trace elements (Iizuka 2012).

Due to the increased mobility of fish, the palaeoceanographic information recorded by otoliths is more complex than for most marine molluscs. Nonetheless, there is some previous literature available for the species *G. macrocephalus* which suggests that the species can be successfully used in palaeothermometry (Uzawa 1992; West, Wischniowski, and Johnston 2012; Helser, Kastelle, McKay, et al. 2018). Trace element analysis and stable isotope analysis are the two main methodologies used for otolith palaeothermometry, though the field is still relatively young, with meta-analysis by Campana (2005) showing that by the early 21st century studies aimed at palaeoenvironmental reconstruction made up less than 1% of total otolith research papers. West et al. (2012) provides a useful summary of palaeothermometry using oxygen stable isotope analysis on Pacific cod otoliths, concluding that they provide a useful record of past ocean temperature. Helser et al. (2018) also used stable oxygen isotope analysis on Pacific cod in an archaeological context, and other researchers have used similar techniques on otoliths of the species' Atlantic cousin *G. morhua* (Radtke et al. 1996; Hufthammer et al. 2010; Ritchie, Folkvord, and Hufthammer 2013; Edvardsson et al. 2019). Otolith shell aragonite is expected to precipitate in equilibrium with the isotopic composition of surrounding water, and $\delta^{18}O$ is inversely correlated with water temperature (Radtke 1983; Thorrold et al. 1997; Kastelle et al. 2017; Helser, Kastelle, McKay, et al. 2018). There has also been recent research exploring the potential archaeological utility of strontium stable isotope analysis on cod otoliths, used to determine fishing location between isotopically distinct water sources (Glykou et al. 2021). It has been shown that cod migration patterns can vary according to stock groups (Moss 2011), so the ability to distinguish movement between different regions isotopically is particularly important.

In the context of this thesis, stable isotope anlaysis of Pacific cod otoliths helps reduce chronological gaps in the sequence by providing additional marine carbonate material from the Early and Final Okhotsk deposits. While the basic principles of the methodology and the relationship between $\delta^{18}O_{carbonate}$ (the oxygen isotope ratio of the carbonate material) and water temperature are the same in both species, the records produced by each should not be directly compared owing to the differences in the species' ecology. As already outlined, Pacific cod are primarily a deep water demersal species, while surf clams occupy the shallow littoral zone. This means that the results from each species will need to be interpreted with respect to their specific ecological niche, and how that niche relates to broader oceanorgaphic and atmospheric conditions that may have impacted coastal hunter-gatherer behaviours.

Research Questions

The project's initial aim was to investigate season of collection, but the specific biological histories of these taxa mean they are not well suited. Instead, the project has shifted to focus more on these resources as archaeologically relevant environmental records. Of course, this comes with its own analytical and interpretational challenges. In order to overcome these issues, it was necessary to establish techniques for sampling and preparation at the Oxford Research Laboratory for Archaeology and the History of Art, locate modern specimens of the target species, and use the modern data to validate archaeological isotopic sequences. The overarching research questions are presented below, beginning with methodological concerns and then moving onto wider-scale archaeological questions.

1. Do modern examples of the bivalve *Spisula sachalinensis* reliably record sea surface temperature?

Before palaeoclimatic analysis of archaeological *S. sachalinensis*, it is important to validate the species as an ocean temperature proxy. To answer this question, modern examples of the species

were sourced from a known fishing location, where the stable oxygen isotope values could be compared with known sea surface temperatures. The results are presented in Paper 1.

2. Can *S. sachalinensis* provide a marine palaeotemperature record for the northwest Pacific, and more specifically for northern Japan?

Based on the outcome of the modern validation study outlined under question 1, it is then necessary to judge the utility of *S. sachalinensis* for palaeotemperature studies. There are specific concerns affecting palaeothermometry that should be considered and addressed, most importantly our ability to accurately determine ancient $\delta^{18}O_{seawater}$ (the oxygen isotope ratio of seawater). The preservation of the shell in the archaeological or palaeontological record should also be discussed, including the potential for post-depositional diagenetic recrystallisation of shell aragonite and ways this can be tested. Although aragonite is metastable, in certain conditions such as heating/cooking or ground-water percolation, primary aragonite can recrystallise into secondary calcite (Andrus and Crowe 2002; Prendergast 2014; Zhang et al. 2014; Larsen 2015). As a result, the isotope composition of the carbonate will no longer reflect the palaeoenvironmental conditions of its original formation. It is therefore key to test that the aragonite being sampled and measured is pristine and unaltered.

3. Does sample preparation and sampling technique have an impact on marine carbonate stable isotope palaeothermometry?

This is another methodological question which became increasingly important following the results of the modern validation study on *S. sachalinensis* in Paper 1. To answer this question, two sampling methods – hand drilling and micromilling – are compared directly in Paper 2. The results of this comparison are relevant not only to this thesis and the species *S. sachalinensis* in particular, but are also more widely applicable to stable isotope sampling on other carbonate materials, including other species of shell, otoliths and speleothems.

4. What cultural or palaeoenvironmental information can be gained from stable oxygen and carbon isotope analysis of Pacific cod otoliths from Hamanaka 2?

As described in above, the marine niche of Pacific cod is more variable than that of *S. sachalinensis*, and the relationship between stable isotope results and archaeologically-relevant climate is more difficult to establish. As part of the discussions in this thesis key ecological information on Pacific cod will be summarised, and the extent to which stable isotope results from these otoliths can inform our archaeological understanding will be assessed. It will also be important to discuss the extent to which results can be interpreted alongside those from marine bivalves.

5. How can marine resources from Hamanaka 2 be integrated in the site's chronological model?

At Hamanaka 2, ceramic typology provides a relative chronological sequence, giving a cultural attribution for each stratigraphic layer, and existing radiometric models (Müller et al. 2016; Leipe et al. 2017; Miyata et al. 2016; Junno et al. 2021). However, the relative chronology of particular shell specimens within each unit is unknown, and marine dates have been excluded from previous modelling owing to uncertainty over the regional marine reservoir effect (Junno et al. 2021). In order to integrate marine samples into the chronological modelling for the site, new marine reservoir effect ΔR values will need to be calculated to account for variation in ΔR between different time periods and different marine habitats.

In order to further investigate the extent to which marine resources can be a chronological aid, this project will also test whether paired dates on incrementally-grown marine carbonates could inform Bayesian modelling to improve radiocarbon chronology. This idea is based on similar paired dating used to good effect on wooden artefacts (Brock et al., 2012), and relies on a model in which two dates (from the beginning and end of a shell's life) are constrained by an intervening age gap estimated via counting of the growth increments. This is novel approach using marine carbonates, although their incremental growth should make them a suitable candidate.

6. Can environmental change be linked to cultural change at Hamanaka 2?

This is a primary archaeological question of interest in this thesis, which many of the methodological questions above work to support. By employing high-resolution subannual $\delta^{18}O$ analyses of marine carbonates from the site, the project aims to estimate past sea surface temperatures (SST) and detect local oceanographic and climatic shifts. With the existing chronological information available (Miyata et al. 2016; Müller et al. 2016; Leipe et al. 2017; Junno et al. 2021) and the addition of new marine radiocarbon dating, it may be possible to correlate proxy palaeotemperature records with the cultural sequence at Hamanaka 2 and investigate how environmental change may have impacted human behaviour, and vice versa.

7. Do proxy palaeotemperature records from marine carbonates at Hamanaka fit with pre-existing regional proxies, and with historical records from southern Japan?

At the wider scale, this project will also assess the extent to which local archaeologically-derived climate and oceanographic records from the far north of Japan match with historical evidence from the south. As already discussed, Hokkaido was not colonised until the late 19th century, and primary occupation by hunter-gatherer groups until this point means that fewer historical climate records are available. This means that much of our understanding of late Holocene climate in Japan as a whole is biased towards Honshu and the southern islands. The provision of new Hokkaido-specific palaeothermometry data will help to fill this gap, as well as providing an opportunity to assess the extent to which climate in Honshu and Hokkaido diverged during this period.

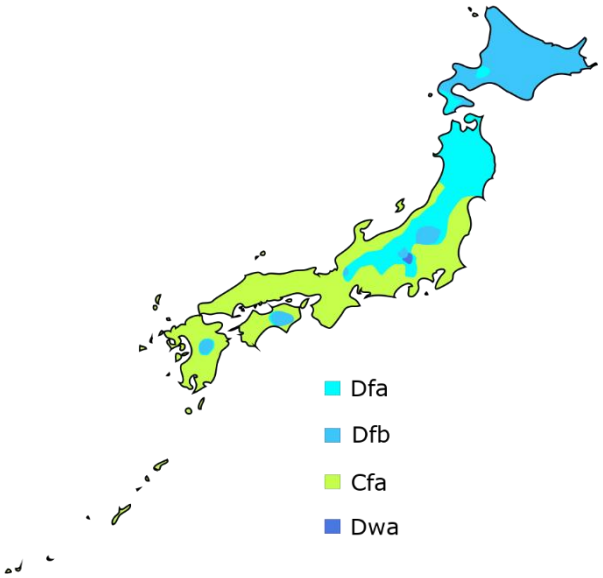


Figure 11: Koppen-Geiger climate map of Japan. Edited from image by Ali Zifan via Wikimedia Commons

Climate and Environment in Japan

The Japanese archipelago is situated in East Asia, spanning from the East China Sea at its most southwestern point to the Sea of Okhotsk in the northeast. The large geographic range of Japan (24° to 46° latitudinally, 123° to 146° longitudinally) encompasses a variety of different climatic and ecological niches, and the presence of several major ocean currents around the archipelago produces variation in oceanographic conditions. While this thesis focuses on palaeoclimate, in order to address questions of palaeoclimate it is important to first understand the modern climatic context. The focus will be on the north island of Hokkaido, but conditions in central and southern Japan will also be briefly discussed before moving on to summarise the current state of palaeoenvironmental reconstruction in northern Japan.

Modern Japan

Hokkaido is the northern-most major island in the Japanese archipelago, and at 83,453.6 km2 also forms the country's largest prefecture in terms of area. According to the Köppen-Geiger climate classification system (Peel, Finlayson, and McMahon 2007), most of Hokkaido falls into the `Dfb' climate, with small pockets in the southwest in the `Dfa' (Figure 11). These climatic categories are described in **Error! Reference source not found.**, which show that in general the Hokkaido climate can be classified as cool, with a warm summer and no dry season. Hokkaido's winters are influenced by the

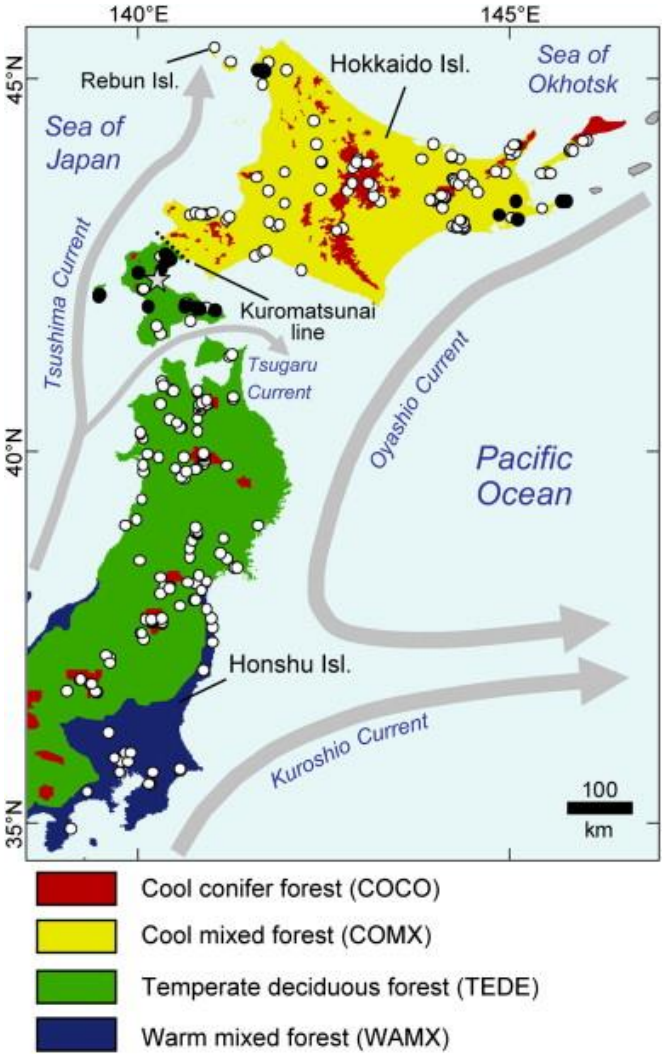


Figure 12: Northern Japanese biomes and currents. Reproduced from Leipe et al. (2013)

East Asian Winter Monsoon (EAWM) air currents, which bring cold air from the north/northwest (Abe et al. 2016), and summer are influenced by the warm, wet conditions of the East Asian Summer Monsoon (EASM) (McColl 2016).

In the rest of Japan, the Köppen-Geiger system classifies climate as mostly 'Dfa' (cold, no dry season, hot summer) or 'Cfa' (temperate, no dry season, hot summer). As with Hokkaido, areas of high elevation diverge from this trend showing both 'Dfb' and 'Dwa' (fig. 1). The main difference compared to Hokkaido is in the winter temperatures, which do not generally reach below freezing in southern Honshu and the Ryukyu Islands (Figure 11, **Error! Reference source not found.**).

Table 3: Descriptions and criteria for selected Koppen-Geiger identifiers, as per Peel et al. (2007)

Köppen-Geiger Identifier	**Description**	**Criteria***
Dfb	Cold, without dry season, warm summer	• $T_{hot}>10$ & $T_{cold}\leq 0$ • Not (Ds) or (Dw) • Not (a) & $T_{mon10}\geq 4$
Dfa	Cold, without dry season, hot summer	• $T_{hot}>10$ & $T_{cold}\leq 0$ • Not ($P_{sdry}<40$ & $P_{sdry}<P_{wwet}/3$) or ($P_{wdry}<P_{swet}/10$) • $T_{hot}\geq 22$
Cfa	Temperate, without dry season, hot summer	• $T_{hot}>10$ & $0<T_{cold}<18$ • Not ($P_{sdry}<40$ & $P_{sdry}<P_{wwet}/3$) or ($P_{wdry}<P_{swet}/10$) • $T_{hot}\geq 22$
Dwa	Cold, dry winter, hot summer	• $T_{hot}>10$ & $T_{cold}\leq 0$ • $P_{wdry}<P_{swet}/10$ • $T_{hot}\geq 22$

***** T_{hot} = temperature of the hottest month, T_{cold} = temperature of the coldest month, T_{mon10} = number of months where temperature is above 10, P_{wdry} = precipitation of the driest month in winter, P_{swet} = precipitation of the wettest month in summer, P_{wwet} = precipitation of the wettest month in winter, P_{sdry} = precipitation of the driest month in summer

In terms of vegetation, Japan is an exceptionally forested country. Figure 12 shows an overview of the biomes from Hokkaido and northeast Honshu. Cool mixed forest is the most abundant on Hokkaido, dominated by *Abies sachalinensis* and *Picea jezoensis* (Leipe et al. 2013). As evident from

figure 12, there is a distinct vegetation shift to temperate deciduous forest in the southwest of Hokkaido, which is dominated by *Fagus crenata* (Leipe et al. 2013). This shift correlates with climatic zoning from figure 11, with temperate forest present in Dfb areas and cool mixed forest present in Dfa areas. This climatic and vegetational divided by what is known as the 'Kuromatsumai Line' as shown in figure 12 (Crawford and Bleed 1998; Leipe et al. 2013). The third vegetational biome in Hokkaido is the cool conifer forest, located mainly in areas of higher elevation and comprises mostly of *P. jezoensis*, *P. glehnii* and *A. sachalinensis* (Leipe et al. 2013). Throughout the rest of Japan, the predominant vegetation is the warm mixed forest visible at the southernmost point of figure 12. This extends throughout the lower elevations of Honshu, Shikoku and Kyushu, with the addition of more temperate deciduous forest in the mountains (Takahara et al. 2000).

Climatic differences, along with the obstacle posed by the Tsugaru Strait (which separates Hokkaido and Honshu), contribute to differences between the faunal compositions on Hokkaido and Honshu. These differences were first recognised by Thomas Blakiston in the late 19th century. Since then, the biogeographical boundary between the two islands has been known as the Blakiston's Line. To the south of this line the fauna on Honshu includes the Japanese macaque (*Macaca fuscata*), Asiatic black bear (*Ursus thibetanus*), pheasant (*Phasianus versicolor*), Japanese serow (*Capricornis crispus*) and Japanese boar (*Sus scrofa leucomystax*). North of this line on Hokkaido species include the brown bear (*Ursus arctos*), northern fox (*Vulpes vulpes schrencki*), red squirrel (*Sciurus vulgaris*) and in the past the now-extinct Hokkaido wolf (*Canis lupus hattai*) (Ohnuki-Tierney 1976; Motokawa and Kajihara 2017).

The Japanese archipelago is surrounded by two major bodies of water: the Sea of Japan to the west and the Pacific Ocean to the east. Figure 13 shows the bathymetric context of Japan, as well as the

major ocean currents in surrounding waters. The most important currents affecting Hokkaido are the Tsushima and Oyashio currents. Tsushima is a warm water current, which flows from the East China Sea into the Sea of Japan around the west coast of Japan. The warm-water Soya current branches from the Tsushima current and flows around Hokkaido's north coast, primarily influencing shallow waters (Matsuyama et al. 2006). The Oyashio is a cold water current that flows down the northeast coast of Japan. In combination, these create a temperature gradient in sea temperature (and in turn terrestrial temperature) from the warmer west to the cooler east (Abe et al. 2016). The Tsushima current prevents the formation of sea ice around western Hokkaido (Nikolaeva and Schebakova 1990), but also encourages evaporation during winter monsoon winds resulting in high snowfall in the region (Kuroyanagi et al. 2006; Abe et al. 2016; Müller et al. 2016).

Seasonality in ocean temperature around Hokkaido is influenced by waxing and waning ocean currents. For the Tsushima and Soya currents, minimum transport volume occurs in the winter (Toba

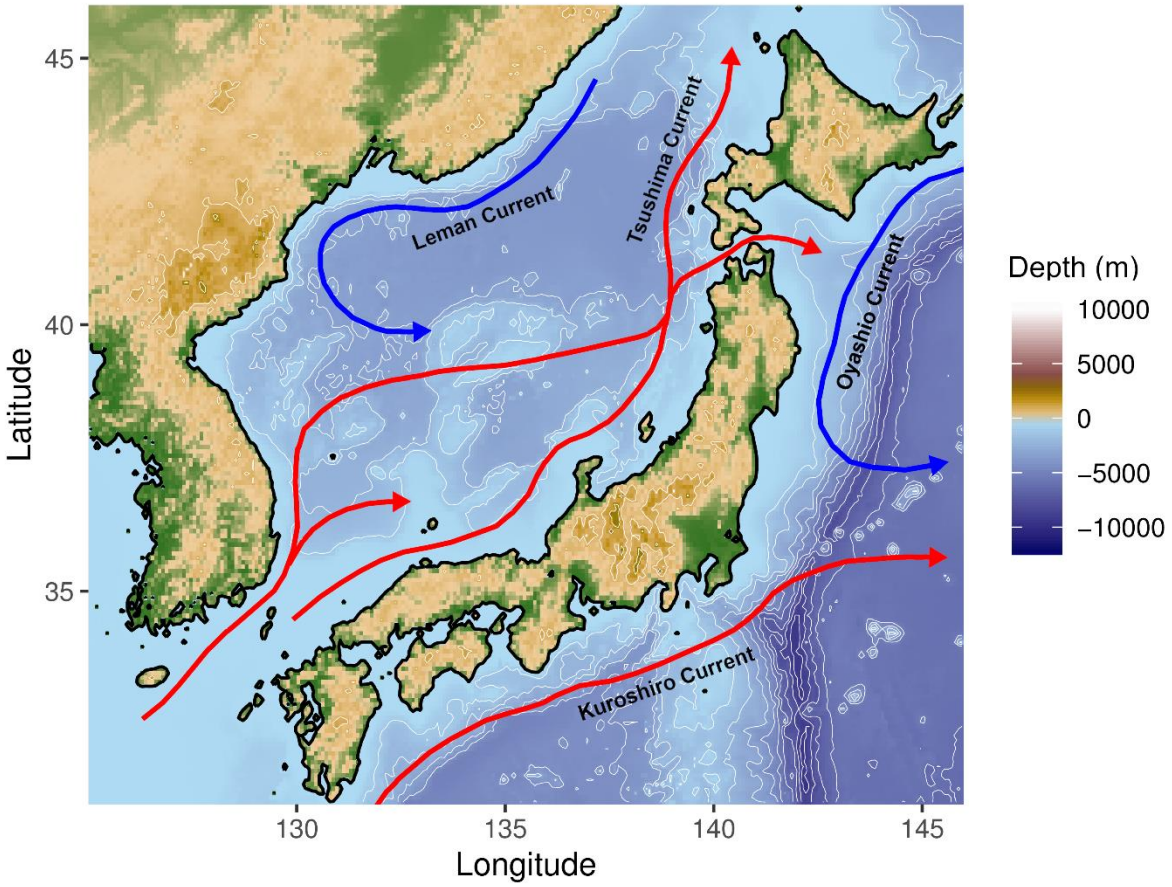


Figure 13: Bathymetric map of Japan showing major ocean currents. Bathymetric data from NOAA (National Oceanic and Atmospheric Administration)

et al. 1982; Ebuchi et al. 2006) and maximum in the summer, perhaps due to additional input from the southern warm Kuroshio current (Isobe 1999). Seasonal currents and sea surface temperature (SST) are strongly interconnected with atmospheric climate. Atmospheric conditions are a primary driver of SST (Imada et al. 2017), while higher (lower) SSTs in the Sea of Japan increase (decrease) wind speed and evaporation, driving regional precipitation especially during the winter monsoon season (Hirose and Fukudome 2006; Takano, Tachibana, and Iwamoto 2008; Seo, Kwon, and Park 2013; Abe et al. 2016).

In the modern context, SST is recorded in a number of ways, including direct measurements from coastal weather stations, drifting and stationary buoys, and indirect satellite measurements. Satellite data is the most widely used measurement, as it does not depend on the limited coverage of ships, buoys and weather stations (Maurer 2002). Infrared satellite data measures the skin surface temperature, which is the temperature of the uppermost 10 μm of water, via either thermal or passive microwave radiometry (Njoku and Brown 1993; Maurer 2002; Wick 2002). Blended satellite datasets, including the Level 4 Physical Oceanography Distributed Active Archive Centre (PODAAC) dataset used in Paper 1, provide an estimate of foundation temperature, which is 'defined as the temperature of the water column just below the diurnal warm layer' (Marullo et al. 2016 p. 8357) by combining infrared measurements with in-situ ship and buoy data.

Palaeoclimatic Reconstructions

For much of Japan, a strong corpus of historical documentary sources exist from which historical climate information can be extrapolated. A combination of recorded cherry blossom flowering dates, lake-freezing dates and diary records can be used to construct a picture of historical climatic variation in Japan (Mikami 2008; Zaiki, Grossman, and Mikami 2012). Records of spring blossoming dates provide a particularly long-lived climatic proxy, with records dating back to 1001 AD which can be used to estimate March temperatures (Aono and Omoto 1994). Using these proxies, evidence of the Medieval Warm Period and Little Ice Age have been recorded from Honshu (Aono and Omoto

1994). While useful, these records unfortunately have a strong bias towards Honshu and southern Japan, and in any case only cover the latest part of the Holocene. The lack of historical documentation pertaining to Hokkaido is unsurprising, given that Hokkaido (then known as Ezo) was not colonised and incorporated into the Japanese state until the Meiji restoration in 1868.

In the absence of historical documentation, we must rely on other palaeoenvironmental proxies to form an understanding of Hokkaido's climate during the mid-late Holocene. Figures 14 and 15 illustrate palaeoenvironmental proxies from lake Toyoni in Hokkaido (Figure 14), and the northwest Pacific and beyond (Figure 15). Broadly speaking, major international-scale climatic trends and events such as the Mediaeval Warm Period (MWP) and Little Ice Age (LIA) are visible in records from Hokkaido and the rest of Japan, as illustrated by Figure 14. Pollen analysis from central Honshu places the MWP in Japan at ~700-1300 AD (Y. Sakaguchi 1976; Y. Sakaguchi 1983; Batten 2008). Using sediment core Inc/Coh, Si/Rb and C/N ratios from lake Toyoni, southern Hokkaido, McColl (2016) shows increased organic input and high productivity from ~1000-1300 AD. This suggests that the peak of the MWP period may have been felt slightly later in Hokkaido than southern Japan. McColl's work at lake Toyoni places the Little Ice Age (LIA), another major global climate event, at 1300-1850 AD. This palaeoenvironmental archive from lake Toyoni also provides evidence for a cold period between 1110-1180 AD and a warmer period from 1200-1266 AD (McColl 2016).

As already discussed with respect to the modern climate in Hokkaido, the EASM and EAWM both have a strong influence on regional seasonal climate. The westerly winds and the EAWM bring cold, dry air across Hokkaido (Fukusawa 1999; McColl 2016), and intensification of the EAWM is associated with the climate deterioration of the LIA period (McColl 2016). Weakening of both the summer and winter monsoon during the late Holocene has been recorded from multiple environmental proxies (e.g. Hu et al. 2008; Steinke et al. 2011), related to a decrease in insolation anomalies during this period (Leipe et al. 2013; Leipe et al. 2018). However, McColl (2016) outlines significant inconsistencies in proxies used to infer strengthening/weakening of the EAWM and

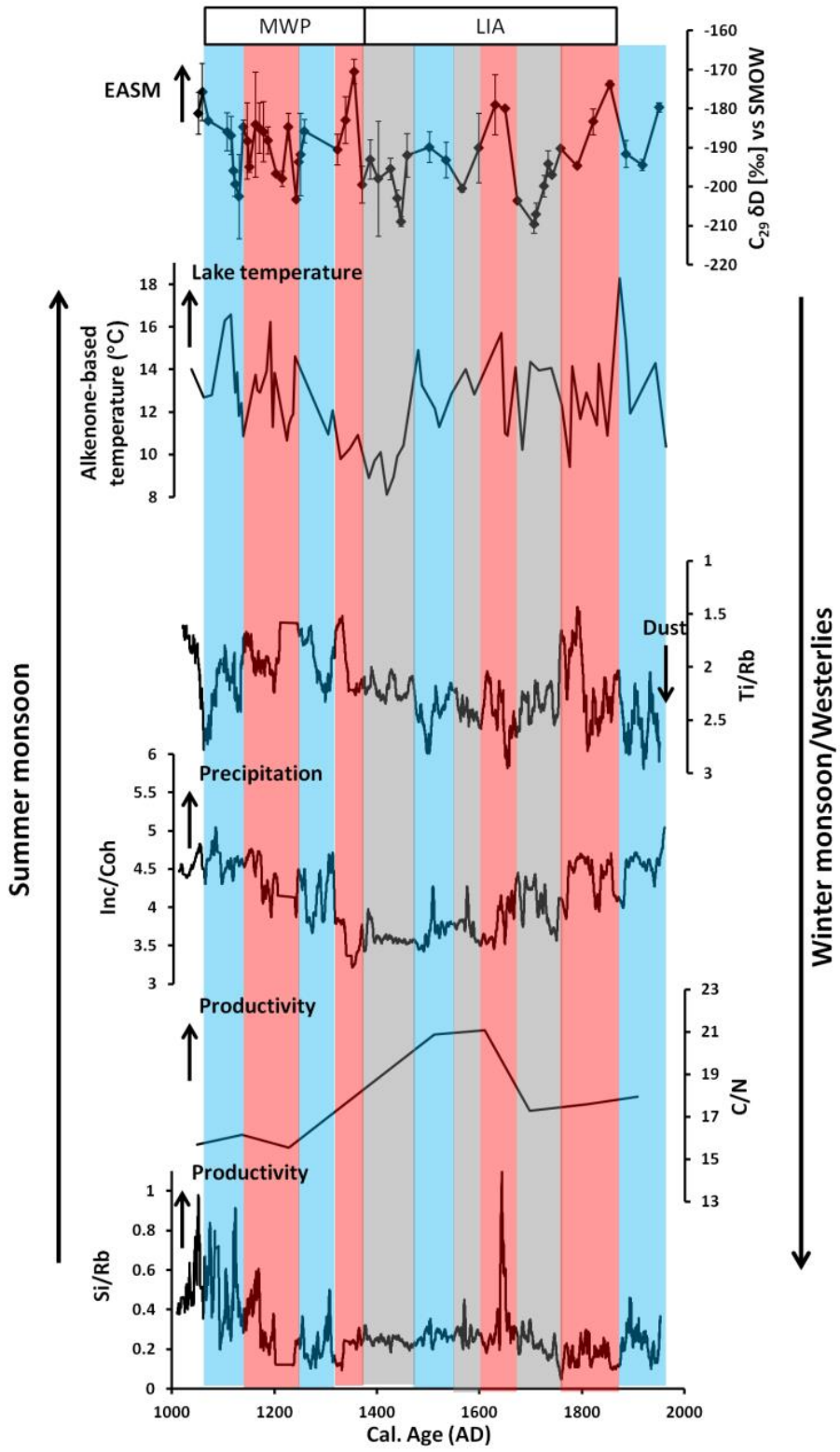


Figure 14: Multi-proxy climate reconstructions from Lake Toyoni over the past 1000 years. From top to bottom; δDHPW as a proxy for temperature and source of precipitation, alkenones as a LST proxy, Ti/Rb as an aeolian input proxy, Inc/Coh ratio as a precipitation proxy, C/N ratio and Si/Rb ratio as productivity proxies. Higher values on graphs indicate a stronger EASM (highlighted in red) and lower values indicate a stronger EAWM (highlighted in grey) and/or Westerlies input (highlighted in blue). Image reproduced from McColl (2016).

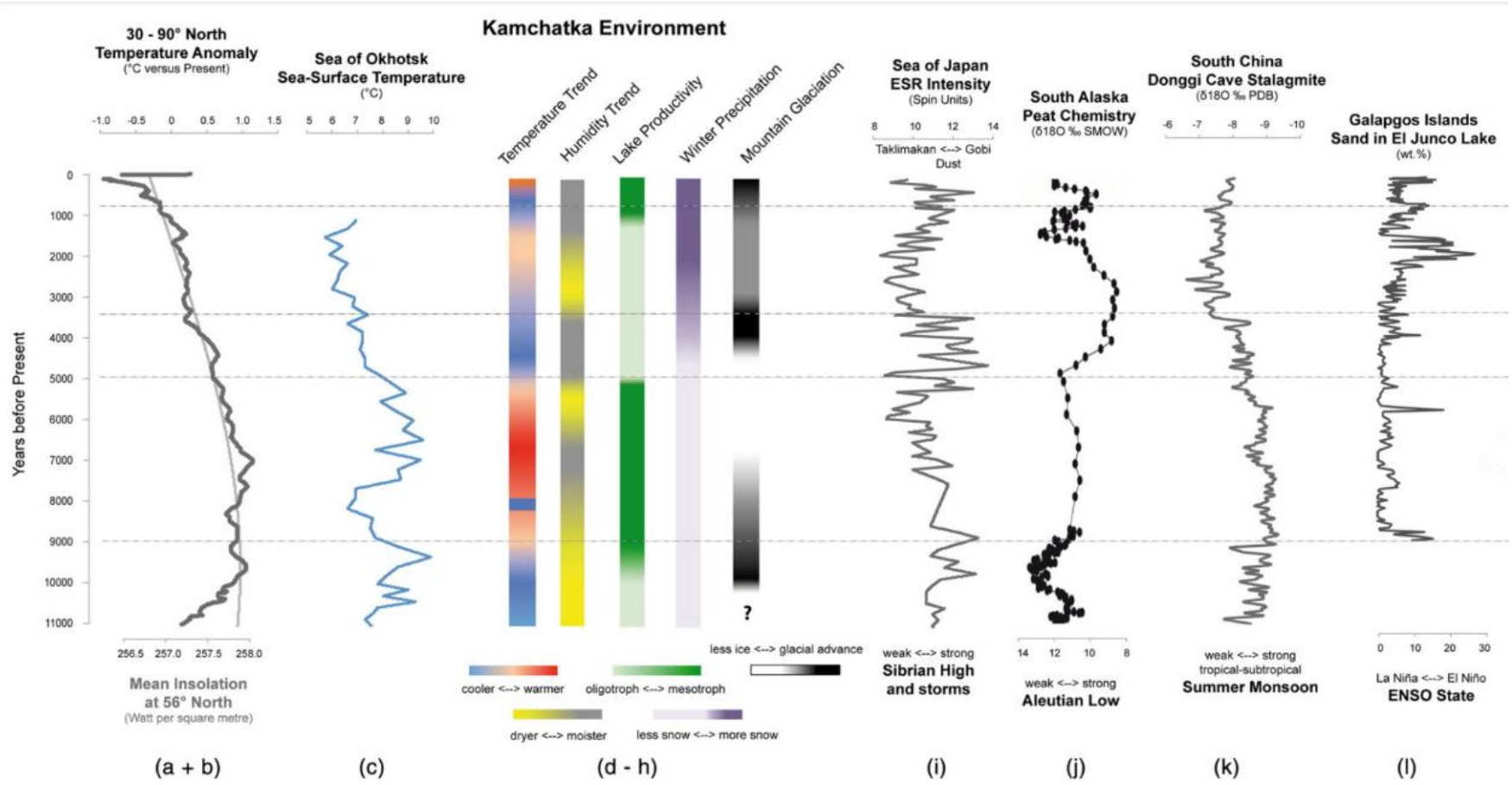


Figure 15: Holocene palaeoenvironmental proxies: (a) mean Holocene temperature anomalies across the mid- to high latitudes of the northern hemisphere (Marcott et al., 2013) and its relation to, (b) climate forcing by mean annual insolation changes at 56°N (Laskar et al., 2004); (c) alkenone-based sea-surface temperature reconstructions in the Sea of Okhotsk ate Site LV29-114-3 (Max et al., 2012); (d) temperature trends, and (e) humidity trends, and (f) changes in lake trophy inferred from lake records of Kamchatka (Andrén et al., 2015, Dirksen et al., 2015, Hoff et al., 2015, Self et al., 2015, Solovieva et al., 2015); (g) trends in winter precipitation inferred from vegetation dynamics and stable isotope signals in lake records of Kamchatka (Hammarlund et al., 2015, Meyer et al., 2015); (h) timing of mountain glaciation on Kamchatka (Barr and Solomina, 2014, Meyer et al., 2015); (i) source signal of aeolian silt-sized quartz in the Japan Sea revealed by electron spin resonance, as a proxy of atmospheric circulation (Nagashima et al., 2013, Harada et al., 2014); (j) stable oxygen isotope data of cellulose in the Horse Trail Fen of South Alaska, as a proxy of Aleutian Low strength (Jones et al., 2014); (k) monsoon signals in the Dongge Cave (Dykowski et al., 2005); (l) reconstruction of El-Niño-Southern Oscillation (ENSO) dynamics from grain-size signals in lake sediments of El Junco Lake on the Galapagos Islands (Conroy et al., 2008). Image reproduced from Brooks et al (2015).

EASM, including between stalagmite, lake sediment, and marine sediment data. These inconsistencies span into researchers' interpretations of the relationship between the EAWM and EASM, with disagreement on whether they are inversely or positively correlated, or a mix of the two during different periods (Leipe et al. 2013; McColl 2016).

As has already been mentioned in this introduction, the main palaeoclimatic variable that will be discussed in this thesis is sea surface temperature (SST). SST has the benefit of being well-established inverse relationship to marine carbonate $\delta^{18}O$, meaning that it is a common choice for palaeoclimatic reconstruction. Not only is it an accessible variable palaeoclimatically, it is also an important one archaeologically, as a variable relevant to atmospheric climate and human-environment interactions (Burke et al. 2021). In the modern context, rising average SST has been closely aligned with rising atmospheric temperatures aroung Japan[1], with atmospheric temperature change identified as the key factor in determining SST variability (Chu, Chen, and Lu 1998). Over the last two decades, SST variability as a result of climate change has also been shown significant negative impacts on the Japanese fishing industry (Kuroda et al. 2020). This relationship between fish stocks and ocean temperatures illustrates the potential impact that changes in past SST conditions could have had on archaeological hunter-gatherers, particularly for maritime-focused hunter-gatherers in an island context such as on Rebun. Indeed, environmental change and its relationship to hunter-gatherer ecology was emphasised as key research topic of the Baikal-Hokkaido Archaeology Project, with recognition that environmental varaibliity had a large impact on the Holocene hunter-gatherers of Hokkaido, potentally contirbuting to key cultural transitions in the region (Weber, Jordan, and Kato 2013).

Looking at the oceanographic palaeoenvironment around Hokkaido, the Tsushima current is thought to have reached its modern volume by ~8,000 cal BP (Oba et al. 1991; Lutaenko et al. 2007),

[1] https://www.data.jma.go.jp/gmd/kaiyou/english/long_term_sst_japan/sea_surface_temperature_around_japan.html

however diatom and pollen analysis from marine and lake cores (Koizumi 1987; Igarashi 2013) have indicated that there were several warm 'pulses' in the late Holocene. Research from the Sea of Okhotsk shows such 'pulses' occurring at 2800-2400 and 1700-1400 cal BP (Kawahata et al. 2003). In Sakhalin, the shellfish assemblage from East Taraika midden suggests that water temperature during the 10th century AD was warmer than modern day (Akamatsu and Ushiro 1995; Hudson 2004). This coincides with the beginning of the MWP, or 'mediaeval climatic optimum' (Hudson 2004).

Palaeoclimatic reconstructions are also available from lake Kushu, Rebun Island. These are particularly relevant to this thesis, as Rebun Island is also home to the archaeological site where samples were collected. Multiple publications have used sediment cores from this lake to produce estimates of regional palaeoclimatic and palaeoenvironmental change (Leipe et al. 2013; Müller et al. 2016; Schmidt et al. 2016; Leipe et al. 2018; Schmidt et al. 2019). The pollen record shows that the local vegetation shifted from largely oak-based to more beech-, pine- and fir-based forest during the period between 4,000 - 2,000 BP, coinciding with a change to warm, wet climatic conditions (Leipe et al. 2013; Müller et al. 2016). A further reduction in arboreal pollen overall is recorded after 1,100 BP, although Müller et al. (2016) suggest that this shift is anthropogenically driven. The lake Kushu pollen records also record rapid cooling events in the local area that coincide with some of the major global/hemispheric climate events already discussed, including the LIA, and the '4.2k event' (Leipe et al. 2018).

Archaeometric Methods

The two main archaeometric methods used in this thesis are stable isotope palaeothermometry, and radiocarbon dating. All three papers make at least some use of stable isotope analysis, including significant discussion of sampling and analytical methodology and its application in an archaeological context. The final paper draws on both stable isotope analysis and radiocarbon dating as applied to the archaeological marine carbonates from Hamanaka 2. Although radiocarbon dating these specimens does have standalone benefits in terms of improving site-wide chronology and regional

marine reservoir corrections, it also has an important role alongside stable isotope analysis. Without radiocarbon dating, it is impossible to conclusively correlate between palaeoclimatic indicators from Hamanaka 2, local indicators from lake Kushu, and regional-/global-scale climate patterns. By directly dating the materials from which stable isotope samples were analysed, you can confirm the stratigraphic integrity of the samples and that the palaeotemperatures they provide are contemporaneous with other archaeological material from the deposit.

Stable Isotope Palaeothermometry

As a technique for inferring environmental/climatic information, stable isotope analysis of marine carbonates has been recognised since the mid twentieth century. Improvements in methods and equipment since the new millennium have offered new ways that these techniques can be approached and applied. This section will provide a literature review of the development of oxygen and carbon stable isotope analysis and palaeoenvironmental reconstruction.

The existence of isotopes was first established in the early twentieth century, when researchers interested in radioactive materials made the discovery that some radioactive elements had corresponding non-radioactive counterparts which were otherwise chemically identical (Urey 1947). The first of these pairs, 'ionium' (thorium-230) and thorium, was identified by Bertran Boltwood (1907) who will perhaps be a recognisable name for scientific archaeologists as one of the founding fathers of radiometric dating. Only a few years later the existence of stable (non-radioactive) isotopes was demonstrated in neon-20 and neon-22 by J.J. Thompson (1912).

Stable and radioactive isotopes continued to be a growing field of study into the middle of the twentieth century, when researchers began to identify variation in the thermodynamic properties of different isotopes. Urey (1947 p. 563) suggests that oxygen isotopes may prove some of the least difficult to differentiate and study, owing to 'the sensitivity with which the density of water may be determined'. He continues to discuss what will become the foundations of stable isotope thermometry, outlining how temperature changes should be reflected in the oxygen and carbon

isotopic composition of accretionary carbonates. This relationship relies on changes in the fractionation factor in equilibrium reactions depending on the ambient temperature (Urey et al. 1954). Urey also predicted that oxygen in particular would be well-suited to (palaeo)thermometry, owing to its atmospheric and oceanic availability, the stable nature of its isotopes and the ability to more precisely measure the abundance of its isotopes using newly (and soon-to-be) developed mass spectrometers (Thode, Graham, and Ziegler 1945; Nier 1947; Urey 1947).

Stable isotope analysis was indeed first applied to palaeothermometry using oxygen isotopes, by Urey and colleagues (Urey et al. 1951). They use Upper Cretaceous belemnites from Europe (England and Denmark) and the United States to produce estimated water temperature from the period of deposition. This geological use case was important in showing the enormous potential of oxygen isotope palaeothermometry, but the authors also note a number of potentially confounding factors (e.g. mass spectrometry precision, diagenetic alteration, changing oceanic isotope composition over time), which remain extremely pertinent in modern palaeothermometry. Urey et al (1954) expand on some of these issues, highlighting how natural temperature ranges and isotopically-calculated temperature ranges are not interchangeable where calcium carbonate precipitation only occurs in a certain temperature range, and that an estimate of the isotopic composition of ancient seawater is also necessary to adequately convert carbonate $\delta^{18}O$ into temperature using a paleotemperature equation. Nonetheless, these studies demonstrated the enormous potential for oxygen isotope analysis to provide a proxy record for ancient water temperatures.

Archaeological (rather than purely geological) interest in this potential palaeotemperature record followed. Emiliani et al. (1964) used human food waste molluscs shells to estimate palaeotemperature at sites in Italy and Libya, and Shackleton (1973) pioneered the use of stable oxygen isotope analysis to estimate season of collection in archaeological mollusc assemblages. He sampled the final growth increment of the *Patella tabularis* from South African 'Wilton' middens and compared the results from these to incremental seasonal sampling along the shells to identify the

shell's season of death. Since then, this technique has become an important component of archaeomalacological investigation, used successfully across a wide variety of species and locations (Deith 1983; Kennett and Voorhies 1996; Mannino et al. 2007; Colonese et al. 2012; Burchell et al. 2013; Branscombe, Nigst, and Miracle 2020).

The basic theoretical foundation of such research - the relationship between precipitated carbonates and ambient temperature - has remained largely unchanged since the beginning of its archaeological application: water $\delta^{18}O$ is temperature-regulated, and most incrementally-grown carbonates precipitate calcareous material in equilibrium with surrounding water and consequently produce a proxy record of temperature change over the period of growth. However, in the decades since the technique was developed, our understanding of the complicating factors originally identified by Urey et al. (1951; 1954) has increased, as has our technological capacity to measure and interpret stable oxygen isotopes.

The first marine carbonate palaeotemperature equation was published by Epstein et al (1951; 1953):

$$t = 11.88 - 5.91*\delta^{18}O$$

This equation saw the amount of O-18 in a sample expressed as a per mille (‰) ratio of O-18 to O-16, relative to a standard sample of Pee Dee Belemnite (PDB):

$$\delta^{18}O = ((Rsample/Rstandard)-1)*1000$$

This delta notation continues to be the standard way to present stable isotope values, although towards the end of the 10th century depletion of the original PDB standard led to its replacement by the new Vienna Pee Dee Belemnite (VPDB) standard (Coplen 1994). A notable update to the original carbonate-water temperature scale (Epstein et al. 1953) is that from Grossman and Ku (1986), who calculated a biogenic aragonite-specific temperature equation:

$$t = (19.73\pm0.6)-(4.34\pm0.24)*((\delta^{18}O_{arag/pdb})-(\delta^{18}O_{wat/smow}))$$

This dealt with the issue of differences in fractionation between water-calcite and water-aragonite, which leads to ^{18}O enrichment in the latter and means that the same temperature equation shouldn't be applied to both.

Ideally, as described by Carre et al. (2005), carbonate temperature equations would be devised for each species of interest, as no single equation accounts for the effect of unique biological processes, e.g. through biologically controlled pathways during aragonite precipitation or the influence of the organic matrix on aragonite crystal nucleation. Species-specific temperature equations have been successfully devised in some cases, e.g. Carré et al. (2005) for *Mesodesma donacium* and Hollyman et al (2020) for *Buccinum undatum*. However, it is often not feasible to produce such species-specific equations as they require significant time to either closely monitor wild specimens, or complete laboratory-rearing experiments. As such, these species specific aragonite fractionation-temperature relationships, often known as 'vital effects' are still poorly understood, and the general assumption when working with biogenic aragonite remains that precipitation will occur broadly in equilibrium.

The history of palaeotemperature reconstruction through carbonate stable isotope analysis is mostly concerned with stable oxygen isotopes, but there is also evidence that carbon isotope fractionation in carbonates can be temperature dependent. Sommer and Rye (1978) proposed that this temperature scale could be especially useful to those interested in palaeotemperature, as it would bypass the need for accurate estimation of seawater $\delta^{18}O$ (Grossman and Ku 1986). Unfortunately in the intervening years it has become clear that $\delta^{13}C_{carbonate}$ has a very complex relationship to water conditions, involving biological metabolic effects, water salinity and dissolved inorganic carbon (DIC) (McConnaughey and Gillikin 2008). $\delta^{13}C_{seawater}$ and DIC can in turn be sensitive to primary productivity, volcanic input, sedimentation rates, sea level change, methane bursts, upwelling, prevailing currents and other oceanographic changes (Arthur et al. 1983; Arthur, Williams, and Jones 1983; Korte, Kozur, and Veizer 2005; Gillikin et al. 2006; McConnaughey and Gillikin 2008). This level of complexity does not preclude the possibility of interpreting $\delta^{13}C$ results in terms of temperature

or oceanography, but does certainly make it a more difficult task especially in the palaeo-context where most of these factors will be hard to model. This has meant that stable isotope palaeotemperature reconstruction generally focuses more heavily on $\delta^{18}O$ results.

While the basic principles of the use of oxygen isotope as a palaeothermometer have remained the same since the early days of the technique, there have been significant developments in sampling techniques and mass spectrometry. In modern carbonate IRMS (isotope-ratio mass spectrometry), techniques differ depending on the material to be analysed and the research questions to be answered. In terms of sample collection, hand drilling (sometimes referred to as microdrilling), micromilling (also known as microsampling), SIMS (Secondary Ion Mass Spectrometry) and laser ablation techniques are the most commonly used (Spötl and Mattey 2006; Lachniet 2009; Zhang et al. 2014; Twaddle et al. 2016; Helser, Kastelle, McKay, et al. 2018).

Hand drilling involved the use of a handheld (usually dental) drill to spot sample regions/transects of interest. Twaddle et al. (2016) highlight some potential issues of this approach, including that spatial resolution is limited by drill bit size and hand drilled samples can therefore 'smooth' minimum and maximum isotope values. An alternative approach, micromilling using computer-controlled drills, has been possible since the 1990s (Dettman and Lohmann 1995), and can provide an extremely high degree of spatial resolution and precision. These two sampling techniques are both discussed in more detail in Paper 2 (Branscombe et al. 2022).

Precise and high resolution sampling strategies would be impossible to exploit if progress had not also been made in the field of mass spectrometry: in most cases, high spatial resolution also means smaller sample sizes. The method describe by Urey et al. (1951) required a minimum of 50 mg of carbonate powder per sample, which is ~1,667 times more than the micromilled samples discussed in this thesis, which were often as small as 30 µg. Vonhof et al. (2020) have recently published results from a new continuous-flow mass spectrometer which can consistently analyse <5 µg carbonate samples. These extremely small samples were measured to a precision of ≤0.1‰. By

contrast, Urey et al. (1951) describe the highest precision achieved at that point as in the region of ±1 ‰. When modern $\delta^{18}O$ palaeothermometry is not using samples at the limits of current sample size requirements the precision can be higher still. Taking the example of the isotope facility at the British Geological Survey (where the analysis in this thesis was completed), the precision of their small carbonate device (dual inlet Isoprime mass spectrometer interfaced with a Multiprep autosampler) is regularly <0.05 ‰.

New spectroscopy approaches have also been developed which bypass the need for powdered sample collection altogether. Secondary Ion Mass Spectrometry (SIMS) is not a completely new approach, having originally been used in the 1960s (Williams 1985), but it has only recently become a common alternative to IRMS. SIMS utilises in situ sampling by bombarding the sample with a heavy ion beam which causes the sample to emit secondary ions (Williams 1985; Twaddle et al. 2016). Done in a vacuum, these secondary ions then move directly into a mass spectrometer. While this is technically a destructive process, the amount of material destroyed is far less than by any milling/drilling technique. Using SIMS presents the opportunity of extremely high resolution isotope profiles (e.g. Helser, Kastelle, McKay, et al. 2018), this comes at the loss of some measurement precision (Kita et al. 2009; Valley and Kita 2009; Twaddle et al. 2016; Helser, Kastelle, McKay, et al. 2018) versus traditional IRMS analysis. In the last two decades the precision of oxygen isotope analysis using SIMS has been improving though and is now regularly in the region of 0.3 ‰ (Kita et al. 2009; Yang et al. 2018; He et al. 2021; C. T. Edwards et al. 2022), although this is still significantly below the sub 1 ‰ precision achieved in IRMS so the use of SIMS is still trade-off between precision and resolution requirements.

LA-ICP-MS (Laser Ablation Inductively Coupled Plasma Mass Spectrometry) is another in situ modern mass spectrometry technique used to measure stable isotopes. Since its initial demonstration in the 1980s, LA-ICP-MS has become a key method used to analyse solid materials that are otherwise difficult to break down (Koch and Günther 2016), but there is also a history of its use in

sclerochronological analysis of marine carbonates (Smalley et al. 1992; Toland et al. 2000; Klünder et al. 2008). In laser ablation mass spectrometry, a laser is focused on the sample surface to produce CO_2 which is then analysed in an attached mass spectrometer. Like SIMS, this has the benefit of combining the sampling and analysis into one rapid in situ process, and the further benefit that trace element ratios - also regularly used to investigate environmental change - can be obtained simultaneously (e.g. Wanamaker and Gillikin 2019). However, as Twaddle et al. (2016) describe, the spatial resolution achieved with laser ablation does not reach the same level as micromilling or SIMS, as the laser heats the surrounding sample surface which potentially affects the isotopic composition of those areas and limits how closely you can group samples.

A new development in modern isotope palaeothermometry is the use of 'clumped' oxygen and carbon isotopes. This combines the measurement of $\delta^{13}C$ and $\delta^{18}O$ along with measurement of how many heavy ^{13}C and ^{18}O atoms are 'clumped' together in a carbonate group. As described by Ghosh et al. (2006), this depends on stable isotope exchange within the carbonate crystalline structure, which is a homogenous equilibrium and is thermodynamically regulated. At cooler temperatures heavy isotopes are more likely to group together to form rare carbonate isotopologues, which have unique and identifiable vibrational characteristics (Ghosh et al. 2006; Eiler 2011). These thermodynamic relationships were first discussed by Urey (1947), but the approach wasn't applied to palaeoclimatic research until the 21st century (Eiler 2011), with studies by Eagle et al. (2013) and de Winter et al. (2018) demonstrating its potential utility in marine molluscs.

A major benefit of this approach is that this relationship between temperature and carbonate isotopic makeup is independent of the isotopic composition of the water (Ghosh et al. 2006; Ghosh et al. 2007). As already discussed, existing carbonate (palaeo)temperature equations rely on accurate estimation of $\delta^{18}O_{seawater}$ to calculate water temperature (Grossman and Ku 1986; Eiler 2011). The addition of clumped isotope thermometry could potentially overcome this issue, although there are still some instrumental and methodological challenges. Clumped isotope

thermometry currently requires high precision and large carbonate sample sizes, and is particularly susceptible to organic contamination (Eiler 2011). This means that studies including clumped isotope analysis often need to use bulk measurements rather than higher resolution incremental sampling (e.g. de Winter et al. 2018) and that clumped isotope analysis is currently most useful as an addition to, rather than replacing, traditional $\delta^{18}O$ thermometry.

Radiocarbon Dating

Radiocarbon dating was first conceived of in the 1940s, when Willard Libby established first that carbon-14 was naturally occurring, and secondly that the amount of carbon-14 in organic matter decreased steadily over time, via the process of decay into nitrogen-14 (Libby 1946; Libby, Anderson, and Arnold 1949; Libby 1967). This is the underlying principle of all radiocarbon dating – that the amount of carbon-14 remaining in a carbonaceous specimen can be directly related to the time of the specimen's 'death' (or its separation from the carbon cycle). Due to the long half-life of radiocarbon, originally thought to be 5,568 years but revised to 5,730 years shortly thereafter, this had enormous potential for archaeology, as well as many other fields such as palaeontology and geology, as it offered the chance to directly date organic archaeological remains for the first time independent of any reliance on stratigraphy or historical documentation.

Originally, it was assumed by researchers that because the level of modern atmospheric carbon was apparently stable worldwide, that this should hold true for pre-modern periods (Libby, Anderson, and Arnold 1949). Soon errors were noticed between radiocarbon dates and calendar dates from known-age objects – usually dendrochronologically-dated wood, or historically-dated archaeological material. At the Sixth International Carbon-14 and Tritium Dating Conference in 1965, the first calibration curves (as they are now known) were presented, which reconstructed atmospheric carbon-14 levels over the past ~6,000 years (Damon, Long, and Grey 1966; Dyck 1967; Libby 1967). In the intervening 60 years, the atmospheric calibration curve has undergone significant elaboration, recalculation and extension, and the most recent available curve – IntCal20 – now extends to 55,000

cal BP (P. J. Reimer et al. 2020; Hogg et al. 2020). Modern calibration uses statistical modelling to calculate the date range most likely to include the true calendar date for a sample, and is most commonly reported as 95.4% probability range (Millard 2014). This is most commonly done using calibration software, such as OxCal (Bronk Ramsey 2009) or CALIB (Stuiver, Reimer, and Reimer 2022).

Another consideration in radiocarbon dating is the marine reservoir effect. This term was coined in 1977, and is the recognition that oceans and other bodies of water constitute carbon reservoirs with distinct radiocarbon content as-compared to the atmosphere, due to upwelling of deep water containing 'old carbon' (Berger, Taylor, and Libby 1966; Stuiver and Polach 1977). In order to correct for this reservoir effect, marine calibration curves have been developed for use with material from a marine context, or for the dating of terrestrial animals ingesting marine material (e.g. Stuiver, Pearson, and Braziunas 1986; Heaton et al. 2020). Due to geological and oceanographic differences across the world's oceans, the global marine calibration curve is used alongside an additional ΔR value, which is the local correction added or subtracted to the global correction during calibration (Stuiver, Pearson, and Braziunas 1986; R. W. Reimer and Reimer 2017).

Several methods are used to calculate local ΔR values for radiocarbon calibration. These include the use of U-Th dates, known-age marine samples, and paired marine and terrestrial dates (R. W. Reimer and Reimer 2017). In each case, a sample dated independently of the marine reservoir effect – whether that be via marine-independent U-Th dating, dating of a terrestrial sample, or using a pre-bomb marine sample with a known collection date – is compared to the radiocarbon age of a marine sample, taking into account the uncertainties of each date, and a ΔR offset is produced. It has been widely shown that ΔR can vary both chronologically and depending on the species being analysed, as marine reservoirs change over time and the marine reservoir effect differs depending on the way and extent to which a species incorporates carbon from the marine reservoir (Ascough et al. 2005; Ascough et al. 2006; Holmquist et al. 2015; Ascough, Church, and Cook 2017). Given the time-

dependence of local ΔR values, in archaeological contexts it is beneficial to utilise either U-Th dating of stratigraphically contemporaneous samples or stratigraphically paired marine and terrestrial samples, as in each case this will provide a ΔR value specific to the time period represented by the stratigraphic unit. Miyata et al. (2016) illustrate how for multi-period sites it may be necessary to calculate a number of ΔR offsets. This process is simplified using the online tool presented by Reimer and Reimer (2017), which is capable of calculating ΔR offsets using all three of the methods mentioned above without the need for researchers to calculate them by hand.

As with stable isotope palaeothermometry, since the early days of radiocarbon dating there have been significant developments in the equipment and statistical methods used which have led to vast improvements in the accuracy and precision of the technique. Originally, carbon-14 could only be indirectly measured through its decay products, but the advent of accelerator mass spectrometry (AMS) in the late 1970s introduced the possibility of counting individual carbon-14 atoms themselves (Libby 1967; Linick et al. 1989; Povinec, Litherland, and von Reden 2009). This not only sped up the measurement time, but also drastically reduced the required sample size, which went from 500-10,000 mg of carbon for β-counting methods, all the way down to <1 mg samples for modern AMS dating (Linick et al. 1989; Cersoy et al. 2017; Gottschalk et al. 2018). Furthermore, using the Mini Carbon Dating System (MICADAS), uncertainty of the dates is also significantly reduced and the dating of 1μg samples may soon be possible (Gottschalk et al. 2020).

Palaeogeography, Palaeoclimatology, Palaeoecology 582 (2021) 110634

Contents lists available at ScienceDirect

Palaeogeography, Palaeoclimatology, Palaeoecology

journal homepage: www.elsevier.com/locate/palaeo

The potential of marine bivalve *Spisula sachalinensis* as a marine temperature record

Tansy Branscombe [a,*], Rick Schulting [a], Julia Lee-Thorp [a], Melanie J. Leng [b]

[a] School of Archaeology, University of Oxford, 1 South Parks Road, OX1 3TG, United Kingdom
[b] National Environmental Isotope Facility, British Geological Survey, Nicker Hill, Keyworth, Nottingham NG12 5GG, United Kingdom

ARTICLE INFO

Editor: Dr. A. Dickson

Keywords:
Palaeoclimate
Northwest pacific
Oxygen isotopes
Sclerochronology
Seasonality

ABSTRACT

This paper presents a four year subannual isotope marine temperature record using modern *Spisula sachalinensis* specimens from Tomakomai (Hokkaido's Pacific coast, Japan). This species is commonly found in pre- and protohistoric shell middens and faunal assemblages from around the Seas of Japan and Okhotsk, so has significant potential as an indicator of past marine and, by inference, climatic conditions. However, previous sclerochronological research on the species' growth has shown significant geographical variation in growth pattern, rendering palaeoclimatic interpretation difficult. To address this issue, this study applied sequential isotopic analysis to two sectioned modern valves, providing a proxy for sea surface temperature (SST) and allowing the direct identification of seasonality during shell growth. The sequences span four years of growth, as confirmed by visually identified growth patterns and the oxygen stable isotope results, which show clear annual cycles in $\delta^{18}O$. $\delta^{13}C$ seasonality is less clear, but shows a weak inverse correlation with temperature potentially relating to primary productivity. Annual growth lines show that shell growth occurs during both warmer and cooler SSTs, but is more rapid during the cooler seasons. This is consistent with warm-season growth minima seen in shells from Hakodate Bay by Kato and Hamai (1975), but not with their suggestion that it is associated with shells growing at the southern limits of their distribution. Comparison to average local SST shows that $\delta^{18}O$-derived temperature falls within the expected range, but, contrary to expectations given preferential cool-season shell growth, appears biased towards warmer temperatures. Factors that could contribute to this are discussed. Overall, stable isotope analysis of *Spisula sachalinensis* is considered a useful complement to macro/microscopic sclerochronological research in building a holistic picture of shell growth, and has significant potential as a high resolution proxy for palaeoenvironmental studies of past SST.

1. Introduction

The value of marine bivalve shells as temperature archives has long been recognised (e.g. Emiliani et al., 1964), with high resolution sampling and increasingly precise stable isotope mass spectrometry allowing the interpretation of data at subannual scales. Following the recognition that some species of clam, e.g. *Arctica islandica*, can live for more than 500 years (Butler et al., 2013; Schöne et al., 2005), researchers have noted the importance of long-lived molluscs as 'sentinel species' in marine climate research (Mann et al., 2013). The shells of such large clams grow incrementally allowing for correlation between annual growth increments and calendar dates (e.g. Khim et al., 2000). Furthermore, their shell oxygen and carbon stable isotope ratios ($\delta^{18}O_{shell}$ and $\delta^{13}C_{shell}$) reflect information about ambient water conditions. Water temperature and salinity in particular drive $\delta^{18}O_{shell}$, while $\delta^{13}C_{shell}$ has a more complex relationship to water conditions involving animal metabolic effects, salinity and dissolved inorganic carbon (DIC) (McConnaughey and Gillikin, 2008). This means that the growth increments can be interpreted as subannual proxy records for these variables (Emiliani et al., 1964).

Spisula (*Mactra/Pseudocardium*) *sachalinensis* (Fig. 1), or the Sakhalin surf clam, is a large bivalve found in the Northwest Pacific, notably in Japan, the Korean peninsula and the Russian Far East (including the eponymous Sakhalin Island). In Japanese this species is known as ubagai (ウバガイ) or hokkigai (ホッキ貝). It is easily recognised by its bright pink muscle and is eaten both raw and cooked. The majority of Japanese

* Corresponding author.
E-mail addresses: tansy.branscombe@arch.ox.ac.uk (T. Branscombe), rick.schulting@arch.ox.ac.uk (R. Schulting), julia.lee-thorp@arch.ox.ac.uk (J. Lee-Thorp), mjl@bgs.ac.uk (M.J. Leng).

https://doi.org/10.1016/j.palaeo.2021.110634
Received 18 January 2021; Received in revised form 18 August 2021; Accepted 19 August 2021
Available online 8 September 2021
0031-0182/Crown Copyright © 2021 Published by Elsevier B.V. All rights reserved.

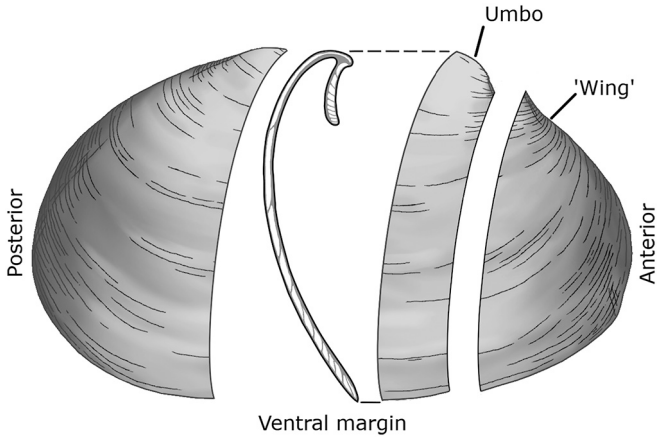


Fig. 1. Schematic illustration of *Spisula sachalinensis* showing section along the axis of maximum growth.

surf clam harvest occurs from the port city of Tomakomai on the south coast of Hokkaido (Fig. 2), where clams are dredged using jet stream seine fishing. As of 1999, 50,000 tons of clam were caught from the Tomakomai coast annually, and it remains a specialty dish of the region (Sasaki and Ohta, 1999).

Previous research on the species has been guided by its commercial importance, focusing on its nutritional value and optimal growth and spawning conditions (e.g. Golikov and Scarlato, 1970; Kato and Hamai, 1975; Lee et al., 1996; Sakurai and Seto, 1998; Sasaki, 1981; Sasaki and Ohta, 1999; Tabakaeva and Tabakaev, 2017; Takahashi and Yamamoto, 1970).

The potential of this species for climate science has not gone unrecognised. For example Mann et al. (2013) list it as one of four major long-lived mactrid clam species, and note that the genus *Spisula* has been suggested as a good continental shelf sentinel species covering both the

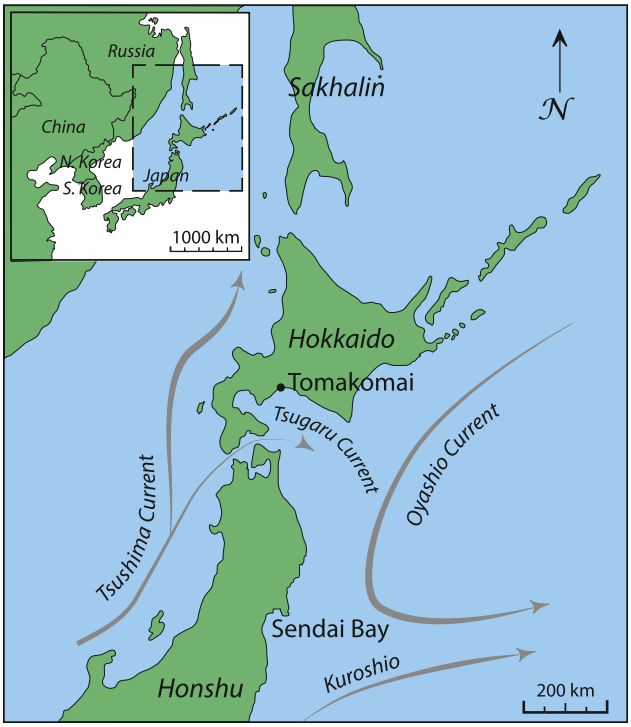


Fig. 2. Map showing the location of Tomakomai within northern Honshu, and the surrounding ocean currents.

North Pacific and North Atlantic. The only isotopic study to specifically test the species as a climatic indicator, however, is that by Khim et al. (2000), confirming the expected relationship between $\delta^{18}O_{shell}$ and sea surface temperature in specimens from the east coast of Korea. They also discuss trends in $\delta^{13}C_{shell}$, suggesting that as in other bivalve species (e.g. McConnaughey and Gillikin, 2008; Gillikin et al., 2006) this is partially a reflection of the $\delta^{13}C$ of DIC. Khim et al. (2000) focus on the utility of *S. sachalinensis* as a monitor for modern hydrological conditions, but do briefly mention possibilities for palaeoclimatic research.

Our study continues this research, but focuses on the region of Hokkaido as opposed to the Korean coast. Not only is this region notable for the modern commercial harvest of *S. sachalinensis* as previously outlined, it is also an important area for Japanese archaeology. In Hokkaido, unlike central/southern Japan, coastally-adapted indigenous hunter-gatherers remained the primary occupants into the late 19th century (Ohnuki-Tierney, 1976; Hudson, 2014; Seaton, 2017). The maritime adaptations of Jomon, Epi-Jomon, Okhotsk and Ainu groups - representing a span of c. 7000 years – mean that shell middens are a frequent element of the archaeological record in Hokkaido (Habu et al., 2011; Oikawa, 1995; Okada, 1998), and the surf clam is a common species found at sites in northern Japan and Hokkaido (Nagasaki, 1994; Okada, 1998; Makino, 2011). Use of the species as a palaeothermometer could provide an important subannual oceanographic and palaeoclimatic proxy, given the interdependence of oceanographic and atmospheric factors and their effect on regional SST (e.g. Abe et al., 2016; Imada et al., 2017; Hirose and ichi Fukudome, 2006; Seo et al., 2013; Takano et al., 2008).

For Honshu and the southern islands of Japan much of the historical period is well-documented climatically by instrumental measurements (back to the late 18th century (Können et al., 2003; Demaree et al., 2013)) and historical documents (back to the 11th century (Mikami, 2008)). However, as Hokkaido was not colonised by the Japanese state until after the Meiji restoration of 1868 there is relatively little historical climatic documentation that specifically relates to this region. Therefore, the use of shellfish (and other marine carbonates) have the potential to fill significant gaps in palaeoclimatic knowledge, both due to their archaeological prevalence and the gap in historical climatic data specific to this island.

We aim to use high-resolution analysis of $\delta^{18}O_{shell}$ and $\delta^{13}C_{shell}$ to identify seasonality of growth through isotope analysis of two specimens of modern, known-age *S. sachalinensis*. A focus is placed on identifying the season of growth decrease/cessation, which has been a point of disagreement in previous research, as outlined below. We aim to investigate the relationship between $\delta^{18}O_{shell}$ and sea surface temperature, in order to demonstrate the potential of *S. sachalinensis* for palaeoclimatic reconstruction in the Northwest Pacific.

2. Growth and ecology

S. sachalinensis is a species that prefers sandy substrates in the littoral zone, growing rapidly for c. eight years, when shell length reaches its maximum size of around 10 cm in length and subsequent growth becomes negligible (Sasaki, 1981). Large shells are often 20–30 years old, with one individual from the Sea of Japan even reported to have reached 70 years (Selin, 2010). The species reaches sexual maturity at three years (Golikov and Scarlato, 1970), after which spawning takes place annually during the spring/early summer in Hokkaido (Kinoshita and Shibuya, 1920; Sasaki, 1981; Sakurai et al., 1992; Takamaru, 1976). In Primorje, Russian Far East, Golikov and Scarlato (1970) report spawning between late June and October. It seems likely that these differences relate to temperature variation between regions, as Lee et al. (1996) have shown that water temperature can be a limiting factor for egg development in *S. sachalinensis*.

Water depth estimates for living colonies vary from 1–5 m (Golikov and Scarlato, 1970), to 3–6 m (Sasaki and Ohta, 1999) and up to 12–15 m (Sasaki, 1989). Golikov and Scarlato (1970) discuss seasonal

change in depth distribution, although the extent of this variation does not account for the wide differences in depth range described in the literature. Sasaki (1989) suggests that a maximum depth of 15 m is common across a number of fishing spots, as a result of sediment conditions. Coarser-grained sand particles found at greater depths inhibit the shellfish's burrowing behaviour. Differences in sediment composition across the species' geographical distribution could therefore be responsible for different depth ranges given in the literature.

As is common in marine bivalves, growth is not constant throughout the year, resulting in the formation of annual growth increments and lines (Kato and Hamai, 1975; Sasaki, 1981). Growth increments show a prismatic structure and represent rapid shell growth. Growth lines are a nacreous layer (due to a difference in the orientation of the crystal structure or the organic compounds therein) and represent a period of slowed or ceased shell growth (Kato and Hamai, 1975). Both of these layers are composed of aragonite ($CaCO_3$). In *S. sachalinensis*, previous work suggests three potential triggers for the formation of annual growth lines: low winter SST (Yamamoto, 1947), high summer SST (Sasaki, 1981) and the end of the spawning season (Kato and Hamai, 1975). As with variation in spawning season, it seems likely that these multiple triggers relate to different environmental conditions across the species' geographic distribution; the warm-season growth lines reported by Sasaki (1981) occurred in shells near the southern end of the *S. sachalinensis* distribution in Sendai Bay, Honshu, whereas the cool-season lines reported by Yamamoto (1947) were from its northern distribution on Sakhalin. Given the expected relationship between $\delta^{18}O_{shell}$ and SST, stable isotope analysis of a modern specimen of *S. sachalinensis* from Tomakomai should confirm the species' regional growth pattern.

3. Materials and methods

The modern shells used in this study were collected from the coast of Tomakomai on Hokkaido's Pacific coast (Fig. 2) in August 2019.

The shells were obtained from a Sapporo sushi restaurant, and had been briefly boiled (<20 minutes) by the restaurant to remove any remaining organic material before export to the UK (standard practice as required by the UK Department for Environment Food & Rural Affairs). As these shells were obtained from a restaurant rather than directly from the study site, we are not able to provide exact coordinates, however the restaurant confirm that they were harvested in Tomakomai on 3rd August 2019 at approximately 42°35′N, 141°36′E.

Age estimate of the two shells were obtained via preliminary identification of annual growth lines, which were later confirmed or adjusted

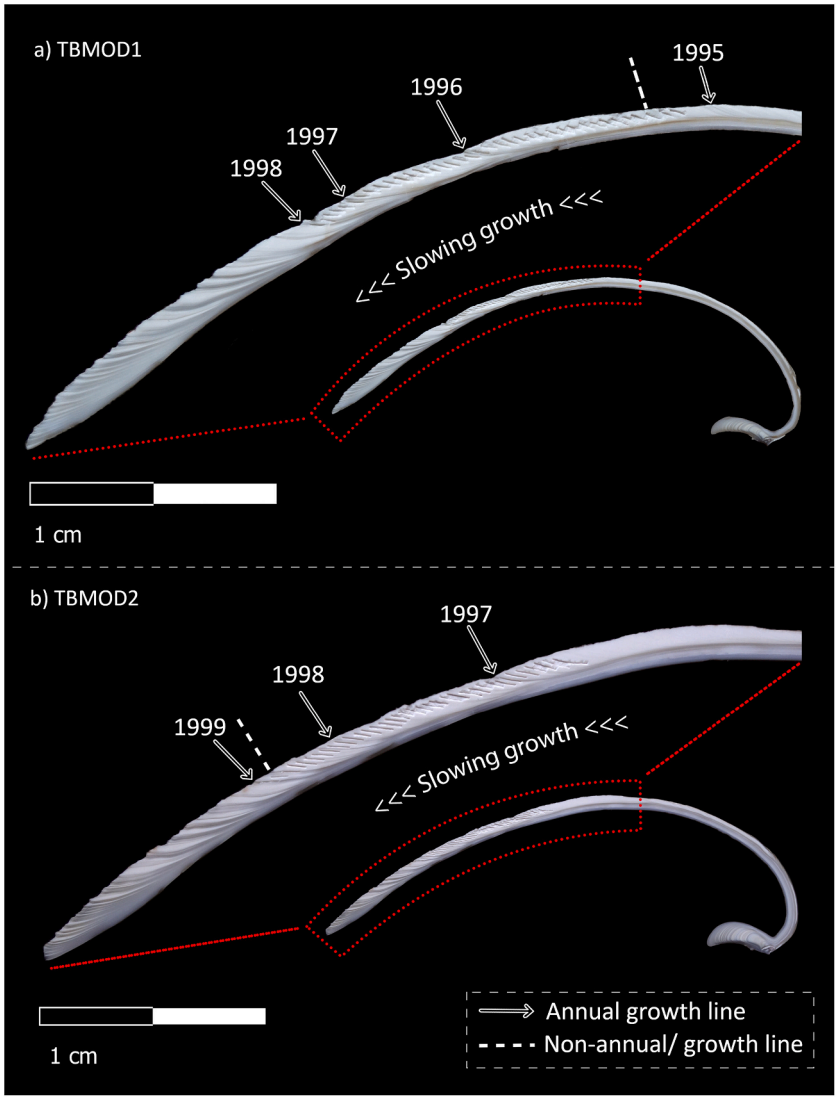


Fig. 3. Image of sectioned *Spisula sachalinensis* valves showing completed micromill sampling and the location of growth lines. NB: the non-annual growth line marked by a dashed line in TBMOD1 has been partially obscured by the milling tracks.

based on the shells' $\delta^{18}O_{shell}$ profiles. One specimen (TBMOD1) is estimated to have been 28 years old at the time of collection, and the other (TBMOD2) is estimated at 26 years old. From this assessment, the four years sampled in this study are considered most likely to represent 1996–1999 (Fig. 3).

Shells were sectioned using a geological trim saw with a 15.24 cm diameter diamond saw blade of 0.1 cm thickness. They were sectioned from the umbo to the shell edge by manually holding the shell in position along the axis of maximum growth, perpendicular to growth banding (Fig. 1). After sectioning, the 'wing' on the anterior side was also cut away to leave a thick section. Sections were embedded with the cut surface corresponding to the axis of maximum growth face down in a plastic mould using MetPrep 'Kleer-Set' polyester resin and hardener, and were left to cure overnight. Once fully cured, the side representing the axis of maximum growth was prepared using a series of silicon carbide grinding and polishing papers. These ranged from P180 up to P4000, producing a polished sampling surface and ensuring that no resin residue remained over the sampling area.

Resin blocks were mounted onto the sampling slide of a New Wave Research microdrill. This allows for high resolution computer-controlled drilling of the growth bands. A 0.3 mm diamond-coated dental drill bit was fitted to the micromill to sample incrementally across the shell section. A section of growth encompassing three annual growth bands was selected for each shell (Fig. 3). This came from the middle of the shell's growth, when the shell is growing fast enough to provide wide increments but not from the earliest years of growth when the outer shell layer being targeted is thinner. The distance between samples (measured from the centre of one sample to the centre of the next) averaged 0.8 mm. The samples that coincided with nacreous growth lines were specifically noted. Samples were drilled over three passes at 100 μm depth per pass (300 μm total depth), with a scan speed of 100 μm/second. A total of 37 samples of aragonite powder were produced, each weighing around 50 μg.

Further samples were hand drilled from each shell to test for diagenetic alteration of the aragonite. These were analysed using FTIR-ATR, using the method outlined by Loftus et al. (2015), which differentiates aragonite and calcite polymorphs using the different vibrational characteristics of their molecular structure. Results showed no evidence of aragonite-to-calcite recrystallisation, but the work of Moon et al. (2018) suggest that a lack of calcite recrystallisation does not preclude diagenetic shifts in $\delta^{18}O_{shell}$.

Isotope ratio mass spectrometry was undertaken at the British Geological Survey in Keyworth, using an IsoPrime dual inlet mass spectrometer and Multiprep device. Samples are loaded into glass vials and sealed with septa. The automated system evacuates vials and delivers anhydrous phosphoric acid to the carbonate at 90 °C. The evolved CO_2 is collected for 15 minutes, cryogenically cleaned, and passed to the mass spectrometer. Isotope values are reported using the delta notation ($\delta^{18}O$, $\delta^{13}C$) as per mille (‰) deviations of the isotopic ratios ($^{13}C/^{12}C$, $^{18}O/^{16}O$) calculated to the VPDB scale using a within-run laboratory standard (KCM) calibrated against international standard NBS-19. The calcite-acid fractionation factor applied to the gas values is 1.00813. Due to the long run time of 21 hours a drift correction is applied across the run, calculated using the standards that bracket the samples. Craig correction (Craig, 1957) is also applied to account for $\delta^{17}O$. The standard calcite values for KCM are for +2.00‰ for $\delta^{13}C$, and -1.73‰ $\delta^{18}O$ with an average analytical reproducibility is of 0.05‰.

Nine KCM standards were measured alongside every 31 samples. The average analytical precision for these was ±0.05‰ for $\delta^{18}O$ and ±0.03‰ for $\delta^{13}C$. An uncertainty of ±0.05‰ $\delta^{18}O$ would in turn correspond to an error of ±0.24 °C in the reconstruction of water temperature at the time of formation, using the aragonite-SST equation:

$$SST = 20.6 - 4.34(\delta^{18}O_{carbonate} - (\delta^{18}O_{seawater} - 0.27)) \quad (1)$$

This is a slightly modified version of the original equation (Grossman and Ku, 1986), where a -0.27‰ correction has been applied to the seawater $\delta^{18}O$ value ($\delta^{18}O_{seawater}$) to account for measuremenets on the modern VSMOW (Vienna Standard Mean Oceanic Water) scale rather than the now-defunct SMOW scale originally used (Leng and Lewis, 2016; Dettman et al., 1999). $\delta^{18}O_{seawater}$ was set at a constant −0.85‰, based on data from NASA's Global Seawater Oxygen-18 Database (Schmidt et al., 1999) (https://data.giss.nasa.gov/o18data/).

The modern observed SST range for the Tomakomai coast was accessed using the Physical Oceanography Distributed Active Archive Centre (PODAAC) satellite imagery database. Specifically, we used Level 4 data from the Canadian Meterological Center, which provides daily global SST measurements at a 0.2 degree resolution, combining infrared imagery with in-situ readings from ships and buoys to provide an estimate of foundation temperature, 'defined as the temperature of the water column just below the diurnal warm layer' (Marullo et al., 2016, p. 8357). While several global satellite SST datasets exist within the Group for High Resolution Sea Surface Temperature (GHRSST), this particular dataset was the only one at Level 4 resolution to provide the required data through the 1990s. The *ghrsst* Python package developed for the present paper Stuart (2020) was used to access daily SST observations from the Tomakomai coast, from January 1992 to December 2002. From this, monthly averages were calculated (Table 1) to provide a general picture of the observed temperature range contemporary with the sampled period of shell growth. The annual range in average monthly temperature is 17.43 °C, while the maximum average annual temperature range (the difference between the average February minimum and August maximum) is 18.93 °C.

4. Results

Of the 78 samples analysed for isotope composition, seven failed to produce enough gas for isotopic measurement. Results are shown in Table 2. $\delta^{18}O_{shell}$ shows a range of 3.46‰, while $\delta^{13}C_{shell}$ range is 1.55‰. Linear regression analysis shows a weak and statistically insignificant correlation between $\delta^{18}O_{shell}$ and $\delta^{13}C_{shell}$ ($r = -0.19$, $p = 0.13$). $\delta^{18}O_{shell}$ results equated to a temperature range of 15.01 °C, with a minimum of 5.40 °C and a maximum of 20.41 °C (Table 2).

The stable isotope data (Fig. 4) show clear peaks and troughs in $\delta^{18}O_{shell}$ in three cycles, matching the expected three-year sampling periods. In general the $\delta^{18}O_{shell}$ peaks appear broader than the corresponding troughs, leading to a 'cuspate' rather than sinusoidal wave appearance, as defined by Goodwin et al. (2003). As samples move towards the ventral growth edge (Fig. 1) the periodicity of the wave decreases, corresponding to shortening growth increments.

Fig. 5 shows SST calculations from $\delta^{18}O_{shell}$ overlain on observed SST variation for Tomakomai, illustrating how the $\delta^{18}O_{shell}$-derived temperatures fit against observed annual SST range for the local coast. In Fig. 5, the $\delta^{18}O_{shell}$-derived SST results have been normalised to account for this slowing growth (and therefore decreasing width in annual growth increments) using a piecewise constant dilation factor. The distance between samples within a growth increment was multiplied by *maximum increment width/width of particular growth increment*. This means that each year of growth appears equal in length, whilst maintaining the original relative spacing between samples within each increment. This was then placed over the satellite-observed SST curve for the relevant years to provide the best visual fit.

5. Discussion

5.1. How well does $\delta^{18}O_{shell}$ data match modern SST observations?

Overall, it is clear that estimates of SST based on $\delta^{18}O_{shell}$ follow a broadly sinusoidal pattern, and none fall outside of the observed range for the collection location. This reinforces the conclusion of Khim et al. (2000), that $\delta^{18}O_{shell}$ in *S. sachalaninensis* can be interpreted as a proxy for subannual cycling of SST. The results in Fig. 4 show shortening

Table 1
Summary of average monthly observed SST (°C) for the Tomakomai coast for the period of 1992–2002. Daily readings were used to produce a minimum, maximum and mean reading for each month, which were then averaged over all years of available data. Raw data at: https://podaac-opendap.jpl.nasa.gov/opendap/hyrax/allData/ghrsst/data/GDS2/L4/GLOB/CMC/CMC0.2deg/v2/contents.html.

	Jan	Feb	Mar	Apr	May	Jun	Jul	Aug	Sep	Oct	Nov	Dec
Average Min	3.40	2.27	2.38	3.16	5.79	10.55	14.72	19.21	17.82	13.43	9.26	5.68
Average	4.66	2.97	3.01	4.38	8.01	12.72	17.14	20.40	19.47	15.66	11.11	7.41
Average Max	6.03	3.01	3.71	5.86	10.36	14.87	19.36	21.20	21.20	17.79	13.26	9.27

period in the later years of shell growth, in keeping with expectations from the ecological literature for *S. sachalinensis*, which suggests significantly slowed growth after individuals reach &eight years in age (Sasaki, 1981).

Due to the nature of shell growth, as well as the sampling methodology used, some 'dampening' of the true seasonal signal Goodwin et al. (2003) is to be expected in such proxies; although micromill sampling resolution is high compared to other techniques, it will still result in some averaging over the true extremes in $\delta^{18}O_{shell}$, which is exacerbated by decreasing increment width as a shell's ontological age increases. We can see this 'dampening' effect in these results, with a calculated temperature range of 15.01 °C, while the range for average observed SST range was higher at 17.43 °C. The overall average temperature across the observed satellite data was 10.62 °C, while the average of the $\delta^{18}O_{shell}$-derived SST calculations is two degrees higher at 12.7 °C. Nonetheless, we can observe a good fit between observed and calculated temperatures, particularly in the overall shape of the temperature curve and around the seasonal peaks in SST. As will be discussed in Section 4.3, this bias towards warmer temperatures and poorer fit around SST minima is unexpected given the seasonality of growth line formation.

5.2. Interpretation of $\delta^{13}C_{shell}$ Results

Interpreting variation in $\delta^{13}C_{shell}$ values in marine carbonates is complex, because it involves several interacting biological and chemical processes such as surface productivity and dissolved carbon content, which in turn depend on the particular oceanographic context in terms of, for example, thermocline depth, prevailing currents, upwelling and salinity (Arthur et al., 1983a,b; Gillikin et al., 2006; McConnaughey and Gillikin, 2008). In this case, $\delta^{13}C_{shell}$ results show significantly less cyclicity than $\delta^{18}O_{shell}$, with a total amplitude of just 1.55‰ (Fig. 4), and a very weak negative correlation between $\delta^{13}C_{shell}$ and $\delta^{18}O_{shell}$. This is similar to the findings of Khim et al. (2000), who also see a smaller overall range and relative stability in $\delta^{13}C_{shell}$ compared to $\delta^{18}O_{shell}$ for this species. They argue that this is related to the shallow growth-depth of *S. sachalinensis*, which live primarily above the thermocline and therefore do not record any major seasonal cycling in DIC. Although we lack growth-depth information for the shells sampled here, we consider that the situation is likely to be similar. The small degree of seasonal cycling that is seen (slightly higher $\delta^{13}C_{shell}$ in the summer/autumn) could relate to increased primary productivity and phytoplankton biomass in the warmer season (Agboola et al., 2013). Overall though, the lack of *in situ* instrumental records (e.g. DIC, salinity) from Tomakomai Bay, as well as detailed species-specific information on the metabolism and physiological incorporation of $\delta^{13}C$, prevents us from drawing more definitive conclusions on the potential of $\delta^{13}C_{shell}$ as a palaeoenvironmental indicator in *S. sachalinensis*.

5.3. Potential confounding factors to $\delta^{18}O_{shell}$ interpretation

One of the main aims of this work was to identify the seasonality of growth minima in *S. sachalinensis* from Tomakomai, as regular interruptions in shell growth result in biased (towards the season of fastest growth) or incomplete SST reconstructions. The ecological literature suggests that growth lines can be triggered variously by excessively warm water (Sasaki, 1981), cold water (Yamamoto, 1947) or by the end of the spawning season (Kato and Hamai, 1975) which falls in spring/early summer for Hokkaido (Kinoshita and Shibuya, 1920; Sasaki, 1981; Sakurai et al., 1992; Takamaru, 1976). In this project, nacreous growth lines were identified during sampling so that the samples representing these minima could be identified in the results. Based on the relationship we have established between $\delta^{18}O_{shell}$ and SST, we can use these results to identify when growth lines form in the seasonal growth cycle.

The dashed lines in Fig. 5 show the locations of growth lines identified during sampling. These data confirm that growth lines occurred on an annual basis, matching expectations from the literature. In all cases where the growth line sample yielded $\delta^{18}O$ data, that sample or one directly adjacent provided the annual peak in SST. This indicates that the growth lines form in later summer/autumn when SST is highest (Table 1). This matches the findings of Sasaki (1981), who attributes this aestival growth interruption to shells located at the southern limits of the species' distribution. Our results show that an aestival growth minimum is not restricted to the southernmost distribution, and extends at least 500 km north of Sendai Bay to southern Hokkaido (the region of most importance for modern commercial harvesting).

For each shell sampled, there was one growth line identified that did not fit this warm-season growth pattern. These are labeled in Fig. 3. On the basis of the isotope results, we suggest that these represent non-annual growth interruptions. Although regular growth lines are expected to form due to predictable annual factors (e.g. seasonal SST, spawning), it is well known that other stressful events can also trigger the formation of growth lines in mollusc species. For example, Schöne (2008) notes that significant storms, or the exposure of shells during neap tides, can also cause this response. In this case, it is possible that a non-annual environmental stressor is responsible for the growth line at sample three, which was then (mis)interpreted as an annually formed growth line. While it is not obvious from the satellite-observed record, it is worth noting that spring 1995 to spring 1996 saw a La Niña event recorded in Japanese waters, indicating colder than average SST (http://ds.data.jma.go.jp/tcc/tcc/products/elnino/ensoevents.html). A potential connection between non-annual growth interruptions and ENSO events in this region warrants further investigation. In cases with sub-annual sampling and clear seasonal cycling, we do not anticipate that misinterpretation of non-annual growth interruptions will be an issue for palaeoenvironmental reconstructions based on isotope evidence, as the combination of macroscopic sclerochronology and $\delta^{18}O_{shell}$ measurements allows for annual and exceptional growth lines to be differentiated.

If researchers were to target annual samples based on growth line analysis of this species then misinterpretation of growth lines could result in errors where certain years are inadvertently sampled twice. This also poses a problem for the accurate aging of individual *S. sachalinensis* specimens, for example in this study the assignment of calendar years to the growth increments was carried out using a count of growth lines seen on the shell. While the isotope results from the region of shell sampled meant that the non-annual lines identified could be factored into this assignment, it is certainly possible that further non-annual lines in the region of shell not sampled could also have been misinterpreted which would shift the calendar age of the sampled region. While none of the discussion in this study rests upon exactly accurate identification of the increments' calendar dates (excepting the

Table 2
Stable isotope data from shells TBMOD1 and TBMOD2 alongside $\delta^{18}O_{shell}$-derived sea surface temperature (SST). Failed samples are greyed out. SST calculations have an uncertainty of ±0.24 °C due to analytical precision based on the aragonite-SST conversion defined in Eq. (1).

Number	Sample ID	$\delta^{18}O$ (‰) VPDB	$\delta^{13}C$ (‰) VPDB	SST (°C)	Comments
1	TBMOD1-101	+0.64	+0.20	13.0	
2	TBMOD1-102	+0.50	+0.26	13.6	
3	TBMOD1-103	+0.40	+0.13	14.0	
4	TBMOD1-104	NA	NA	NA	Growth stoppage
5	TBMOD1-105	+0.26	+0.45	14.6	
6	TBMOD1-106	+0.05	+0.48	15.5	
7	TBMOD1_1	NA	NA	NA	
8	TBMOD1_2	+1.12	+0.17	10.9	
9	TBMOD1_3	NA	NA	NA	Growth stoppage
10	TBMOD1_4	+1.84	+0.25	7.8	
11	TBMOD1_5	+1.90	+0.46	7.5	
12	TBMOD1_6	+2.04	+0.47	6.9	
13	TBMOD1_7	+1.78	+0.49	8.0	
14	TBMOD1_8	+1.98	+0.58	7.2	
15	TBMOD1_9	NA	NA	NA	
16	TBMOD1_10	+1.75	+0.59	8.1	
17	TBMOD1_11	NA	NA	NA	
18	TBMOD1_12	+1.18	+0.77	10.6	
19	TBMOD1_13	+0.97	+0.92	11.5	
20	TBMOD1_14	+1.11	+1.15	10.9	
21	TBMOD1_15	-0.02	+0.69	15.8	
22	TBMOD1_16	+0.17	+0.97	15.0	
23	TBMOD1_17	NA	NA	NA	
24	TBMOD1_18	+0.28	+1.07	14.5	
25	TBMOD1_19	-0.82	+0.34	19.3	Growth stoppage
26	TBMOD1_20	-0.24	+0.28	16.8	
27	TBMOD1_21	+0.01	+0.37	15.7	
28	TBMOD1_22	+1.15	+0.07	10.8	
29	TBMOD1_23	+1.38	+0.15	9.7	
30	TBMOD1_24	+1.68	+0.12	8.5	
31	TBMOD1_25	+1.55	+0.14	9.0	
32	TBMOD1_26	+1.71	+0.23	8.3	
33	TBMOD1_27	+1.60	+0.26	8.8	
34	TBMOD1_28	+1.17	+0.16	10.7	
35	TBMOD1_29	+0.65	+0.19	12.9	
36	TBMOD1_30	+0.46	+0.43	13.7	
37	TBMOD1_31	-0.22	+0.79	16.7	

(*continued on next page*)

Table 2 (*continued*)

38	TBMOD1_32	-0.16	+0.22	16.45	Growth stoppage
39	TBMOD1_33	+0.37	+0.48	14.15	
40	TBMOD1_34	+1.40	+0.22	9.68	
41	TBMOD1_35	NA	NA	NA	
42	TBMOD1_36	+1.33	-0.13	9.96	
43	TBMOD1_37	-0.74	+0.58	18.93	Growth stoppage
44	TBMOD2-1	-0.47	+1.02	17.79	
45	TBMOD2-2	-0.44	+0.91	17.66	
46	TBMOD2-3	+0.04	+0.96	15.57	
47	TBMOD2-4	-0.30	+0.93	17.05	
48	TBMOD2-5	-0.45	+0.84	17.71	
49	TBMOD2-6	-0.26	+0.65	16.89	
50	TBMOD2-7	-0.79	-0.08	19.16	Growth stoppage
51	TBMOD2-8	+0.28	+0.41	14.51	
52	TBMOD2-9	+1.40	+0.72	9.66	
53	TBMOD2-10	+1.73	+1.04	8.21	
54	TBMOD2-11	+1.57	+0.36	8.91	
55	TBMOD2-12	+2.22	+0.41	6.09	
56	TBMOD2-13	+1.35	+0.05	9.89	
57	TBMOD2-14	+1.87	+0.30	7.60	
58	TBMOD2-15	+2.38	+0.57	5.40	
59	TBMOD2-16	+2.23	+0.51	6.06	
60	TBMOD2-17	+1.50	+0.52	9.25	
61	TBMOD2-18	+1.73	+0.74	8.23	
62	TBMOD2-19	+1.62	+0.99	8.72	
63	TBMOD2-20	+1.11	+0.77	10.91	
64	TBMOD2-21	+0.48	+0.25	13.67	
65	TBMOD2-22	-0.21	+0.61	16.67	
66	TBMOD2-23	-0.37	+0.68	17.37	
67	TBMOD2-24	-0.76	+0.74	19.05	
68	TBMOD2-25	-0.37	+0.89	17.36	
69	TBMOD2-26	-0.81	+0.68	19.24	Growth stoppage
70	TBMOD2-27	-0.78	+0.18	19.13	Growth stoppage
71	TBMOD2-28	+0.04	+0.35	15.59	
72	TBMOD2-29	-0.04	+0.38	15.92	
73	TBMOD2-30	+0.80	+0.16	12.28	
74	TBMOD2-31	+1.29	-0.23	10.15	
75	TBMOD2-32	+2.07	-0.40	6.76	
76	TBMOD2-33	+1.78	+0.10	8.03	
77	TBMOD2-34	+0.21	-0.27	14.83	
78	TBMOD2-35	-0.70	+0.61	18.76	
79	TBMOD2-36	-1.08	-0.09	20.41	Growth stoppage
	MIN	-1.08	-0.40	5.40	
	MAX	+2.38	+1.15	20.41	
	RANGE	3.46	1.55	15.01	
	AVERAGE	+0.70	+0.45	12.72	

possible connection between the non-annual growth line and 1995/6 La Niña event mentioned above), in future research this is certainly an issue which should be examined closely and we suggest that where possible isotope analysis should supplement visual examination of growth lines to accurately identify whether they represent an annual growth stoppage.

Based on the positions of the growth lines in the $\delta^{18}O_{shell}$ cycle (aside from the exception outlined above), the shells grew preferentially in the

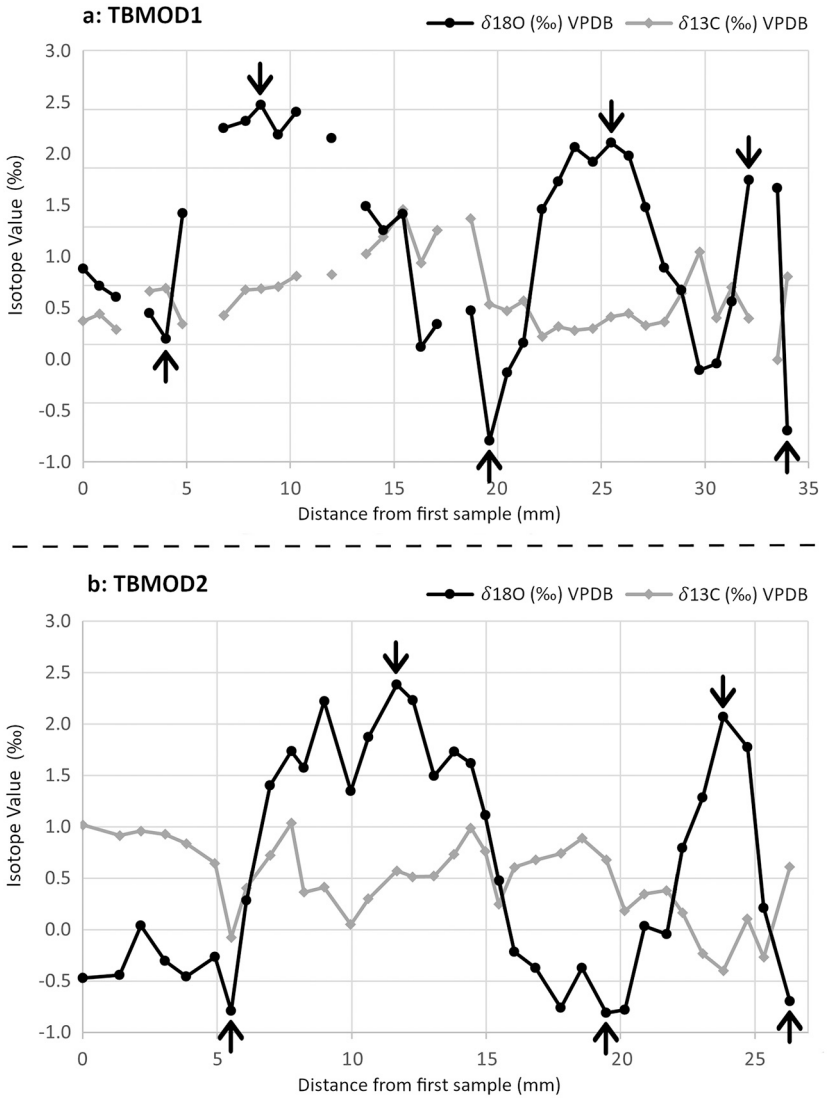


Fig. 4. Graph plotting oxygen and carbon stable isotope results. Peaks and troughs in $\delta^{18}O_{shell}$ marked with arrows. Earliest/closest to umbo shell growth on the left.

cooler part of the year, with growth slowing or stopping completely during the warmest SSTs in late summer/autumn. By comparison to observed satellite data Fig. 5, it appears that growth stoppage occurs during approx. August/September/October. This might suggest that $\delta^{18}O_{shell}$ would not reflect SST extremes during the warmer period of the year. As previously discussed, we would ordinarily expect some degree of 'dampening' of the seasonal temperature extreme from $\delta^{18}O_{shell}$, meaning that it is difficult to tell whether growth slows or stops completely during the formation of the growth line. In either case, we would expect that SST reconstruction would be biased towards the cooler part of the year. In practice, our results show annual SST minima consistently falling outside of the observed range and a minimum calculated SST at 6.9 °C compared to a satellite-observed minimum of 2.27 °C. This suggests that the isotope SST results are slightly offset from the observed satellite data towards warmer temperatures, which in turn means it is difficult to give a more precise estimate of the exact timing and duration of the growth stoppages. In explaining this offset, there are several potential contributing factors that we should consider, all of which are also more generally relevant in terms of the 'dampening' and palaeoclimatic interpretation of seasonal marine carbonate isotope proxies, as discussed below.

5.3.1. *Estimating $\delta^{18}O_{seawater}$*

As the other variable alongside $\delta^{18}O_{shell}$ in the aragonite palaeotemperature equation, misestimation of $\delta^{18}O_{seawater}$, as well as seasonally variable $\delta^{18}O_{seawater}$ has a significant impact on the accuracy of SST reconstructions. In modern cases such as this, the NOAA database can provide a regional measurement, although this is not necessarily a close geographical match, and does not account for variation relating to seasonal currents or depth. In our data, for the difference between observed and calculated minimum SST to be accounted for by a misestimation of $\delta^{18}O_{seawater}$, the $\delta^{18}O_{seawater}$ used would have needed to be at least &0.25‰ lower (at -1.1‰). This would bring the average $\delta^{18}O_{shell}$-derived SST down to 10.68 °C and in line with the average SST observed from satellite data (10.62 °C). A $\delta^{18}O_{seawater}$ value of -1.1‰ would be out of the expected range for the wider region; according to NASA data, within a c. 10 degree (lat/long) radius of Tomakomai Bay, the minimum observed $\delta^{18}O_{seawater}$ was -0.89‰. Furthermore, based on salinity data from the Japan Oceanographic Data Center (https://data.giss.nasa.gov/cgi-bin/o18data) and the salinity:$\delta^{18}O_{seawater}$ equation for the Tsushima current provided by Kodaira et al. (2016), we see that minimum $\delta^{18}O_{seawater}$ is not reached until May, and total seasonal variation is only c. 0.4‰. As the placement of the growth lines indicate warm-season growth interruptions, we would expect that the SST recorded in shell growth to be biased towards colder-season growth with an average

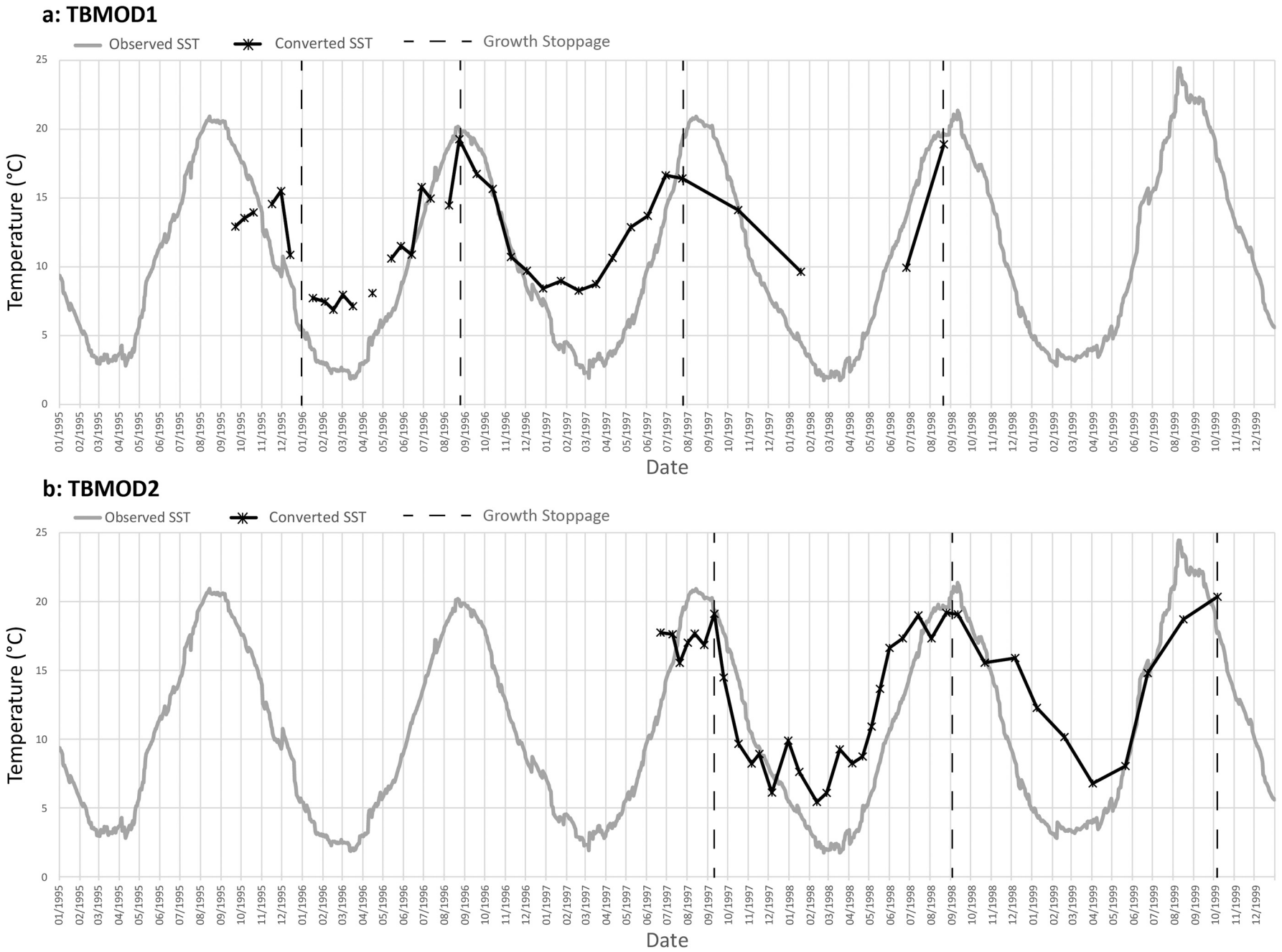


Fig. 5. Temperature estimation based on $\delta^{18}O_{shell}$ results, overlain on average annual SST range for Tomakomai (Table 1) where the annual period has been piece-wise linearly transformed to account for decreasing growth rate.

temperature less than that of the observed data. To achieve this, an even larger reduction in $\delta^{18}O_{seawater}$ would be needed.

Freshwater fluvial input is another consideration, and has the potential to affect coastal $\delta^{18}O_{seawater}$ values without necessarily impacting the measurements of the NOAA database which have been taken further from the shore. Tomakomai bay receives fluvial input from several minor rivers, the largest of which is the Yufutsu River, but unfortunately no $\delta^{18}O$ measurements appear to have be published relating to these inputs. Measurements of precipitation from Tomakomai provide an average annual $\delta^{18}O$ of -9.7‰ (Li, 2017). If shells were harvested from an area of the bay particularly affected by riverine input then this could result in more negative $\delta^{18}O_{seawater}$ values than the -0.85‰ used in the palaeotemperature equation here which would help to explain the temperature offset. Unfortunately, without more precise knowledge of the shell harvest location or in-situ measurements of near-shore $\delta^{18}O_{seawater}$ we are unable to confirm that this is the case. This is therefore an avenue which should be further explored in future studies of this species and region.

5.3.2. Diurnal temperature variation

If extremes of temperature can inhibit shell growth on a seasonal basis, it follows that this could also affect growth on a daily basis if diurnal variation is regularly bringing seawater temperature outside of the preferred range. This could also contribute to biases or 'dampening' in the proxy record. For the Tomakomai coast, diurnal warming (ΔSST) is expected to be small, with models predicting <1 °C ΔSST (Noh et al., 2011). This small variation is confirmed by comparing combined day- and night-time satellite SST data. Therefore, even if *S. sachalinensis* consistently precipitated preferentially during the warmest part of the day during the cooler months, this would not account for the offset in $\delta^{18}O_{shell}$-derived winter temperatures.

5.3.3. Growth depth

In the other available paper addressing stable isotope results for *S. sachalinensis*, the extent to which the full SST range was recorded varied between sampled individuals (Khim et al., 2000). The authors compare $\delta^{18}O_{shell}$-derived SST range to observed SST (using the Grossman and Ku (1986) equation), although they do not present the specific SST calculations or specify the $\delta^{18}O_{seawater}$ value used. Nevertheless, they did not posit any species-wide offset in estimated SST and were confident in the use of *S. sachalinensis* as a SST proxy. Non-equilibrium precipitation is rare in marine molluscs (Twaddle et al., 2016; McConnaughey and Gillikin, 2008), and it would be surprising in this species given that isotopic equilibrium has been shown for its Atlantic sibling, *S. solidissima* (Jones et al., 1983). Instead, Khim et al. (2000) suggest that the differences they observe could relate to the depth at which shells precipitated, although conflicting evidence exists as to whether shallower growth-depth corresponds to increased or decreased annual $\delta^{18}O_{shell}$ range (Krantz et al., 1987; Geary et al., 1992).

As this study is based on data from just two shells, and without detailed information on growth-depth, it is difficult to discuss the potential effects of this factor. Still, it is logical that growth-depth would significantly impact calculated SST, as variable temperature stratification in the top 10 metres of the water column may generate differences between growth-depth water temperature and foundation SST (Göttsche and Olesen, 2017) as modelled from satellite data. For example, Sakaizawa et al. (2018) show that for the Tomakomai coast the temperature at 5 m depth in February is &0.5 °C warmer than the surface temperature. This magnitude of difference would go some, but not all the way to explaining the differences seen between $\delta^{18}O_{shell}$-derived SST results and observed cool-season temperatures. Increased species-specific understanding of the relationship between growth depth and $\delta^{18}O_{shell}$ would be also useful, especially for studies which discuss modern ecology or oceanography.

5.3.4. Sample treatment

Another possible explanation for anomalies seen in the proxy record could be the treatment of the samples after the shell collection that might lead to temperature offsets. Boiling of the shells is a potential concern for stable isotope analysis, as it has the potential to encourage isotopic exchange and so alter the original $\delta^{18}O_{shell}$ value. Milano et al. (2016) showed that for the aragnoitic portion of gastropod *Phorcus turbinatus*, boiling at 100 °C did not produce significant isotopic exchange. They did see isotopic exchange in hotter temperatures (e.g. 300+ °C) and roasting conditions, but shifts in $\delta^{18}O_{shell}$ were also accompanied by visible changes in shell microstructure. Müller et al. (2017) suggested that $\delta^{18}O_{shell}$ may be slightly lowered by boiling, but do acknowledge that the differences seen between theirs and Milano et al.'s (2016) results were likely primarily due to experimental design. On the other hand, Moon et al. (2018) found that for *Spisula solidissima*, a shift in $\delta^{18}O_{shell}$ can occur even with 'negligible' mineralogical change and no calcite recrystallisation. This study looked at dry heat rather than boiling, but nonetheless raises the issue of heat-induced shifts in $\delta^{18}O_{shell}$, even for shells which appear to preserve seasonal cycling. For the shells used in this study, the length of boiling was <20 minutes, so significantly under the 40 minutes used by Müller et al. (2017), and no changes in shell microstructure are visible to the naked eye.

Moon et al. (2018) suggest that isotopic exchange is possible even without visible change in shell microstructure, and according to Müller et al. (2017), boiling for 15 minutes can result in a change of -0.5‰ in $\delta^{18}O_{shell}$. In the present study FTIR-ATR (attenuated total reflectance Fourier transform infrared spectroscopy) was used to specifically check for recrystallisation of shell aragonite, for which no evidence was found. This means that extreme diagenetic alteration (of aragonite into calcite) has not occurred, but there is still the possibility that a small but significant systemic shift in $\delta^{18}O_{shell}$ could have occurred. Correcting for a -0.5‰ shift, as per Müller et al. (2017) would result in the $\delta^{18}O_{shell}$-derived SST results shifting down towards colder temperatures with an overall average temperature of 9.60 °C. This would be more in keeping with the observed SST.

5.4. Implications for palaeothermometry

One aim of this research was to assess the utility of *S. sachalinensis* as a palaeothermometer in archaeological studies. As outline in the introduction, the importance of marine resources over the past 7000 years of Hokkaido's history means that shellfish remains are a common element of archaeological assemblages, and the unique hunter-gatherer development in Hokkaido means that there are gaps in our palaeoenvironemntal understanding of this region as compared to much of the rest of Japan,

In terms of carbon isotopes, our results show a slight but statistically insignificant covariance between high $\delta^{18}O_{shell}$/low $\delta^{13}C_{shell}$, with slightly higher $\delta^{13}C_{shell}$ values in summer and autumn potentially related to primary productivity. However, due to the lack of clear seasonal cycling and the complex relationship between $\delta^{13}C_{shell}$, oceanography and climate in similar species, we can't currently suggest a way that $\delta^{13}C_{shell}$ in *S. sachalinensis* can be employed as an effective sub-annual palaeoclimatic indicator.

By contrast, there is a strong case for the use of stable isotope analysis on *S. sachalinensis* as a palaeothermometer. Clear cyclicity can be seen in $\delta^{18}O_{shell}$, and based on comparison to observed SST and the position of growth lines, we are confident that ambient water temperature is the main driver. $\delta^{18}O_{shell}$ therefore has the potential to provide information on annual and sub-annual climate which should add important climatic and oceanographic context to the archaeological record.

However, as previously discussed and as expected for proxies of this kind, $\delta^{18}O_{shell}$ in this species does not necessarily appear to record the complete annual range of SST. There are a number of factors relating to the specific growth conditions, local oceanography and sample treatment that should be considered as far as possible within a palaeoclimatic

or archaeological context. For example, exact specimen growth depth will always be an unknown quantity when dealing with archaeological material, but assuming a relatively consistent depth range of 1–15 m for *S. sachalinensis* as well as the fact that prehistoric gatherers would have been more likely to collect preferentially at relatively shallow depths, this uncertainty can be fairly well constrained.

The growth pattern of the species, with rapid growth allowing sub-annual incremental sampling until eight to nine years of age, means that *S. sachalinensis* could be used to produce a SST proxy at either an inter- or intra-annual resolution. Furthermore, if young, fast-growing, shells are found in an archaeological context it should be possible to use growth-edge samples to estimate season of collection and/or site occupation. This technique was first proposed by Shackleton (1973), and has since been a common feature of stable isotope research in archaeomalacology (e.g. Bosch et al., 2018; Burchell et al., 2013; Jew et al., 2013; Mannino et al., 2007). However, it relies on fast-growing increments at the shell edge so would only be appropriate for archaeological *S. sachalinensis* ontogenetically younger than &eight years. Given archaeological biases towards larger, more meat-rich specimens, suitable shells are not likely to be commonly encountered except in cases of local resource over-exploitation.

Clumped isotope measurements as a palaeoclimatic proxy within *Spisula sachalinensis* may be a means to circumvent some of the issues identified here. This approach has been successfully used to provide seasonal climate reconstructions from Cretaceous bivalves (de Winter et al., 2020), and has the benefit of being independent from estimations of past $\delta^{18}O_{seawater}$ (Eiler, 2007; Henkes et al., 2013), which we have already noted among the confounding factors of temperature interpretation. This will be especially relevant for prehistoric and deep-time bivalves where historical records of seawater composition can't be relied upon, but could also be useful in cases of extreme seasonal variation in $\delta^{18}O_{seawater}$ which can be hard to incorporate into palaeoclimate models.

6. Conclusions

These results confirm the inverse relationship between $\delta^{18}O_{shell}$ and SST in *Spisula sachalinensis*, as previously identified for long-lived clam species in other regions, and indicate that shells from Tomakomai form a warm-season growth line. When compared to satellite-recorded SST, $\delta^{18}O_{shell}$-derived temperatures fall within the expected range for the region and show clear seasonal cycling. This demonstrates the potential utility of this species as a SST archive in both modern and palaeoclimatic contexts. Possible biases in this record include sample treatment, growth depth and $\delta^{18}O_{seawater}$, but further investigation is required to determine the extent to which these affect SST estimation.

This study also highlights complexities in *S. sachalinensis* growth that suggest the need for caution during macro/microscopic sclerochronological assessment. For example, not only is there is evidence for variation in growth line formation both between geographically distant shells (e.g. at the southern or northern limits of distribution) but we have also shown that this variation can occur within a single shell (e.g. the anomalous cool-season line observed in TBMOD1). Given these issues, we suggest that stable oxygen isotope analysis in combination with visual macro- and microscopic assessment of shell growth is the most reliable route to *S. sachalinensis* palaeothermometry.

Declaration of Competing Interest

The authors declare that they have no known competing financial interests or personal relationships that could have appeared to influence the work reported in this paper.

Acknowledgements

This work was supported by a NEIFSC project grant [IP-1944-1119]; and a Clarendon Fund Scholarship. Thanks also to Taena Uemura for her help in arranging access to the samples, and to Hilary Sloane for her role in the sample preparation and mass spectrometry process.

References

Abe, C., Leipe, C., Tarasov, P.E., Müller, S., Wagner, M., 2016. Spatio-temporal distribution of hunter-gatherer archaeological sites in the Hokkaido region (northern Japan): an overview. Holocene 26, 1627–1645. https://doi.org/10.1177/0959683616641745.

Agboola, J.I., Uchimiya, M., Kudo, I., Osawa, M., Kido, K., 2013. Seasonality and environmental drivers of biological productivity on the western hokkaido coast, ishikari bay, japan. Estuar. Coast. Shelf Sci. https://doi.org/10.1016/j.ecss.2013.03.008.

Arthur, M.A., Anderson, T.F., Kaplan, I.R., Veizer, J., Land, L.S., 1983a. Stable Isotopes in Sedimentary Geology. SEPM Society for Sedimentary Geology. https://doi.org/10.2110/scn.83.10.

Arthur, M.A., Williams, D.F., Jones, D.S., 1983b. Seasonal temperature- salinity changes and thermocline development in the mid- Atlantic Bight as recorded by the isotopic composition of bivalves. Geology 11, 655–659 doi:10.1130/0091-7613(1983)11<655:STCATD>2.0.CO;2.

Bosch, M.D., Mannino, M.A., Prendergast, A.L., Wesselingh, F.P., O'Connell, T.C., Hublin, J.J., 2018. Year-round shellfish exploitation in the Levant and implications for Upper Palaeolithic hunter-gatherer subsistence. J. Archaeol. Sci. Rep. 21, 1198–1214. https://doi.org/10.1016/j.jasrep.2017.08.014.

Burchell, M., Hallmann, N., Martindale, A., Cannon, A., Schöne, B.R., 2013. Seasonality and intensity of shellfish harvesting on the north coast of british columbia. J. Island Coast. Archaeol. https://doi.org/10.1080/15564894.2013.787566.

Butler, P.G., Wanamaker, A.D., Scourse, J.D., Richardson, C.A., Reynolds, D.J., 2013. Variability of marine climate on the North Icelandic Shelf in a 1357-year proxy archive based on growth increments in the bivalve Arctica islandica. Palaeogeogr. Palaeoclimatol. Palaeoecol. https://doi.org/10.1016/j.palaeo.2012.01.016.

Craig, H., 1957. Isotopic standards for carbon and oxygen and correction factors for mass-spectrometric analysis of carbon dioxide. Geochim. Cosmochim. Acta. https://doi.org/10.1016/0016-7037(57)90024-8.

Demaree, G.R., Mikami, T., Tsukahara, T., Zaiki, M., 2013. The meteorological Observations of the "Vereenigde Oost-Indische Compagnie (VOC)"-What can be learned from them? 歴史地理学 55-5, 99–106.

Dettman, D.L., Reische, A.K., Lohmann, K.C., 1999. Controls on the stable isotope composition of seasonal growth bands in aragonitic fresh-water bivalves (unionidae). Geochim. Cosmochim. Acta 63, 1049–1057. https://doi.org/10.1016/S0016-7037(99)00020-4.

Eiler, J.M., 2007. Clumped-isotope" geochemistry - The study of naturally-occurring, multiply-substituted isotopologues. Earth Planet. Sci. Lett. 262, 309–327. https://doi.org/10.1016/j.epsl.2007.08.020.

Emiliani, C., Cardini, L., Mayeda, T., McBurney, C., Tongiorgi, E., 1964. Palaeotemperature analysis of marine molluscs (food refuse) from the site of Arene Candide cave, Italy and the Haua Fteah cave, Cyrenaica. In: Craig, H., Miller, S., Wasserburg, G. (Eds.), Isotopic and Cosmic Chemistry. North-Holland Publishing Company, Amsterdam, pp. 133–156.

Geary, D.H., Brieske, T.A., Bemis, B.E., 1992. The influence and interaction of temperature, salinity, and upwelling on the stable isotopic profiles of strombid gastropod shells. PALAIOS. https://doi.org/10.2307/3514797.

Gillikin, D.P., Lorrain, A., Bouillon, S., Willenz, P., Dehairs, F., 2006. Stable carbon isotopic composition of Mytilus edulis shells: relation to metabolism, salinity, δ13CDIC and phytoplankton. Org. Geochem. 37, 1371–1382. https://doi.org/10.1016/j.orggeochem.2006.03.008.

Golikov, A.N., Scarlato, O.A., 1970. Abundance, dynamics and production properties of populations of edible bivalves Mizuhopecten yessoensis and Spisula sachalinensis related to the problem of organization of controllable submarine farms at the Western shores of the Sea of Japan. Helgoländer Wissenschaftliche Meeresuntersuchungen 20, 498–513. https://doi.org/10.1007/BF01609925.

Goodwin, D.H., Schöne, B.R., Dettman, D.L., Goodwin, D.H., Schone, B.R., Dettman, D.L., 2003. Resolution and Fidelity of Oxygen Isotopes as Paleotemperature Proxies in Bivalve Mollusk Shells: Models and Observations, 18. SEPM Society for Sedimentary Geology, pp. 110–125.

Göttsche, F., Olesen, F.S., 2017. Fiducial Reference Measurements for Validation of Surface Temperature from Satellites (FRM4STS) Technical Report 3: A Framework to Verify the Field Performance of TIR FRM, European Space Agency Technical Reports, 3.

Grossman, E.L., Ku, T.L., 1986. Oxygen and carbon isotope fractionation in biogenic aragonite: temperature effects. Chem. Geol. Isot. Geosci. Sect. 59, 59–74. https://doi.org/10.1016/0168-9622(86)90057-6.

Habu, J., Matsui, A., Yamamoto, N., Kanno, T., 2011. Shell midden archaeology in Japan: aquatic food acquisition and long-term change in the Jomon culture. Quat. Int. 239, 19–27. https://doi.org/10.1016/j.quaint.2011.03.014.

Henkes, G.A., Passey, B.H., Wanamaker, A.D., Grossman, E.L., Ambrose, W.G., Carroll, M.L., 2013. Carbonate clumped isotope compositions of modern marine mollusk and brachiopod shells. Geochim. Cosmochim. Acta 106, 307–325. https://doi.org/10.1016/j.gca.2012.12.020.

Hirose, N., ichi Fukudome, K., 2006. Monitoring the Tsushima warm current improves seasonal prediction of the regional snowfall. Sci. Online Lett. Atmos. 2, 61–63. https://doi.org/10.2151/sola.2006-016.

Hudson, M.J., 2014. The Ethnohistory and Anthropology of 'Modern' Hunter-Gatherers: North Japan (Ainu). In: Cummings, V., Jordan, P., Zvelebil, M. (Eds.), The Oxford Handbook of the Archaeology and Anthropology of Hunter-Gatherers. Oxford Unversity Press.

Imada, Y., Maeda, S., Watanabe, M., Shiogama, H., Mizuta, R., Ishii, M., Kimoto, M., 2017. Recent enhanced seasonal temperature contrast in Japan from large ensemble high-resolution climate simulations. Atmosphere 8, 1–13. https://doi.org/10.3390/atmos8030057.

Jew, N.P., Erlandson, J.M., Rick, T.C., Watts, J., 2013. Shellfish, seasonality, and sedentism: δ18O analysis of california mussels from early holocene shell middens on san miguel island, California. Pac. Archaeol. 4.

Jones, D.S., Williams, D.F., Arthur, M.A., 1983. Growth history and ecology of the Atlantic surf clam, Spisula solidissima (Dillwyn), as revealed by stable isotopes and annual shell increments. J. Exp. Mar. Biol. Ecol. 73, 225–242. https://doi.org/10.1016/0022-0981(83)90049-7.

Kato, Y., Hamai, I., 1975. Growth and shell formation of the surf clam, spisula sachalinensis (Schrenck). Bulletin of the faculty of fisheries. Hokkaido University 25, 291–303.

Khim, B.K., Woo, K.S., Je, J.G., 2000. Stable isotope profiles of bivalve shells: seasonal temperature variations, latitudinal temperature gradients and biological carbon cycling along the east coast of Korea. Cont. Shelf Res. 20, 843–861. https://doi.org/10.1016/S0278-4343(00)00004-2.

Kinoshita, T., Shibuya, S., 1920. Muroran Oyobi Kamiiso San Hokkigai No Sanranki. Hokusuisi Jumpo, 4-5.

Kodaira, T., Horikawa, K., Zhang, J., Senjyu, T., 2016. 日本海対馬暖流域における海水の酸素同位体比と塩分の関係 (relationship between seawater oxygen isotope ratio and salinity in the tsushima current, the sea of japan). Chikyukagaku (Geochemistry) 50, 263–277. https://doi.org/10.14934/chikyukagaku.50.263.

Können, G.P., Zaiki, M., Baede, A.P., Mikami, T., Jones, P.D., Tsukahara, T., 2003. Pre-1872 extension of the Japanese instrumental meteorological observation series back to 1819. J. Clim. 16, 118–131 doi:10.1175/1520-0442(2003)016<0118:PEOTJI>2.0.CO;2.

Krantz, D.E., Williams, D.F., Jones, D.S., 1987. Ecological and paleoenvironmental information using stable isotope profiles from living and fossil molluscs. Palaeogeogr. Palaeoclimatol. Palaeoecol. https://doi.org/10.1016/0031-0182(87)90064-2.

Lee, J.Y., Chang, Y.J., Park, Y.J., 1996. Spawning induction and egg development of surf clam, spisula sachalinensis. J. Aquac. (한국양식학회지) 9, 419–427.

Leng, M.J., Lewis, J.P., 2016. Oxygen isotopes in Molluscan shell: applications in environmental archaeology. Environ. Archaeol. 21, 295–306. https://doi.org/10.1179/1749631414y.0000000048.

Li, X., 2017. Study on Stable Isotopes of Precipitation in Hokkaido, North Japan. https://doi.org/10.14943/doctoral.r7033. Ph.D. thesis.

Loftus, E., Rogers, K., Lee-Thorp, J., 2015. A simple method to establish calcite: aragonite ratios in archaeological mollusc shells. J. Quat. Sci. 30, 731–735. https://doi.org/10.1002/jqs.2819.

Makino, M., 2011. Fisheries Management in Japan: Its Institutional Features and Case Studies. https://doi.org/10.1007/978-94-007-1777-0.

Mann, R., Munroe, D., Powell, E., Hofmann, E., Klinck, J., 2013. Bivalve Molluscs: Barometers of Climate Change in Arctic Marine Systems. In: Mueter, F., Dickson, D., Huntingdon, H., Irvine, J., Logerwell, E., MacLean, S., Quakenbush, L., Rosa, C. (Eds.), Responses of Arctic Marine Ecosystems to Climate Change. University of Alaska Fairbanks, pp. 61–82. https://doi.org/10.4027/ramecc.2013.04.

Mannino, M.A., Thomas, K.D., Leng, M.J., Piperno, M., Tusa, S., Tagliacozzo, A., 2007. Marine resources in the mesolithic and neolithic at the Grotta dell'Uzzo (Sicily): evidence from isotope analyses of marine shells. Archaeometry 49, 117–133. https://doi.org/10.1111/j.1475-4754.2007.00291.x.

Marullo, S., Minnett, P., Santoleri, R., Tonani, M., 2016. The diurnal cycle of sea-surface temperature and estimation of the heat budget of the mediterranean sea. J. Geophys. Res. Oceans 121, 6762–6778. https://doi.org/10.1002/2016JC012132.Received.

McConnaughey, T.A., Gillikin, D.P., 2008. Carbon isotopes in mollusk shell carbonates. Geo-Mar. Lett. 28, 287–299. https://doi.org/10.1007/s00367-008-0116-4.

Mikami, T., 2008. Climatic variations in Japan reconstructed from historical documents. Weather 63, 190–193. https://doi.org/10.1002/wea.281.

Milano, S., Prendergast, A.L., Schöne, B.R., 2016. Effects of cooking on mollusk shell structure and chemistry: implications for archeology and paleoenvironmental reconstruction. J. Archaeol. Sci. Rep. 7, 14–26. https://doi.org/10.1016/j.jasrep.2016.03.045.

Moon, L.R., Judd, E.J., Thomas, J., Ivany, L.C., 2018. Out of the oven and into the fire: Unexpected preservation of the seasonal δ18O cycle following heating experiments on shell carbonate. Palaeogeogr. Palaeoclimatol. Palaeoecol. 532.

Müller, P., Staudigel, P.T., Murray, S.T., Vernet, R., Barusseau, J.P., Westphal, H., Swart, P.K., 2017. Prehistoric cooking versus accurate palaeotemperature records in shell midden constituents. Sci. Rep. https://doi.org/10.1038/s41598-017-03715-8.

Nagasaki, F., 1994. Beef-Eating Culture and Fish-Eating Culture. Nousangyoson-bunka-kyokai, Tokyo.

Noh, Y., Lee, E., Kim, D.H., Hong, S.Y., Kim, M.J., Ou, M.L., 2011. Prediction of the diurnal warming of sea surface temperature using an atmosphere-ocean mixed layer coupled model. J. Geophys. Res. Oceans 116, 1–15. https://doi.org/10.1029/2011JC006970.

Ohnuki-Tierney, E., 1976. Regional variations in ainu culture. Am. Ethnol. 3, 297–329. https://doi.org/10.1525/ae.1976.3.2.02a00080. URL: http://onlinelibrary.wiley.com/doi/10.1525/ae.1976.3.2.02a00080/abstract.

Oikawa, A., 1995. Kaizuka database no suryo-teki bunseki. (Quantitative analysis of shell-mound database). Jinbun Kagaku to Computer (Humanities and Computer) 25, 59–66.

Okada, H., 1998. Maritime adaptations in Northern Japan. Arct. Anthropol. 35, 335–339. URL: http://muse.jhu.edu/content/crossref/journals/asian_perspectives/v045/45.1matsumura.pdf.

Sakaizawa, R., Kawai, T., Sato, T., Oyama, H., Tsumune, D., Tsubono, T., Goto, K., 2018. The inclusion of ocean-current effects in a tidal-current model as forcing in the convection term and its application to the mesoscale fate of CO2 seeping from the seafloor. Ocean Model. 123, 40–54. https://doi.org/10.1016/j.ocemod.2018.01.001.

Sakurai, I., Miyamoto, T., Kurata, M., 1992. Breeding season of the Japanese surf clam Pseudocardium sybillae in Tomakomai and Shizunai, southwest Hokkaido. Scientific Reports of the Hokkaido Fisheries Experimental Station 39, 45–52.

Sakurai, I., Seto, M., 1998. Behavioral characteristics of the juvenile japanese surf clam pseudocardium sachalinensis in response to sand erosion and deposition associated with oscillatory water flow. Fish. Sci. 64, 367–372.

Sasaki, K., 1981. Growth of the sakhalin surf clam, spisula sachalinensis (SCHRENCK), in Sendai Bay. Tohoku J. Agric. Res. 32, 168–180.

Sasaki, K., 1989. Characteristics of the bottom sediments inhabited by the surf clam spisula sachalinensis in Sendai Bay. Nippon Suisan Gakkaishi. 55, 1127–1131.

Sasaki, S., Ohta, T., 1999. Seasonal variation of chemical components in surf clam (Spisula sachalinensis). Food Sci.Technol.Res. 5, 313–315.

Schmidt, G.A., Bigg, G.R., Rohling, E.J., 1999. Global Seawater Oxygen-18 Database - v1.22. URL: https://data.giss.nasa.gov/o18data/.

Schöne, B.R., 2008. The curse of physiology - Challenges and opportunities in the interpretation of geochemical data from mollusk shells. Geo-Mar. Lett. 28, 269–285. https://doi.org/10.1007/s00367-008-0114-6.

Schöne, B.R., Fiebig, J., Pfeiffer, M., Gleß, R., Hickson, J., Johnson, A.L., Dreyer, W., Oschmann, W., 2005. Climate records from a bivalved methuselah (Arctica islandica, Mollusca; Iceland). Palaeogeogr. Palaeoclimatol. Palaeoecol. 228, 130–148. https://doi.org/10.1016/j.palaeo.2005.03.049.

Seaton, P., 2017. Japanese empire in Hokkaido. https://doi.org/10.1093/acrefore/9780190277727.013.76. URL: http://asianhistory.oxfordre.com/view/10.1093/acrefore/9780190277727.001.0001/acrefore-9780190277727-e-76.

Selin, N.I., 2010. The growth and life span of bivalve mollusks at the northeastern coast of Sakhalin Island. Russ. J. Mar. Biol. 36, 258–269. https://doi.org/10.1134/S1063074010040048.

Seo, H., Kwon, Y.O., Park, J.J., 2013. On the effect of the East/Japan Sea SST variability on the North Pacific atmospheric circulation in a regional climate model. J. Geophys. Res. 119, 418–444. https://doi.org/10.1038/175238c0.

Shackleton, N.J., 1973. Oxygen isotope analysis as a means of determining season of occupation of prehistoric midden sites. Archaeometry 15, 133–141. https://doi.org/10.1111/j.1475-4754.1973.tb00082.x.

Stuart, C., 2020. Python Script for Extracting SST Data from NOAA Database. URL: https://github.com/christuart/ghrsst.

Tabakaeva, O.V., Tabakaev, A.V., 2017. Lipids and fatty acids from soft tissues of the bivalve mollusk Spisula Sachalinensis. Chem. Nat. Comp. 53, 16–20. https://doi.org/10.1007/s10600-017-1900-z.

Takahashi, N., Yamamoto, K., 1970. Histological studies on the reproductive cycle of the surf clam, Spisula sachalinensis. Seasonal changes in the ovary. Bull. Jap. Soc. Sci. Fish. 36, 345–352.

Takamaru, N., 1976. On the breeding season of the surf clam, Spisula sachalinensis (Schrenk) in Tokachi. Journal of Hokkaido Fisheries Experimental Station 33, 1–8.

Takano, Y., Tachibana, Y., Iwamoto, K., 2008. Influences of large-scale atmospheric circulation and local sea surface temperature on convective activity over the sea of Japan in December. Sci. Online Lett. Atmos. 4, 113–116. https://doi.org/10.2151/sola.2008-029.

Twaddle, R.W., Ulm, S., Hinton, J., Wurster, C.M., Bird, M.I., 2016. Sclerochronological analysis of archaeological mollusc assemblages: methods, applications and future prospects. Archaeol. Anthropol. Sci. 8, 359–379. https://doi.org/10.1007/s12520-015-0228-5.

de Winter, N., Müller, I., Kocken, I., Thibault, N., Ullmann, C.V., Farnsworth, A., Lunt, D., Claeys, P., Ziegler, M., 2020. First absolute seasonal temperature estimates for greenhouse climate from clumped isotopes in bivalve shells. (Preprint). https://doi.org/10.21203/rs.3.rs-39203/v1.

Yamamoto, K., 1947. Hokkigai no seicho ni tsuite. Sapporo norin-gakkin-ho (Journal of the Sapporo Society of Agriculture and Forestry) 36, 51–62.

Check for updates

Received: 4 February 2022 | Revised: 5 April 2022 | Accepted: 24 April 2022

DOI: 10.1002/rcm.9318

RESEARCH ARTICLE

Rapid Communications in Mass Spectrometry WILEY

Micromilling vs hand drilling in stable isotope analyses of incremental carbonates: The potential for $\delta^{13}C$ contamination by embedding resin

Tansy Branscombe[1] | Julia Lee-Thorp[1] | Rick Schulting[1] | Melanie Leng[2,3]

[1]School of Archaeology, University of Oxford, Oxford, UK

[2]National Environmental Isotope Facility, British Geological Survey, Nottingham, UK

[3]School of Biosciences, University of Nottingham, Loughborough, UK

Correspondence
T. Branscombe, School of Archaeology, University of Oxford, 1 South Parks Road, Oxford OX1 3TG, UK.
Email: tansy.branscombe@bnc.ox.ac.uk

Funding information
Clarendon Fund; National Environmental Isotope Facility, Grant/Award Number: IP-1944-1119

Rationale: Embedding resins are commonly used to facilitate high-resolution sampling for stable isotope analysis but anomalous $\delta^{13}C$ values have been observed in some cases. Here we compare the results of microsampling strategies for hand-drilled versus resin-embedded micromilled samples from the same marine shells to assess whether resin contamination is implicated in $\delta^{13}C$ spikes. The comparison allows assessment of the relative benefits for spatial resolution, seasonal range for both $\delta^{18}O$ and $\delta^{13}C$, and sample failure rates.

Methods: Hand-drilled samples were obtained from two bivalve shells (*Spisula sachalinensis*), corresponding to micromilled samples on the same shells where high $\delta^{13}C$ spikes were observed. All carbonate powders were analysed using a dual-inlet Isoprime mass spectrometer and Multiprep device. Results from both sample sets were compared statistically.

Results: No anomalous high $\delta^{13}C$ values and no failures due to insufficient gas were observed in the hand-drilled samples in contrast to the embedded micromilled sequences. Spatial resolution was reduced ($\sim$2.5$\times$) in the former compared with the latter, resulting in a small reduction in the total range observed in the micromilled $\delta^{13}C$ and $\delta^{18}O$ values. Reduced sampling resolution between the two datasets was only significant for $\delta^{18}O$.

Conclusions: For *S. sachalinensis* (as with other similar bivalves), rapid growth mitigates the reduced sampling resolution of hand drilling and does not significantly impact observed isotopic range and seasonal patterning. Occurrence of anomalous $\delta^{13}C$ values were eliminated and failure rates due to insufficient sample size greatly reduced in the hand-drilled dataset. We can find no other explanation for the occurrence of $\delta^{13}C$ spikes than contamination by the embedding agent. We conclude that the logistical and interpretational benefits of careful hand drilling may be preferable to resin embedding for micromilling in marine shells, corals or speleothems where growth rate is rapid and the highest resolution is not required.

This is an open access article under the terms of the Creative Commons Attribution License, which permits use, distribution and reproduction in any medium, provided the original work is properly cited.
© 2022 The Authors. *Rapid Communications in Mass Spectrometry* published by John Wiley & Sons Ltd.

10970231, 2022, 14, Downloaded from https://analyticalsciencejournals.onlinelibrary.wiley.com/doi/10.1002/rcm.9318 by Test, Wiley Online Library on [20/10/2022]. See the Terms and Conditions (https://onlinelibrary.wiley.com/terms-and-conditions) on Wiley Online Library for rules of use; OA articles are governed by the applicable Creative Commons License

1 | INTRODUCTION

Carbon and oxygen stable isotope ($\delta^{13}C/\delta^{18}O$) analysis of marine bivalves can be used to provide (palaeo)environmental information on marine conditions, including water temperature,[1–4] salinity[5] and productivity,[6,7] as well as biogeographic information on the species analysed.[8–10] Depending on the size and shape of the material/species being sampled, and the resolution and precision requirements of the study, a variety of sampling techniques can be used to produce powder samples for mass spectrometry analysis. These have been discussed by other authors, primarily referring to hand drilling (sometimes known as microdrilling, but referred to as hand drilling throughout this paper), micromilling, SIMS (Secondary Ion Mass Spectrometry) and laser ablation techniques in the sampling of marine and freshwater carbonates such as mollusc shells, corals and otoliths,[9,11] as well as in the related field of speleothem research.[12–15]

Although SIMS and laser ablation are increasingly used, hand drilling and micromilling remain the most commonly used sampling methods,[11,16] due to their balance of accessibility, precision and resolution, and because they produce the powdered samples necessary for high-precision MC-ICPMS (Multicollector Inductively Coupled Plasma Mass Spectrometry) and ICP-AES (Inductively Coupled Plasma Atomic Emission Spectroscopy).[17–19] Micromilling provides the opportunity to precisely mill from very specific regions of the sample and at high resolution, but is more time consuming than hand drilling and the equipment is often temperamental. The collection of micromilled powder samples is most commonly accomplished manually using a combination of scalpels and razor blades,[16] so the process requires a flat and relatively wide sampling surface. This means that in order to be micromilled, most materials need sectioning in order to provide such a surface. In the case of fragile or small/thin material (including, e.g., shells and otoliths) this also necessitates embedding specimens in a stabilising medium to make them less susceptible to breakage, and to increase the size of the flat surface available when collecting samples. The embedding and sectioning process can be laborious, further increasing the time and resources required for this approach.

By contrast, hand drilling is expedient and inexpensive. Depending on the size of the drill bit, it usually produces larger sample sizes, although with lower resolution due to increased time averaging within and between samples. Unlike micromilling, hand drilling can be performed on flat or curved surfaces. This allows sampling to be done around the curve of a shell and reduces the need for extensive preparation of the sampling surface.

This study was prompted by the results of $\delta^{13}C$ and $\delta^{18}O$ analysis on archaeological samples of the marine bivalve *Spisula sachalinensis* – a large and long-lived bivalve found in the northwest Pacific.[20] Results were obtained from a resin-embedded specimen which had been sampled using a computer-operated New Wave Research MicroMill. $\delta^{18}O$ values show a seasonal annual temperature curve as expected, but the $\delta^{13}C$ record of two of the seven shells showed regions where the values were significantly more positive than expected (up to ~5‰). These positive spikes were especially apparent when compared with the rest of the sequences from these individual shells, as well as results from other shells analysed, where $\delta^{13}C$ is relatively stable at $\sim +1 \pm 0.5$‰.

S. sachalinensis is a well-researched species,[20–29] and sudden positive $\delta^{13}C$ excursions of this nature are ecologically implausible. The species lives above the thermocline at depths <15 m,[23,28–30] where there is not a high degree of seasonal change in surrounding seawater DIC (dissolved inorganic carbon). We therefore expect relative stability in shell $\delta^{13}C$ values. Moreover, $\delta^{13}C$ values as high as ~5‰ would be considered implausibly high in all cases for marine bivalves. In McConnaughey and Gillikin's[6] overview of the physiological and environmental controls affecting shell $\delta^{13}C$ values, there is no mention of any condition or species where marine shell $\delta^{13}C$ would near 5‰, nor any mechanism that could account for such large and sudden spikes in $\delta^{13}C$. We are unaware of any literature that reports shell $\delta^{13}C$ values this high and considers it a true reflection of the growing shell's isotopic composition. The large $\delta^{13}C$ excursions seen in these two specific shells (labelled II_1 and VIII_3) discussed in this paper were therefore considered highly anomalous, leading us to investigate the potential role of sample preparation and sampling strategy in affecting $\delta^{13}C$ results.

As the micromilled shells were embedded in polyester resin prior to sampling, one possible consideration is resin contamination. Polyester and epoxy resins are both complex organic polymers[31] commonly used in stable isotope analysis of carbonates to impregnate or embed materials and enable sampling. Despite the widespread use of these resins, and the fact that the tiny carbonate sample sizes mean that even miniscule contaminant contributions could significantly influence isotope results, research into their potential as an isotopic contaminant is uncommon. Mortensen et al[32] undertook a direct comparison between $\delta^{13}C$ and $\delta^{18}O$ values in aragonite coral septa, analysing a series of resin-embedded septa alongside a non-embedded control sample. They saw a 0.12‰ enrichment in $\delta^{18}O$ and a 0.17‰ depletion in $\delta^{13}C$, but in the context of their analysis this was not considered significant as these differences were smaller than their inter-sample variation. This study has since been cited as evidence that polyester resin 'does not contribute to the CO_2 evolved by acid digestion that is used for the isotopic measurements'.[33]

However, the study of Mortensen et al[32] dates to 1998, and the effects of a 0.12‰ $\delta^{18}O$ enrichment and a 0.17‰ $\delta^{13}C$ depletion are greater than the average analytical precision of modern mass spectrometry, which is usually ~ ±0.06‰ for carbonate samples (e.g. Radke et al[34]). At the British Geological Survey (BGS), where the isotopic analysis used in this study was carried out, precision is routinely <0.05‰. A more recent study by Schöne et al[35] investigated a number of different pretreatment methods and sample preparation materials, finding that contamination of carbonate standards by commonly used resin 'glues', including the Kleer-Set resin discussed in this paper, can produce *at least* moderate isotopic shifts. Furthermore, Rodríguez de Vera et al[31] suggest that polyester resins can have a significant 'interference effect' on compound-specific mass spectrometry of lipids in archaeological sediments, particular affecting $\delta^{13}C_{18:0}$. Resin-associated analytical issues have

10970231, 2022, 14, Downloaded from https://analyticalsciencejournals.onlinelibrary.wiley.com/doi/10.1002/rcm.9318 by Test, Wiley Online Library on [20/10/2022]. See the Terms and Conditions (https://onlinelibrary.wiley.com/terms-and-conditions) on Wiley Online Library for rules of use; OA articles are governed by the applicable Creative Commons License

also been previously noted by the BGS in high-resolution speleothem work, but these were never fully investigated. This existing evidence highlights the issue of resin contamination in carbonate palaeothermometry, but has not yet dissuaded the common use of sample pretreatment, embedding, and gluing in subsequent studies (e.g. [36,37]). Moreover, previous studies do not explore whether changes to sampling strategy to avoid such contaminants results in an unacceptable loss of precision and/or resolution.

Here we tested corresponding hand-drilled, non-embedded samples from the same valves to assess whether the high $\delta^{13}C$ values occurred in both datasets. If so, then we must re-examine our initial position and examine how these high $\delta^{13}C$ results could be otherwise explained. Alternatively, if these $\delta^{13}C$ peaks are not present in the hand-drilled samples then we can consider how sampling strategy and/or polyester resin contamination are potential issues for future carbonate stable isotope analyses. This would have relevance not only to the shells used in this particular study, but also to any researcher contemplating the use of embedding resin in a strategy for high-resolution sampling of carbonates for stable isotopes.

2 | METHODS

The samples used in this experiment came from two archaeological *S. sachalinensis* valves (labelled VIII_3 and II_1) both collected from the site of Hamanaka 2, Rebun Island, Japan. In the initial stable isotope analysis undertaken on these shells, the valves had been sectioned as per Figure 1, with the central section of the shell (corresponding to the axis of maximum growth) then embedded in MetPrep 'Kleer-Set' polyester resin (https://metprep.co.uk/product/kleer-set/). Samples were milled incrementally from these resin-embedded sections using a computer-controlled New Wave Research MicroMill at the BGS. Milling was carried out up to 300 μm depth in multiple milling passes of 50 μm depth/pass, and using a 0.3 mm diameter diamond-coated dental drill bit. No chemical or physical pretreatments were applied to the samples before analysis. The non-embedded halves of the same valves were sampled using a Buehler hand drill, from the area corresponding to the original sampling locations (Figure 3). For both the micromilled and hand-drilled samples, the cross-lamellar layer of the shell was targeted, as is most common with shell palaeothermometry studies.[38] In this large species, the cross-lamellar layer is relatively thick (ca. 4 mm width after the second year of growth; Figure 3), so it was possible to avoid mixing material from the surrounding outer and inner layers by eye during hand drilling. In other smaller species of shell, it may be more difficult to specifically target one microstructural layer during hand drilling. Samples were spot drilled using a 1 mm diameter drill bit, and aluminium foil was used to collect the resulting aragonite powder before transferring it into microcentrifuge tubes. During hand drilling, the shell was supported using the non-dominant hand, which rested firmly on the lab bench and provided a 'cushion' between the shell itself and the bench to prevent direct contact between the two which could cause damage to the specimen. The sectioned surface of the shell was held

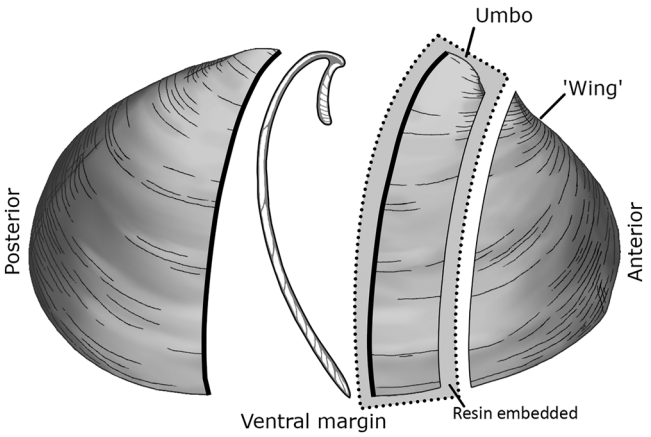


FIGURE 1 Illustration of *Spisula sachalinensis* showing section along the axis of maximum growth. The bolded lines show the sampled surfaces

angled down towards the aluminium foil to direct the shell powder onto the foil and reduce sample loss. Each sample was checked for purity of the aragonite using Fourier-transform infrared spectroscopy,[20] as per Loftus et al.[39]

Once in the microcentrifuge tubes, the powders obtained using both the hand-drilling and micromilling methods were analysed identically, using a dual-inlet Isoprime mass spectrometer interfaced with a Multiprep autosampler (hereafter referred to as the Isoprime plus Multiprep) at the BGS. We aimed to produce 50 to 100 μg of carbonate per sample for isotope analysis; however, micromilled samples were often below 50 μg, smaller than those produced by hand drilling which were typically >100 μg (with 50–100 μg sub-samples used for analysis). Samples are loaded into glass vials and sealed with septa, evacuated and anhydrous phosphoric acid delivered to the carbonate at 90°C. Evolved CO_2 is collected for 15 min, H_2O is removed, and pure, dry CO_2 introduced into the mass spectrometer for measurement. Isotope ratios of carbon and oxygen ($^{13}C/^{12}C$, $^{18}O/^{16}O$) are expressed as per mille (‰) deviations of the isotopic ratios ($^{13}C/^{12}C$, $^{18}O/^{16}O$) calculated to the VPDB (Vienna Pee Dee Belemnite) scale using a within-run laboratory standard (KCM) calibrated against international standard NBS-19. Nine KCM calcite standards were measured alongside every 31 samples. The Craig correction[40] was applied to correct for $\delta^{17}O$, as well as a calcite-acid fractionation factor of 1.00813. Due to the long run time of 21 h a drift correction is applied across the run, calculated using the standards that bracket the samples. The standard calcite values for KCM are +2.00‰ for $\delta^{13}C$ and −1.73‰ for $\delta^{18}O$ with an average analytical reproducibility of 0.05‰.

A small aliquot of the resin was analysed separately on an Elementar vario ISOTOPE cube elemental analyser (EA) coupled to an Isoprime precisION isotope ratio mass spectrometer also at the BGS, in an attempt to provide a baseline $\delta^{13}C$ isotope ratio for the embedding resin. The significant drawback to this approach is that the resin is fully combusted, including organic components, while the phosphoric acid in the Multiprep preferentially reacts with

10970231, 2022, 14, Downloaded from https://analyticalsciencejournals.onlinelibrary.wiley.com/doi/10.1002/rcm.9318 by Test, Wiley Online Library on [20/10/2022]. See the Terms and Conditions (https://onlinelibrary.wiley.com/terms-and-conditions) on Wiley Online Library for rules of use; OA articles are governed by the applicable Creative Commons License

carbonates, and therefore likely does not dissolve all components. Therefore, this was not the best approach to determine the effects of resin traces on the shell carbonates; it would have been preferable to analyse the resin sample on the Multiprep, but this ran the risk of a costly contamination of the instrument and could not be justified.

3 | RESULTS AND DISCUSSION

Of the 36 hand-drilled samples added for this paper, all produced sufficient gas for isotopic measurement. Of the pre-existing micromilled samples from these two shells, 21 of the 91 samples failed to produce enough gas to measure isotopic composition. This represents a failure rate of 23%, likely due to challenges with handling very small amounts of powder during the period between micromilling and mass spectrometry. The results of all (hand-drilled and micromilled) samples are summarised in Table 1. The $\delta^{18}O$ results show clear cyclicity, with a range of 2.98‰ for shell II_1 and 2.28‰ for VIII_3. The $\delta^{13}C$ results for hand-drilled samples show a smaller range of 0.87‰ for II_1 and 1.55‰ for VIII_3. Figure 2 shows the results of the hand-drilled samples alongside the original results from the corresponding micromilled samples.

Compared with the micromilled samples, the hand-drilling approach provided ~2.5× lower spatial sampling resolution. Shell II_1 produced 20 hand-drilled samples over the same area that produced 50 micromilled samples, and VIII_3 produced 16 hand-drilled samples compared with 41 micromilled. The difference in resolution relates to the relative size of the drill bits used in each case (0.3 mm for

TABLE 1 Summary of stable isotope results from shells II_1 and VIII_3

		Maximum $\delta^{18}O$ (‰)	Minimum $\delta^{18}O$ (‰)	$\delta^{18}O$ range (‰)	Maximum $\delta^{13}C$ (‰)	Minimum $\delta^{13}C$ (‰)	$\delta^{13}C$ range (‰)
II_1	Micromilled/resin-embedded	+2.11	−1.37	+3.48	+4.86	+0.62	+4.24
	Hand drilled/unembedded	+1.65	−1.33	+2.98	+1.36	+0.49	+0.87
VIII_3	Micromilled/resin-embedded	+1.63	−1.13	+2.76	+2.59	−0.03	+2.62
	Hand drilled/unembedded	+1.01	−1.27	+2.28	+1.62	+0.07	+1.55

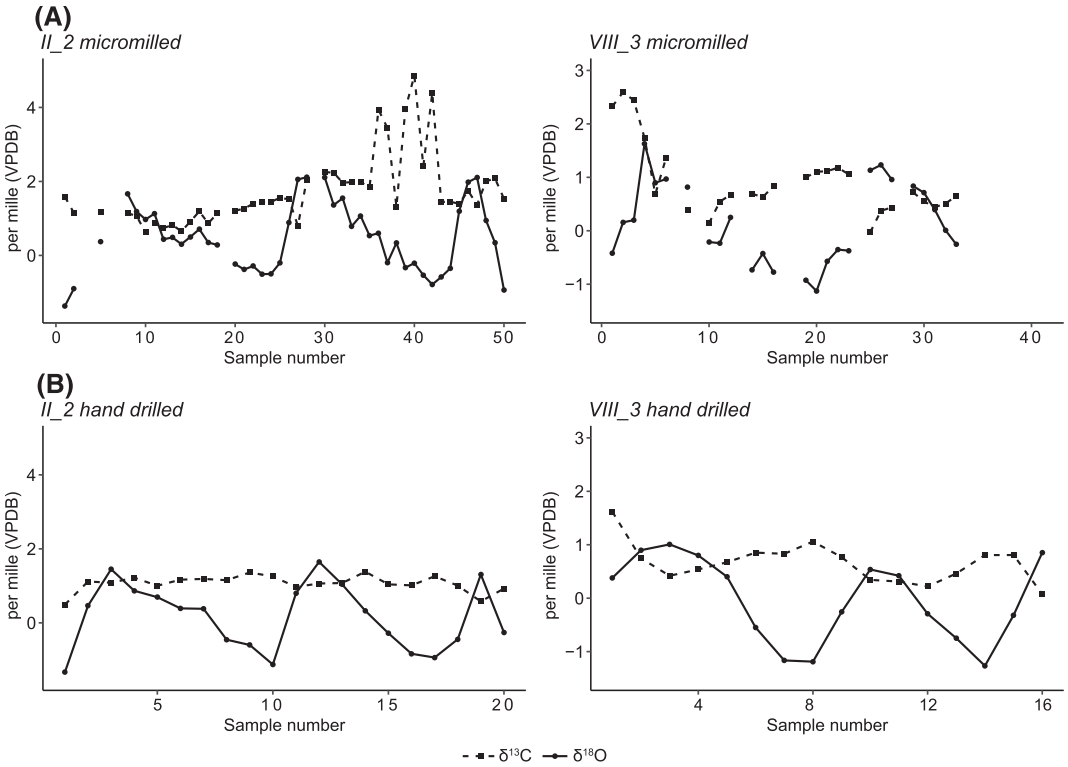


FIGURE 2 Plots showing the $\delta^{13}C$ and $\delta^{18}O$ results for shells II_1 and VIII_3 for A, the micromilled samples and B, the hand-drilled samples

10970231, 2022, 14, Downloaded from https://analyticalsciencejournals.onlinelibrary.wiley.com/doi/10.1002/rcm.9318 by Test, Wiley Online Library on [20/10/2022]. See the Terms and Conditions (https://onlinelibrary.wiley.com/terms-and-conditions) on Wiley Online Library for rules of use; OA articles are governed by the applicable Creative Commons License

micromilling vs 1 mm for hand drilling), and the increased spatial precision obtainable when using a computer-operated system. These results, unsurprisingly, show that hand drilling results in reduced sampling resolution compared with micromilling, which is one of the main reasons cited by Twaddle et al[11] that micromilling is the method of choice for most researchers. In this study, hand drilling produced a resolution of approximately one sample per 1.7 mm distance along the shell. Drill bits smaller than 1 mm diameter could be sourced to increase the resolution of hand drilling, but the spatial precision achievable by hand drilling will still be limited by the steadiness and coordination of the drill operator, and the fragility of increasingly small drill bits. Furthermore, this study does not represent the maximum spatial precision achievable with micromilling, as we sampled using discrete consecutive milling trenches (as seen in Figure 3) with some material remaining between each sample. Other researchers have shown that continuous sampling can be achieved where each sampling pass is less wide than the diameter of the drill bit, no material remains between samples, and spatial resolution can go under 100 μm.[12,14]

Figure 4 shows a close fit between the $\delta^{18}O$ data for both sequences, with the aforementioned slightly reduced $\delta^{18}O$ ranges seen in the hand-drilled sequences for both shells (Table 1). For shell II_1 the $\delta^{18}O$ range for the non-embedded hand-drilled samples was reduced by 0.50‰, and for VIII_3 the range was similarly reduced by 0.48‰. This means that for II_1 and VIII_3, respectively, the $\delta^{18}O$ ranges of the hand-drilled samples were 85.6% and 82.6% of the micromilled samples. A reduction of 0.5‰ in $\delta^{18}O$ equates to a reduction of ~2°C in the calculated temperature range, using the aragonite/temperature equation from Grossman and Ku,[3] as modified by Leng and Lewis.[41] Therefore, if the intended research outcome requires very precise calculations of maximum and minimum ocean temperatures then hand drilling is likely to dampen these extremes (especially in slow-growing species) and micromilling is therefore preferable. However, if the intended outcome is to identify seasonal cycles or season of collection then higher resolution may be surplus to requirements.

Despite the lower spatial resolution and compression of $\delta^{18}O$ values in the hand-drilled samples, the sequences appear more coherent and are easier to interpret in terms of seasonal shifts compared with the micromilled results (Figure 2). This is at least partly because the increased resolution achieved in the micromilled results (Figure 2A) is more complex and appears 'noisy', rendering seasonal 'patterns' more difficult to interpret as compared with the hand-drilled results (Figure 2B). The gaps in the micromilled results further contribute to this difficulty, whereas the hand-drilled sequence is continuous. We believe the problem relates to the smaller sample sizes obtained via micromilling, and subsequent powder loss when transferring the powder between vessels, so that failure rate due to small quantities of CO_2 is relatively high. Hand-drilled samples produced material easily in or above the 50–100 μg range typically run on the Isoprime plus Multiprep device, while micromilling regularly produced smaller samples of ~30 μg (weighed in microcentrifuge tubes immediately after sample collection). Small samples such as this are harder to transfer and powder will be lost due to static on transfer between microcentrifuge tubes and septa. Larger samples have a much lower failure rate, and in the case that samples do fail there is usually enough leftover powder to repeat those samples. The sample sizes obtained through micromilling could be increased by targeting larger areas or drilling deeper into the shell section, but this would compromise the sampling precision (one of the

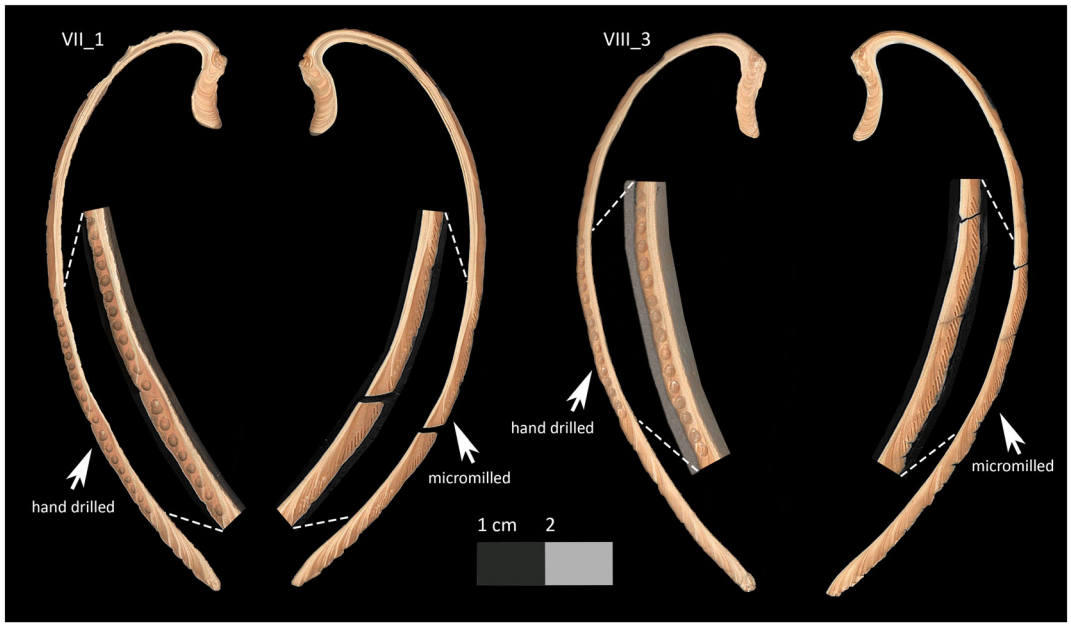


FIGURE 3 Scan of sampled sections for shells II_1 and VIII_3 showing the corresponding micromilled and hand-drilled regions [Color figure can be viewed at wileyonlinelibrary.com]

10970231, 2022, 14, Downloaded from https://analyticalsciencejournals.onlinelibrary.wiley.com/doi/10.1002/rcm.9318 by Test, Wiley Online Library on [20/10/2022]. See the Terms and Conditions (https://onlinelibrary.wiley.com/terms-and-conditions) on Wiley Online Library for rules of use; OA articles are governed by the applicable Creative Commons License

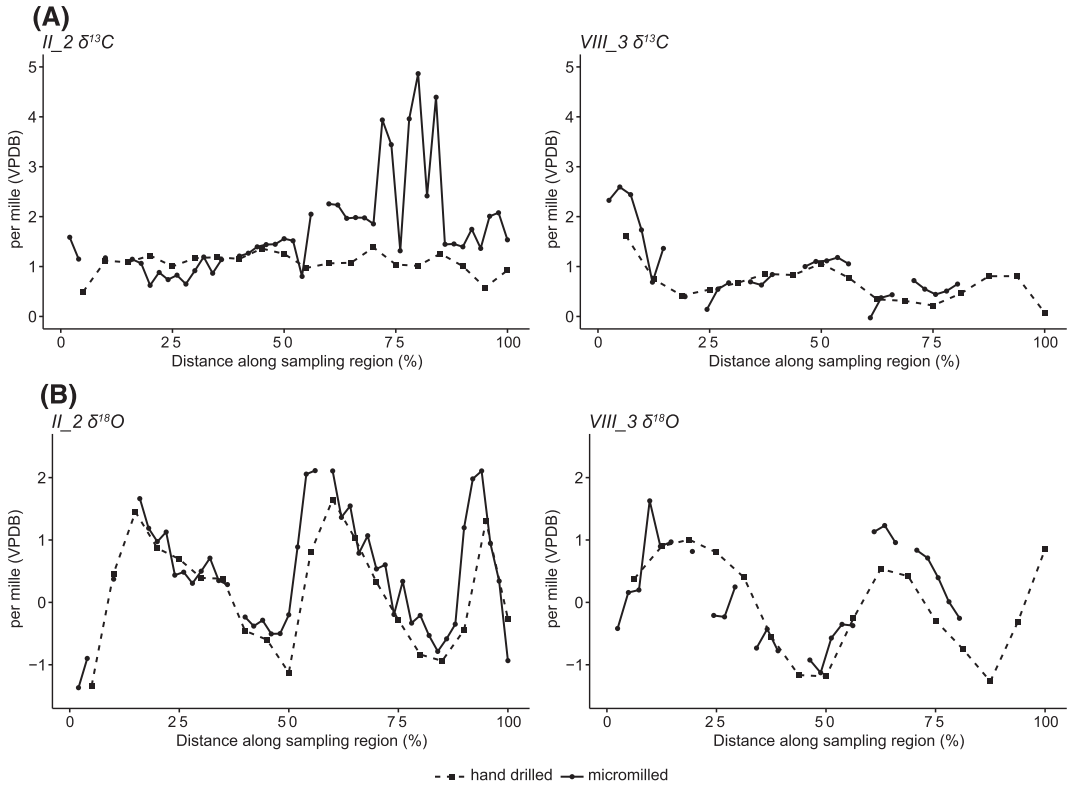


FIGURE 4 Plot showing A, $\delta^{13}C$ results from hand-drilled and micromilled samples plotted against distance along the shell (as a percentage along the sampling region) and B, $\delta^{18}O$ results from hand-drilled and micromilled samples plotted against distance along the shell

main benefits of micromilling), while prolonging the already-slow milling time. Similarly, statistically smoothing the data (e.g. [42]) to reduce the apparent noise obviates the point of having higher sampling resolution.

The differences between the micromilled and hand-drilled samples were greater for the $\delta^{13}C$ results. The range of $\delta^{13}C$ for the hand-drilled samples was reduced by 3.37‰ for II_I and by 1.07‰ for VIII_3. In both cases, the difference is due to a reduction in the maximum observed $\delta^{13}C$ value. This strongly suggests that the highest $\delta^{13}C$ values observed in the original micromilled samples are indeed erroneous. As they were not replicated in the hand-drilled results it suggests that this issue was resolved by the change in sampling strategy to hand drilling unembedded material. The other possibility, that the high $\delta^{13}C$ values were completely missed in the hand-drilled sampling spots, is very remote. This is even more the case since the sampling locations for each method overlap significantly in terms of their position along the growth increments of each shell. For the hand-drilled samples to cover the regions of high $\delta^{13}C$ but still to average out to the same ~1‰ value as the rest of the sequence, it would be necessary to suppose very localised areas of very high $\delta^{13}C$ (which coincidentally aligned with the micromilled sampling locations) surrounded by areas of shell with $\delta^{13}C$ values lower than 1‰ (which would also need to have been coincidentally missed by the higher resolution sampling). Given the extreme unlikelihood of this scenario, along with the aforementioned implausibility of DIC conditions that would result in such high values of $\delta^{13}C$, we do not consider this a feasible interpretation.

One other possible explanation for the differences in results between the micromilled and hand-drilled samples could be the smaller sample size in the micromilled samples, as already discussed with reference to their higher failure rate. Particularly tiny samples can lead to greater errors, with uncertainty generally attributed to the enhanced influence of exchange with the reference gas during mass spectrometry. As anomalous results in our study appear to be present only in the $\delta^{13}C$ results, mixing with the reference gas is only a plausible cause if the reference gas has a very similar $\delta^{18}O$ value to the samples but a very different $\delta^{13}C$ value. If such a scenario is correct, in order to cause high $\delta^{13}C$ values the reference gas would have to show positive $\delta^{13}C$ values. However, in this case the reference gas is slightly negative (~ -2‰) for both $\delta^{13}C$ and $\delta^{18}O$. We can eliminate this as a likely explanation for the erroneous $\delta^{13}C$ values. Moreover, the stable isotope facility at the BGS routinely runs small sample sizes successfully, down to 5 μg, with no loss of precision or anomalous values.

Instead, it is more likely that polyester embedding resin contaminated the aragonite powders during the micromilling sampling process. The possibility of resin contamination has been observed previously by the stable isotope facility at the BGS in results from embedded speleothems, although these issues were not further investigated at the time. On examination of the sampling locations for

10970231, 2022, 14, Downloaded from https://analyticalsciencejournals.onlinelibrary.wiley.com/doi/10.1002/rcm.9318 by Test, Wiley Online Library on [20/10/2022]. See the Terms and Conditions (https://onlinelibrary.wiley.com/terms-and-conditions) on Wiley Online Library for rules of use; OA articles are governed by the applicable Creative Commons License

the high $\delta^{13}C$ samples in Figure 3 there is no obvious difference visible between those and the other sampling tracks, and nothing unusual was noted about these samples during milling. However, the method of sample collection used during micromilling – the use of a scalpel to push the powder onto the edge of a razor blade – does mean that the blades of the scalpel and the razor blade both make contact with (and potentially scrape) the surface of the polyester resin. It therefore seems possible for trace amounts of the resin to be scraped into the samples without it being visually clear to the micromill operator. Given the relatively sporadic appearance of $\delta^{13}C$ anomalies in the micromilled data, it appears that this type of contamination is unpredictable and difficult to avoid when using such manual sample retrieval methods. The continuous section of anomalously high $\delta^{13}C$ in shell II_1 may also suggest that this kind of contamination can 'linger' in the mass spectrometer and affect subsequent samples.

We had hoped to be able to demonstrate more clearly that resin contamination was the cause of these high values, but unfortunately were unable to measure the resin alone on the Isoprime plus Multiprep due to the risk of instrument contamination. A resin sample measured on the EA as organic material produced an average $\delta^{13}C$ value of $-27.97‰$ ($\sigma = 0.15$), but it does not represent the effect of resin contamination on samples measured by H_3PO_4 acid digestion on the Isoprime plus Multiprep. The EA completely combusts the organic material, while incomplete acid digestion of organic components on the Isoprime plus Multiprep could result in particular $\delta^{13}C$-positive components of the resin being analysed rather than the compound as a whole. The previous work of Schöne et al[35] helps to resolve this issue by the addition of known small quantities of resin to carbonate reference material for acid digestion, which better mimics the typical conditions required for sampling in palaeoclimatological studies.

Where there is concern about the possibility of resin contamination, a replacement embedding material could be used, but it would be necessary to gauge whether this replacement too would suffer the same problem if it were to contaminate the sample material. An alternative sample retrieval method, replacing the scalpel/razor blade approach, might also reduce the chance of contamination from the embedding material if it involved less physical contact with the embedding material. One alternative method was proposed by Sakai and Kodan[16] in 2011, where milled powder is sucked up using a vacuum pump. While this method achieves a high (>90%) sample retrieval rate, it requires specialist equipment since the apparatus structure must be specifically modified to fit the particular type of reaction vial being used such that one design is not universally applicable between labs. Likely for these reasons, the technique has not been widely used.

As this study illustrates for *S. sachalinensis*, the sampling resolution gained by micromilling is not always necessary or may even be undesirable, producing problematically small samples and resolution at a high enough level to distract from seasonal patterns. In this case, rather than overcoming the issues of small sample size by changing powder collection methods, a simpler solution would be to avoid micromilling altogether. Hand drilling can provide a simpler alternative which eliminates the need for a large flat sampling surface and embedding materials, effectively bypassing the issue of resin contamination and powder loss during sample collection. For large and/or fast-growing species such as *S. sachalinensis*, the reduced resolution provided by hand drilling is in our opinion outweighed by these benefits. The balance would change in favour of micromilling with very small specimens or slow-growing species, or if specific research questions necessitate extremely high-resolution sampling of faster-growing species.

4 | CONCLUSIONS

The question that prompted this study was whether a number of unusually high $\delta^{13}C$ values in our micromilled dataset were an artefact of the approach taken to sample preparation and collection. By comparing the stable isotope values of micromilled samples with hand-drilled samples from the same area on two halves of the same valve, we were able to show that the highest $\delta^{13}C$ results only occurred in the micromilled samples. We are confident that they do not represent a true reflection of marine conditions.

We conclude that these high $\delta^{13}C$ values are most likely related to contamination from the polyester resin in which the samples were embedded, which could have entered the powdered samples during retrieval post-milling. During the period of analysis there were no instrumental issues, and the internal reproducibility of each analysis and standard results were all checked for consistency. Reference gases continued to show normal, negative $\delta^{13}C$ values, which suggests that exchange with the reference gas in particularly small samples did not contribute to these high $\delta^{13}C$ values. Although the resin we analysed on the EA mass spectrometer produced a strongly negative $\delta^{13}C$ value, we suggest that the Isoprime mass spectrometer and Multiprep device used to analyse the original carbonate samples resulted in less complete breakdown of the resin (by phosphoric acid in the Isoprime plus Multiprep instrument as opposed to combustion in the EA) and so the measured sample was only contaminated by one or more $\delta^{13}C$-positive component(s) of the resin. In order to further investigate the resin contamination issue, we recommend analysis of carbonate reference material with known (small) amounts of resin contamination to better understand how the resin affects $\delta^{13}C$ values and how predictable this is; however, there is the possibility of contamination of the organic material within the mass spectrometer (hence not tried here). $\delta^{18}O$ values appeared unaffected by contamination issues specifically relating to resin embedding.

A further outcome of this study is a direct comparison of micromilling versus hand-drilling microsampling approaches in terms of spatial resolution, sample failure rates, ease of interpretation and accessibility. Whilst it can be tempting to opt for the increased resolution of micromilling wherever possible, in this case we conclude that the higher resolution gained from micromilling is not always advantageous. Practically speaking, hand drilling saves time and analytical costs. Our results also show that in a large and relatively fast-growing species such as *S. sachalinensis*, hand-drilled samples

10970231, 2022, 14, Downloaded from https://analyticalsciencejournals.onlinelibrary.wiley.com/doi/10.1002/rcm.9318 by Test, Wiley Online Library on [20/10/2022]. See the Terms and Conditions (https://onlinelibrary.wiley.com/terms-and-conditions) on Wiley Online Library for rules of use; OA articles are governed by the applicable Creative Commons License

show clear and easily interpreted seasonal cycles with a lower sample failure rate than those obtained via micromilling. This will be of interest to researchers working on many other long-lived and fast-growing sentinel species commonly targeted for stable isotope palaeothermometry and marine conditions, for example the species noted by Mann et al.[43] The hand-drilling approach can effectively bypass the potential issue of contamination from embedding materials, and while some other methods have been discussed to mitigate this issue, avoiding embedding in the first instance is of course chief among these. Our results, however, suggest that in cases where sampling resolution must be particularly high, or where it is important to show extremes in $\delta^{18}O$ as precisely as possible, then micromilling remains the best option. With increased knowledge of the interpretational consequences and relative sampling resolution of the method, researchers across the field of carbonate stable isotope thermometry should be better equipped to decide which is more appropriate for their material and specific research questions.

ACKNOWLEDGMENTS

This work was supported by a NEIFSC project grant (IP-1944-1119) and a Clarendon Fund Scholarship. The authors thank Hilary Sloane and Jack Lacey for their assistance in the sample preparation and mass spectrometry processes. They are also grateful to two anonymous reviewers for their helpful comments and encouragement.

PEER REVIEW

The peer review history for this article is available at https://publons.com/publon/10.1002/rcm.9318.

DATA AVAILABILITY STATEMENT

The data that support the findings of this study are available from the corresponding author upon reasonable request.

ORCID

Tansy Branscombe https://orcid.org/0000-0002-7205-4740
Julia Lee-Thorp https://orcid.org/0000-0002-3291-0258
Rick Schulting https://orcid.org/0000-0002-4444-766X
Melanie Leng https://orcid.org/0000-0003-1115-5166

REFERENCES

1. Emiliani C, Cardini L, Mayeda T, McBurney C, Tongiorgi E. Palaeotemperature analysis of marine molluscs (food refuse) from the site of Arene Candide cave, Italy and the Haua Fteah cave, Cyrenaica. In: Craig H, Miller S, Wasserburg G, eds. *Isotopic and Cosmic Chemistry*. Amsterdam: North-Holland Publishing Company; 1964.
2. Branscombe T, Bosch MD, Miracle P. Seasonal shellfishing across the east Adriatic Mesolithic-Neolithic Transition: Oxygen isotope analysis of *Phorcus turbinatus* from Vela Spila (Croatia). *Environ Archaeol*. 2020; 26(5):497-510. doi:10.1080/14614103.2020.1721695
3. Grossman EL, Ku TL. Oxygen and carbon isotope fractionation in biogenic aragonite: Temperature effects. *Chem Geol Isot Geosci Sect*. 1986;59(C):59-74. doi:10.1016/0168-9622(86)90057-6
4. Goodwin DH, Schöne BR, Dettman DL, Goodwin DH, Schone BR, Dettman DL. Resolution and fidelity of oxygen isotopes as paleotemperature proxies in bivalve mollusk shells: Models and observations published by: SEPM Society for Sedimentary Geology Linked references are available on JSTOR for this article: Paleotemperature pro. *SEPM Soc Sediment Geol*. 2003;18(2):110-125.
5. Reynolds DJ, Hall IR, Slater SM. An integrated carbon and oxygen isotope approach to reconstructing past environmental variability in the northeast Atlantic Ocean. *Palaeogeogr Palaeoclimatol Palaeoecol*. 2019;523(December 2018):48-61. doi:10.1016/j.palaeo.2019.03.005
6. McConnaughey TA, Gillikin DP. Carbon isotopes in mollusk shell carbonates. *Geo-Marine Lett*. 2008;28(5–6):287-299. doi:10.1007/s00367-008-0116-4
7. Gillikin DP, Lorrain A, Bouillon S, Willenz P, Dehairs F. Stable carbon isotopic composition of *Mytilus edulis* shells: Relation to metabolism, salinity, $\delta^{13}C_{DIC}$ and phytoplankton. *Org Geochem*. 2006;37(10):1371-1382. doi:10.1016/j.orggeochem.2006.03.008
8. Kastelle CR, Helser TE, McKay JL, et al. Age validation of Pacific cod (*Gadus macrocephalus*) using high-resolution stable oxygen isotope ($\delta^{18}O$) chronologies in otoliths. *Fish Res*. 2017;185:43-53. doi:10.1016/j.fishres.2016.09.024
9. Helser TE, Kastelle CR, McKay JL, Orland IJ, Kozdon R, Valley JW. Evaluation of micromilling/conventional isotope ratio mass spectrometry and secondary ion mass spectrometry of $\delta^{18}O$ values in fish otoliths for sclerochronology. *Rapid Commun Mass Spectrom*. 2018;32(20):1781-1790. doi:10.1002/rcm.8231
10. Darnaude AM, Sturrock A, Trueman CN, Mouillot D, Campana SE, Hunter E. Listening in on the past: What can otolith $\delta^{18}O$ values really tell us about the environmental history of fishes? *PLoS ONE*. 2014;9(10):e108539. doi:10.1371/journal.pone.0108539
11. Twaddle RW, Ulm S, Hinton J, Wurster CM, Bird MI. Sclerochronological analysis of archaeological mollusc assemblages: Methods, applications and future prospects. *Archaeol Anthropol Sci*. 2016;8(2):359-379. doi:10.1007/s12520-015-0228-5
12. Spötl C, Mattey D. Stable isotope microsampling of speleothems for palaeoenvironmental studies: A comparison of microdrill, micromill and laser ablation techniques. *Chem Geol*. 2006;235(1–2):48-58. doi:10.1016/j.chemgeo.2006.06.003
13. Zhang H, Cai Y, Tan L, Qin S, An Z. Stable isotope composition alteration produced by the aragonite-to-calcite transformation in speleothems and implications for paleoclimate reconstructions. *Sediment Geol*. 2014;309:1-14. doi:10.1016/j.sedgeo.2014.05.007
14. Lachniet MS. Climatic and environmental controls on speleothem oxygen-isotope values. *Quat Sci Rev*. 2009;28(5–6):412-432. doi:10.1016/j.quascirev.2008.10.021
15. Baldini JUL, McDermott F, Hoffmann DL, Richards DA, Clipson N. Very high-frequency and seasonal cave atmosphere P_{CO2} variability: Implications for stalagmite growth and oxygen isotope-based paleoclimate records. *Earth Planet Sci Lett*. 2008;272(1–2):118-129. doi:10.1016/j.epsl.2008.04.031
16. Sakai S, Kodan T. Micropowder collecting technique for stable isotope analysis of carbonates. *Rapid Commun Mass Spectrom*. 2011; 25(9):1205-1208. doi:10.1002/rcm.4980
17. Linge KL. Recent developments in trace element analysis by ICP-AES and ICP-MS with particular reference to geological and environmental samples. *Geostand Geoanal Res*. 2005;29(1):7-22. doi:10.1111/j.1751-908X.2005.tb00650.x
18. Halicz L, Galy A, Belshaw N, O'Nions R. High precision measurement of calcium isotopes in carbonates and related minerals by multi-collector inductively coupled plasma mass spectrometry (MC-ICP-MS). *J Anal At Spectrom*. 1999;14(12):1835-1838. doi:10.1039/a906422b
19. He D, Zhu Z, Zhao L, et al. A practical method for measuring high precision calcium isotope ratios without chemical purification for calcium carbonate samples by multiple collector inductively coupled plasma mass spectrometry. *Chem Geol*. 2019;514:105-111. doi:10.1016/j.chemgeo.2019.03.020

10970231, 2022, 14, Downloaded from https://analyticalsciencejournals.onlinelibrary.wiley.com/doi/10.1002/rcm.9318 by Test, Wiley Online Library on [20/10/2022]. See the Terms and Conditions (https://onlinelibrary.wiley.com/terms-and-conditions) on Wiley Online Library for rules of use; OA articles are governed by the applicable Creative Commons License

20. Branscombe T, Schulting R, Lee-Thorp J, Leng MJ. The potential of marine bivalve *Spisula sachalinensis* as a marine temperature record. *Palaeogeogr Palaeoclimatol Palaeoecol*. 2021;582(September):110634. doi:10.1016/j.palaeo.2021.110634
21. Sasaki K. Growth of the Sakhalin surf clam, *Spisula sachalinensis* (SCHRENCK), in Sendai Bay. *Tohoku J Agric Res*. 1981;32(4):168-180.
22. Kang YJ, Kim CK. Studies on the structure and production processes of biotic communities in the coastal shallow waters of Korea. Age and growth of *Spisula sachalinensis* from the eastern waters of Korea. *Korean J Fish Aquat Sci*. 1983;16(2):82-87.
23. Golikov AN, Scarlato OA. Abundance, dynamics and production properties of populations of edible bivalves *Mizuhopecten yessoensis* and *Spisula sachalinensis* related to the problem of organization of controllable submarine farms at the western shores of the Sea of Japan. *Helgoländer Wissenschaftliche Meeresuntersuchungen*. 1970; 20(1–4):498-513. doi:10.1007/BF01609925
24. Takahashi N, Yamamoto K. Histological studies on the reproductive cycle of the surf clam, *Spisula sachalinensis* – II. Seasonal changes in the ovary. *Bull Japanese Soc Sci Fish*. 1970;36(4):345-352. doi:10.2331/suisan.36.345
25. Takamaru N. On the breeding season of the surf clam, *Spisula sachalinensis* (Schrenk) in Tokachi. *J Hokkaido Fish Exp Stn*. 1976;33: 1-8.
26. Lee J-Y, Chang Y-J, Park Y-J. Spawning induction and egg development of surf clam, *Spisula sachalinensis*. *J Aquac*. 1996;9(4): 419-427.
27. Tabakaeva OV, Tabakaev AV. Lipids and fatty acids from soft tissues of the bivalve mollusk *Spisula sachalinensis*. *Chem Nat Compd*. 2017; 53(1):16-20. doi:10.1007/s10600-017-1900-z
28. Sasaki K. Characteristics of the bottom sediments inhabited by the surf clam *Spisula sachalinensis* in Sendai Bay. *Nippon Suisan Gakkaishi*. 1989;55(7):1127-1131. doi:10.2331/suisan.55.1127
29. Sasaki S, Ohta T. Seasonal variation of chemical components in surf clam (*Spisula sachalinensis*). *Food SciTechnolRes*. 1999;5(3):313-315. doi:10.3136/fstr.5.311
30. Khim BK, Woo KS, Je JG. Stable isotope profiles of bivalve shells: Seasonal temperature variations, latitudinal temperature gradients and biological carbon cycling along the east coast of Korea. *Cont Shelf Res*. 2000;20(8):843-861. doi:10.1016/S0278-4343(00)00004-2
31. Rodríguez de Vera C, Herrera-Herrera AV, Jambrina-Enríquez M, et al. Micro-contextual identification of archaeological lipid biomarkers using resin-impregnated sediment slabs. *Sci Rep*. 2020; 10(1):20574. doi:10.1038/s41598-020-77257-x
32. Mortensen PB, Rapp HT, Båmstedt U. Oxygen and carbon isotope ratios related to growth line patterns in skeletons of *Lophelia pertusa* (L) (Anthozoa, Scleractinia): Implications for determination of linear extension rate. *Sarsia*. 1998;83(5):433-446. doi:10.1080/00364827.1998.10413702
33. Mentzer SM, Quade J. Compositional and isotopic analytical methods in archaeological micromorphology. *Geoarchaeology*. 2013;28(1):87-97. doi:10.1002/gea.21425
34. Radke J, Haubold P, Hilkert A. Isotope analysis of 6–130 μg samples with the KIEL IV carbonate device. Application Note No. 30176. Thermo Fisher Scientific, Bremen, Germany; 2009.
35. Schöne BR, Schmitt K, Maus M. Effects of sample pretreatment and external contamination on bivalve shell and Carrara marble $\delta 1^{8}O$ and $\delta^{13}C$ signatures. *Palaeogeogr Palaeoclimatol Palaeoecol*. 2017;484:22-32. doi:10.1016/j.palaeo.2016.10.026
36. Dias R, Estrella-Martínez J, Butler P, et al. Mesolithic human occupation and seasonality: Sclerochronology, $\delta^{18}O$ isotope geochemistry, and diagenesis verification by Raman and LA-ICP-MS analysis of *Argyrosomus regius* (meagre) sagittae otoliths from layer 1 of Cabeço da Amoreira Mesolithic shell midd. *Archaeol Anthropol Sci*. 2018;11(2):1-24. doi:10.1007/s12520-017-0569-3
37. Hollyman PR, Leng MJ, Chenery SRN, Sloane HJ, Richardson CA. Calibration of shell $\delta^{18}O$ from the common whelk *Buccinum undatum* highlights potential for palaeoenvironmental reconstruction. *Palaeogeogr Palaeoclimatol Palaeoecol*. 2020;560:109995. doi:10.1016/j.palaeo.2020.109995
38. Surge D, Walker KJ. Geochemical variation in microstructural shell layers of the southern quahog (*Mercenaria campechiensis*): Implications for reconstructing seasonality. *Palaeogeogr Palaeoclimatol Palaeoecol*. 2006;237(2):182-190. doi:10.1016/j.palaeo.2005.11.016
39. Loftus E, Rogers K, Lee-Thorp J. A simple method to establish calcite: aragonite ratios in archaeological mollusc shells. *J Quat Sci*. 2015; 30(8):731-735. doi:10.1002/jqs.2819
40. Craig H. Isotopic standards for carbon and oxygen and correction factors for mass-spectrometric analysis of carbon dioxide. *Geochim Cosmochim Acta*. 1957;12(1–2):133-149. doi:10.1016/0016-7037(57)90024-8
41. Leng MJ, Lewis JP. Oxygen isotopes in molluscan shell: Applications in environmental archaeology. *Environ Archaeol*. 2016;21(3):295-306. doi:10.1179/1749631414y.0000000048
42. Chute AS, Wainright SC, Hart DR. Timing of shell ring formation and patterns of shell growth in the sea scallop *Placopecten Magellanicus* based on stable oxygen isotopes. *J Shellfish Res*. 2012;31(3):649-662. doi:10.2983/035.031.0308
43. Mann R, Munroe DM, Powell EN, Hofmann EE, Klinck JM. Bivalve molluscs: Barometers of climate change in Arctic marine systems. In: Mueter FJ, Dickson DM, Huntingdon H, et al., eds. *Responses of Arctic Marine Ecosystems to Climate Change*. University of Alaska Fairbanks; 2013. doi:10.4027/ramecc.2013.04

How to cite this article: Branscombe T, Lee-Thorp J, Schulting R, Leng M. Micromilling vs hand drilling in stable isotope analyses of incremental carbonates: The potential for $\delta^{13}C$ contamination by embedding resin. *Rapid Commun Mass Spectrom*. 2022;36(14):e9318. doi:10.1002/rcm.9318

10970231, 2022, 14, Downloaded from https://analyticalsciencejournals.onlinelibrary.wiley.com/doi/10.1002/rcm.9318 by Test, Wiley Online Library on [20/10/2022]. See the Terms and Conditions (https://onlinelibrary.wiley.com/terms-and-conditions) on Wiley Online Library for rules of use; OA articles are governed by the applicable Creative Commons License

Stable Isotope Palaeothermometry and Radiocarbon Chronology of Marine Carbonates from Hamanaka 2, Rebun Island (Japan)

Tansy Branscombe[1], Julia Lee-Thorp[1], Takao Sato[2], Rick Schulting[1], Hirofumi Kato[3]

Abstract

The site of Hamanaka 2 (Rebun Island, northern Japan) provides a good opportunity to study long term hunter-gatherer behavioural change during the late Holocene. As Hokkaido was occupied by coastally adapted hunter-gatherers until its colonisation by Imperial Japan in 1868, sites in the region offer a particularly long sequence of hunter-gatherer archaeology. Hamanaka 2 provides evidence from the Late Jomon to historical Ainu period (~4000-80 cal BP), benefitting from ongoing excavation and previous chronological modelling. This study uses $\delta^{18}O$ results from archaeological marine carbonates from Hamanaka 2 as a direct proxy for palaeotemperature. Sakhalin surf clams (*Spisula sachalinensis*) from the Epi-Jomon (~3000-1500 cal BP) and Okhotsk (~1500-1000 cal BP) periods showed a similar range of palaeotemperature, while Pacific cod (*Gadus macrocephalus*) otoliths from the Okhotsk levels indicate cooler temperatures. We discuss the extent to which this can be considered a true reflection of climatic variability or whether this difference relates to the ecological differences between shallow-water clams and deep-water cod. Radiocarbon dating on marine samples for this region has previously been avoided due to concerns about the variability of the local marine reservoir effect; however, recent terrestrial dates from Hamanaka 2 can be used to provide marine reservoir corrections across the stratigraphic sequence and enable marine samples to contribute to site chronology. We demonstrate this through radiocarbon dating of shells and otoliths, providing a robust chronology for the palaeotemperature results discussed as well as presenting new ΔR marine reservoir corrections for Hamanaka 2 and the wider region. Overall, our results highlight the utility of archaeological marine carbonates (shells, otoliths), representing direct and archaeologically-relevant proxies for palaeotemperature, as well as a useful radiocarbon dating material.

Keywords
Palaeothermometry, archaeomalacology, Hokkaido, Northwest Pacific, radiocarbon chronology, marine carbonates

Introduction
Understanding palaeoenvironmental change is a key element of archaeological research, both for hunter-gatherer communities who rely heavily on the seasonal availability of resources, and for agricultural groups whose crop yields vary heavily depending on the climate. For much of Japan, historical sources dating back to the 11th century provide a valuable document of recent climatic change. This is less true for Hokkaido (then known as Ezo), which remained predominantly occupied by maritime hunter-gatherer groups until its colonisation by Imperial Japan in 1868. This makes sites such as Hamanaka 2, a long-lived late Holocene site on Rebun Island off Hokkaido's northern coast, particularly important to capture the specific behavioural and environmental development of this region.

Hamanaka 2 is located on the north coast of Rebun next to the large, shallow Funadomari Bay (Figure 1). It is a well-stratified sand dune site, in a location that has seen near-continuous occupation since the Late Jomon period (~4000 cal BP) to modern day. This provides an extremely useful record of the development of hunter-gatherer cultures in Hokkaido, which is also relevant for nearby Sakhalin Island to the north which has a similar cultural history. The site has been the subject of recent excavations led by the Hokkaido University Center for Ainu and Indigenous Studies. Due to the sandy sediment, the site shows good preservation of faunal remains (Hirasawa and Kato 2019; Hirasawa 2018), and due to the site's coastal location and the maritime-adapted cultural groups that occupied the site, its faunal assemblage includes considerable marine material.

Marine zooarchaeological remains provide a useful opportunity to access palaeotemperature, through the inverse relationship between the stable isotope signature of incrementally-grown marine carbonates and sea surface temperatures (Urey et al. 1951, 1954; Emiliani et al. 1964; Deith 1983; Leng and Lewis 2016). While marine material is relatively abundant at Hamanaka 2, shells and

otoliths have not been a focus of recent research, and have therefore not been targeted during excavation. This means that there have been no previous attempts to use marine carbonates from the site as the basis for an archaeologically-relevant palaeotemperature record. One potential reason that marine carbonate material from Hamanaka 2 has not previously been a research focus is the issue of dating these materials. While marine carbonate is in theory directly dateable via radiocarbon dating, the region has shown variable and potentially large marine reservoir effects. This variability relates to the key oceanographic influences in the region, the Soya and Oyashio currents (Figure 1). The warm-water Soya current branches from the Tsushima current and flows around Hokkaido's north coast, primarily influencing shallow waters (Matsuyama et al. 2006). The marine currents affecting Rebun are variable over time (Koizumi 1987; Oba et al. 1991; Igarashi 2013), and affect different marine habitats differently, for example in shallow vs. deep water or sheltered vs. exposed coast. ΔR values calculated in a previous study by Miyata et al. (2016) confirmed variability in the marine reservoir effect between marine niches, ranging from 172 ±39 ^{14}C yrs for *S. sachalinensis* shells to 447±55 ^{14}C yrs for charred material – presumed to be of marine origin – from the inner surface of potsherds. Moreover, with shells there is also the possibility of encountering 'old' specimens, for example those transported – whether by human or natural agents – from the nearby beach long after the death of the organism, which also decreases confidence in shell-derived dates.

Thus, in Junno et al.'s (2021) recent study of the chronology of Hamanaka 2, previous marine radiocarbon dates were excluded due to justified concerns over the issue of variable and species/diet-specific marine reservoir effects. This leads to the loss of information not only from marine organisms such as fish, molluscs and marine mammals, but also terrestrial domesticated animals (i.e., pigs and dogs) likely to have consumed marine foods, and human remains where diet is known through isotopic studies to have depended heavily on marine resources (Tsutaya et al. 2013, 2014), and pottery crusts where biochemical composition analysis has shown marine mammal processing as a likely source (Miyata et al. 2016). While the study by Miyata et al. (2016) is useful in

providing ΔR values relevant to the Late Jomon, these are not likely to be transferable across the chronological sequence at Hamanaka 2 as confirmed by conflicting ΔR values calculated from historically-collected shell specimens (Yoneda et al. 2007).

Considering these factors, the ability to reliably incorporate marine materials from the site into its overall chronology has myriad benefits. Firstly, comparison between paired terrestrial radiocarbon dated samples and marine carbonate samples from throughout the sequence at Hamanaka 2 would provide important new information on the relative (in)stability of regional ΔR values over time. These ΔR values will also be important for other sites in northern Japan, where shell middens are a common archaeological feature (Oikawa 1995; Habu et al. 2011; Edwards 2005). Similar work on the variability of ΔR values over time has been undertaken successfully in other regions, for example the work of Ascough et al. in northern and western Scotland (Ascough et al. 2004, 2006; Ascough, Church, and Cook 2017). Secondly, the ability to combine marine and terrestrial dates into the chronological model for the site will dramatically increase the amount of dateable material produced at the site and will allow for more robust modelling to be done in combination with existing dates. Lastly, if marine carbonates can be reliably radiocarbon dated, the information gained from stable isotope palaeothermometry will be all-the-more important as a record that combines directly-dateable evidence of human subsistence and resource management with an independent archive of palaeoenvironmental information.

In this study, we aim to make steps towards these goals using a combination of incremental stable isotope analysis and radiocarbon dating on a selection of marine carbonate materials. The targeted species were *Spisula sachalinensis* and *Gadus macrocephalus*. The former, the Sakhalin surf clam, is a species of large and long-lived marine bivalve, and member of a genus with an established record as a temperature archive (Jones, Williams, and Arthur 1983; Khim, Woo, and Je 2000; Branscombe et al. 2021) and as a dietary resource across archaeological sites of the northwest Pacific (Vladimir and Gorbunov 2004; Nikitin, Sayenko, and Lutaenko 2016; Nishimoto 1985; Amano and Vasilevski 2002).

G. macrocephalus, commonly known as the Pacific cod, is a key dietary resource at Hamanaka 2 (Tsutaya et al. 2021). Through stable oxygen isotope analysis on shell and otolith samples from the Final/Epi-Jomon and Okhotsk periods, it may be possible to present palaeotemperature information to provide a local picture or regional- and global-scale climatic events, such as the Medieval Warm Period (Y. Sakaguchi 1976, 1983; Batten 2008) and pulses of the warm Tsushima current which feeds the Soya current (Koizumi 1987; Igarashi 2013; Kawahata et al. 2003). Via radiocarbon dating of shells and otoliths from across the sequence at Hamanaka 2, we also hope to tackle some of the issues relating to local marine reservoir effects and investigate the dating potential of marine carbonates – not only from Hamanaka 2 but also from other sites in the region where marine resources form a significant portion of the archaeological assemblage.

Materials and methods

The archaeological material used in this study all came from recent excavations at Hamanaka 2. The shells were collected during the 2018 and 2019 field seasons and include material excavated between 2015-2018. The otoliths were provided by the research lab of Professor Takao Sato, University of Keio, where zooarchaeological analysis on the Hamanaka 2 remains is being undertaken. The otoliths sampled were all excavated during the 2011 field season. Samples were taken primarily depending on the stratigraphic unit represented, attempting to cover a significant portion of the site's chronology between the shell and otolith samples. The stratigraphic location of the samples is shown in Figure 2. Most stratigraphic units did not produce a large number of *S. sachalinensis* shells or *G. macrocephalus* otoliths, so all suitably intact specimens were used where possible. Valves were also checked to make sure that none 'refit' so as to ensure that two valves from the same individual were not sampled. The paucity of marine material from some layers is primarily an artefact of the site sampling strategy, where prior to 2018 shells and otoliths were not routinely retained unless they were worked or formed a notable deposit (e.g. an abalone midden from an Ainu context (Hirasawa and Kato 2020; Kato 2020)).

Shells were manually washed and cleaned of sediment, and then sectioned using a geological trim saw fitted with a 15.24 cm diameter, 0.1 cm thickness diamond saw blade. Two cuts were made, the first from umbo to shell edge along the axis of maximum growth, and the second to cut away the 'wing' section on the anterior side (Figure 3). The shells were handheld and supported during sectioning. This process left behind a thick section, which was embedded in MetPrep 'Kleer-Set' polyester resin. Once cured, the face showing the shell's maximum axis of growth was ground and polished using silicon carbide papers ranging from P180 to P4000. The embedded section was used for stable isotope analysis, while the unembedded posterior section was used for radiocarbon dating.

Otoliths were also manually cleaned and were embedded in polyester resin in 25 mm rounds. The otoliths were held with support clips during embedding, so that each specimen was upright when embedded. The embedded otoliths were sectioned using a Buehler Isomet low-speed diamond saw and wafering blade. Each was cut once, along the posterior-anterior axis aiming to bisect the nucleus in order to expose a transect across the region where annuli is thickest. The thinner of the two resulting halves was used for stable isotope analysis, and the thicker for radiocarbon dating.

Powdered samples for stable isotope analysis were milled using a computer-operated New Wave Research microdrill. The resin-embedded samples were fixed to the sampling plate and milled using a 0.3 mm diameter diamond-coated drill bit. For shells, the cross-lamellar region was targeted, milling incrementally across a section constituting 3-4 years of shell growth. This region was from the middle of the shell, where the shell is still growing fast enough to produce wide annual increments and the cross-lamellar layer is thick enough for sampling. For otoliths, incremental samples were milled from the edge of the nucleus to (but not overlapping) the edge of the otolith, from the region where growth increments appeared thickest and most clear. Samples were milled as consecutive but discrete trenches following the pattern of the growth increments and were spaced at ~0.8 mm intervals. Trenches were milled up to 300 µm depth in multiple milling passes of 50 µm depth/pass.

Separate powdered samples were taken to test for diagenetic recrystallisation of the aragonite using FTIR-ATR (Loftus, Rogers, and Lee-Thorp 2015), for which no evidence was found. All isotope ratio mass spectrometry was undertaken at the British Geological Society Stable Isotope Facility (Keyworth, Nottingham, UK). See Branscombe et al. (2021) for a full description of the lab protocols.

For the shells, two powdered radiocarbon samples were drilled from each specimen; one from the umbo, representing the date the shell began to grow, and one from the shell edge representing the year of death. This strategy intended to utilise incremental carbonate deposition to provide 'stratigraphic' information to further constrain modelled dates, a method which has been used to good effect on wooden artefacts (Brock et al. 2012). These samples were taken from the external surface of the shell, which was first cleaned using a shot blaster. As the otoliths are significantly smaller, it was not possible to produce paired samples. Instead, one powdered sample was taken from each otolith across its entire width and homogenised. In the case of layer IV, some otoliths that were not suitable for $\delta^{18}O$ sampling (as they did not provide a complete-enough shell transect) were included as additional radiocarbon-only specimens. Radiocarbon samples were processed at the Oxford Radiocarbon Accelerator Unit. Details of the chemical pretreatment, target preparation and AMS measurements can be found in Brock et al. (2010).

Dates were calibrated in OxCal version 4.4 (Bronk Ramsey 2009) using the Marine20 calibration curve (Heaton et al. 2020). Dates were incorporated into a Bayesian model based on stratigraphic phases identified during excavation at Hamanaka 2, the code for which can be found in appendix 1. A total of 14 phases were included, spanning the Late Jomon to Ainu period. A sequential model was used, with start and end boundaries between each period (in order to allow for the possibility of hiatuses in site activity), except in the case of the Towada 1-Motochi 2 Okhotsk sequence (~1550-1000 cal BP), in which the phases were deemed contiguous (Junno et al. 2021). For the three charcoal samples (Miyata et al. 2009; Müller et al. 2016) a charcoal outlier model was used to account for the old wood effect (Dee and Ramsey 2014). For the rest of the samples a general outlier

model was used to down-weight samples likely to be outliers in the chronological model (Ramsey 2009; Junno et al. 2021). For the non-charcoal samples, 8 dates were identified as outliers: Poz-91170, Nuta2-21213, Poz-73802, Poz-73801, Poz-91165, OxA-41455, Poz-91167 and Poz-91169.

Results

Uncalibrated radiocarbon results from the shell and otolith samples are shown in Table 1. All dates cluster within their expected stratigraphic sequence except the two dates from shell II2, which produced an uncalibrated date of ~2000 years earlier than the two other shells from layer II. As a result, this shell is considered intrusive to the layer and is excluded when modelling the Motochi 2 and overall Okhotsk periods. Other than II2, the shell and otolith dates all show good agreement within stratigraphic units, and the two dates from each shell also show close agreement to one another. Calibrated dates span from 3718-3180 cal BP from intrusive shell II2, to 1124-990 cal BP for the youngest Okhotsk shell II1 (Figure 4, appendix 2). Throughout this text, calibrated radiocarbon dates will be referred to using the 95.4% probability range, as recommended by Millard (2014).

Sample ID	**Lab code**	**Material**	**Species**	**^{14}C Age BP**	**1σ (±)**	**δ^{13}C (‰)**
VIII1-umbo	OxA-41446	shell	*S. sachalinensis*	2761	17	0.46
VIII1-edge	OxA-41447	shell	*S. sachalinensis*	2800	17	0.36
VIII2-umbo	OxA-41448	shell	*S. sachalinensis*	2790	17	0.49
VIII2-edge	OxA-41449	shell	*S. sachalinensis*	2814	17	0.41
VIII4-umbo	OxA-41450	shell	*S. sachalinensis*	2769	17	1.33
VIII4-edge	OxA-41451	shell	*S. sachalinensis*	2801	17	0.55
II1-umbo	OxA-41452	shell	*S. sachalinensis*	1655	17	1.88
II1-edge	OxA-41453	shell	*S. sachalinensis*	1646	17	0.4
II2-umbo	OxA-41454	shell	*S. sachalinensis*	3704	18	1.5
II2-edge	OxA-41455	shell	*S. sachalinensis*	3759	18	-0.29
II3-umbo	OxA-41456	shell	*S. sachalinensis*	1647	17	0.73
II3-edge	OxA-41457	shell	*S. sachalinensis*	1676	17	-0.4
IIIa1	OxA-42197	otolith	*G. macrocephalus*	1778	17	-1.2
IIIa2	OxA-42198	otolith	*G. macrocephalus*	1711	17	-2.1
IVa1	OxA-42199	otolith	*G. macrocephalus*	1849	17	-1.8
IV2	OxA-42200	otolith	*G. macrocephalus*	1873	18	-1.2
IV3	OxA-42201	otolith	*G. macrocephalus*	1826	17	-0.7
IV4	OxA-42202	otolith	*G. macrocephalus*	1835	17	-1.1
IV5	OxA-42237	otolith	*G. macrocephalus*	1769	29	-2.72

IV6	OxA-42238	otolith	*G. macrocephalus*	1747	30	-4.55

Table 1: List of ^{14}C dates from marine samples at Hamanaka II obtained in this project

Paired shell dates from the umbo and edge samples are marked in Table 1 by 'X-edge' and 'X-umbo'. The age of the shells was estimated by counting the shell growth increments under light microscopy, and are presented in Table 2, ranging from 11 to 24 years. These paired dates and shell ages (with a ±2 year error for each shell age to account for miscounted and non-annual growth lines) were combined into a model which aimed to use incremental carbonate deposition similarly to 'stratigraphic' information, with a known-age gap separating the two dates in the model. A similar paired date technique has previously been used to good effect using tree rings within carved wooden objects (Brock et al. 2012). Although initial testing – done using models with simulated dates and a 10-15 year age gap – was promising, this was carried out before the release of the Marine20 calibration curve (Heaton et al. 2020). When carried out using the paired archaeological shell dates and the new Marine20 calibration curve, the Bayesian models provides only minimal improvement to the resolution of the shell dates. This is the result of the additional uncertainty incorporated into the new curve. For this reason, the model shown in Figure 4 utilised the edge dates only.

Specimen	VIII1	VIII2	VIII4	II1	II2	II3
Age (years)	24 ±2	12 ±2	18 ±2	11 ±2	17 ±2	20 ±2

Table 2: Estimations of age for each ^{14}C-dated S. sachalinensis *specimen*

A total of 328 archaeological samples were analysed for $\delta^{18}O$ and $\delta^{13}C$, across 7 shells and 3 otoliths. Of these, 285 produced $\delta^{18}O$ and $\delta^{13}C$ measurements, with the remaining 43 samples producing insufficient gas for measurement. This is an overall sample failure rate of 13.1% (approximately equal for shell (13.2%) and otolith (12.5%) samples), and is likely related to the handling of small, powdered samples, where material can be lost on transfer between micromilling and mass spectrometry leading to samples that fall below the minimum size required (Branscombe et al. 2022).

Layer	Period	Count	Mean $\delta^{18}O$	Median $\delta^{18}O$	IQR* $\delta^{18}O$	Min $\delta^{18}O$	Max $\delta^{18}O$	Amplitude $\delta^{18}O$
IIc	Motochi 2	75	0.63	0.53	1.83	−1.37	2.42	3.79
IIIa	Motochi 1	20	1.87	1.90	0.81	0.68	3.39	2.71
IV	Towada 2	7	2.54	2.64	1.10	1.72	3.36	1.64
VIII	Final/Epi-Jomon	149	0.55	0.57	1.47	−1.37	3.23	4.60

*Table 3: Summary results of shell and otolith $\delta^{18}O$ analysis. *IQR = Interquartile range*

Results of $\delta^{18}O$ analysis are summarised by archaeological period in Table 3, excluding the intrusive shell II2 from the Okhotsk levels. $\delta^{13}C$ and $\delta^{18}O$ data are presented in Figure 5, although it should be noted that issues with potential contamination from embedding resin (Branscombe et al. 2022) resulted in some erroneously high $\delta^{13}C$ results. The median $\delta^{18}O$ values for the Motochi 2 and Final/Epi-Jomon periods were very similar (at 0.53 and 0.57‰ respectively), and the minimum $\delta^{18}O$ values are the same for each (to two decimal places) at −1.37‰. The total $\delta^{18}O$ range of the two periods would also be very similar, excepting one particularly high $\delta^{18}O$ value of 4.86‰ which falls just short of the upper limit (*Q3+1.5×IQR*) so is not statistically considered an outlier. Shapiro-Wilk tests performed on the data for each period show that results from the Okhotsk (Towada 2 and Motochi 1) otoliths $\delta^{18}O$ are normally distributed (p=0.39, p=0.84), but that the Motochi 2 and Final/Epi-Jomon shell $\delta^{18}O$ results are non-normally distributed (P=0.02 in both cases). Q-Q plots for the Motochi 2 and Final/Epi-Jomon $\delta^{18}O$ data show the data are under-dispersed or platykurtic, with fewer datapoints in the tails than expected for a normal distribution. $\delta^{13}C$ results were not statistically analysed due to the issues relating to resin contamination as previously mentioned.

To convert $\delta^{18}O$ to SST (°C), a modified version of Grossman and Ku's (1986) aragonite palaeotemperature equation was used:

$$SST = 20.6 - 4.34(\delta^{18}O_{aragonite} - (\delta^{18}O_{seawater} - 0.27))$$

This uses a −0.27‰ correction on the value of $\delta^{18}O_{seawater}$ to account for the use of the VSMOW (Vienna Standard Mean Oceanic Water) scale rather than the older SMOW scale (Leng and Lewis 2016). For $\delta^{18}O_{seawater}$ a constant value of −0.85‰ was used, based on regional data from the NASA

Global Seawater Oxygen-18 Database (Schmidt, Bigg, and Rohling 1999)[1]. Table 4 and Figure 6 show estimated ocean palaeotemperatures for each period studied. Overall, these range from 1.02 °C to 21.68 °C.

As a constant value was used for $\delta^{18}O_{seawater}$, the similarities between Motochi 2 and Final/Epi-Jomon $\delta^{18}O$ results are directly reflected in the SST estimates. The data are not normally distributed, so the Kruskal-Wallis test is used to determine whether differences between periods are statistically significant. When comparing the Motochi 2 and Final/Epi-Jomon shell-derived SST there is no statistical difference between the two groups, with the Kruskal-Wallis test returning a P-value of 0.61. As is clear from Figure 6, there is minimal overlap between the interquartile range of the Towada 2 and Motochi 1 otolith-derived SST compared and that of the Motochi 2 and Final/Epi-Jomon shell-derived temperatures. The difference between the Okhotsk data and the other periods studied is statistically confirmed with a Kruskal-Wallis test returning a P-value of <0.01.

Period	*Material*	*Count*	*Mean (°C)*	*Median (°C)*	*IQR* (°C)*	*Min (°C)*	*Max (°C)*	*Mid-range (°C)*
Motochi 2	Shell	75	13.02	13.42	7.92	5.22	21.68	13.45
Motochi 1	Otolith	20	7.61	7.47	3.53	1.02	12.78	6.90
Towada 2	Otolith	7	4.71	4.27	4.78	1.12	8.28	6.95
Final/Epi-Jomon	Shell	149	13.35	13.27	6.40	1.72	21.69	11.71
3718-3180 cal BP	Shell	33	12.03	11.50	8.80	−0.33	21.98	10.83

*Table 4: Summary of SST estimations by period, as calculated using $\delta^{18}O$. *IQR = Interquartile range*

[1] https://data.giss.nasa.gov/o18data/

Discussion

New ΔR values

As previously outlined, the inter-species variability in ΔR shown by Miyata et al. (2016), and for Hokkaido more generally (Kuzmin et al. 2007; Yoneda et al. 2007), has meant that subsequent chronological modelling from Hamanaka 2 beyond the Late Jomon period has excluded dates on material affected by marine reservoir effects (Junno et al. 2021). However, as Junno et al. (2021) point out in their conclusion, by modelling the site's stratigraphy based on terrestrial botanical samples, the issue of this complex marine system can be circumvented. Using the existing terrestrial results from Hamanaka 2 (Miyata et al. 2016; Müller et al. 2016; Leipe et al. 2017, 2018a; Junno et al. 2021), we suggest it is now be possible to reintegrate marine samples into the chronological model, using this terrestrial model as a basis from which to calculate new ΔR values which can unlock the potential of marine material to shed further light on site chronology, and by extension increase the potential for the use of marine material in future regional chronologies.

Table 5 shows the Late Jomon marine reservoir effects calculated by Miyata et al. (2016), which were calculated by reference to terrestrial dates from wood samples excavated from the same layer. The values have been updated from their original publication, in order to reflect changes to the marine calibration curve with the introduction of Marine20 (Heaton et al. 2020). Table 6 shows new ΔR values calculated using the shell and otolith dates produced in the present study. ΔR values were calculated using the online http://calib.org/deltar/ tool presented by Reimer and Reimer (2017). The marine radiocarbon age and σ was calculated for each layer using the R_combine function in OxCal to produce a single age estimate for each layer (see appendix 1). The umbo dates for each shell were excluded, as were the dates from shell II_2, which was clearly identifiable as an intrusively old shell based on its ^{14}C age. The independent age determination used was a combined terrestrial date for each of the layers in question, using R_combine in OxCal to combine terrestrial results from previous dating at Hamanaka 2 (Leipe et al. 2017, 2018b; Junno et al. 2021). Outliers identified in Model 2 from Junno et al. (2021) were also excluded when combining terrestrial dates.

As is clear from the results presented in Table 5 and Table 6, the ΔR values vary between both species and stratigraphic units, i.e., age. Chronological variation is clearest when comparing within a species; for example, coastal bivalve shells have a ΔR value of 30 ±58 in the Late Jomon, 102 ±58 in the Final/Epi-Jomon, and then −57 ±62 during the Late Okhotsk (Motochi 2) period. The re-calculated values for the Late Jomon shells (Miyata et al. 2016) and our results from the Final/Epi-Jomon are similar, which indicates that despite the time gap between these periods of ~700 years these periods share a similar marine carbon reservoir. The younger Motochi 2 shells show a smaller ΔR value of −57 ±62. Although there is overlap between the uncertainty ranges of all three ΔR values, the lower value for layer IIc suggests that the marine reservoir during this period had a 'younger' carbon reservoir than during the Final Jomon to Final/Epi-Jomon periods.

Layer	*Material*	*Period*	*ΔR*	*±*	*n*
V	charred material	Late Jomon	304	70	4
V	shell	"	30	58	4
V	alcidae	"	148	52	1
V	sea lion	"	248	52	1

Table 5: ΔR values from Miyata et al. (2016), updated using the Marine20 radiocarbon curve

Layer	*Material*	*Period*	*ΔR*	*±*	*n*
IIc	shell	Motochi 2	−57	62	2
IIIa	otolith	Motochi 1	21	40	2
IV	otolith	Towada 2	−203	57	6
VIII	shell	Final/Epi-Jomon	102	58	3

Table 6: New ΔR values calculated using the marine ^{14}C results from this thesis

As is visible in the results of Miyata et al. (2016), the material being sampled – and more specifically the carbon reservoir incorporated by that material – can make a key difference to ΔR offsets. In our case, the otolith ΔR values are not directly comparable to shell ΔR values. While it is possible that this reflects diachronic change in the MRE, a more likely explanation is that *S. sachalinensis* and *G. macrocepahlus* occupy two different marine niches with correspondingly different carbon reservoirs. *S. sachalinensis* is a shallow water species which lives and feeds in coastal waters above the thermocline at 1-15 m depth (Golikov and Scarlato 1970; K. Sasaki 1989; S. Sasaki and Ohta 1999), where the carbon reservoir around Rebun Island is primarily influenced by the prevailing Soya Warm Current. By contrast, *G. macrocephalus* live largely offshore in deeper waters (Boeing, Martin, and Duffy-Anderson 2007; Savin 2008; West, Wischniowski, and Johnston 2012; West et al. 2020), out of

the Soya Current's direct influence. For comparison, pre-bomb shells with known collection ages in southwest Hokkaido, where the current dominates, provide a ΔR of -96 ±42 yrs (n = 2) (Yoneda et al. 2007) when re-calculated using the Marine20 curve.

In terms of the existing reservoir corrections from Hamanaka 2, we expected the ΔR values of the cod otoliths to look most similar to that of the Japanese sea lion (the recently extinct *Zalophus japonicus*) (Miyata et al. 2016), which feeds on deep water species such as cod that should have a larger reservoir correction reflecting the deep water 'older' carbon environment. However, the results in Table 6 show that the corrections produced for otoliths from this study – for both the Towada 2 and Motochi 1 periods – are actually much smaller than those presented for Late Jomon sea lions in Table 5. These low ΔR values could indicate reduced upwelling during the Okhostk period compared to the Late Jomon (Dewar et al. 2012). The results in Table 6 again demonstrate the temporal variability in ΔR in this region, and highlight the importance of calculating period- and species-specific ΔR values when incorporating marine dates into a model.

While it is clearly important to account for marine reservoir effects in sites occupied by marine-adapted groups, it is unavoidable that the logic used to calculate ΔR values has an element of circularity (Elias 2007; Martindale et al. 2018). This is because the method for calculating ΔR forces marine dates to correspond to existing terrestrial dates, which relies on those dates themselves being reliable. The extent to which this is actually true depends on the confidence with which the existing site chronology is known. We should also acknowledge that reservoir effects calculated based on only a small number of dates should be treated with less confidence than those supported by a larger pool of data. In the case of the present study, we feel confident that the terrestrial modelling done by Junno et al. (2021) is a reliable starting point for ΔR calculation, even where layers are represented by only a single terrestrial date (e.g. Towada 2, Motochi 2), since such cases are well-constrained by surrounding phases.

An updated chronological model for Hamanaka 2

Using the new ΔR values in Table 6 alongside the existing chronological model of Junno et al. (2021), including dates from Müller et al. (2016), Leipe et al. (2017), and Leipe et al. (2018b), and existing marine dates from Miyata et al. (2016), we can present an updated model of site chronology at Hamanaka 2 which benefits from both terrestrial and marine materials. Figure 4 shows the resulting OxCal model, which spans from ~3351 cal BP to present day. As with Junno et al.'s (2021) previous model, the period of site occupation is discontinuous, with hiatuses in the radiocarbon record between the Late Jomon and Final/Epi-Jomon, the Epi-Jomon and Okhotsk, and Okhotsk to the Satsumon and Ainu periods. The major difference between the two models is the final hiatus in the previous model occurs between the Motochi 1 and Motochi 2 periods, whereas the model in this paper instead shows a hiatus following the Motochi 2 period. The extension of the model to 'present day' by radiocarbon standards is not unexpected, since the dates from layer I – the historical Ainu – are recent enough that the 95.4% probability range extends to the post-bomb pulse period. There is not much discussion in the literature concerning Ainu occupation at Hamanaka 2 and its (dis)continuity with 'modern' occupation, but the Junno et al. (2021) model suggests that the Ainu phase lasts until potentially as late as 1930 CE, so it seems reasonable to suggest that there is significant continuity and overlap between what we consider to be historical Ainu and 'modern' occupation at the site.

One of the major recommendations made by Junno et al. (2021) was that more samples from layer IIc/Motochi 2 were needed, in order to constrain the timing of the Final Okhotsk at Hamanaka 2. In their paper, Junno et al. produce two models for site chronology at Hamanaka 2, one based on the results of Bayesian modelling of all dates in OxCal – Model 1 – and another – Model 2 – which specifically focused on layers VIII-IIC (Final/Epi-Jomon to Motochi 2). Model 1 showed an extended age range for the Okhotsk periods (specifically layer IIc) and particularly young age ranges for layers IIb and IIa, none of which were supported by prior understanding of cultural development at the site (nor in Hokkaido more generally). They considered that this was likely due to the small number of

samples representing layers IIc-IIa (Motochi to Satsumon), and that anthropogenic soil disturbances and bioturbation had led to the redeposition of botanical remains. Although the use of terrestrial macrobotanical material in radiocarbon dating overcomes the issue of marine reservoir correction, these small, light remains are far more susceptible to mixing between layers and redeposition than larger, heavier shell remains. Where layers IIb and younger were excluded in Model 2, Junno et al. found an end-date for the Okhotsk period of 1103-1070 cal BP, which is more closely aligned to existing archaeological understanding.

The current study adds new dates from two *S. sachalinensisi* valves from the Motochi 2 layer (excluding II2, identified as an older intrusion predating the Final Jomon period). The addition of these dates does indeed prove useful, as they provide confirmation that the terrestrial result extending the Motochi 2 phase in Model 1 from Junno et al. (2021) is a younger outlier and likely the result of the redeposition of more recent plant macroremains into the Motochi 2 layer. The model presented here in Figure 4 differs from Junno et al.'s Model 1, and despite the inclusion of samples from layers IIb-I, results in an estimate for the end of the Okhotsk period of 1107-958 cal BP which is much more similar to that suggested by Junno et al.'s Model 2. This new model unfortunately does not help constrain the dating of the Satsumon period, with no new samples added for layers IIb or IIa. As noted by Junno et al., the stratigraphic continuity between layers IIa-c, combine with the relative stratigraphic insecurity of seeds excavated from these layers, means that dates representing layers IIb and IIa in Figure 4 are also likely to be misleadingly young.

$\delta^{13}C$ results

Marine carbonate $\delta^{13}C$ results are notoriously difficult to interpret, especially in a palaeo- or archaeological context. Several oceanographic factors can influence $\delta^{13}C$, including prevailing currents, upwelling, salinity, temperature, and thermocline depth (Arthur et al. 1983; Gillikin et al. 2006; McConnaughey and Gillikin 2008). In a recent paper on modern *S. sachalinensis* from southern Hokkaido, we were unable to demonstrate any clear relationship between shell $\delta^{13}C$ and

environment, even with the knowledge of time/place of collection and modern environmental records against which to compare (Branscombe et al. 2021). Given this, we are reticent to interpret variation in shell $\delta^{13}C$ as related to palaeoenvironmental change, especially given the issues with resin contamination that affected $\delta^{13}C$ results in this case. More detailed discussion of this issue can be found in Branscombe et al. (2022).

That being said, it is clear from the otolith results that $\delta^{13}C$ is positively correlated with $\delta^{18}O$. This is confirmed by linear regression which shows a positive correlation between otolith $\delta^{13}C$ and $\delta^{13}C$ and $\delta^{18}O$ (r^2 = 0.4, p = <0.01). By comparison, the relationship between the two for the *S. sachalinensis* shells is only a weak negative correlation. There is certainly more difference between the $\delta^{13}C$ of shells and otoliths than between the different cultural periods at Hamanaka 2, which means that in combination with the complex relationship between environment and carbonate precipitation, it is not possible to reach any firm conclusions on diachronic changes in the ocean based on $\delta^{13}C$ results from Hamanaka 2.

$\delta^{18}O$ results

The relationship between sea surface temperature (SST) and the $\delta^{18}O$ of incrementally-grown marine carbonates is well known, including the species of fish and shellfish used in this study (Khim, Woo, and Je 2000; Alaska Fisheries Science Center 2015; Helser et al. 2018; Branscombe et al. 2021). The results from the archaeological shells in this show clear seasonal cycles in $\delta^{18}O$. Peaks in shell $\delta^{18}O$ correspond to seasonal temperature minima. The otolith $\delta^{18}O$ results do not show seasonal cycles in $\delta^{18}O$, and instead show a gradual increase in $\delta^{18}O$ across the sampling transect, consistent across all specimens. As with $\delta^{13}C$, the difference between the ecological niches of the fish/shellfish are much greater than the palaeothermometric differences between periods.

The lack of visible seasonal cycles is likely due to the small size of the otoliths, which means that annual growth increments are much thinner than those sampled in the *S. sachalinensis* specimens and each sample will represent an averaged $\delta^{18}O$ over a longer span of shell growth. The increase in

$\delta^{18}O$ across the fish's life history can also be seen in previous studies of Pacific cod (Gao et al. 2005; Helser, Kastelle, Crowell, et al. 2018), so we are confident that it does not relate to the specific oceanographic context of Rebun Island. Helser et al. (2018) suggest that this ontogenetic trend relates to migration from warmer coastal waters to deeper water over the first year of the fish's life. This, along with the visibility of multiple growth lines in each otolith section, confirm that all otoliths sampled in this study are those of adult fish greater than one year in age (Catherin West, pers. comm.). In terms of fishing adaptations at Hamanaka 2, there is increased evidence for year-round fishing activity from the Okhotsk period (T. Sakaguchi 2007b, 2007a; Tsutaya et al. 2021), with Eda et al. (2016) suggesting that this period could have seen the development of advanced seafaring technology. Such technology would have increased the ability of occupants at Hamanaka 2 to catch adult cod in deeper oceanic waters.

Even without subannual temperature information from otolith $\delta^{18}O$ series, Figure 6 still demonstrates that the overall temperature range displayed by the otoliths is cooler than that of the shells. As we do not expect significant climatic variation between the successive (Figure 4) Motochi 1 and Motochi 2 periods, we can use comparison of the otoliths and shells excavated from these layers to see that the temperature difference is primarily due to ecological niche rather than broader palaeoclimate; the fish are living in a cooler (pelagic) environment than the coastal shells. West et al. (2012) noted a relatively consistent trend in which the annulus $\delta^{18}O$ was significantly lower than that of the rest of the otolith; we may have seen more overlap in temperature between the otoliths and shells had we incorporated the annulus into our sampling transect.

Of the otolith oxygen data, the specimen from the Towada 2 phase (early Okhotsk) shows a narrower and lower temperature range than the data from Motochi 2 (Final Okhotsk). Leipe et al. (2018b) demonstrate that the beginning of the Okhotsk period coincides with deforestation on Rebun Island (~1400-1500 cal BP), potentially related to climatic deterioration, anthropogenic activity, or a combination thereof. The slightly warmer temperatures inferred here from otoliths of

the Final Okhotsk period may indicate that this period of climatic deterioration was relatively short-lived, and that by the latter stages of Okhotsk occupation at Hamanaka 2 the climate had once again ameliorated. However, given small sample size of otoliths, both the number of specimens and the number of samples taken from each specimen, it is not possible to draw firm conclusions from this evidence and more samples from throughout the Okhotsk period would be needed to confirm this. Preferably, *S. sachalinensis* shells from the Okhotsk period would be sampled to provide a more direct comparison with other layers, and because palaeoclimatic interpretation of otoliths is also confounded by the fact that they – unlike the surf clams – are a mobile species which can adjust their habitat, feeding pattern sand behavioural range in response to environmental change.

In terms of interpreting the data from the Final/Epi-Jomon *S. sachalinensis* samples, the results from Branscombe et al. (2021) show that although $\delta^{18}O$ is a useful temperature proxy, it does not reliably detect extremes in temperature, as growth stoppages occur during times of extreme weather, seasonal temperature extremes and predation. Due to this, we should assume that the temperature ranges suggested by these archaeological shells are a *minimum* rather than complete range, and that the true maximum and minimum annual atmospheric temperatures will usually be outside this range. Nevertheless, the shells do produce useful palaeotemperature information. For all three periods represented by shells (Final/Epi-Jomon, Motochi 2, and the single intrusive shell dated to 3718-3180 cal BP), the vast majority of samples fall between ~5-22 °C, and the median temperatures for the Final/Epi-Jomon and Motochi 2 periods are particularly similar at 13.27 and 13.42 °C, respectively (Table 3, Figure 6). This suggests that there is no significant difference in SST between these periods. Again, the similarity in temperature range of pre-Okhotsk (Final/Epi-Jomon) and Final Okhostk (Motochi 2) shells indicates that any climatic deterioration occurring the onset of the Okhotsk period did not last until the end of the Okhotsk. In future research at Hamanaka 2, it would be beneficial to seek shell and otolith specimens from a wider range of periods in order to facilitate the study of diachronic change in nearshore and pelagic water temperature.

Compared to modern day temperatures at Rebun, it is difficult to establish any clear differences compared to those from the archaeological periods studied here. Modern water temperature around Rebun reaches an average minimum of 3.8 °C in Feb/March and maximum of 20.8 °C in August[2]. The minimum temperatures shown by the *S. sachalinensis* are slightly lower than this (Table 4), although we would argue that difference is more likely to relate slow shell growth during the coldest part of the year. Without modern *S. sachalinensis* specimens from Rebun Island itself, it is difficult to compare the shell records directly to modern observed water temperatures as our previous research indicated that seasonal extremes in SST are not always well-represented by shell $\delta^{18}O$ records (Branscombe et al. 2021). Consequently, we are also reticent to draw conclusions about whether the effects of the Medieval Warm Period can be seen in the Final Okhotsk shells and otoliths as we cannot conclusively argue that the archaeological shells show temperature differences as compared to one another nor modern day local climate.

Conclusions

This study presents new ΔR values for the Final/Epi-Jomon, Early Okhotsk (Towada 2), and Final Okhostk (Motochi 1 and Motochi 2) periods, which will be applicable to a variety of sites in northern Japan influence by similarly influenced by the Soya and Oyashio currents. As samples were taken from both *S. sachalinensis* valves and *G. macrocephalus* otoliths, these ΔR values should be used with the understanding that they relate to species with different ecological niches, and therefore accessing different radiocarbon reservoirs. Otolith ΔR values are a better representation of deep-water pelagic species, while shell values reflect the shallow coastal environment above the thermocline. The ΔR values we calculated for otoliths were surprisingly small, given that we would expect pelagic species to have a greater ΔR offset reflecting deep 'old' water. However, the close agreement of ^{14}C yr ages between otoliths from layer IV (excepting IV5 and IV6) does suggest that they are all contemporaneous to the layer so we do have relatively high confidence in this ΔR

[2] https://en.climate-data.org/asia/japan/hokkaido/rebun-770592/#water

calculation. The existence of species-specific ΔR offsets has important implications for how radiocarbon dates on humans (and other terrestrial animals) with a strong marine dietary component – such as those pertaining at Hamanaka and other Jomon and Okhotsk sites in Hokkaido (Tsutaya et al. 2013, 2014) – are calibrated. Bone collagen stable carbon and especially nitrogen values may provide some indication of which resources dominate (e.g., higher $\delta^{15}N$ values will be associated with the consumption of piscivorous fish and/or marine mammals), and so which ΔR to use, but the mixed diets of most coastal hunter-gatherers will complicate this and lead to increased uncertainty in the calibrated date (e.g. Okamoto et al. 2016).

Our results build on those of Miyata et al. (2016), and show how ΔR is variable over time as well as between species. However, following the example of Miyata et al., through the combination of paired terrestrial and marine dates throughout the sequence, it is still possible to incorporate marine dates into the overall chronological model of the site. In this paper we demonstrate the benefits of this marine integration. Increasing the sample size for the Motochi 2 (IIc) layer allows the overall OxCal model for the site (Figure 4) to align more closely with existing archaeological understanding of cultural chronology in Hokkaido. Our results offer promise for dating marine materials from the poorly dated layers in the uppermost section of the stratigraphy (IIb – I, post-Okhotsk to Historical Ainu). Marine evidence, such as the shells and otoliths utilised in this study, will be larger and easier to sample than macrobotanical remains, more stratigraphically secure due to their larger size, and can be collected directly during excavation prior to flotation. Palaeobotanical remains from the uppermost layers also appear to suffer from the most disturbance, likely related to continued modern land use.

Palaeoclimatically, our results do not show evidence of any dramatic shift in climate when comparing Final/Epi-Jomon shell $\delta^{18}O$ records. As discussed above, the single otolith sampled from layer IV does appear to show a cooler temperature range than those in the later Motochi 1 phase. However, this relies on only one specimen and additional samples would be needed to confirm this.

Preferably, *S. sachalinensis* would be sampled for all stratigraphic layers, as these show a more reliable record of near-coastal palaeotemperature which is more closely related to coastal and atmospheric temperature conditions than those for pelagic-dwelling fish. These larger shells also provide longer-lived records, with wider growth increments to allow for subannual sampling via either hand drilling or micromilling (Branscombe et al. 2022), and do not suffer from the ontogenetic shift in $\delta^{18}O$ evident in the otoliths (Figure 5).

Overall, we show that previous researchers have been sensible to approach marine dates from Hamanaka 2 (and the northern Hokkaido region more generally) with caution, as there is an issue of chronologically-variable and species-specific marine reservoir effects. However, for coastal sites occupied by maritime adapted hunter-gatherers such as Hamanaka 2, marine materials are not only a valuable source of information on subsistence and resource management (Tsutaya et al. 2021), but also present an important archive of palaeotemperature which can be directly ^{14}C-dated to accurately contextualise the palaeotemperature information within the site's chronology. In the future, these records could be a vital means of accessing subanually-resolved and Hokkaido-specific climatic information. This will be key in constructing an archaeology of Hokkaido that properly recognises its distinct cultural development within the wider context of Japanese archaeology.

Acknowledgements

This work was supported by NEIFSC project grant [IP-1944-1119]; NEIFSC project grant [IP-2278-0320]; and a Clarendon Fund Scholarship. Fieldwork funding was also provided by the Sasakawa Foundation, Hokkaido University, Oxford University's Travel Abroad Bursary, and the Brasenose College Student Support Find and Graduate Research Grant. Samples from the 2011 excavations were provided by the Baikal-Hokkaido Archaeology Project and Keio University, and samples from the 2018 excavations were provided by the Core-to-Core Project and Hokkaido University. Thanks to researchers and staff members at the BGS Stable Isotope Facility in Keyworth, the Sclerochronology Research Group at Exeter University's Penryn campus, the Oxford University radiocarbon laboratory

and the Oxford University Earth Sciences department, all of whom provided guidance and assistance throughout the project.

Figures

Figure 1: Map of Hokkaido showing the location of Hamanaka II, and the major oceanographic currents influencing the region. Image reproduced from Müller et al. 2016

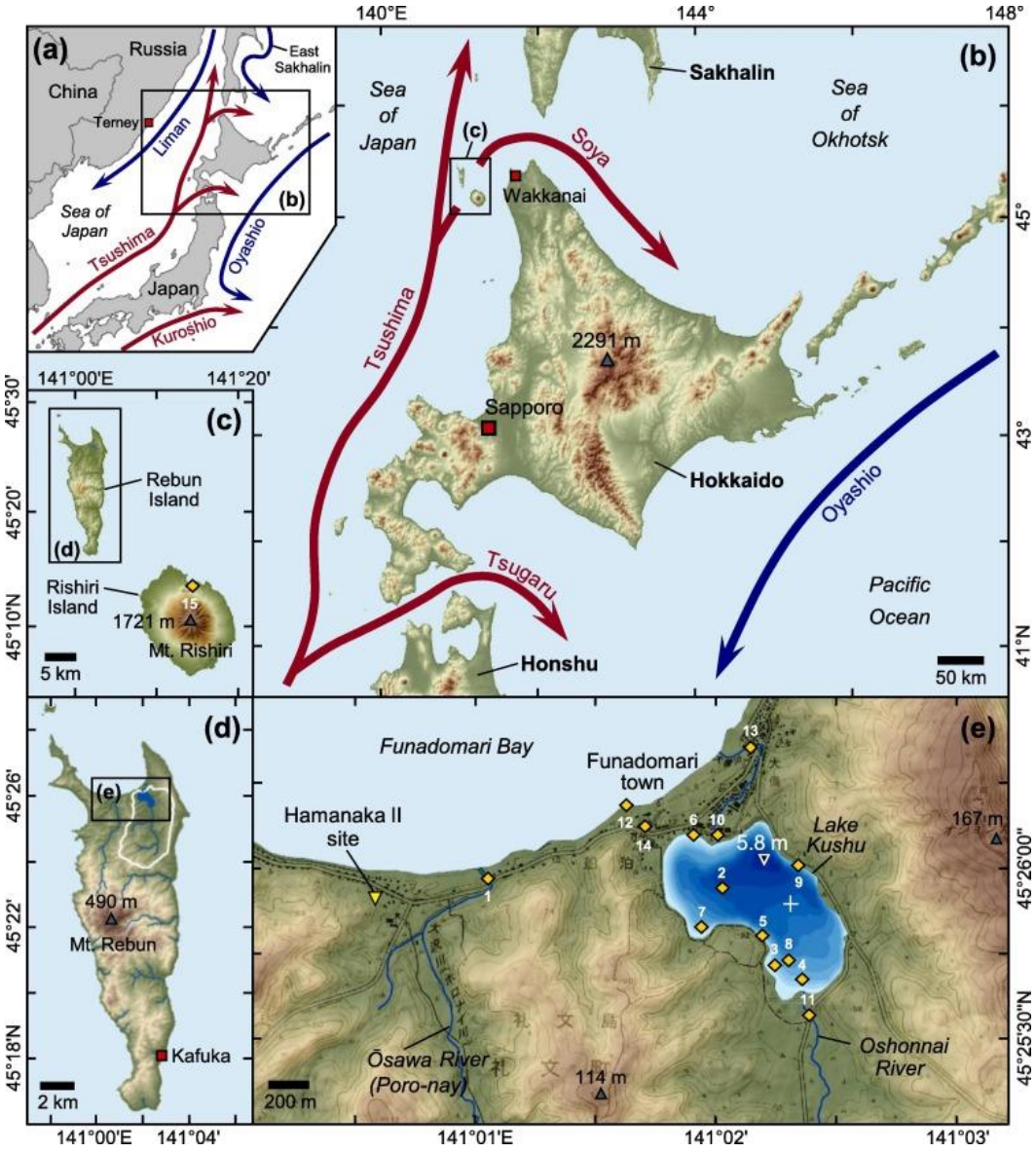


Figure 2: Stratigraphic profile for Hamanaka II (modified from Müller et al. 2016), showing locations of proposed samples, existing chronology, and key climatic events

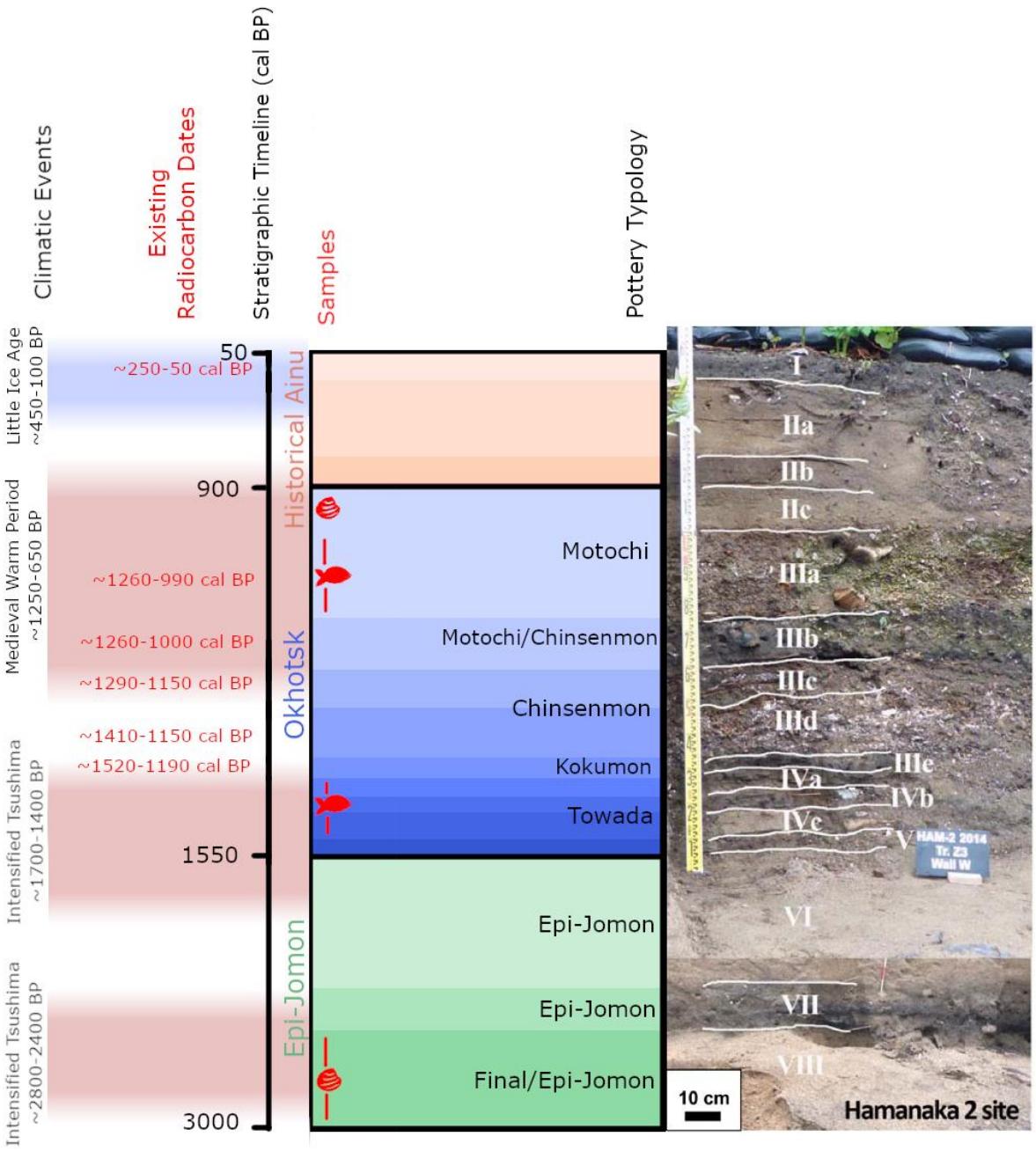


Figure 3: illustration showing the way in which Spisula sachalinensis *shells were sectioned from umbo to shell edge, along the axis of maximum growth*

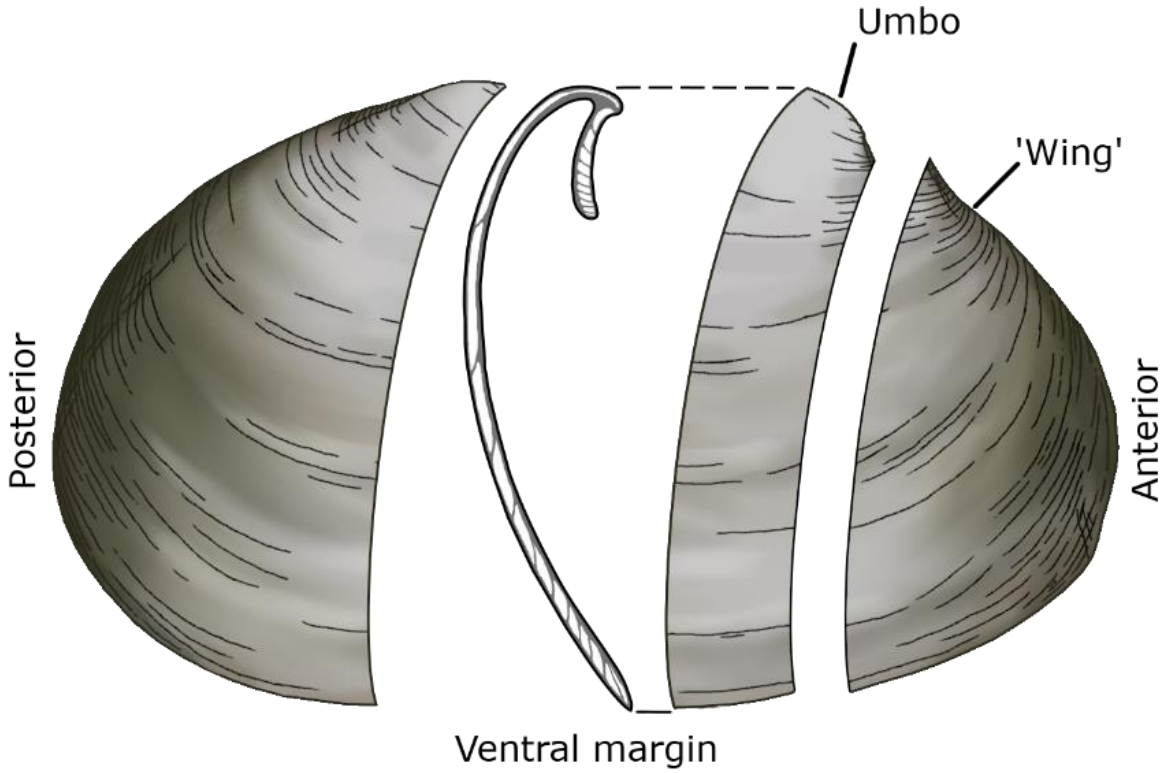
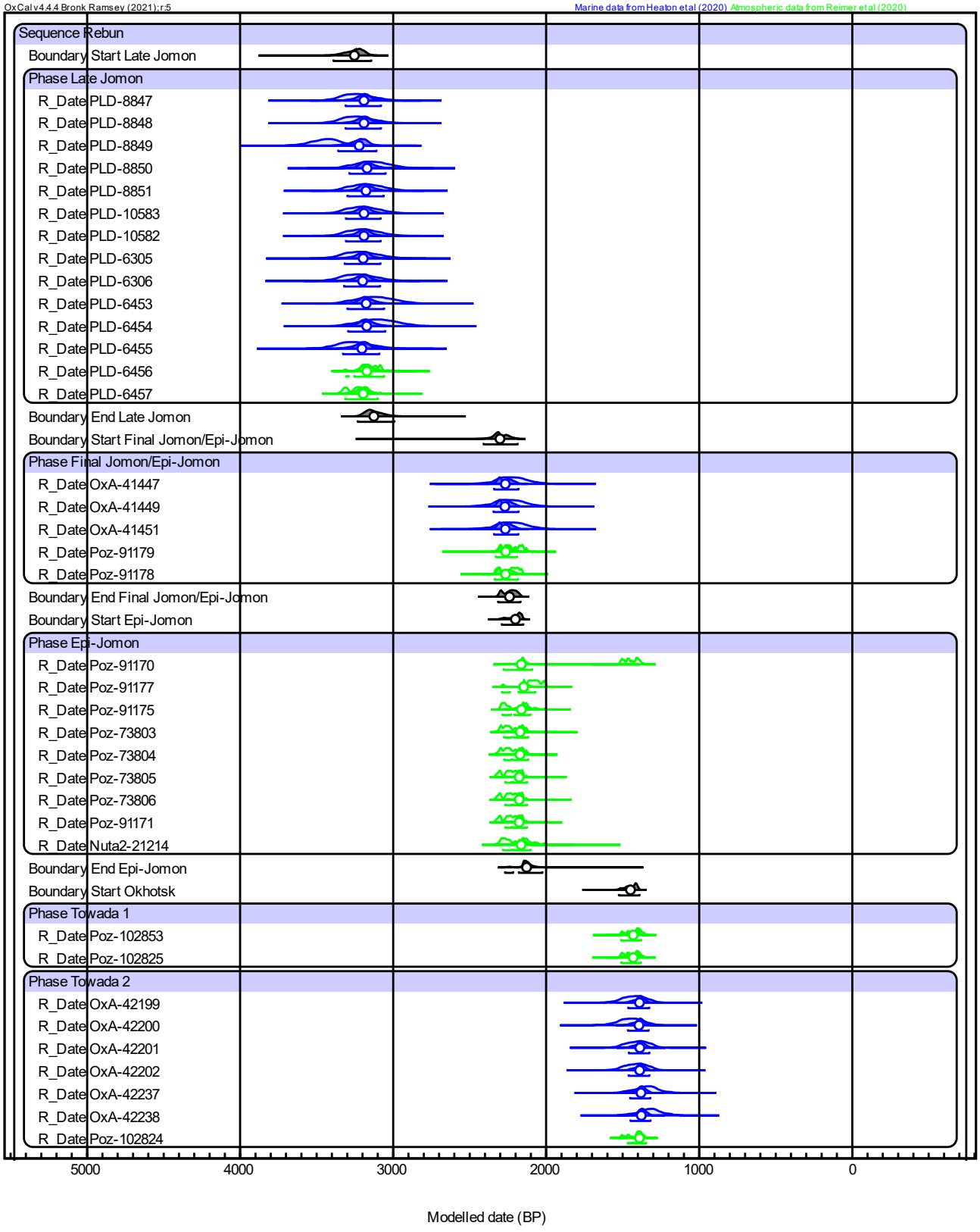


Figure 4: Results plot of radiocarbon sequence for Hamanaka 2, including 73 dates over 14 phases. Existing ^{14}C data coming from Miyata et al. (2009), Muller et al. (2016), Leipe et al. (2017, 2018), and Junno et al. (2021). Cont. overleaf.



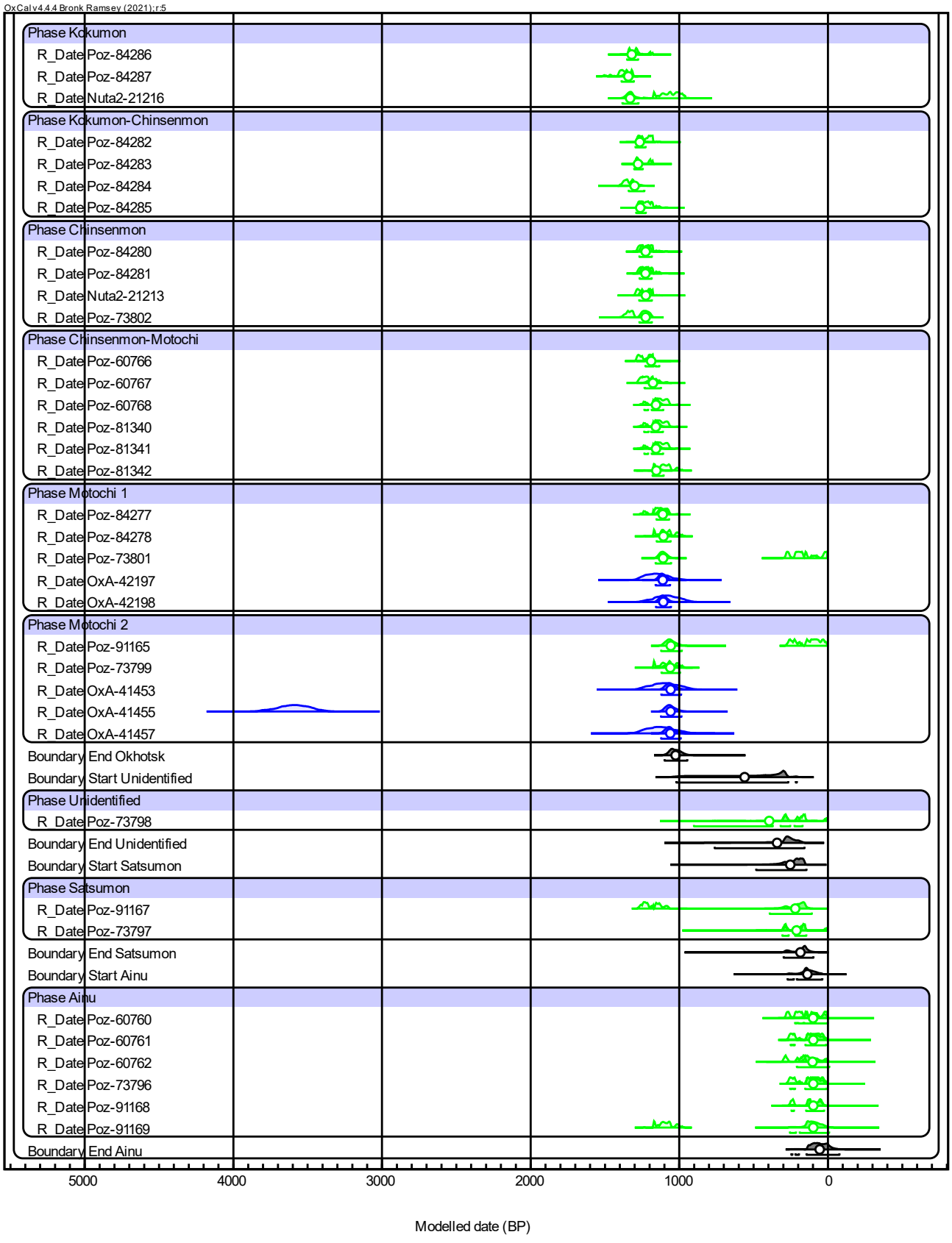

OxCal v4.4.4 Bronk Ramsey (2021); r:5
Phase Kokumon
R_Date Poz-84286
R_Date Poz-84287
R_Date Nuta2-21216
Phase Kokumon-Chinsenmon
R_Date Poz-84282
R_Date Poz-84283
R_Date Poz-84284
R_Date Poz-84285
Phase Chinsenmon
R_Date Poz-84280
R_Date Poz-84281
R_Date Nuta2-21213
R_Date Poz-73802
Phase Chinsenmon-Motochi
R_Date Poz-60766
R_Date Poz-60767
R_Date Poz-60768
R_Date Poz-81340
R_Date Poz-81341
R_Date Poz-81342
Phase Motochi 1
R_Date Poz-84277
R_Date Poz-84278
R_Date Poz-73801
R_Date OxA-42197
R_Date OxA-42198
Phase Motochi 2
R_Date Poz-91165
R_Date Poz-73799
R_Date OxA-41453
R_Date OxA-41455
R_Date OxA-41457
Boundary End Okhotsk
Boundary Start Unidentified
Phase Unidentified
R_Date Poz-73798
Boundary End Unidentified
Boundary Start Satsumon
Phase Satsumon
R_Date Poz-91167
R_Date Poz-73797
Boundary End Satsumon
Boundary Start Ainu
Phase Ainu
R_Date Poz-60760
R_Date Poz-60761
R_Date Poz-60762
R_Date Poz-73796
R_Date Poz-91168
R_Date Poz-91169
Boundary End Ainu
5000
4000
3000
2000
1000
0
Modelled date (BP)

Figure 5: Scatter graphs showing $\delta^{13}C$ and $\delta^{18}O$ results for shells from the Final-/Epi-Jomon, Towada 2, Motochi 1 and Motochi 2 units at Hamanaka 2. X-axes labelled in red (TBVIII3 & TBII1) are measured in % across the sampled shell transect.

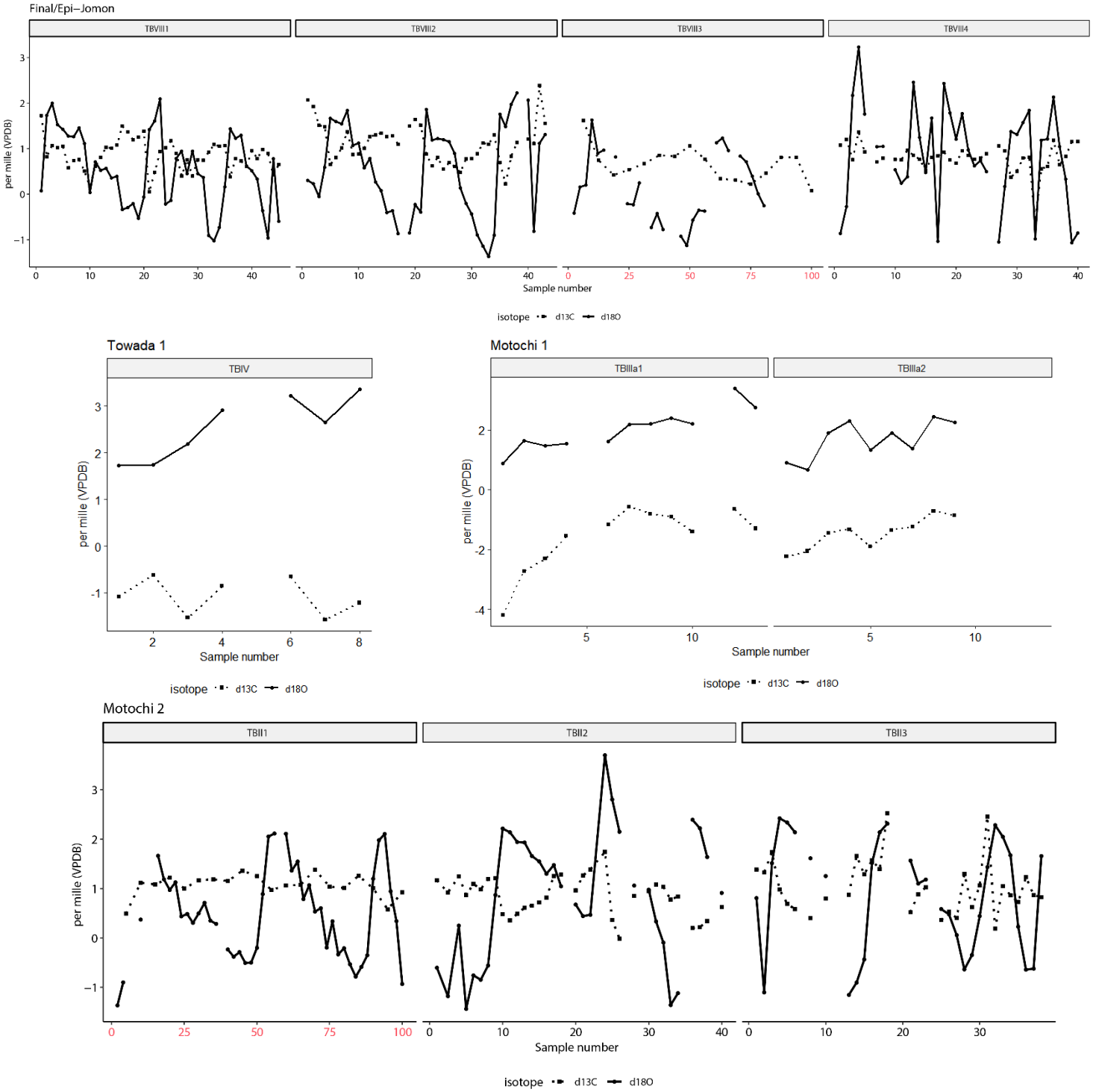
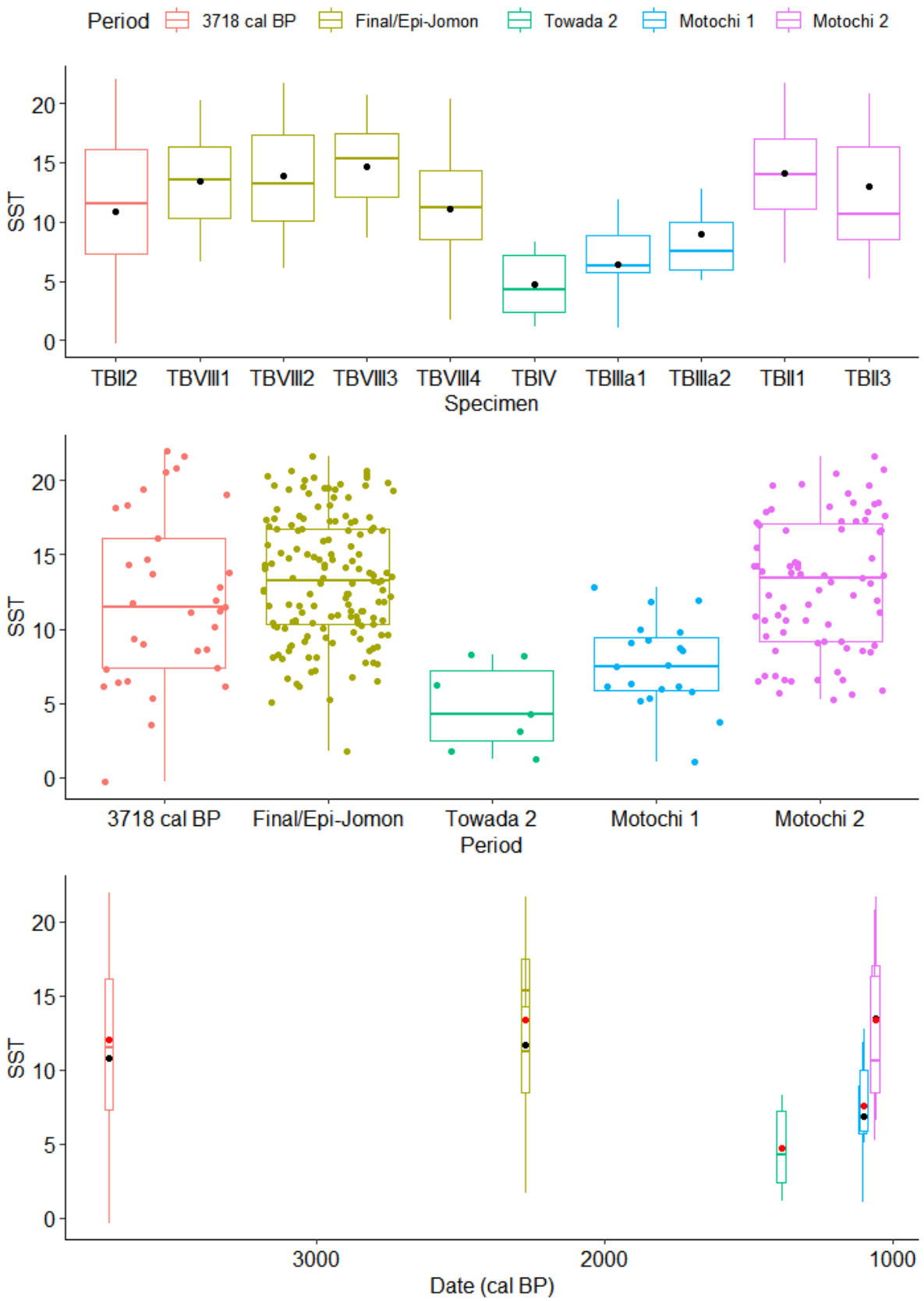


Figure 6: Boxplots showing SST range. Top: SST by specimen, black circles show the mid-range point ((minSST+maxSST)/2). Middle: SST by period, jitter shows distribution of samples. Bottom: SST by specimen with cal BP on x-axis to show relative age gaps between each period, black circles show the mid-range point, red circles show the median



Bibliography

"Age Validation of Pacific Cod Using Stable Oxygen Isotope (Δ18O) in Otoliths." 2015. https://www.fisheries.noaa.gov/feature-story/age-validation-pacific-cod-using-stable-oxygen-isotope-d18o-otoliths.

Amano, T, and A Vasilevski. 2002. "Okhotsk culture formation, metamorphosis and ending: Japan and Russia cooperative symposium TT - サハリンにおけるオホーツク文化の形成と変容・消滅 : 日ロ共同シンポジウム." In *The 5th open symposium of the Hokkaido University Museum*. 北海道大学総合博物館. http://hdl.handle.net/2115/48121.

Arthur, Michael A., Thomas F. Anderson, Isaac R. Kaplan, Jan Veizer, and Lynton S. Land. 1983. *Stable Isotopes in Sedimentary Geology*. *Stable Isotopes in Sedimentary Geology*. SEPM Society for Sedimentary Geology. https://doi.org/10.2110/scn.83.10.

Ascough, Philippa L, Mike J Church, and Gordon T Cook. 2017. "Marine Radiocarbon Reservoir Effects for the Mesolithic and Medieval Periods in the Western Isles of Scotland." *Radiocarbon* 59 (1): 17–31. https://doi.org/DOI: 10.1017/RDC.2016.99.

Ascough, Philippa L, G T Cook, M J Church, A J Dugmore, S V Arge, and T H McGovern. 2006. "Variability in North Atlantic Marine Radiocarbon Reservoir Effects at c. AD 1000." *The Holocene* 16 (1): 131–36. https://doi.org/10.1191/0959683606hl913rr.

Ascough, Philippa L, Gordon T Cook, Andrew J Dugmore, John Barber, Elaine Higney, and E Marian Scott. 2004. "Holocene Variations in the Scottish Marine Radiocarbon Reservoir Effect." *Radiocarbon* 46 (2): 611–20. https://doi.org/DOI: 10.1017/S0033822200035657.

Batten, Bruce L. 2008. "Climate Change in Japanese History and Prehistory: A Comparative Overview."

Boeing, Wiebke J., Michael H. Martin, and Janet T. Duffy-Anderson. 2007. "4.6 - Groundfish." In *Long-Term Ecological Change in the Northern Gulf of Alaska*, edited by Robert B B T - Long-term Ecological Change in the Northern Gulf of Alaska Spies, 259–418. Amsterdam: Elsevier. https://doi.org/https://doi.org/10.1016/B978-044452960-2/50005-9.

Branscombe, Tansy, Julia Lee-Thorp, Rick Schulting, and Melanie J Leng. 2022. "Micromilling Vs Hand Drilling in Stable Isotope Analyses of Incremental Carbonates: The Potential for Δ13C Contamination by Embedding Resin." *Rapid Communications in Mass Spectrometry*. https://doi.org/https://doi.org/10.1002/rcm.9318.

Branscombe, Tansy, Rick Schulting, Julia Lee-Thorp, and Melanie J. Leng. 2021. "The Potential of Marine Bivalve Spisula Sachalinensis as a Marine Temperature Record." *Palaeogeography, Palaeoclimatology, Palaeoecology* 582 (September): 110634. https://doi.org/10.1016/j.palaeo.2021.110634.

Brock, Fiona, Thomas Higham, Peter Ditchfield, and Christopher Bronk Ramsey. 2010. "Current Pretreatment Methods for AMS Radiocarbon Dating at the Oxford Radiocarbon Accelerator Unit (Orau)." *Radiocarbon* 52 (1): 103–12. https://doi.org/DOI: 10.1017/S0033822200045069.

Brock, Fiona, Joanna Ostapkowicz, Christopher Bronk Ramsey, Alex Wiedenhoeft, and Caroline Cartwright. 2012. "Paired Dating of Pith and Outer Edge (Terminus) Samples from Pre-Hispanic Caribbean Wooden Sculptures." *Radiocarbon*. https://doi.org/10.1017/s0033822200047342.

Bronk Ramsey, Christopher. 2009. "Bayesian Analysis of Radiocarbon Dates." *Radiocarbon* 51 (1):

337–60. https://doi.org/DOI: 10.1017/S0033822200033865.

Dee, M W, and C Bronk Ramsey. 2014. “High-Precision Bayesian Modeling of Samples Susceptible to Inbuilt Age.” *Radiocarbon* 56 (1): 83–94. https://doi.org/10.2458/56.16685.

Deith, Margaret R. 1983. “Molluscan Calendars: The Use of Growth-Line Analysis to Establish Seasonality of Shellfish Collection at the Mesolithic Site of Morton, Fife.” *Journal of Archaeological Science* 10 (5): 423–40. https://doi.org/10.1016/0305-4403(83)90058-4.

Dewar, Genevieve, Paula J Reimer, Judith Sealy, and Stephan Woodborne. 2012. “Late-Holocene Marine Radiocarbon Reservoir Correction (ΔR) for the West Coast of South Africa.” *The Holocene* 22 (12): 1481–89. https://doi.org/10.1177/0959683612449755.

Eda, Masaki, Hiroko Koike, and Hiroyoshi Higuchi. 2016. “Understanding Prehistoric Maritime Adaptations in Northern Japan: Indirect Evidence from Ancient DNA and Histological Observations of Albatross (Aves: Diomedeidae) Bones.” *Quaternary International* 419: 159–64. https://doi.org/10.1016/j.quaint.2015.06.067.

Edwards, Walter. 2005. “Japanese Archaeology and Cultural Properties Management: Prewar Ideology and Postwar Legacies.” In *A Companion to the Anthropology of Japan*, edited by Jennifer Robertson, 36–49. Blackwell.

Elias, Scott A. 2007. *Encyclopedia of Quaternary Science*. *Quaternary Science*. Amsterdam, Netherlands : Elsevier.

Emiliani, C., L. Cardini, T. Mayeda, C. McBurney, and E. Tongiorgi. 1964. “Palaeotemperature Analysis of Marine Molluscs (Food Refuse) from the Site of Arene Candide Cave, Italy and the Haua Fteah Cave, Cyrenaica.” In *Isotopic and Cosmic Chemistry*, edited by H. Craig, S. Miller, and G Wasserburg. Amsterdam: North-Holland Publishing Company.

Gao, Yongwen, Greg G. Bargmann, Uwe Brand, and David L.G. Noakes. 2005. “Stable Isotopic and Trace Elemental Compositions of Otoliths and the Stock Structure of Pacific Cod, Gadus Macrocephalus.” *Environmental Biology of Fishes* 74 (3–4): 335–48. https://doi.org/10.1007/s10641-005-1332-7.

Gillikin, David Paul, Anne Lorrain, Steven Bouillon, Philippe Willenz, and Frank Dehairs. 2006. “Stable Carbon Isotopic Composition of Mytilus Edulis Shells: Relation to Metabolism, Salinity, Δ13CDIC and Phytoplankton.” *Organic Geochemistry* 37 (10): 1371–82. https://doi.org/10.1016/j.orggeochem.2006.03.008.

Golikov, A. N., and O. A. Scarlato. 1970. “Abundance, Dynamics and Production Properties of Populations of Edible Bivalves Mizuhopecten Yessoensis and Spisula Sachalinensis Related to the Problem of Organization of Controllable Submarine Farms at the Western Shores of the Sea of Japan.” *Helgoländer Wissenschaftliche Meeresuntersuchungen* 20 (1–4): 498–513. https://doi.org/10.1007/BF01609925.

Grossman, Ethan L., and Teh Lung Ku. 1986. “Oxygen and Carbon Isotope Fractionation in Biogenic Aragonite: Temperature Effects.” *Chemical Geology: Isotope Geoscience Section* 59 (C): 59–74. https://doi.org/10.1016/0168-9622(86)90057-6.

Habu, Junko, Akira Matsui, Naoto Yamamoto, and Tomonori Kanno. 2011. “Shell Midden Archaeology in Japan: Aquatic Food Acquisition and Long-Term Change in the Jomon Culture.” *Quaternary International* 239 (1–2): 19–27. https://doi.org/10.1016/j.quaint.2011.03.014.

Heaton, Timothy J, Peter Köhler, Martin Butzin, Edouard Bard, Ron W Reimer, William E N Austin, Christopher Bronk Ramsey, et al. 2020. “Marine20—The Marine Radiocarbon Age Calibration Curve (0–55,000 Cal BP).” *Radiocarbon* 62 (4): 779–820. https://doi.org/DOI:

10.1017/RDC.2020.68.

Helser, Thomas, Craig Kastelle, Aron Crowell, Takayuki Ushikubo, Ian J Orland, Reinhard Kozdon, and John W Valley. 2018. “A 200-Year Archaeozoological Record of Pacific Cod (Gadus Macrocephalus) Life History as Revealed through Ion Microprobe Oxygen Isotope Ratios in Otoliths.” *Journal of Archaeological Science: Reports* 21: 1236–46. https://doi.org/https://doi.org/10.1016/j.jasrep.2017.06.037.

Helser, Thomas, Craig R. Kastelle, Jennifer L. McKay, Ian J. Orland, Reinhard Kozdon, and John W. Valley. 2018. “Evaluation of Micromilling/Conventional Isotope Ratio Mass Spectrometry and Secondary Ion Mass Spectrometry of Δ18O Values in Fish Otoliths for Sclerochronology.” *Rapid Communications in Mass Spectrometry* 32 (20): 1781–90. https://doi.org/10.1002/rcm.8231.

Hirasawa, Yu. 2018. “Rebun Island Field Guide.”

Hirasawa, Yu, and Hirofumi Kato. 2019. “Preliminary Archaeological Field Report of Excavation at Hamanaka 2 Site, Rebun Island, Hokkaido, JAPAN.” Sapporo.

———. 2020. “Preliminary Archaeological Field Report at Hamanaka 2 Site, Rebun Island, Hokkaido, JAPAN.” Sapporo.

Igarashi, Yaeko. 2013. “Holocene Vegetation and Climate on Hokkaido Island, Northern Japan.” *Quaternary International* 290–291: 139–50. https://doi.org/10.1016/j.quaint.2012.09.030.

Jones, Douglas S., Douglas F. Williams, and Michael A. Arthur. 1983. “Growth History and Ecology of the Atlantic Surf Clam, Spisula Solidissima (Dillwyn), as Revealed by Stable Isotopes and Annual Shell Increments.” *Journal of Experimental Marine Biology and Ecology* 73 (3): 225–42. https://doi.org/10.1016/0022-0981(83)90049-7.

Junno, Ari, Jack P.R. Dury, Christian Leipe, Mayke Wagner, Pavel E. Tarasov, Yu Hirasawa, Peter D. Jordan, and Hirofumi Kato. 2021. “Building a High-Resolution Chronology for Northern Hokkaido – A Case Study of the Late Holocene Hamanaka 2 Site on Rebun Island, Hokkaido (Japan).” *Journal of Archaeological Science: Reports* 36 (February): 102867. https://doi.org/10.1016/j.jasrep.2021.102867.

Kato, Hirofumi. 2020. “Hokkaido Sequence and the Archaeology of the Ainu People BT - Encyclopedia of Global Archaeology.” In , edited by Claire Smith, 5213–28. Cham: Springer International Publishing. https://doi.org/10.1007/978-3-030-30018-0_33.

Kawahata, H., H. Ohshima, C. Shimada, and T. Oba. 2003. “Terrestrial-Oceanic Environmental Change in the Southern Okhotsk Sea during the Holocene.” *Quaternary International* 108 (1): 67–76. https://doi.org/10.1016/S1040-6182(02)00195-7.

Khim, Boo Keun, Kyung Sik Woo, and Jong Geel Je. 2000. “Stable Isotope Profiles of Bivalve Shells: Seasonal Temperature Variations, Latitudinal Temperature Gradients and Biological Carbon Cycling along the East Coast of Korea.” *Continental Shelf Research* 20 (8): 843–61. https://doi.org/10.1016/S0278-4343(00)00004-2.

Koizumi, I. 1987. “Pulses of Tsushima Current during the Holocene.” *第四紀研究(The Quaternary Research)* 26 (1): 13–25.

Kuzmin, Y. V., G. S. Burr, S. V. Gorbunov, V. A. Rakov, and N. G. Razjigaeva. 2007. “A Tale of Two Seas: Reservoir Age Correction Values (R, ΔR) for the Sakhalin Island (Sea of Japan and Okhotsk Sea).” *Nuclear Instruments and Methods in Physics Research, Section B: Beam Interactions with Materials and Atoms* 259 (1): 460–62. https://doi.org/10.1016/j.nimb.2007.01.308.

Leipe, Christian, Stefanie Müller, Konrad Hille, Hirofumi Kato, Franziska Kobe, Mareike Schmidt,

Konrad Seyffert, et al. 2018a. “Vegetation Change and Human Impacts on Rebun Island (Northwest Pacific) over the Last 6000 Years.” *Quaternary Science Reviews* 193: 129–44. https://doi.org/10.1016/j.quascirev.2018.06.011.

———. 2018b. “Vegetation Change and Human Impacts on Rebun Island (Northwest Pacific) over the Last 6000 Years.” *Quaternary Science Reviews* 193: 129–44. https://doi.org/10.1016/j.quascirev.2018.06.011.

Leipe, Christian, Elena A. Sergusheva, Stefanie Muller, Robert N. Spengler, Tomasz Goslar, Hirofumi Kato, Mayke Wagner, Andrzej W. Weber, and Pavel E. Tarasov. 2017. “Barley (Hordeum Vulgare) in the Okhotsk Culture (5th-10th Century AD) of Northern Japan and the Role of Cultivated Plants in Hunter-Gatherer Economies.” *PLoS ONE* 12 (3). https://doi.org/10.1371/journal.pone.0174397.

Leng, Melanie J, and Jonathan P Lewis. 2016. “Oxygen Isotopes in Molluscan Shell: Applications in Environmental Archaeology.” *Environmental Archaeology* 21 (3): 295–306. https://doi.org/10.1179/1749631414y.0000000048.

Loftus, Emma, Keith Rogers, and Julia Lee-Thorp. 2015. “A Simple Method to Establish Calcite: Aragonite Ratios in Archaeological Mollusc Shells.” *Journal of Quaternary Science* 30 (8): 731–35. https://doi.org/10.1002/jqs.2819.

Martindale, Andrew, Gordon T Cook, Iain McKechnie, Kevan Edinborough, Ian Hutchinson, Morley Eldridge, Kisha Supernant, and Kenneth M Ames. 2018. “Estimating Marine Reservoir Effects in Archaeological Chronologies: Comparing ΔR Calculations in Prince Rrupert Harbour, British Columbia, Canada.” *American Antiquity* 83 (4): 659–80. https://doi.org/DOI: 10.1017/aaq.2018.47.

Matsuyama, Masaji, Makiko Wadaka, Taizo Abe, Masaaki Aota, and Yoshio Koike. 2006. “Current Structure and Volume Transport of the Soya Warm Current in Summer.” *Journal of Oceanography* 62 (2): 197–205. https://doi.org/10.1007/s10872-006-0044-8.

McConnaughey, Ted A., and David Paul Gillikin. 2008. “Carbon Isotopes in Mollusk Shell Carbonates.” *Geo-Marine Letters* 28 (5–6): 287–99. https://doi.org/10.1007/s00367-008-0116-4.

Millard, Andrew R. 2014. “Conventions for Reporting Radiocarbon Determinations.” *Radiocarbon* 56 (2): 555–59. https://doi.org/10.2458/56.17455.

Miyata, Yoshiki, Akiko Horiuchi, Megumi Kondo, Shin Onbe, Kunio Yoshida, Seiya Nagao, and Toyohiro Nishimoto. 2016. “Marine Reservoir Effects Deduced from 14C Dates on Pottery Residues, Bones, and Molluskan Shells from the Hamanaka 2 Archaeological Site, Rebun Island, Hokkaido, Japan.” *Radiocarbon* 58 (4): 755–70. https://doi.org/10.1017/RDC.2016.93.

Miyata, Yoshiki, Akiko Horiuchi, Paleo Labo, and A M S Dating. 2009. “Traces of Sea Mammals on Pottery from the Hamanaka 2 Archaeological Site , Rebun Island , Japan : Implications from Sterol Analysis , Stable Isotopes , and Radiocarbon Dating.” *Res. Org. Geochem* 25: 15–27.

Müller, S., M. Schmidt, A. Kossler, C. Leipe, T. Irino, M. Yamamoto, H. Yonenobu, et al. 2016. “Palaeobotanical Records from Rebun Island and Their Potential for Improving the Chronological Control and Understanding Human–Environment Interactions in the Hokkaido Region, Japan.” *Holocene* 26 (10): 1646–60. https://doi.org/10.1177/0959683616641738.

Nikitin, Yu. G, E M Sayenko, and K A Lutaenko. 2016. “Mollusks from the Archaeological Site Chernyatino-2 in Primorye.” *The Bulletin of the Russian Far East Malacological Society* 20 (2): 55–80.

Nishimoto, Toyohiro. 1985. “The Transition of Hunting and Fishing Activities in Hokkaido. Bulletin of

National Museum of Japanese History (in Japanese).” *Bulletin of the National Museum of Japanese History* 6: 53–74.

Oba, T, M Kato, H Kitazato, I Koizumi, A Omura, T Sakai, and T Takayama. 1991. “Palaeoenvironmental Changes in the Japan Sea During the Last 85,000 Years.” *Paleoceanography* 6 (4): 499–518.

Oikawa, A. 1995. “Kaizuka Database No Suryo-Teki Bunseki. (Quantitative Analysis of Shell-Mound Database).” *Jinbun Kagaku to Computer (Humanities and Computer)* 25 (7): 59–66.

Okamoto, Yuka, Hajime Ishida, Ryosuke Kimura, Takehiro Sato, Nanae Tsuchiya, Sadayuki Murayama, Hitoshi Fukase, et al. 2016. “An Okhotsk Adult Female Human Skeleton (11th/12th Century Ad) with Possible Sapho Syndrome from Hamanaka 2 Site, Rebun Island, Northern Japan.” *Anthropological Science* 124 (2): 107–15. https://doi.org/10.1537/ase.160608.

Ramsey, Christopher Bronk. 2009. “Dealing with Outliers and Offsets in Radiocarbon Dating.” *Radiocarbon* 51 (3): 1023–45. https://doi.org/10.1017/s0033822200034093.

Reimer, Ron W, and Paula J Reimer. 2017. “An Online Application for ΔR Calculation.” *Radiocarbon* 59 (5): 1623–27. https://doi.org/DOI: 10.1017/RDC.2016.117.

Sakaguchi, Takashi. 2007a. “Refuse Patterning and Behavioral Analysis in a Pinniped Hunting Camp in the Late Jomon Period: A Case Study in Layer V at the Hamanaka 2 Site, Rebun Island, Hokkaido, Japan.” *Journal of Anthropological Archaeology* 26 (1): 28–46. https://doi.org/10.1016/j.jaa.2006.07.001.

———. 2007b. “Site Formation Processes and Long-Term Changes in Land Use among Maritime Hunter-Gatherers: A Case Study at the Hamanaka-2 Site, Rebun Island, Hokkaido.” *Arctic Anthropology* 44 (2): 31–50. https://doi.org/10.1353/arc.2011.0031.

Sakaguchi, Y. 1976. “Characteristics of Ozegahara Deposits and Climatic Changes since Late Glacial in Central Japan.” *Bull. Dept. Geology, Univ. Tokyo* 15: 1–24.

———. 1983. “Warm and Cold Stages in the Past 7600 Years in Japan and Their Global Correlation - Especially on Climatic Impacts to the Global Sea Level Changes and the Ancient Japanese History.” *Bulletin of the Department of Geography, University of Tokyo* 15: 1–31.

Sasaki, Koichi. 1989. “Characteristics of the Bottom Sediments Inhabited by the Surf Clam Spisula Sachalinensis in Sendai Bay.” *Nippon Suisan Gakkaishi* 55 (7): 1127–31.

Sasaki, Shigefumi, and Tomoki Ohta. 1999. “Seasonal Variation of Chemical Components in Surf Clam (Spisula Sachalinensis).” *Food Sci.Technol.Res.*

Savin, A. B. 2008. “Seasonal Distribution and Migrations of Pacific Cod Gadus Macrocephalus (Gadidae) in Anadyr Bay and Adjacent Waters.” *Journal of Ichthyology* 48 (8): 610–21.

Schmidt, G. A., G. R. Bigg, and E. J. Rohling. 1999. “Global Seawater Oxygen-18 Database - v1.22.” 1999. https://data.giss.nasa.gov/o18data/.

Tsutaya, Takumi, Yuichi I Naito, Hajime Ishida, and Minoru Yoneda. 2014. “Carbon and Nitrogen Isotope Analyses of Human and Dog Diet in the Okhotsk Culture: Perspectives from the Moyoro Site, Japan.” *Anthropological Science* 122 (2): 89–99. https://doi.org/10.1537/ase.140604.

Tsutaya, Takumi, Junmei Sawada, Yukio Dodo, Hitoshi Mukai, and Minoru Yoneda. 2013. “Isotopic Evidence of Dietary Variability in Subadults at the Usu-Moshiri Site of the Epi-Jomon Culture, Japan.” *Journal of Archaeological Science* 40 (11): 3914–25. https://doi.org/https://doi.org/10.1016/j.jas.2013.05.015.

Tsutaya, Takumi, Tomonari Takahashi, Takayuki Omori, Kohei Yamazaki, Takao Sato, Minoru Yoneda, Rick J Schulting, Hirofumi Kato, and Andrzej W Weber. 2021. “Reconstruction of Diachronic Changes in Human Fishing Activity and Marine Ecosystems from Carbon and Nitrogen Stable Isotope Ratios of Archaeological Fish Remains.” *Quaternary International*. https://doi.org/https://doi.org/10.1016/j.quaint.2021.12.005.

Urey, H.C., S. Epstein, H.A. Lowenstam, and C. Emiliani. 1954. “Final Report, Task Order XXVIII, Contract N6or1-02028, NR 081-096.”

Urey, H.C., H.A. Lowenstam, S. Epstein, and C.R. McKinney. 1951. “Measurement of Paleotemperatures and Temperatures and the Southeastern United States.” *Bulletin of the Geological Society of America* 62 (April): 399–416.

Vladimir, A. Rakov, and S.V. Gorbunov. 2004. “The Development of Malacofauna and Reconstruction Paleoenvironmental Changes in Coastal Areas of Sakhalin during the Holocene.” In *Proceedings of the Third Workshop on the Okhotsk Sea and Adjacent Areas*, edited by Skip McKinnell. North Pacific Marine Science Organization (PICES).

West, Catherine F., Stephen Wischniowski, and Christopher Johnston. 2012. “Pacific Cod (Gadus Macrocephalus) as a Paleothermometer: Otolith Oxygen Isotope Reconstruction.” *Journal of Archaeological Science* 39 (10): 3277–83. https://doi.org/10.1016/j.jas.2012.05.009.

West, Catherine F, Michael A Etnier, Steven Barbeaux, Megan A Partlow, and Alexei M Orlov. 2020. “Size Distribution of Pacific Cod (Gadus Macrocephalus) in the North Pacific Ocean over 6 Millennia.” *Quaternary Research*, 1–21. https://doi.org/DOI: 10.1017/qua.2020.70.

Yoneda, Minoru, Hikaru Uno, Yasuyuki Shibata, Ryo Suzuki, Yuichiro Kumamoto, Kunio Yoshida, Takenori Sasaki, Atsushi Suzuki, and Hodaka Kawahata. 2007. “Radiocarbon Marine Reservoir Ages in the Western Pacific Estimated by Pre-Bomb Molluscan Shells.” *Nuclear Instruments and Methods in Physics Research, Section B: Beam Interactions with Materials and Atoms*. https://doi.org/10.1016/j.nimb.2007.01.184.

Appendix 1: OxCal code

```
// Delta_R values updated for Marine20

 Plot()

 {

  Outlier_Model("General",T(5),U(0,4),"t");

  Outlier_Model("Charcoal",Exp(1,-10,0),U(0,3),"t");

  Sequence("Rebun")

  {

   Boundary("Start Late Jomon");

   Phase("Late Jomon")

   {

    Curve("Marine20","marine20.14c");
```

```
Delta_R("JomonShell",30,58);
R_Date("PLD-8847", 3550, 25)
{
 Outlier("General", 0.05);
};
R_Date("PLD-8848", 3550, 25)
{
 Outlier("General", 0.05);
};
R_Date("PLD-8849", 3715, 25)
{
 Outlier("General", 0.05);
};
R_Date("PLD-8850", 3470, 25)
{
 Outlier("General", 0.05);
};
R_Date("PLD-8851", 3500, 25)
{
 Outlier("General", 0.05);
};
Curve("=Marine20");
Delta_R("JomonAlcidae",148,52);
R_Date("PLD-10583", 3635, 30)
{
 Outlier("General", 0.05);
};
Curve("=Marine20");
Delta_R("JomonSeaLion",248,52);
R_Date("PLD-10582", 3735, 30)
{
```

```
 Outlier("General", 0.05);
};
Curve("=Marine20");
Delta_R("CharredMaterial",304,70);
R_Date("PLD-6305", 3805, 20)
{
 Outlier("General", 0.05);
};
R_Date("PLD-6306", 3815, 20)
{
 Outlier("General", 0.05);
};
R_Date("PLD-6453", 3730, 35)
{
 Outlier("General", 0.05);
};
R_Date("PLD-6454", 3715, 35)
{
 Outlier("General", 0.05);
};
R_Date("PLD-6455", 3840, 35)
{
 Outlier("General", 0.05);
};
Curve("IntCal20","intcal20.14c");
R_Date("PLD-6456", 2980, 35)
{
 Outlier("Charcoal", 1);
};
R_Date("PLD-6457", 3035, 35)
{
```

```
 Outlier("Charcoal", 1);
 };
};
Boundary("End Late Jomon");
Boundary("Start Final Jomon/Epi-Jomon");
Phase("Final Jomon/Epi-Jomon")
{
 Curve("=Marine20");
 Delta_R("Final/Epi-JomonShell",102,58);
 R_Date("OxA-41447", 2800, 17)
 {
  Outlier("General", 0.05);
 };
 R_Date("OxA-41449", 2814, 17)
 {
  Outlier("General", 0.05);
 };
 R_Date("OxA-41451", 2801, 17)
 {
  Outlier("General", 0.05);
 };
 Curve("=IntCal20");
 R_Date("Poz-91179", 2200, 30)
 {
  Outlier("General", 0.05);
 };
 R_Date("Poz-91178", 2240, 30)
 {
  Outlier("General", 0.05);
 };
};
```

```
Boundary("End Final Jomon/Epi-Jomon");
Boundary("Start Epi-Jomon");
Phase("Epi-Jomon")
{
 Curve("=IntCal20");
 R_Date("Poz-91170", 1555, 30)
 {
  Outlier("General", 0.05);
 };
 R_Date("Poz-91177", 2115, 30)
 {
  Outlier("General", 0.05);
 };
 R_Date("Poz-91175", 2170, 30)
 {
  Outlier("General", 0.05);
 };
 R_Date("Poz-73803", 2195, 30)
 {
  Outlier("General", 0.05);
 };
 R_Date("Poz-73804", 2200, 35)
 {
  Outlier("General", 0.05);
 };
 R_Date("Poz-73805", 2220, 30)
 {
  Outlier("General", 0.05);
 };
 R_Date("Poz-73806", 2220, 30)
 {
```

```
 Outlier("General", 0.05);
 };
 R_Date("Poz-91171", 2220, 30)
 {
  Outlier("General", 0.05);
 };
 R_Date("Nuta2-21214", 2176, 43)
 {
  Outlier("General", 0.05);
 };
};
Boundary("End Epi-Jomon");
Boundary("Start Okhotsk");
Phase("V")
{
 Curve("=IntCal20");
 R_Date("Poz-102853", 1540, 30)
 {
  Outlier("General", 0.05);
 };
 R_Date("Poz-102825", 1550, 30)
 {
  Outlier("General", 0.05);
 };
};
Phase("IV")
{
 Curve("=Marine20");
 Delta_R("OkhotskIV",-178,45);
 R_Date("OxA-42199", 1849, 17)
 {
```

```
 Outlier("General", 0.05);
 };
 R_Date("OxA-42200", 1873, 18)
 {
  Outlier("General", 0.05);
 };
 R_Date("OxA-42201", 1826, 17)
 {
  Outlier("General", 0.05);
 };
 R_Date("OxA-42202", 1835, 17)
 {
  Outlier("General", 0.05);
 };
 R_Date("OxA-42237", 1769, 29)
 {
  Outlier("General", 0.05);
 };
 R_Date("OxA-42238", 1747, 30)
 {
  Outlier("General", 0.05);
 };
 Curve("=IntCal20");
 R_Date("Poz-102824", 1535, 30)
 {
  Outlier("General", 0.05);
 };
};
Phase("IIIe")
{
 R_Date("Poz-84286", 1350, 30)
```

```
 {
  Outlier("General", 0.05);
 };
 R_Date("Poz-84287", 1520, 30)
 {
  Outlier("General", 0.05);
 };
 R_Date("Nuta2-21216", 1154, 45)
 {
  Outlier("General", 0.05);
 };
};
Phase("IIId")
{
 R_Date("Poz-84282", 1295, 30)
 {
  Outlier("General", 0.05);
 };
 R_Date("Poz-84283", 1335, 30)
 {
  Outlier("General", 0.05);
 };
 R_Date("Poz-84284", 1475, 30)
 {
  Outlier("General", 0.05);
 };
 R_Date("Poz-84285", 1275, 30)
 {
  Outlier("General", 0.05);
 };
};
```

```
Phase("IIIc")
{
 R_Date("Poz-84280", 1285, 30)
 {
  Outlier("General", 0.05);
 };
 R_Date("Poz-84281", 1275, 30)
 {
  Outlier("General", 0.05);
 };
 R_Date("Nuta2-21213", 1320, 40)
 {
  Outlier("General", 0.05);
 };
 R_Date("Poz-73802", 1455, 30)
 {
  Outlier("General", 0.05);
 };
};
Phase("IIIb")
{
 R_Date("Poz-60766", 1305, 30)
 {
  Outlier("General", 0.05);
 };
 R_Date("Poz-60767", 1265, 30)
 {
  Outlier("General", 0.05);
 };
 R_Date("Poz-60768", 1215, 30)
 {
```

```
 Outlier("General", 0.05);
 };
 R_Date("Poz-81340", 1220, 30)
 {
  Outlier("General", 0.05);
 };
 R_Date("Poz-81341", 1215, 30)
 {
  Outlier("General", 0.05);
 };
 R_Date("Poz-81342", 1180, 30)
 {
  Outlier("General", 0.05);
 };
};
Phase("IIIa")
{
 R_Date("Poz-84277", 1215, 30)
 {
  Outlier("General", 0.05);
 };
 R_Date("Poz-84278", 1170, 30)
 {
  Outlier("General", 0.05);
 };
 R_Date("Poz-73801", 170, 30)
 {
  Outlier("General", 0.05);
 };
 Curve("=Marine20");
 Delta_R("OkhotskIIIa",21,40);
```

```
 R_Date("OxA-42197", 1778, 17)
 {
  Outlier("General", 0.05);
 };
 R_Date("OxA-42198", 1711, 17)
 {
  Outlier("General", 0.05);
 };
};
Phase("IIc")
{
 Curve("=IntCal20");
 R_Date("Poz-91165", 130, 30)
 {
  Outlier("General", 0.05);
 };
 R_Date("Poz-73799", 1165, 30)
 {
  Outlier("General", 0.05);
 };
 Curve("=Marine20");
 Delta_R("OkhotskShell",-57,62);
 R_Date("OxA-41453", 1646, 17)
 {
  Outlier("General", 0.05);
 };
 R_Date("OxA-41455", 3759, 18)
 {
  Outlier("General", 0.05);
 };
 R_Date("OxA-41457", 1676, 17)
```

```
 {
  Outlier("General", 0.05);
 };
};
Boundary("End Okhotsk");
Boundary("Start Unidentified");
Phase("Unidentified")
{
 Curve("=IntCal20");
 R_Date("Poz-73798", 210, 30)
 {
  Outlier("General", 0.05);
 };
};
Boundary("End Unidentified");
Boundary("Start Satsumon");
Phase("Satsumon")
{
 Curve("=IntCal20");
 R_Date("Poz-91167", 1245, 30)
 {
  Outlier("General", 0.05);
 };
 R_Date("Poz-73797", 215, 30)
 {
  Outlier("General", 0.05);
 };
};
Boundary("End Satsumon");
Boundary("Start Ainu");
Phase("I")
```

```
 {
  Curve("=IntCal20");
  R_Date("Poz-60760", 165, 30)
  {
   Outlier("General", 0.05);
  };
  R_Date("Poz-60761", 115, 30)
  {
   Outlier("General", 0.05);
  };
  R_Date("Poz-60762", 210, 30)
  {
   Outlier("Charcoal", 1);
  };
  R_Date("Poz-73796", 120, 30)
  {
   Outlier("General", 0.05);
  };
  R_Date("Poz-91168", 80, 30)
  {
   Outlier("General", 0.05);
  };
  R_Date("Poz-91169", 1175, 30)
  {
   Outlier("General", 0.05);
  };
 };
 Boundary("End Ainu");
};
```

Appendix 2: full radiocarbon results

Full calibrated radiocarbon results. '…' marks where ranges extend to or beyond radiocarbon 'present'.

	Unmodelled (BP) 95.4%		Modelled (BP) 95.4%	
Lab code	from	to	from	to
R_Date PLD-8847	3437	3024	3292	3088
R_Date PLD-8848	3437	3024	3291	3088
R_Date PLD-8849	3640	3225	3592	3242
R_Date PLD-8850	3350	2922	3270	3068
R_Date PLD-8851	3375	2955	3278	3075
R_Date PLD-10583	3388	2981	3282	3081
R_Date PLD-10582	3388	2981	3282	3082
R_Date PLD-6305	3430	2979	3289	3084
R_Date PLD-6306	3440	2990	3291	3086
R_Date PLD-6453	3353	2873	3272	3066
R_Date PLD-6454	3340	2858	3267	3064
R_Date PLD-6455	3474	3000	3298	3090
R_Date PLD-6456	3326	3005	3249	3073
R_Date PLD-6457	3358	3083	3299	3084
R_Date OxA-41447	2428	2006	2341	2185
R_Date OxA-41449	2459	2030	2344	2184
R_Date OxA-41451	2430	2007	2341	2185
R_Date Poz-91179	2317	2122	2329	2193
R_Date Poz-91178	2339	2151	2337	2185
R_Date Poz-91170	1522	1371	1522	1372
R_Date Poz-91177	2291	1996	2291	1996
R_Date Poz-91175	2309	2052	2277	2120
R_Date Poz-73803	2315	2120	2271	2128
R_Date Poz-73804	2327	2119	2269	2129
R_Date Poz-73805	2334	2146	2266	2145
R_Date Poz-73806	2334	2146	2266	2144
R_Date Poz-91171	2334	2146	2266	2145
R_Date Nuta2-21214	2320	2009	2273	2123
R_Date Poz-102853	1517	1353	1495	1368
R_Date Poz-102825	1520	1363	1495	1369
R_Date OxA-42199	1630	1280	1430	1288
R_Date OxA-42200	1668	1304	1438	1292
R_Date OxA-42201	1609	1265	1425	1285
R_Date OxA-42202	1617	1271	1427	1286
R_Date OxA-42237	1547	1189	1404	1282
R_Date OxA-42238	1529	1172	1399	1281
R_Date Poz-102824	1517	1350	1418	1315
R_Date Poz-84286	1310	1176	1307	1271
R_Date Poz-84287	1515	1314	1515	1314

R_Date Nuta2-21216	1177	959	1177	960
R_Date Poz-84282	1291	1175	1292	1225
R_Date Poz-84283	1304	1176	1299	1242
R_Date Poz-84284	1397	1305	1397	1305
R_Date Poz-84285	1286	1129	1289	1221
R_Date Poz-84280	1290	1131	1268	1185
R_Date Poz-84281	1286	1129	1267	1186
R_Date Nuta2-21213	1305	1174	1269	1185
R_Date Poz-73802	1383	1300	1383	1300
R_Date Poz-60766	1292	1176	1236	1134
R_Date Poz-60767	1285	1079	1240	1123
R_Date Poz-60768	1262	1061	1240	1104
R_Date Poz-81340	1263	1062	1241	1107
R_Date Poz-81341	1262	1061	1240	1104
R_Date Poz-81342	1179	978	1180	1099
R_Date Poz-84277	1262	1061	1152	1069
R_Date Poz-84278	1178	977	1151	1059
R_Date Poz-73801	291	...	291	3
R_Date OxA-42197	1290	992	1157	1063
R_Date OxA-42198	1243	932	1156	1058
R_Date Poz-91165	275	8	276	7
R_Date Poz-73799	1178	975	1122	1004
R_Date OxA-41453	1271	923	1126	1002
R_Date OxA-41455	3815	3390	3735	3378
R_Date OxA-41457	1290	945	1126	1005
R_Date Poz-73798	308	...	428	165
R_Date Poz-91167	1274	1072	1273	1072
R_Date Poz-73797	309	...	297	143
R_Date Poz-60760	289	...	185	1
R_Date Poz-60761	270	10	150	9
R_Date Poz-60762	308	...	210	0
R_Date Poz-73796	271	10	151	8
R_Date Poz-91168	260	29	147	15
R_Date Poz-91169	1179	978	1179	979

Appendix 3: combined dates

Combined marine and terrestrial dates used when calculating DR values. Dates combined using OxCal function R_Combine. Marine material shaded in blue, terrestrial material shaded in green.

			Combined date			
Layer	**Period**	**Material**	**Uncal BP**	**σ**	**reference**	**n**
IV	Okhotsk	Otolith	1833	8	thesis	6
IIIa	Okhotsk	Otolith	1745	13	thesis	2
IIc	Okhotsk	Shell	1661	13	thesis	2
V	Late Jomon	Charred material	3794	55	Miyata 2016	4
V	Late Jomon	Shell	3518	39	Miyata 2016	4
V	Late Jomon	Sea lion	3735	30	Miyata 2016	1
V	Late Jomon	Alcidae	3635	30	Miyata 2016	1
VIII	Final/Epi-Jomon	Shell	2805	10	thesis	3
V	Late Jomon	Wood	3008	25	Miyata 2016	2
VIII	Final/Epi-Jomon	Seed	2220	22	Leipe 2018	2
VII	Epi-Jomon	Seed	2202	13	Leipe 2018 & Junno 2021	7
V	Towada 1	Seed	1545	22	Junno 2021	2
IV	Towada 2	Seed	1535	30	Junno 2021	1
IIIe	Kokumon	Seed	1436	22	Leipe 2017	2
IIId	Kokumon-Chinsenmon	Seed	1302	18	Leipe 2017	3
IIIc	Chinsenmon	Seed	1289	19	Leipe 2017 & Junno 2021	3
IIIb	Chinsenmon-Motochi	Seed	1234	13	Muller 2016 & Leipe 2017	6
IIIa	Motochi 1	Seed	1193	22	Leipe 2017	2
IIc	Motochi 2	Seed	1165	30	Leipe 2018	1
IIb	Unidentified	Seed	210	30	Leipe 2018	1
IIa	Satsumon	Seed	215	30	Leipe 2018	1
I	Ainu	Seed	138	14	Muller 2016 & Leipe 2018	5

Discussion and Conclusion

In Chapter 1, several overarching research questions were outlined which this thesis aimed to address. In summarising and discussing my conclusions, it seems appropriate to return to these questions and assess the extent to which these aims have (and have not) been met.

1. Do modern examples of the bivalve *Spisula sachalinensis* reliably record sea surface temperature?

and

2. Can *S. sachalinensis* provide a marine palaeotemperature record for the northwest Pacific, and more specifically for northern Japan?

This first question is dealt with in the first paper presented in this thesis. In some respects, it has a straightforward answer: the results of stable oxygen isotope analysis on a modern examples of *S. sachalinensis* did indeed show that incremental $\delta^{18}O$ values show seasonal cycling which matches well with observed sea surface temperatures. The extent to which this can be considered a *reliable* resource is dependent on a few caveats though. While the results presented show that the average maximum annual temperatures are recorded well, the same was not true for annual minimum temperatures. This was contrary to expectations, as examination of the shells showed that growth increments were forming during the warmest months, which would instead indicate that warmer temperatures should be underrepresented. This is interpreted as indicating an offset in $\delta^{18}O_{shell}$-derived and observed temperatures which should be taken into consideration in palaeo-contexts. It is not easy to pinpoint a reason for this offset. One possibility discussed in paper 1 is that temperatures were calculated using an incorrect value for $\delta^{18}O_{seawater}$, which could be attributed to $\delta^{18}O$-depleted riverine input and freshwater runoff. This is also a possibility for archaeological shells from Hamanaka 2, which show a similar $\delta^{18}O$ range to the modern shells analysed, as Funadomari bay has riverine input from the Osawa and Obi rivers.

In general, proxy temperature ranges produced by $\delta^{18}O_{carbonate}$ produced by any marine carbonate are likely to be somewhat 'dampened' or 'smoothed' due to averaging effects. This effect will be exaggerated with decreasing resolution, although this is not always an issue interpretationally, as exemplified by the relatively smooth $\delta^{18}O$ results from hand drilled sampled in paper 2 versus the higher-resolution micromilled samples. This does mean that in the palaeo-context, temperatures estimated from $\delta^{18}O_{carbonate}$ will often be more straightforward to interpret if looking at average temperature ranges rather than examining specific annual minima and maxima.

Continued research on modern specimens will certainly augment our understanding of the precise relationship between *S. sachalinensis* shell $\delta^{18}O$ and water temperature, as discussed under 'future research directions' below. Nevertheless, the relationship does appear strong enough that $\delta^{18}O_{shell}$ can already be interpreted as a palaeotemperature proxy, especially if interpreted with the appropriate caution regarding the likelihood that maximum and minimum temperatures are likely to be dampened compared to lived conditions. In paper 3, $\delta^{18}O$ results from archaeological *S. sachalinensis* from northern Japan (see Appendix 3) are interpreted based on this established connection between temperature and $\delta^{18}O_{carbonate}$. This discussion focuses on the relative temperature ranges between different archaeological periods, but due to the uncertainties mentioned above, subannual seasonal variation in temperature is not addressed. Overall though, the results presentd do indicate that *S. sachalinensis* has great potential as a marine palaeotemperature record for the northwest Pacific.

3. Does sample preparation and sampling technique have an impact on marine carbonate stable isotope palaeothermometry?

Although this is a question that has been discussed numerous times and from various different angles by previous researchers (e.g. Goodwin et al. 2003; Spötl and Mattey 2006; Schöne, Schmitt, and Maus 2017), throughout this project it was clear that many methodological questions remain underexplored or unanswered. There are also very few studies which use varied sampling

techniques on the same specimens in order to get a direct comparison of how changing preparation and sampling techniques affects results.

The bivalves used in this study presented an excellent opportunity to undertake such research. In order to gain easier access to the cross-lamellar layer of the shell for microscopy and sampling via micromill, each valve was sectioned along the axis of maximum growth (paper 1, figure 1). This not only produces a flat surface suited to micromilling, it also results in two halves of shell, both of which should show matching section of shell growth. By extension, these two halves should also produce near-identical patterns of $\delta^{18}O$ and $\delta^{13}C$ and if different method are used to sample each half then major difference in the results can be attributed to these methods.

Paper 2 in this thesis works on this basis to test whether particularly high $\delta^{13}C$ results found in some of the archaeological samples could be related to contamination from the resin in which shells were embedded. The results of paper 2 ended up confirming the suspicion that the polyester resin embedding medium had contaminated samples, leading to anomalously high $\delta^{13}C$ values – these high values did not appear in the samples drilled from the unembedded half of the shell. This has been posited before, with moderate contamination effects from cured adhesives reported by Schone et al. (2017), but this was the first case in which such an effect was demonstrated to have influenced $\delta^{13}C$ results in a practical archaeological case. Since resins remain a popular method of stabilising archaeological and palaeontological specimens for sectioning and milling, it is important to ensure that the scientific community is fully aware of the potential effects that embedding may have on analytical results. Furthermore, in the case of $\delta^{13}C$ in marine carbonates, any (palaeo)climatic interpretation is already fraught with metabolic and oceanographic complications (see paper 1, section 5.2), so any additional complexity is particularly problematic.

This experiment presented in paper 2 was also used as an opportunity to contrast the resolution and resulting temperature achieved using micromilling – the method used for the majority of the analysis in this thesis – and hand drilling. Hand drilling had originally been disregarded as a viable

sampling method in this thesis, as the increased resolution afforded by micromilling is generally considered desirable when aiming to produce sequential, subannual results. However, the results of paper 2 actually demonstrate that when sampling a region of rapid growth from a large species such as *S. sachalinensis*, the decreased resolution of hand drilling does not necessarily result in significant loss of range in calculated temperatures. As a result, the paper concludes that researchers should carefully consider whether hand drilling unembedded specimens could be an effective way forward, taking into account required sample size, locational precision, and resolution. Retrospectively, it is clear that hand drilling all the shell samples analysed for this thesis would not only have avoided the issue of resin contamination, but would also have allowed more expedient sampling which may have resulted in the ability to measure more specimens. Increasing the total number of shells and otoliths sampled in this way, without significant impact on the temperature ranges calculated using $\delta^{18}O$, would have been a major augmentation to the thesis as a whole.

4. What cultural or palaeoenvironmental information can be gained from stable oxygen and carbon isotope analysis of Pacific cod otoliths from Hamanaka 2?

While this thesis does not offer conclusive answers to this question, it does go some way to show the immense potential for marine carbonates as an archaeological resource at Hamanaka 2, and in the northern Hokkaido region more broadly. As far as the shell results presented in paper 3, the overall picture is one of climatic consistency rather than change, with shells from three periods (including shell II2 which predated the layer from which it was excavated) all showing very similar calculated temperature ranges. It was clear that the greatest difference between archaeological periods was actually a result of the different oceanographic niche inhabited by Pacific cod, vs the coastal Sakhalin surf clam. This caused layers represented by shells to appear warmer than those represented by otoliths. The lack of either available otoliths or shells from all chronological periods across the site was therefore a major impediment to the interpretations of $\delta^{18}O_{carbonate}$-derived temperatures.

One tentative indication from the otolith results is that the single otolith representing the Early Okhotsk layer IV (Towada 2) did show an overall lower temperature range than the otoliths from Final Okhostk layer IIIa (Motochi 1). Paper 3 discusses the fact that Leipe et al. (2018b) previously suggested that vegetation change at the onset of the Okhotsk could have been the result of climatic deterioration. This would fit with the observation that the Early Okhotsk otolith showed lower temperatures than those from the Final Okhotsk, but as already pointed out this conclusion is based on only on specimen from the Early Okhotsk so increased sample size would be required to confirm the existence of this temperature difference.

5. How can marine resources from Hamanaka 2 be integrated in the site's chronological model?

The results presented in Paper 3 show that archaeological marine carbonates can be an important chronological resource, not only for Hamanaka 2 but also the northwest Pacific more widely. By radiocarbon dating of marine specimens from various time periods and across two species, it is clear that the marine reservoir correction is highly variable in the region owing to its oceanographic environment and the interaction of the Soya and Oyashio currents. By combining these new marine dates with existing terrestrial dates from previous research at the site, they were successfully integrated into the site's chronological model and helped to constrain the timing of the local Final Okhotsk. Importantly, this pairing of marine and terrestrial dates also allowed for the calculation of new ΔR values, which can now be used by other researchers investigating the chronology of northern Japan.

When radiocarbon samples were first being planned for the shells and otoliths studied in this thesis, it included modelling whether the sclerochronological information available from *S. sachalinensis* could be harnessed in order to increase dating precision by incorporating paired shell dates into an OxCal model. The idea was that two dates on a single shell, one sampled from the hinge (the oldest part of the shell) and the other from the shell edge (the youngest part of the shell), could be used

alongside a sclerochronological estimate of the shell's ontogenetic shell age to create an age-gap model capable of constraining overall calendar age of the shell. A similar approach has previously been used on wooden artefacts, utilising age gaps estimated from dendrochronology (Brock et al. 2012), but has not previously been translated to sclerochronology. Initial tests run using simulated radiocarbon dates indicated that there was merit to this approach, and that an age gap of 10-15 years could significantly reduce uncertainty, especially in the 95% confidence interval.

In practice, when looking at the growth of individual shells (see Appendix 5) the number of annual growth lines between two radiocarbon samples can indeed be used to constrain the calendar date of the shell. For the shells used, this modelling resulted in a small reduction of the 68.3% and 95.4% confidence ranges, an improvement in precision in the region of 15% of the total range. However, in the context of the site-wide chronological model for Hamanaka 2, this does not make any significant contribution as the model is already fairly tightly constrained, especially during the Okhotsk when successive layers appear to have been rapidly deposited (paper 3, figure 4). Stronger results were anticipated with the Marine13 curve when the radiocarbon grant application was submitted (Appendix 1), but the Marine20 curve incorporates greater uncertainty which was reflected in the final results. Nevertheless, the concept is interesting methodologically, as at other sites this small reduction in chronological uncertainty could prove more important. This is certainly an approach which warrants further investigation (see 'future research directions' below).

6. Can environmental change be linked to cultural change at Hamanaka 2?

Leipe et al. (2018a) suggest that the timing of cooling events – as evidence by changes in the palynological record at nearby lake Kushu – corresponds to cultural shifts on Rebun. Of particular interest here is the cooling event at c. 1550 cal BP, which appears to be contemporaneous with the beginning of the Okhotsk occupation at Hamanaka 2, as well as a period of increasing deforestation. Using palynological records alone, it is difficult to establish whether deforestation occurred as a direct result of climatic deterioration, or as a result of anthropogenic deforestation, or – perhaps the

more likely explanation – a mixture of both of these factors. For example, cooler climate could lead to an increase in tree-felling where wood fires are relied on as a heat source.

The period of intense deforestation at Hamanaka 2 coincides with the Okhotsk otolith specimens from layer IV, which date to between 1462-1308 cal BP. Unfortunately, only one of the otoliths from this layer was complete enough to sample for sequential $\delta^{18}O$ analysis, meaning that the palaeotemperature record for this period is less strong than the chronological one. Having said this, the single otolith sampled from layer IV does show cooler temperatures than those sampled from layer IIIa, during the Final Okhotsk period. More $\delta^{18}O$ evidence from layer IV would be needed to confirm this difference in average temperature, but these initial results do suggest cooler temperature at the beginning of the Okhotsk.

7. Do proxy palaeotemperature records from marine carbonates at Hamanaka 2 fit with pre-existing regional proxies, and with historical records from southern Japan?

This is certainly the question addressed least thoroughly in this thesis. One aspect is discussed above, with comparison between the palynological (indirect) climate record for Rebun and the direct proxy of $\delta^{18}O$. Despite this, given the small number of specimens being considered (albeit some producing large sample sizes representing multiple years), it is hard to undertake meaningful comparison between existing regional proxies, historical records from southern Japan, and $\delta^{18}O_{carbonate}$-derived temperatures. Compared to modern temperatures in Rebun, the average maximum sea water temperature of 20.8 degrees is similar to that estimated based on archaeological shells from layers IIc and VIII. The minimum average temperature recorded in modern Rebun is 3.8 degrees[1], falling below that calculated from the Mototchi 2 shells, and above that calculated from the Final/Epi-Jomon shells and the older shell II2. However, for the latter two the vast majority of samples provided temperatures falling within the range of ~4-22 degrees. Given the offset in minimum temperature recorded in the modern shells from paper 1 versus the observed

[1] https://en.climate-data.org/asia/japan/hokkaido/rebun-770592/#water

temperature, caution is urged when interpreting the archaeological results – differences between modern and archaeological climate do not appear to be evident in the $\delta^{18}O$ data. The lack of clear and statistically significant distinctions between the $\delta^{18}O_{carbonate}$-derived temperature records of the different periods at Hamanaka 2 (at least that which is not more clearly attributable to ecological differences between *S. sachalinensis* and Pacific cod) also hinder comparison with historical documentary records from southern Japan.

According to evidence from Sakhalin – located to the north of Rebun, across the Soya strait and affected by many of the same oceanographic factors – seawater was 3-5 degrees warmer at ~1,100 cal BP than present day (Hudson 2004; Akamatsu and Ushiro 1995). This is based on the presence of warm-water bivalves species at a site on the island's western coast. This would coincide with the Motochi 2 shells and Motochi 1 otoliths analysed at Hamanaka 2 (which date between 1157-1001 cal BP), yet the $\delta^{18}O$ results from these shells do not indicate any such difference compared to modern temperatures from Rebun. As mentioned above, the Motochi 2 shell does show a minimum $\delta^{18}O_{carbonate}$-derived temperature above that observed in modern-day Rebun, but given that a similar result was observed when comparing modern known-age shells to modern temperatures, this is not considered robust evidence.

Future Research Directions

Sample Size

The biggest theme connecting the discussion above is the issue of small numbers of specimens analysed. This is the single biggest issue facing attempts to interpret the archaeological stable isotope results in terms of palaeoclimatic change. Increasing the number of specimens sampled would go a long way towards solving this issue, and more specifically it would be preferable to obtain comparable shells/otoliths across all occupation periods at Hamanaka 2 in order to also overcome the problem of comparing two species with different ecological niches and correspondingly different $\delta^{18}O$ values.

For otoliths the number of samples analysed per specimen was also low, due to the small size of each otolith. In the future, higher-resolution records could be obtained using alternative methods of sampling and/or analysis. For example, Helser et al. (2018) achieve higher-resolution $\delta^{18}O$ records from the otoliths of Pacific cod using secondary ion mass spectrometry (SIMS), and also show that high-precision records can be obtained using micromilling/IRMS (as utilitsed in this study), if trenches are milled sequentially at widths smaller than the drill bit diameter. They do however caution that the spatial resolution of milled samples will be degraded if trenches cross time boundaries or intersect younger material at depth' (Helser et al. 2018 p. 1787).

An alternative approach would be to move away from sequential sampling of the otoliths, and instead focus on analysis of a bulk, homogenised sample from each specimen. In the otoliths studied here, as well as in previous papers (Gao et al. 2005; Helser et al. 2018), seasonal information gained from cod otoliths $\delta^{18}O$ is muddied by the ontogenetic change towards higher $\delta^{18}O$ values over the lifetime of the fish. As a result, palaeoclimatically- and archaeologically-relevant information from high resolution sampling is minimal compared to sedentary, coastal mollusc species. By removing the sequential sampling altogether, bulk sampling would allow for the sampling of otoliths otherwise too fragmented to sample, for instance those from layer IV in this study which were suited to radiocarbon dating but not incremental stable isotope analysis. Moreover, bulk sampling would have the additional benefit of removing the need for embedding specimens, and by extension removing the risk of $\delta^{13}C$ contamination by embedding materials.

In this study, the primary obstacle in increasing specimen numbers was the lack of retained shell/otolith material from the site. Therefore, in order to successfully build on this research in future, it is important to stress the utility of this material during excavation and ensure that it is treated as valuable archaeological evidence. In order to balance the research benefits with the additional time and money spent in post-excavation recording and storage, it may be necessary to place constraints on which species are retained based on their archaeological relevance. For

example, the most abundant bivalve species found at Hamanaka 2 is *Glycymeris vestita*; however, this species is less archaeologically useful than *S. sachalinensis* not only because it is not considered a key food resource (A. O. Junno 2020), but also because it is the species that makes up the majority of substrate at nearby Funadomari bay and 'dead' shells could be easily transported from the beach to the site by humans, animals and extreme weather.

Trace Element Analysis

Various trace elements present in marine carbonates have been considered as potential (palaeo)climatic indicators, including Sr, Ca, Mg, Ba, Na, K, S and Cl (Gunn et al. 1992; Janz and Vennemann 2005; Powell, Shennan, and Thomas 2009; Iizuka 2012; Lazareth et al. 2013; Hausmann et al. 2017, 2019). The combination of stable isotope and trace element proxies from the same material has the potential to increase our understanding of the palaeoenvironmental conditions recorded by marine carbonates (Janz and Vennemann 2005; Batenburg et al. 2011; Lea 2013). Trace element analysis via electron microprobe was explored as part of this thesis, as presented in Appendix 4, using rockfish otoliths from Hamanaka 2 of the genus *Sebastes*. Originally this was intended to form a more significant part of this thesis, with continued trace element analysis using the same Pacific cod otoliths which were also sampled for stable isotope analysis, however this lab work was affected by pandemic lab closures. Once labs reopened, high demand for the equipment led to long lead times, meaning that this research was no longer feasible for inclusion in this thesis. Trace element analysis of these otoliths remains an attractive avenue for future research, especially as the resolution of the microprobe is extremely high so more detailed transects could be achieved than for stable isotope analysis. As certain elements are anticipated to be more closely related with different oceanographic factors (Gunn et al. 1992), via a combination of different trace element ratios and stable isotopes, a clearer picture of fish life history and climate could be achieved.

Stable isotope analysis

Unfortunately, the results of this thesis were not conclusive in terms of interpreting temperature change across the late Holocene at Hamanaka 2. This relates to a combination of the factors discussed above: difficulty directly comparing between the two species sampled, few available specimens, and methodological issues with resin contamination. The adjustments already mentioned – increasing specimen numbers via both changes to excavation practice at Hamanaka 2 and bulk analysis of otoliths – would result in more useful information in terms of palaeoclimatic change. It would also be extremely useful to sample a modern *S. sachalinensis* specimen fished from Rebun itself. This was not achieved as part of the thesis, so instead modern shells from southern Hokkaido were used to confirm the basic principles of stable isotope palaeothermometry for the species. This was useful, but it is obvious from the literature on the species (Yamamoto 1947; Kato and Hamai 1975; Sasaki 1981; Branscombe et al. 2021), that the time when shell growth slows/stops is variable depending on the region. So, although the Tomakomai shells showed growth stoppages in the summer, that does not necessarily apply to the shells from Hamanaka 2 which lived at a higher latitude and in a cooler climate. Another important factor to be improved upon in terms of the stable isotope palaeothermometry is the estimation of $\delta^{18}O_{seawater}$, which is needed to calculate palaeotemperature using aragonite-temperature equations. Finding a suitable $\delta^{18}O_{seawater}$ value to use in a palaeo-context is often challenging, and depending on the method used various potential $\delta^{18}O_{seawater}$ values can be produced. This uncertainty over $\delta^{18}O_{seawater}$ feeds into uncertainty in calculated palaeotemperature. In future research, it would be extremely useful to take a measurement of modern $\delta^{18}O_{seawater}$ for the water surrounding Rebun Island, to provide a decisive modern value from which to evaluate the most likely value for ancient seawater.

Radiocarbon Dating

This study added clarity to the timing of the Final Okhotsk period at Hamanaka 2, and northern Hokkaido more generally. Beyond that though, the timing of the post-Okhotsk period, from layers IIb to I at Hamanaka 2, are still unclear. The dating of these layers still relies on a small number of seed

samples, which are considered likely to be misleadingly young (A. Junno et al. 2021). Given the lack of existing secure terrestrial dates, it will be more difficult to overcome the issue of the marine reservoir effect in these layers. For the Satsumon period, which is likely to have followed on from the Okhotsk relatively rapidly (A. Junno et al. 2021), the Motochi 1 or Motochi 2 ΔR values presented in this thesis will provide a good basis. For the Ainu layers where the intervening time difference is larger, it would be better to obtain new terrestrial dates from this layer, either instead of, or in addition to, marine dates. If both marine and terrestrial dates are analysed then these can be used to calculate a new ΔR value specific to the Ainu period.

Conclusion

This study has confirmed the potential of the large and archaeological common bivalves *S. sachalinensis* as an important proxy for palaeotemperature in the northwest Pacific. Using this species alongside Pacific cod otoliths, the results of stable oxygen isotope analysis have provided a first look at direct and archaeologically-relevant palaeotemperature records from the late Holocene of Rebun Island. Of particular interest is the early Okhotsk period, where the oxygen isotope results begin to indicate that a short-lived period of climatic deterioration may have played a role in increasingly-intense Okhotsk deforestation as previously identified via palynological analysis. With increased attention on the utility of marine carbonates from Hamanaka 2, in future this palaeotemperature record can be built upon to increase the number of specimens analysed and allow more confident conclusions to be drawn on the relationship between human cultural change and palaeoclimate on Rebun.

The stable isotope data analysed in this thesis also prompted investigation of resin contamination effects, which were identified as a potential reason for high $\delta^{13}C$ values. While this is a subject that has received some previous attention, the use of resin is still widely accepted in the isotope palaeothermometry community, with little regard to the effect of embedding material on the results. The results presented in paper 2 are, to the best of the author's knowledge, the first

published case where embedded and unembedded samples from the same individual are directly compared in a practical archaeological context. Not only does this provide a cautionary tale for other researchers looking for ways to secure and stabilise fragile material, it also gives useful information on the relative resolution provided by hand drilling versus the current 'gold standard' of micromilling.

As well as the palaeotemperature application of marine carbonates at Hamanaka 2, this thesis also contributes new radiocarbon dates based on the marine material. This has the dual benefits of 1) building on previous research which targeted the Final Jomon layer (Miyata et al. 2016) to provide new ΔR values across the chronological sequence, and 2) contributing to an updates chronological model for the site with improved constraints on the timing of the Final Okhotsk. The new ΔR values confirm that the marine reservoir effect in this region varies both between species and across time. This makes clear the need for carefully-chosen marine-terrestrial pairings to construct these ΔR values, and that ΔR values used should be chosen based on both the period and species being dated. The addition of the newly calculate values presented will help expand the existing library of known MRE corrections, meaning that new marine dating projects will not need to create new ΔR values if their material can be appropriately matched to existing corrections.

Archaeologically, the new chronological model for Hamanaka 2 confirms and expands on the findings from previous site chronologies (Junno et al. 2021). It confirms that there are significant multi-centennial hiatuses between each cultural period in the record from the site, but that the phases of the Okhotsk cultural period are continuous and closely spaced. Importantly, the new chronology helps to constrain the timing of the final Okhotsk layer, while previous models which excluded marine material had suggested an extended Okhotsk period which was not supported by pre-existing archaeological understanding of the cultural trajectory of Rebun Island.

Overall, this thesis presents new data which begin to establish the palaeoclimatic history of Rebun Island, and bolsters existing chronological models with the addition of new marine dates. The

recognition of *S. sachalinensis* as an archaeologically-important palaeothermometer could have significant impact across the archaeology of the northwest Pacific, and the methodological information presented in these papers will be of significant assistance to the researchers that use it (and other, similar proxies) in the future.

Bibliography

Abe, Chiharu, Christian Leipe, Pavel E. Tarasov, Stefanie Müller, and Mayke Wagner. 2016. “Spatio-Temporal Distribution of Hunter–Gatherer Archaeological Sites in the Hokkaido Region (Northern Japan): An Overview.” Holocene 26 (10): 1627–45. https://doi.org/10.1177/0959683616641745.

Akamatsu, M., and H. Ushiro. 1995. “Ohôtsuku Bunka Iseki No Ritchi to Sono Haikei. Final Reports on ‘Research Project of the Historical and Cultural Exchange of the North.’” Sapporo.

Amano, T, and A Vasilevski. 2002. “Okhotsk culture formation, metamorphosis and ending: Japan and Russia cooperative symposium TT - サハリンにおけるオホーツク文化の形成と変容・消滅 : 日ロ共同シンポジウム.” In The 5th open symposium of the Hokkaido University Museum. 北海道大学総合博物館. http://hdl.handle.net/2115/48121.

Andrén, E., Klimaschewski, A., Self, A.E., St. Amour, N., Andreev, A.A., Bennett, K.D., Conley, D.J., Edwards, T.W.D., Solovieva, N., Hammarlund, D. 2015. “Holocene climate and environmental change in north-eastern Kamchatka (Russian Far East).” Glob. Planet. Chang. 134, 41–54.

Andrus, C. Fred T., and Douglas E. Crowe. 2002. “Alteration of Otolith Aragonite: Effects of Prehistoric Cooking Methods on Otolith Chemistry.” Journal of Archaeological Science 29 (3): 291–99. https://doi.org/10.1006/jasc.2001.0694.

Aono, Yasuyuki, and Yukio Omoto. 1994. “Estimation of Temperature at Kyoto since the 11th Century Using Flowering Data of Cherry Trees in Old Documents.” Journal of Agricultural Meteorology 49 (4): 263–72.

Arnold, Jeanne E. 1996. “The Archaeology of Complex Hunter-Gatherers.” Journal of Archaeological Method and Theory 3 (1): 77–126.

Arthur, Michael A., Thomas F. Anderson, Isaac R. Kaplan, Jan Veizer, and Lynton S. Land. 1983. Stable Isotopes in Sedimentary Geology. Stable Isotopes in Sedimentary Geology. SEPM Society for Sedimentary Geology. https://doi.org/10.2110/scn.83.10.

Arthur, Michael A, Douglas F Williams, and Douglas S Jones. 1983. “Seasonal Temperature-Salinity Changes and Thermocline Development in the Mid-Atlantic Bight as Recorded by the Isotopic Composition of Bivalves.” Geology 11 (11): 655–59. https://doi.org/10.1130/0091-7613(1983)11<655:stcatd>2.0.co;2.

Ascough, Philippa L, Mike J Church, and Gordon T Cook. 2017. “Marine Radiocarbon Reservoir Effects for the Mesolithic and Medieval Periods in the Western Isles of Scotland.” Radiocarbon 59 (1): 17–31. https://doi.org/DOI: 10.1017/RDC.2016.99.

Ascough, Philippa L, G T Cook, M J Church, A J Dugmore, S V Arge, and T H McGovern. 2006. “Variability in North Atlantic Marine Radiocarbon Reservoir Effects at c. AD 1000.” The Holocene 16 (1): 131–36. https://doi.org/10.1191/0959683606hl913rr.

Ascough, Philippa L, Gordon T Cook, Andrew J Dugmore, E Marian Scott, and Stewart P H T Freeman. 2005. “Influence of Mollusk Species on Marine ΔR Determinations.” Radiocarbon 47 (3): 433–440. https://doi.org/10.1017/S0033822200035219.

Barr, I.D., Solomina, O. 2014. “Pleistocene and Holocene glacier fluctuations upon the Kamchatka Peninsula.” Glob. Planet. Chang. 113, 110–120.

Batenburg, Sietske J, Gert-Jan Reichart, Tom Jilbert, Max Janse, Frank P Wesselingh, and Willem Renema. 2011. “Interannual Climate Variability in the Miocene: High Resolution Trace Element and Stable Isotope Ratios in Giant Clams.” Palaeogeography, Palaeoclimatology, Palaeoecology 306 (1): 75–81. https://doi.org/https://doi.org/10.1016/j.palaeo.2011.03.031.

Batten, Bruce L. 2008. “Climate Change in Japanese History and Prehistory: A Comparative Overview.”

Befu, Harumi, and Chester S Chard. 1964. “A Prehistoric Maritime Culture of the Okhotsk Sea.” American Antiquity 30 (1): 1–18.

Berger, Rainer, R. E. Taylor, and W. F. Libby. 1966. “Radiocarbon Content of Marine Shells from the California and Mexican West Coast.” Science 153 (3738): 864–66. https://doi.org/10.1126/science.153.3738.864.

Boltwood, B B. 1907. “Note on a New Radio-Active Element.” American Journal of Science s4-24 (142): 370 LP – 372. https://doi.org/10.2475/ajs.s4-24.142.370.

Branscombe, Tansy, Julia Lee-Thorp, Rick Schulting, and Melanie J Leng. 2022. “Micromilling Vs Hand Drilling in Stable Isotope Analyses of Incremental Carbonates: The Potential for Δ13C Contamination by Embedding Resin.” Rapid Communications in Mass Spectrometry. https://doi.org/https://doi.org/10.1002/rcm.9318.

Branscombe, Tansy, Marjolein Nigst, and Preston Miracle. 2020. “Seasonal Shellfishing across the East Adriatic Mesolithic-Neolithic Transition: Oxygen Isotope Analysis of Phorcus Turbinatus from Vela Spila (Croatia).” Environmental Archaeology. https://doi.org/10.1080/14614103.2020.1721695.

Branscombe, Tansy, Rick Schulting, Julia Lee-Thorp, and Melanie J. Leng. 2021. “The Potential of Marine Bivalve Spisula Sachalinensis as a Marine Temperature Record.” Palaeogeography, Palaeoclimatology, Palaeoecology 582 (September): 110634. https://doi.org/10.1016/j.palaeo.2021.110634.

Brock, Fiona, Joanna Ostapkowicz, Christopher Bronk Ramsey, Alex Wiedenhoeft, and Caroline Cartwright. 2012. “Paired Dating of Pith and Outer Edge (Terminus) Samples from Pre-Hispanic Caribbean Wooden Sculptures.” Radiocarbon. https://doi.org/10.1017/s0033822200047342.

Bronk Ramsey, Christopher. 2009. “Bayesian Analysis of Radiocarbon Dates.” Radiocarbon 51 (1): 337–60. https://doi.org/DOI: 10.1017/S0033822200033865.

Buckley, Brendan, and Osamu Kobayashi. 1990. “Warm-Season Annual to Decadal Temperature Variability for Hokkaido, Japan, Inferred from Maximum Latewood Density and Ring Width Data,Nicole Davi, Etc Climatic Change, 52, 1-2, 2.Pdf,” 201–17.

Burchell, M, A Cannon, N Hallmann, H P Schwartz, and B R Schöne. 2013. “Refining Estimate for the Season of Collection on the Pacific Northwest Coast: Applying High-Resolution Stable Oxygen Isotope Analysis and Sclerochronology.” Archaeometry 55 (2): 258–76. https://doi.org/https://doi.org/10.1111/j.1475-4754.2012.00684.x.

Burke, Ariane, Matthew C Peros, Colin D Wren, Francesco S R Pausata, Julien Riel-Salvatore, Olivier Moine, Anne de Vernal, Masa Kageyama, and Solène Boisard. 2021. “The Archaeology of Climate Change: The Case for Cultural Diversity.” Proceedings of the National Academy of Sciences of the United States of America 118 (30). https://doi.org/10.1073/pnas.2108537118.

Butler, Paul G., Alan D. Wanamaker, James D. Scourse, Christopher A. Richardson, and David J. Reynolds. 2013. “Variability of Marine Climate on the North Icelandic Shelf in a 1357-Year Proxy Archive Based on Growth Increments in the Bivalve Arctica Islandica.” Palaeogeography,

Palaeoclimatology, Palaeoecology. https://doi.org/10.1016/j.palaeo.2012.01.016.

Campana, S E. 2005. “Otolith Science Entering the 21st Century.” Marine and Freshwater Research 56: 485–95.

Carré, Matthieu, Ilhem Bentaleb, Dominique Blamart, Neil Ogle, Freddy Cardenas, Sheyla Zevallos, Robert M. Kalin, Luc Ortlieb, and Michel Fontugne. 2005. “Stable Isotopes and Sclerochronology of the Bivalve Mesodesma Donacium: Potential Application to Peruvian Paleoceanographic Reconstructions.” Palaeogeography, Palaeoclimatology, Palaeoecology 228 (1–2): 4–25. https://doi.org/10.1016/j.palaeo.2005.03.045.

Cersoy, S, A Zazzo, J Rofes, A Tresset, S Zirah, C Gauthier, E Kaltnecker, F Thil, and N Tisnerat-Laborde. 2017. “Radiocarbon Dating Minute Amounts of Bone (3–60 Mg) with ECHoMICADAS.” Scientific Reports 7 (1): 7141. https://doi.org/10.1038/s41598-017-07645-3.

Chen, Ernest. 2014. “Pacific Cod.” Monterey Bay Aquarium Seafood Watch.

Chu, Peter C, Yuchun Chen, and Shihua Lu. 1998. “Temporal and Spatial Variabilities of Japan Sea Surface Temperature and Atmospheric Forcings.” Journal of Oceanography 54 (3): 273–84. https://doi.org/10.1007/BF02751702.

Colonese, André Carlo, Ester Verdún-Castelló, Myrian Álvarez, Ivan Briz i Godino, Débora Zurro, and Lorena Salvatelli. 2012. “Oxygen Isotopic Composition of Limpet Shells from the Beagle Channel: Implications for Seasonal Studies in Shell Middens of Tierra Del Fuego.” Journal of Archaeological Science 39 (6): 1738–48. https://doi.org/10.1016/j.jas.2012.01.012.

Conroy, J.L., Overpeck, J.T., Cole, J.E., Shanahan, T.M., Steinitz-Kannan, M. 2008. “Holocene changes in eastern tropical Pacific climate inferred from a Gala'pagos lake sediment record.” Quat. Sci. Rev. 27, 1166–1180.

Coplen, Tyler B. 1994. “Reporting of Stable Hydrogen, Carbon, and Oxygen Isotopic Abundances (Technical Report).” Pure and Applied Chemistry 66 (2): 273–76. https://doi.org/doi:10.1351/pac199466020273.

Córdova-Rodríguez, Kathy, Jonathan Flye-Sainte-Marie, Ernesto Fernández, Michelle Graco, Anibal Rozas, and Arturo Aguirre-Velarde. 2022. “Effect of Low PH on Growth and Shell Mechanical Properties of the Peruvian Scallop Argopecten Purpuratus (Lamarck, 1819).” Marine Environmental Research 177: 105639. https://doi.org/https://doi.org/10.1016/j.marenvres.2022.105639.

Crawford, Gary W. 2008. “The Jomon in Early Agriculture Discourse: Issues Arising from Matsui, Kanehara and Pearson.” World Archaeology 40 (4): 445–65. https://doi.org/10.1080/00438240802451181.

Crawford, Gary W., and Peter Bleed. 1998. “Scheduling and Sedentism in the Prehistory of Northern.” In Seasonality and Sedentism: Archaeological Perspectives from Old and New World Sites, edited by Thomas R Rocek and Ofer Bar-Yosef. Harvard University Press.

Crawford, Gary W., and H Takamiya. 1990. “The Origins and Implications of Late Prehistoric Plant Husbandry in Northern Japan.” Antiquity iv (1990): 889–911.

Crawford, Gary W., and Masakazu Yoshizaki. 1987. “Ainu Ancestors and Prehistoric Asian Agriculture.” Journal of Archaeological Science 14 (2): 201–13. https://doi.org/10.1016/0305-4403(87)90007-0.

Damon, Paul E, Austin Long, and Donald C. Grey. 1966. “Fluctuation of Atmospheric C 14 during the Last Six Millennia.” Journal of Geophysical Research 71 (4): 1055–63.

https://doi.org/10.1029/jz071i004p01055.

Deith, Margaret R. 1983. “Molluscan Calendars: The Use of Growth-Line Analysis to Establish Seasonality of Shellfish Collection at the Mesolithic Site of Morton, Fife.” Journal of Archaeological Science 10 (5): 423–40. https://doi.org/10.1016/0305-4403(83)90058-4.

Dettman, D. L., and K. C. Lohmann. 1995. “Microsampling Carbonates for Stable Isotope and Minor Element Analysis: Physical Separation of Samples on a 20 Micrometer Scale.” Journal of Sedimentary Research A: Sedimentary Petrology & Processes, no. A65(3): 566–69. https://doi.org/10.1306/d426813f-2b26-11d7-8648000102c1865d.

Dirksen, V., Dirksen, O., van den Bogaard, C., Diekmann, B. 2015. “Holocene pollen record from Lake Sokoch, interior Kamchatka (Russia), and its palaeobotanical and paleoclimatic interpretation.” Glob. Planet. Chang. 134, 129–141.

Dyck, Willy. 1967. “Recent Developments in Radiocarbon Dating: Their Implications for Geochronology and Archaeology.” Current Anthropology 8 (4): 349–51. https://doi.org/10.1086/200812.

Dykowski, C.A., Edwards, R.L., Cheng, H., Yuan, D.X., Cai, Y.J., Zhang, M.L., Lin, Y.S., Qing, J.M., An, Z.S., Revenaugh, J. 2005. “A high-resolution, absolute-dated Holocene and deglacial Asian monsoon record from Dongge Cave, China.” Earth Planet. Sci. Lett. 233, 71–86.

Eagle, R. A., J. M. Eiler, A. K. Tripati, J. B. Ries, P. S. Freitas, C. Hiebenthal, A. D. Wanamaker, et al. 2013. “The Influence of Temperature and Seawater Carbonate Saturation State on 13C-18O Bond Ordering in Bivalve Mollusks.” Biogeosciences 10 (7): 4591–4606. https://doi.org/10.5194/bg-10-4591-2013.

Ebuchi, Naoto, Yasushi Fukamachi, Kay I. Ohshima, Kunio Shirasawa, Masao Ishikawa, Toru Takatsuka, Takaharu Daibo, and Masaaki Wakatsuchi. 2006. “Observation of the Soya Warm Current Using HF Ocean Radar.” Journal of Oceanography. https://doi.org/10.1007/s10872-006-0031-0.

Eda, Masaki, Hiroko Koike, and Hiroyoshi Higuchi. 2016. “Understanding Prehistoric Maritime Adaptations in Northern Japan: Indirect Evidence from Ancient DNA and Histological Observations of Albatross (Aves: Diomedeidae) Bones.” Quaternary International 419: 159–64. https://doi.org/10.1016/j.quaint.2015.06.067.

Edvardsson, Ragnar, William P Patterson, Hlynur Bárðarson, Sandra Timsic, and Guðbjörg Ásta Ólafsdóttir. 2019. “Change in Atlantic Cod Migrations and Adaptability of Early Land-Based Fishers to Severe Climate Variation in the North Atlantic.” Quaternary Research, 1–11. https://doi.org/DOI: 10.1017/qua.2018.147.

Edwards, Cole T, Clive M Jones, Page C Quinton, and David A Fike. 2022. “Oxygen Isotope (Δ18O) Trends Measured from Ordovician Conodont Apatite Using Secondary Ion Mass Spectrometry (SIMS): Implications for Paleo-Thermometry Studies.” GSA Bulletin 134 (1–2): 261–74. https://doi.org/10.1130/B35891.1.

Edwards, Walter. 2005. “Japanese Archaeology and Cultural Properties Management: Prewar Ideology and Postwar Legacies.” In A Companion to the Anthropology of Japan, edited by Jennifer Robertson, 36–49. Blackwell.

Eiler, John M. 2011. “Paleoclimate Reconstruction Using Carbonate Clumped Isotope Thermometry.” Quaternary Science Reviews 30 (25): 3575–88. https://doi.org/https://doi.org/10.1016/j.quascirev.2011.09.001.

Emiliani, C., L. Cardini, T. Mayeda, C. McBurney, and E. Tongiorgi. 1964. “Palaeotemperature Analysis

of Marine Molluscs (Food Refuse) from the Site of Arene Candide Cave, Italy and the Haua Fteah Cave, Cyrenaica." In Isotopic and Cosmic Chemistry, edited by H. Craig, S. Miller, and G Wasserburg. Amsterdam: North-Holland Publishing Company.

Epstein, Samuel, R Buchsbaum, H a Lowenstam, and H C Urey. 1953. "Revised Carbonate-Water Isotopic Temeprature Scale." Geological Society of America Bulletin. https://doi.org/10.1130/0016-7606(1953)64.

Erlandson, Jon M., and M Moss. 2001. "Shellfish Feeders, Carrion Eaters, and the Archaeology of Aquatic Adaptations." American Antiquity 66 (3): 413–32. https://doi.org/10.2307/2694242.

Fukusawa, Hitoshi. 1999. "Varved Lacustrine Sediments in Japan:Recent Progress." The Quaternary Research (Daiyonki-Kenkyu) 38 (3): 237–43. https://doi.org/10.4116/jaqua.38.237.

Gao, Yongwen, Greg G. Bargmann, Uwe Brand, and David L.G. Noakes. 2005. "Stable Isotopic and Trace Elemental Compositions of Otoliths and the Stock Structure of Pacific Cod, Gadus Macrocephalus." Environmental Biology of Fishes 74 (3–4): 335–48. https://doi.org/10.1007/s10641-005-1332-7.

Gauldie, R W, and D G A Nelson. 1988. "Aragonite Twinning and Neuroprotein Secretion Are the Cause of Daily Growth Rings in Fish Otoliths." Comparative Biochemistry and Physiology Part A: Physiology 90 (3): 501–9. https://doi.org/https://doi.org/10.1016/0300-9629(88)90227-7.

Ghosh, Prosenjit, Jess Adkins, Hagit Affek, Brian Balta, Weifu Guo, Edwin A Schauble, Dan Schrag, and John M Eiler. 2006. "13C–18O Bonds in Carbonate Minerals: A New Kind of Paleothermometer." Geochimica et Cosmochimica Acta 70 (6): 1439–56. https://doi.org/https://doi.org/10.1016/j.gca.2005.11.014.

Ghosh, Prosenjit, John Eiler, Steven E Campana, and Richard F Feeney. 2007. "Calibration of the Carbonate 'Clumped Isotope' Paleothermometer for Otoliths." Geochimica et Cosmochimica Acta 71 (11): 2736–44. https://doi.org/https://doi.org/10.1016/j.gca.2007.03.015.

Gillikin, David Paul, Anne Lorrain, Steven Bouillon, Philippe Willenz, and Frank Dehairs. 2006. "Stable Carbon Isotopic Composition of Mytilus Edulis Shells: Relation to Metabolism, Salinity, Δ13CDIC and Phytoplankton." Organic Geochemistry 37 (10): 1371–82. https://doi.org/10.1016/j.orggeochem.2006.03.008.

Glykou, Aikaterini, Kenneth Ritchie, Matthew S Hargrave, Wouter Visch, and Kerstin Lidén. 2021. "Strontium Isotope Analysis in Prehistoric Cod Otoliths by Laser Ablation Multi-Collector Inductively Coupled Plasma Mass Spectrometry." Journal of Archaeological Science: Reports 37: 102976. https://doi.org/https://doi.org/10.1016/j.jasrep.2021.102976.

Golikov, A. N., and O. A. Scarlato. 1970. "Abundance, Dynamics and Production Properties of Populations of Edible Bivalves Mizuhopecten Yessoensis and Spisula Sachalinensis Related to the Problem of Organization of Controllable Submarine Farms at the Western Shores of the Sea of Japan." Helgoländer Wissenschaftliche Meeresuntersuchungen 20 (1–4): 498–513. https://doi.org/10.1007/BF01609925.

Gomes, Amanda, and Shiaki Kondo. 2020. "Reflections on Ethnographic Methods Training at an Archaeological Field School : A Case Study from Rebun International Field School in Japan." Journal of the Faculty of Humanities and Human Sciences 15.

Gompertz, Benjamin. 1825. "XXIV. On the Nature of the Function Expressive of the Law of Human Mortality, and on a New Mode of Determining the Value of Life Contingencies. In a Letter to Francis Baily, Esq. F. R. S." Phil. Trans. R. Soc 115.

Goodwin, David H, Bernd R Schöne, David L Dettman, David H Goodwin, Bernd R Schone, and David L

Dettman. 2003. “Resolution and Fidelity of Oxygen Isotopes as Paleotemperature Proxies in Bivalve Mollusk Shells : Models and Observations Published by : SEPM Society for Sedimentary Geology Linked References Are Available on JSTOR for This Article : Paleotemperature Pro.” SEPM Society for Sedimentary Geology 18 (2): 110–25.

Gottschalk, Julia, R F Anderson, D Hodell, A Martinez-garcia, Alain Mazaud, E Michel, Luke C Skinner, et al. 2020. “On New Developments in Accelerator Mass Spectrometry.” In Presentation from the European Geosciences Union General Assembly. https://presentations.copernicus.org/EGU2020/EGU2020-12768_presentation.pdf.

Gottschalk, Julia, Sönke Szidat, Elisabeth Michel, Alain Mazaud, Gary Salazar, Michael Battaglia, Jörg Lippold, and Samuel L Jaccard. 2018. “Radiocarbon Measurements of Small-Size Foraminiferal Samples with the Mini Carbon Dating System (MICADAS) at the University of Bern: Implications for Paleoclimate Reconstructions.” Radiocarbon 60 (2): 469–91. https://doi.org/DOI: 10.1017/RDC.2018.3.

Grossman, Ethan L., and Teh Lung Ku. 1986. “Oxygen and Carbon Isotope Fractionation in Biogenic Aragonite: Temperature Effects.” Chemical Geology: Isotope Geoscience Section 59 (C): 59–74. https://doi.org/10.1016/0168-9622(86)90057-6.

Gunn, John S., Ian R. Harrowfield, Craig H. Proctor, and Ronald E. Thresher. 1992. “Electron Probe Microanalysis of Fish Otoliths - Evaluation of Techniques for Studying Age and Stock Discrimination.” Journal of Experimental Marine Biology and Ecology 158 (1): 1–36. https://doi.org/10.1016/0022-0981(92)90306-U.

Habu, Junko. 2008. “Growth and Decline in Complex Hunter-Gatherer Societies: A Case Study from the Jomon Period Sannai Maruyama Site, Japan.” Antiquity. https://doi.org/10.1017/S0003598X00097234.

Habu, Junko, Akira Matsui, Naoto Yamamoto, and Tomonori Kanno. 2011. “Shell Midden Archaeology in Japan: Aquatic Food Acquisition and Long-Term Change in the Jomon Culture.” Quaternary International 239 (1–2): 19–27. https://doi.org/10.1016/j.quaint.2011.03.014.

Hammarlund, D., Klimaschewski, A., Amour, N.A.S., Andrén, E., Self, A.E., Solovieva, N., Andreev, A.A., Barnekow, L., Edwards, T.W.D. 2015. “Late Holocene expansion of Siberian dwarf pine (Pinus pumila) in Kamchatka in response to increased snow cover as inferred from lacustrine oxygen isotope records.” Glob. Planet. Chang. 134, 91–100.

Harada, N., Katsuki, K., Nakagawa, M., Matsumoto, A., Seki, O., Addison, J.A., Finney, B.P., Sato, M. 2014. “Holocene sea surface temperature and sea ice extent in the Okhotsk and Bering Seas.” Prog. Oceanogr. 126, 242–253.

Hausmann, N., P. Siozos, A. Lemonis, A. C. Colonese, H. K. Robson, and D. Anglos. 2017. “Elemental Mapping of Mg/Ca Intensity Ratios in Marine Mollusc Shells Using Laser-Induced Breakdown Spectroscopy.” Journal of Analytical Atomic Spectrometry 32 (8): 1467–72. https://doi.org/10.1039/c7ja00131b.

Hausmann, N, A L Prendergast, A Lemonis, J Zech, P Roberts, P Siozos, and D Anglos. 2019. “Extensive Elemental Mapping Unlocks Mg/Ca Ratios as Climate Proxy in Seasonal Records of Mediterranean Limpets.” Scientific Reports 9 (1): 3698. https://doi.org/10.1038/s41598-019-39959-9.

Hausmann, Niklas, Harry K. Robson, and Chris Hunt. 2019. “Annual Growth Patterns and Interspecimen Variability in Mg/ca Records of Archaeological Ostrea Edulis (European Oyster) from the Late Mesolithic Site of Conors Island.” Open Quaternary 5 (1): 1–18. https://doi.org/10.5334/oq.59.

He, Miaohong, Tianyu Chen, Xi Liu, Ya-Nan Yang, Xiaoping Xia, Qing Yang, Pengli He, Jian Di, Yanqiang Zhang, and Gangjian Wei. 2021. “Accurate in Situ Oxygen Isotopic Analysis at High Resolution by Secondary Ion Mass Spectrometry Shows the Potential of Aragonite as a Reference Material.” Journal of Analytical Atomic Spectrometry 36 (7): 1389–98. https://doi.org/10.1039/D1JA00072A.

Heaton, Timothy J, Peter Köhler, Martin Butzin, Edouard Bard, Ron W Reimer, William E N Austin, Christopher Bronk Ramsey, et al. 2020. “Marine20—The Marine Radiocarbon Age Calibration Curve (0–55,000 Cal BP).” Radiocarbon 62 (4): 779–820. https://doi.org/DOI: 10.1017/RDC.2020.68.

Helser, Thomas, Craig Kastelle, Aron Crowell, Takayuki Ushikubo, Ian J Orland, Reinhard Kozdon, and John W Valley. 2018. “A 200-Year Archaeozoological Record of Pacific Cod (Gadus Macrocephalus) Life History as Revealed through Ion Microprobe Oxygen Isotope Ratios in Otoliths.” Journal of Archaeological Science: Reports 21: 1236–46. https://doi.org/https://doi.org/10.1016/j.jasrep.2017.06.037.

Helser, Thomas, Craig R. Kastelle, Jennifer L. McKay, Ian J. Orland, Reinhard Kozdon, and John W. Valley. 2018. “Evaluation of Micromilling/Conventional Isotope Ratio Mass Spectrometry and Secondary Ion Mass Spectrometry of Δ18O Values in Fish Otoliths for Sclerochronology.” Rapid Communications in Mass Spectrometry 32 (20): 1781–90. https://doi.org/10.1002/rcm.8231.

Heuer, A H, X Su, S Kamat, and R Ballarini. 2001. “Shell: Properties.” In , edited by K H Jürgen Buschow, Robert W Cahn, Merton C Flemings, Bernhard Ilschner, Edward J Kramer, Subhash Mahajan, and Patrick B T - Encyclopedia of Materials: Science and Technology Veyssière, 8462–69. Oxford: Elsevier. https://doi.org/https://doi.org/10.1016/B0-08-043152-6/01512-6.

Hirasawa, Yu. 2018. “Rebun Island Field Guide.”

Hirasawa, Yu, and Hirofumi Kato. 2019. “Preliminary Archaeological Field Report of Excavation at Hamanaka 2 Site, Rebun Island, Hokkaido, JAPAN.” Sapporo.

———. 2020. “Preliminary Archaeological Field Report at Hamanaka 2 Site, Rebun Island, Hokkaido, JAPAN.” Sapporo.

Hirose, Naoki, and Ken ichi Fukudome. 2006. “Monitoring the Tsushima Warm Current Improves Seasonal Prediction of the Regional Snowfall.” Scientific Online Letters on the Atmosphere 2: 61–63. https://doi.org/10.2151/sola.2006-016.

Hoff, U., Biskaborn, B.K., Dirksen, V., Dirksen, O., Kuhn, G., Meyer, H., Nazarova, L., Roth, A., Diekmann, B. 2015. “Holocene environment of Central Kamchatka, Russia: implications from a multi-proxy record of Two-Yurts Lake.” Glob. Planet. Chang. 134, 101–117.

Hogg, Alan G, Timothy J Heaton, Quan Hua, Jonathan G Palmer, Chris S M Turney, John Southon, Alex Bayliss, et al. 2020. “SHCal20 Southern Hemisphere Calibration, 0–55,000 Years Cal BP.” Radiocarbon 62 (4): 759–78. https://doi.org/DOI: 10.1017/RDC.2020.59.

Hollyman, Philip R, Melanie J Leng, Simon R.N. Chenery, Hilary J Sloane, and Christopher A Richardson. 2020. “Calibration of Shell Δ18O from the Common Whelk Buccinum Undatum Highlights Potential for Palaeoenvironmental Reconstruction.” Palaeogeography, Palaeoclimatology, Palaeoecology 560. https://doi.org/10.1016/j.palaeo.2020.109995.

Holmquist, James R, Laura Reynolds, Lauren N Brown, John R Southon, Alexander R Simms, and Glen M MacDonald. 2015. “Marine Radiocarbon Reservoir Values in Southern California Estuaries: Interspecies, Latitudinal, and Interannual Variability.” Radiocarbon 57 (3): 449–458. https://doi.org/10.2458/azu_rc.57.18389.

Hu, Chaoyong, Gideon M Henderson, Junhua Huang, Shucheng Xie, Ying Sun, and Kathleen R Johnson. 2008. “Quantification of Holocene Asian Monsoon Rainfall from Spatially Separated Cave Records.” Earth and Planetary Science Letters 266 (3): 221–32. https://doi.org/https://doi.org/10.1016/j.epsl.2007.10.015.

Hudson, Mark J. 1999. “Post-Yayoi Interaction and Ethnogenesis.” In Ruins of Identity : Ethnogenesis in the Japanese Islands. University of Hawaii Press.

———. 2004. “The Perverse Realities of Change: World System Incorporation and the Okhotsk Culture of Hokkaido.” Journal of Anthropological Archaeology 23 (3): 290–308. https://doi.org/10.1016/j.jaa.2004.05.002.

———. 2014. “The Ethnohistory and Anthropology of ‘Modern’ Hunter-Gatherers: North Japan (Ainu).” In The Oxford Handbook of the Archaeology and Anthropology of Hunter-Gatherers, edited by Vicki Cummings, Peter Jordan, and Marek Zvelebil. Oxford Unversity Press.

Hufthammer, Anne Karin, Hans Høie, Arild Folkvord, Audrey J. Geffen, Carin Andersson, and Ulysses S. Ninnemann. 2010. “Seasonality of Human Site Occupation Based on Stable Oxygen Isotope Ratios of Cod Otoliths.” Journal of Archaeological Science 37 (1): 78–83. https://doi.org/10.1016/j.jas.2009.09.001.

Igarashi, Yaeko. 2013. “Holocene Vegetation and Climate on Hokkaido Island, Northern Japan.” Quaternary International 290–291: 139–50. https://doi.org/10.1016/j.quaint.2012.09.030.

Iizuka, Yoshiyuki. 2012. “Electron Microprobe Study of Otolith : Migratory Behavior and Habitat of Three Major Temperate.”

Imada, Yukiko, Shuhei Maeda, Masahiro Watanabe, Hideo Shiogama, Ryo Mizuta, Masayoshi Ishii, and Masahide Kimoto. 2017. “Recent Enhanced Seasonal Temperature Contrast in Japan from Large Ensemble High-Resolution Climate Simulations.” Atmosphere 8 (3): 1–13. https://doi.org/10.3390/atmos8030057.

Ishida, Hajime, Tsunehiko Hanihara, Osamu Kondo, and Naoyuki Ohshima. 1994. “A Human Skeleton of the Early Phase of the Okhotsk Culture Unearthed at the Hamanaka-2 Site, Rebun Island, Hokkaido.” Anthropological Science 102 (January): 363–78. https://doi.org/10.1537/ase.102.363.

Isobe, Atsuhiko. 1999. “On the Origin of the Tsushima Warm Current Water and Its Seasonality.” Acta Oceanologica Sinica 19 (1999): 117–33.

Janz, Horst, and Torsten W Vennemann. 2005. “Isotopic Composition (O, C, Sr, and Nd) and Trace Element Ratios (Sr/Ca, Mg/Ca) of Miocene Marine and Brackish Ostracods from North Alpine Foreland Deposits (Germany and Austria) as Indicators for Palaeoclimate.” Palaeogeography, Palaeoclimatology, Palaeoecology 225 (1): 216–47. https://doi.org/https://doi.org/10.1016/j.palaeo.2005.06.012.

Jeong, Choongwon, Shigeki Nakagome, and Anna Di Rienzo. 2016. “Deep History of East Asian Populations Revealed through Genetic Analysis of the Ainu.” Genetics 202 (1): 261–72. https://doi.org/10.1534/genetics.115.178673.

Jessop, B. M. 2021. “Oceanic Water Temperatures Less Than 20°C May Partly Account for Bias in American Eel Elver Otolith Age Estimates.” Marine and Coastal Fisheries 13 (5): 614–24. https://doi.org/10.1002/mcf2.10154.

Jones, Douglas S. 1980. “Annual Cycle of Shell Growth Increment Formation in Two Continental Shelf

Bivalves and Its Paleoecologic Significance." Paleobiology 3 (3): 331–40. https://doi.org/10.1017/S0094837300006837.

Jones, M.C., Wooller, M., Peteet, D.M., Katsuki, K. 2014. "A deglacial and Holocene record of climate variability in south-central Alaska from stable oxygen isotopes and plant macrofossils in peat. Quat. Sci. Rev. 87, 1–11.

Junno, Ari, Jack P.R. Dury, Christian Leipe, Mayke Wagner, Pavel E. Tarasov, Yu Hirasawa, Peter D. Jordan, and Hirofumi Kato. 2021. "Building a High-Resolution Chronology for Northern Hokkaido – A Case Study of the Late Holocene Hamanaka 2 Site on Rebun Island, Hokkaido (Japan)." Journal of Archaeological Science: Reports 36 (February): 102867. https://doi.org/10.1016/j.jasrep.2021.102867.

Junno, Aripekka Oskari. 2020. "Bringing Home Animals: Final-Stage Jomon and Okhotsk Culture Food Technologies." http://hdl.handle.net/11370/df08ed08-d9a8-408b-a57b-92db0302ff86.

Karakiri, M., and H. von Westernhagen. 1989. "Daily Growth Patterns in Otoliths of Larval and Juvenile Plaice (Pleuronectes Platessa): Influence of Temperature, Salinity and Light Conditions." Rapp. P.-v. Réun. Cons. Perm. Int. Explor. Mer 191.

Kastelle, Craig R., Thomas E. Helser, Jennifer L. McKay, Chris G. Johnston, Delsa M. Anderl, Mary E. Matta, and Daniel G. Nichol. 2017. "Age Validation of Pacific Cod (Gadus Macrocephalus) Using High-Resolution Stable Oxygen Isotope (δ 18O) Chronologies in Otoliths." Fisheries Research 185: 43–53. https://doi.org/10.1016/j.fishres.2016.09.024.

Katayama, Satoshi. 2018. "A Description of Four Types of Otolith Opaque Zone." Fisheries Science 84 (5): 735–45. https://doi.org/10.1007/s12562-018-1228-z.

Kato, Hirofumi. 2020. "Hokkaido Sequence and the Archaeology of the Ainu People BT - Encyclopedia of Global Archaeology." In , edited by Claire Smith, 5213–28. Cham: Springer International Publishing. https://doi.org/10.1007/978-3-030-30018-0_33.

Kato, Yasuhisa, and Ikuso Hamai. 1975. "Growth and Shell Formation of the Surf Clam, Spisula Sachalinensis (Schrenck)." Bulletin of the Faculty of Fisheries, Hokkaido University 25 (4): 291–303.

Kawahata, H., H. Ohshima, C. Shimada, and T. Oba. 2003. "Terrestrial-Oceanic Environmental Change in the Southern Okhotsk Sea during the Holocene." Quaternary International 108 (1): 67–76. https://doi.org/10.1016/S1040-6182(02)00195-7.

Kelly, Robert L. 1983. "Hunter-Gatherer Mobility Strategies" 39 (3): 277–306.

Kennett, Douglas J, and Barbara Voorhies. 1996. "Oxygen Isotopic Analysis of Archaeological Shells to Detect Seasonal Use of Wetlands on the Southern Pacific Coast of Mexico." Journal of Archaeological Science 23 (5): 689–704. https://doi.org/https://doi.org/10.1006/jasc.1996.0065.

Khim, Boo Keun, Kyung Sik Woo, and Jong Geel Je. 2000. "Stable Isotope Profiles of Bivalve Shells: Seasonal Temperature Variations, Latitudinal Temperature Gradients and Biological Carbon Cycling along the East Coast of Korea." Continental Shelf Research 20 (8): 843–61. https://doi.org/10.1016/S0278-4343(00)00004-2.

Kikuchi, Toshihiko. 1978. "The Origin of the Okhotsk Culture and Its Correlation with Cultures of Neighbouring Regions." Bulletin of the Instute for the Study of North Eurasian Cultures, Hokkaido University. 12: 39–76.

Kimura, Y., Y. Yokoyama, and H. Hirano. 2011. "Stratigraphic Trends in Molluscan Paleoecology in

Storm-Generated Shell Beds from the Lower Shoreface Deposits of the Pliocene Dainichi Formation, Kakegawa Group, Central Japan." Fossils 90.

Kita, Noriko T, Takayuki Ushikubo, Bin Fu, and John W Valley. 2009. "High Precision SIMS Oxygen Isotope Analysis and the Effect of Sample Topography." Chemical Geology 264 (1): 43–57. https://doi.org/https://doi.org/10.1016/j.chemgeo.2009.02.012.

Klünder, Maiken Hansen, Dorothee Hippler, Rob Witbaard, and Dirk Frei. 2008. "Laser Ablation Analysis of Bivalve Shells - Archives of Environmental Information." Geological Survey of Denmark and Greenland Bulletin, no. 15: 89–92. https://doi.org/10.34194/geusb.v15.5052.

Koch, Joachim, and Detlef Günther. 2016. "Laser Ablation Inductively Coupled Plasma Mass Spectrometry." Encyclopedia of Spectroscopy and Spectrometry, 526–32. https://doi.org/10.1016/B978-0-12-803224-4.00024-8.

Kodama, D. 2003. "Komakino Stone Circle and Its Significance for the Study of Jomon Social Structure." In Hunter-Gatherers of the North Pacific Rim, edited by J. Habu, J. M. Savelle, S. Koyama, and H. Hongo. National Museum of Ethnology, Osaka.

Koizumi, I. 1987. "Pulses of Tsushima Current during the Holocene." 第四紀研究 (The Quaternary Research) 26 (1): 13–25.

Korte, Christoph, Heinz W Kozur, and Ján Veizer. 2005. "Δ13C and Δ18O Values of Triassic Brachiopods and Carbonate Rocks as Proxies for Coeval Seawater and Palaeotemperature." Palaeogeography, Palaeoclimatology, Palaeoecology 226 (3): 287–306. https://doi.org/https://doi.org/10.1016/j.palaeo.2005.05.018.

Kuroda, Hiroshi, Toshihiko Saito, Toshiki Kaga, Akinori Takasuka, Yasuhiro Kamimura, Sho Furuichi, and Takuya Nakanowatari. 2020. "Unconventional Sea Surface Temperature Regime Around Japan in the 2000s–2010s: Potential Influences on Major Fisheries Resources ." Frontiers in Marine Science . https://www.frontiersin.org/articles/10.3389/fmars.2020.574904.

Kuroyanagi, Azumi, Hodaka Kawahata, Hisashi Narita, Ken'ichi Ohkushi, and Takafumi Aramaki. 2006. "Reconstruction of Paleoenvironmental Changes Based on the Planktonic Foraminiferal Assemblages off Shimokita (Japan) in the Northwestern North Pacific." Global and Planetary Change 53 (1–2): 92–107. https://doi.org/10.1016/j.gloplacha.2006.01.015.

Lachniet, Matthew S. 2009. "Climatic and Environmental Controls on Speleothem Oxygen-Isotope Values." Quaternary Science Reviews 28 (5–6): 412–32. https://doi.org/10.1016/j.quascirev.2008.10.021.

Larsen, Susan C. 2015. "Recrystallization of Biogenic Aragonite Shells from Archaeological Contexts and Implications for Paleoenvironmental Reconstruction." Western Washington Universty.

Laskar, J., Robutel, P., Joutel, F., Gastineau, M., Correia, A.C.M., Levrard, B. 2004. "A long term numerical solution for the insolation quantities of the Earth." Astron. Astrophys. 428, 261–285.

Lazareth, C E, F Le Cornec, F Candaudap, and R Freydier. 2013. "Trace Element Heterogeneity along Isochronous Growth Layers in Bivalve Shell: Consequences for Environmental Reconstruction." Palaeogeography, Palaeoclimatology, Palaeoecology 373: 39–49. https://doi.org/https://doi.org/10.1016/j.palaeo.2011.04.024.

Lea, D. W. 2013. Elemental and Isotopic Proxies of Past Ocean Temperatures. Treatise on Geochemistry: Second Edition. 2nd ed. Vol. 8. Elsevier Ltd. https://doi.org/10.1016/B978-0-08-095975-7.00614-8.

Lebedintsev, Aleksandr I, Richard L Bland, Anna Gokhman, William Workman, Karen Workman, Aleksandr I Lebedintsev, William Workman, and Karen Workman. 1998. “Maritime Cultures of the North Coast of the Sea of Okhotsk.” Arctic Anthropology 35 (1): 296–320.

Lee, Jeong-Yong, Young-Jin Chang, and Young-Je Park. 1996. “Spawning Induction and Egg Development of Surf Clam, Spisula Sachalinensis.” Journal of Aquaculture (한국양식학회지) 9 (4): 419–27.

Leipe, Christian, Norio Kito, Yumi Sakaguchi, and Pavel E. Tarasov. 2013. “Vegetation and Climate History of Northern Japan Inferred from the 5500-Year Pollen Record from the Oshima Peninsula, SW Hokkaido.” Quaternary International 290–291: 151–63. https://doi.org/10.1016/j.quaint.2012.07.014.

Leipe, Christian, Stefanie Müller, Konrad Hille, Hirofumi Kato, Franziska Kobe, Mareike Schmidt, Konrad Seyffert, et al. 2018a. “Vegetation Change and Human Impacts on Rebun Island (Northwest Pacific) over the Last 6000 Years.” Quaternary Science Reviews 193: 129–44. https://doi.org/10.1016/j.quascirev.2018.06.011.

———. 2018b. “Vegetation Change and Human Impacts on Rebun Island (Northwest Pacific) over the Last 6000 Years.” Quaternary Science Reviews 193: 129–44. https://doi.org/10.1016/j.quascirev.2018.06.011.

Leipe, Christian, Elena A. Sergusheva, Stefanie Muller, Robert N. Spengler, Tomasz Goslar, Hirofumi Kato, Mayke Wagner, Andrzej W. Weber, and Pavel E. Tarasov. 2017. “Barley (Hordeum Vulgare) in the Okhotsk Culture (5th-10th Century AD) of Northern Japan and the Role of Cultivated Plants in Hunter-Gatherer Economies.” PLoS ONE 12 (3). https://doi.org/10.1371/journal.pone.0174397.

Libby, W. F. 1946. “Atmospheric Helium Three and Radiocarbon from Cosmic Radiation.” Physical Review 69 (11–12): 671–72. https://doi.org/10.1103/PhysRev.69.671.2.

Libby, W. F., E. C. Anderson, and J. R. Arnold. 1949. “Age Determination by Radiocarbon Content: World-Wide Assay of Natural Radiocarbon.” Science 109 (2827): 227–28. https://doi.org/10.1126/science.109.2827.227.

Libby, W.F. 1967. “History of Radiocarbon Dating.” Radioactive Dating and Methods of Low-Level Counting, 3–26.

Linick, T. W., P. E. Damon, D. J. Donahue, and A. J.T. Jull. 1989. “Accelerator Mass Spectrometry: The New Revolution in Radiocarbon Dating.” Quaternary International 1 (C): 1–6. https://doi.org/10.1016/1040-6182(89)90004-9.

López, R A, P E Penchaszadeh, and S C Marcomini. 2008. “Storm-Related Strandings of Mollusks on the Northeast Coast of Buenos Aires, Argentina.” Journal of Coastal Research 2008 (244): 925–35. https://doi.org/10.2112/05-0621.1.

Lutaenko, Konstantin, Irina Zhushchikhovskaya, Yuri Mikishin, and Alexander Popov. 2007. “Mid-Holocene Climatic Changes and Cultural Dynamics in the Basin of the Sea of Japan and Adjacent Areas.” In Climate Change and Cultural Dynamics, 331–406. https://doi.org/10.1016/B978-012088390-5.50015-7.

Lutz, Richard A., and Donald C. Rhoads. 1977. “Anaerobiosis and a Theory of Growth Line Formation.” Science 198 (4323): 1222–26. https://doi.org/10.1126/science.198.4323.1222.

———. 1980. “Growth Patterns within the Molluscan Shell.” In Skeletal Growth of Aquatic Organisms, edited by Richard A. Lutz and Donald C. Rhoads. Boston: Springer US.

Mann, R., D.M. Munroe, E.N. Powell, E.E. Hofmann, and J.M. Klinck. 2013. “Bivalve Molluscs: Barometers of Climate Change in Arctic Marine Systems.” In Responses of Arctic Marine Ecosystems to Climate Change, edited by F.J. Mueter, D.M.S Dickson, H.P Huntingdon, J.R. Irvine, E.A. Logerwell, S.A. MacLean, L.T. Quakenbush, and C. Rosa. University of Alaska Fairbanks. https://doi.org/10.4027/ramecc.2013.04.

Mannino, Marcello A., K. D. Thomas, M. J. Leng, M. Piperno, S. Tusa, and A. Tagliacozzo. 2007. “Marine Resources in the Mesolithic and Neolithic at the Grotta Dell’Uzzo (Sicily): Evidence from Isotope Analyses of Marine Shells.” Archaeometry 49 (1): 117–33. https://doi.org/10.1111/j.1475-4754.2007.00291.x.

Marali, Soraya, and Bernd R Schöne. 2015. “Oceanographic Control on Shell Growth of Arctica Islandica (Bivalvia) in Surface Waters of Northeast Iceland — Implications for Paleoclimate Reconstructions.” Palaeogeography, Palaeoclimatology, Palaeoecology 420: 138–49. https://doi.org/https://doi.org/10.1016/j.palaeo.2014.12.016.

Marcott, S.A., Shakun, J.D., Clark, P.U., Mix, A. 2013. “A reconstruction of regional and global temperature for the past 11,300 years.” Science 339, 1198–1201.

Martineau, Robert-Giles. 2012. “JAPANESE SHELLFISH SPECIES 12: SURF CLAM-UBAGAI-姥貝.” 2012. https://shizuokagourmet.com/en/2012/03/30/japanese-shellfish-species-surf-clam-ubagai-姥貝/.

Marullo, S., P.J. Minnett, R. Santoleri, and M. Tonani. 2016. “The Diurnal Cycle of Sea-Surface Temperature and Estimation of the Heat Budget of the Mediterranean Sea.” Journal of Geophysical Research: Oceans 121 (9): 6762–78. https://doi.org/10.1002/2016JC012132.Received.

Matsumura, Hirofumi, Mark J. Hudson, Kenichiro Koshida, and Yoichi Minakawa. 2006. “Embodying Okhotsk Ethnicity: Human Skeletal Remains from the Aonae Dune Site, Okushiri Island, Hokkaido.” Asian Perspectives 45 (1): 1–23. https://doi.org/10.1353/asi.2006.0010.

Matsutaro, Shibata. 1970. “On the Punctations Scattered over the Shell Surface of Glycymeris (Veletuceta) Albolineata (Lischke).” Chikyu Kagaku (Earth Science) 24 (5): 167–70. https://eurekamag.com/research/019/604/019604971.php.

Matsuyama, Masaji, Makiko Wadaka, Taizo Abe, Masaaki Aota, and Yoshio Koike. 2006. “Current Structure and Volume Transport of the Soya Warm Current in Summer.” Journal of Oceanography 62 (2): 197–205. https://doi.org/10.1007/s10872-006-0044-8.

Maurer, John. 2002. “Infrared and Microwave Remote Sensing of Sea Surface Temperature (SST).” 2002. http://www2.hawaii.edu/~jmaurer/sst/.

Max, L., Riethdorf, J.-R., Tiedemann, R., Smirnova, M., Lembke-Jene, L., Fahl, K., Nürnberg, D., Matul, A., Mollenhauer, G. 2012. “Sea surface temperature variability and sea-ice extent in the subarctic northwest Pacific during the past 15,000 years.” Paleoceanography 27, PA3213. http://dx.doi.org/10.1029/2012PA002292.

McColl, Jill Louise. 2016. “Climate Variability of the Past 1000 Years in the NW Pacific: High Resolution, Multi-Biomarker Records from Lake Toyoni.” University of Glasgow.

McConnaughey, Ted A., and David Paul Gillikin. 2008. “Carbon Isotopes in Mollusk Shell Carbonates.” Geo-Marine Letters 28 (5–6): 287–99. https://doi.org/10.1007/s00367-008-0116-4.

Meyer, H., Chapligin, B., Hoff, U., Nazarova, L., Diekmann, B. 2015. “Oxygen isotope composition of diatoms as Late Holocene climate proxy at Two-Yurts-Lake, Central Kamchatka, Russia.” Glob.

Planet. Chang. 134, 118–128.

Mikami, Takehiko. 2008. “Climatic Variations in Japan Reconstructed from Historical Documents.” Weather 63 (7): 190–93. https://doi.org/10.1002/wea.281.

Millard, Andrew R. 2014. “Conventions for Reporting Radiocarbon Determinations.” Radiocarbon 56 (2): 555–59. https://doi.org/10.2458/56.17455.

Mishima, S. 1984. “Stock Assessment and Biological Aspects of Pacific Cod Gadus Macrocephalus in Japanese Waters,” January, 180–88. https://eurekamag.com/research/029/216/029216129.php.

Miyata, Yoshiki, Akiko Horiuchi, Megumi Kondo, Shin Onbe, Kunio Yoshida, Seiya Nagao, and Toyohiro Nishimoto. 2016. “Marine Reservoir Effects Deduced from 14C Dates on Pottery Residues, Bones, and Molluskan Shells from the Hamanaka 2 Archaeological Site, Rebun Island, Hokkaido, Japan.” Radiocarbon 58 (4): 755–70. https://doi.org/10.1017/RDC.2016.93.

Miyata, Yoshiki, Akiko Horiuchi, Paleo Labo, and A M S Dating. 2009. “Traces of Sea Mammals on Pottery from the Hamanaka 2 Archaeological Site , Rebun Island , Japan : Implications from Sterol Analysis , Stable Isotopes , and Radiocarbon Dating.” Res. Org. Geochem 25: 15–27.

MolluscaBase. 2022. “Spisula Sachalinensis (Schrenck, 1862).” Accessed through: World Register of Marine Species. https://www.marinespecies.org/aphia.php?p=taxdetails&id=505775.

Morales-Nin, Beatriz. 2000. “Review of the Growth Regulation Processes of Otolith Daily Increment Formation.” Fisheries Research 46 (1): 53–67. https://doi.org/https://doi.org/10.1016/S0165-7836(00)00133-8.

Moss, Madonna L. 2011. “Pacific Cod in Southeast Alaska.” The Archaeology of North Pacific Fisheries, 149–233.

Motokawa, Masaharu, and Hiroshi Kajihara. 2017. Species Diversity of Animals in Japan. Tokyo: Springer.

Müller, S., M. Schmidt, A. Kossler, C. Leipe, T. Irino, M. Yamamoto, H. Yonenobu, et al. 2016. “Palaeobotanical Records from Rebun Island and Their Potential for Improving the Chronological Control and Understanding Human–Environment Interactions in the Hokkaido Region, Japan.” Holocene 26 (10): 1646–60. https://doi.org/10.1177/0959683616641738.

Nagashima, K., Tada, R., Toyoda, S. 2013. “Westerly Jet — East Asian summer monsoon connection during the Holocene.” Geochem. Geophys. Geosyst. 14, 5041–5053.

Naito, Yuichi I., Yoshito Chikaraishi, Naohiko Ohkouchi, Hitoshi Mukai, Yasuyuki Shibata, Noah V. Honch, Yukio Dodo, et al. 2010a. “Dietary Reconstruction of the Okhotsk Culture of Hokkaido, Japan, Based on Nitrogen Composition of Amino Acids: Implications for Correction of 14C Marine Reservoir Effects on Human Bones.” Radiocarbon 52 (2): 671–81. https://doi.org/10.1017/S0033822200045690.

———. 2010b. “Dietary Reconstruction of the Okhotsk Culture of Hokkaido, Japan, Based on Nitrogen Composition of Amino Acids: Implications for Correction Of14C Marine Reservoir Effects on Human Bones.” Radiocarbon 52 (2): 671–81. https://doi.org/10.1017/S0033822200045690.

Nakazawa, Yuichi. 2011. “Dual Nature in the Creation of Disciplinary Archaeology in Japan.” Asian Perspectives 49 (2): 231–50.

Nier, Alfred O. 1947. “A Mass Spectrometer for Isotope and Gas Analysis.” Review of Scientific

Instruments 18 (398).

Nikitin, Yu. G, E M Sayenko, and K A Lutaenko. 2016. “Mollusks from the Archaeological Site Chernyatino-2 in Primorye.” The Bulletin of the Russian Far East Malacological Society 20 (2): 55–80.

Nikolaeva, A. S., and V. I. Schebakova. 1990. “Physical Map.” In Geograficheskii LAtlas SSSR, edited by A. S. Nikolaeva and V. I. Schebakova, 10–11. Moscow: GUGK.

Nishimoto, Toyohiro. 1984. “The Hunting and Fishing Activities of the Jomon and the Epi-Jomon Culture - An Analysis of the Faunal Remains.” Bulletin of the National Museum of Japanese History.

————. 1985. “The Transition of Hunting and Fishing Activities in Hokkaido. Bulletin of National Museum of Japanese History (in Japanese).” Bulletin of the National Museum of Japanese History 6: 53–74.

Njoku, E.G., and O.B. Brown. 1993. “Sea Surface Temperature.” In Atlas of Satellite Observations Related to Global Change, edited by Gurney, Foster, and Parkinson. Cambridge University Press.

Oba, T, M Kato, H Kitazato, I Koizumi, A Omura, T Sakai, and T Takayama. 1991. “Palaeoenvironmental Changes in the Japan Sea During the Last 85,000 Years.” Paleoceanography 6 (4): 499–518.

Ohnuki-Tierney, E. 1976. “Regional Variations in Ainu Culture.” American Ethnologist 3 (2): 297–329. https://doi.org/10.1525/ae.1976.3.2.02a00080.

Oikawa, A. 1995. “Kaizuka Database No Suryo-Teki Bunseki. (Quantitative Analysis of Shell-Mound Database).” Jinbun Kagaku to Computer (Humanities and Computer) 25 (7): 59–66.

Okada, Hiroaki. 1998. “Maritime Adaptations in Northern Japan.” Arctic Anthropology 35 (1): 335–39. http://muse.jhu.edu/content/crossref/journals/asian_perspectives/v045/45.1matsumura.pdf.

Okamoto, Yuka, Hajime Ishida, Ryosuke Kimura, Takehiro Sato, Nanae Tsuchiya, Sadayuki Murayama, Hitoshi Fukase, et al. 2016. “An Okhotsk Adult Female Human Skeleton (11th/12th Century Ad) with Possible Sapho Syndrome from Hamanaka 2 Site, Rebun Island, Northern Japan.” Anthropological Science 124 (2): 107–15. https://doi.org/10.1537/ase.160608.

Omoto, Keiichi, and Naruya Saitou. 1997. “Genetic Origins of the Japanese: A Partial Support for the Dual Structure Hypothesis.” American Journal of Physical Anthropology. https://doi.org/10.1002/(SICI)1096-8644(199704)102:4<437::AID-AJPA1>3.0.CO;2-P.

Ōnishi, Hideyuki. 2014. “The Formation of the Ainu Cultural Landscape: Landscape Shift in a Hunter-Gatherer Society in the Northern Part of the Japanese Archipelago.” Journal of World Prehistory 27 (3–4): 277–93. https://doi.org/10.1007/s10963-014-9080-2.

Pannella, G. 1971. “Fish Otoliths: Daily Growth Layers and Periodical Patterns.” Science 173: 1124–27.

Pearson, Richard. 1992. “The Nature of Japanese Archaeology.” Asian Perspectives 31 (2): 115–27.

————. 2007. “Debating Jomon Social Complexity.” Asian Perspectives 46 (2): 361–88.

Peel, M. C., B. L. Finlayson, and T. A. McMahon. 2007. “Updated World Map of the Köppen-Geiger Climate Classification.” Hydrology and Earth System Sciences 11 (5): 1633–44.

https://doi.org/10.5194/hess-11-1633-2007.

Petersen, Erik, and Christopher Meiklejohn. 2007. “Historical Context of the Term ‘Complexity’: In the South Scandinavian Mesolithic.” Acta Archaeologica 78 (2): 181–92.

Povinec, Pavel P., A. E. Litherland, and Karl F. von Reden. 2009. “Developments in Radiocarbon Technologies: From the Libby Counter to Compound-Specific Ams Analyses.” Radiocarbon 51 (1): 45–78. https://doi.org/10.1017/S0033822200033701.

Powell, Adam, Stephen Shennan, and Mark G Thomas. 2009. “Late Pleistocene Demography and the Appearance of Modern Human Behavior.” Science 324 (5932): 1298–1301. https://doi.org/10.1126/science.1170165.

Prendergast, Amy L. 2014. “Molluscs (Isotopes) – Analyses in Environmental Archaeology . In The Encyclopedia of Global Archaeology . Springer,” no. January. https://doi.org/10.1016/j.palaeo.2012.11.026.S.

Radtke, R. L. 1983. “Cod Fish Otoliths: Information Storage Structures.” In The Propagation of Cod Gadus Morhua L.: An International Symposium, Arendal, 14 - 17 June, edited by E Moksness, P. Solemdal Dahl, and D.S. Danielssen. Havforskningsinstituttet.

Radtke, R L, P Lenz, W Showers, and E Moksness. 1996. “Environmental Information Stored in Otoliths: Insights from Stable Isotopes.” Marine Biology 127 (1): 161–70. https://doi.org/10.1007/BF00993656.

Reimer, Paula J, William E N Austin, Edouard Bard, Alex Bayliss, Paul G Blackwell, Christopher Bronk Ramsey, Martin Butzin, et al. 2020. “The IntCal20 Northern Hemisphere Radiocarbon Age Calibration Curve (0–55 Cal KBP).” Radiocarbon 62 (4): 725–57. https://doi.org/DOI: 10.1017/RDC.2020.41.

Reimer, Ron W, and Paula J Reimer. 2017. “An Online Application for ΔR Calculation.” Radiocarbon 59 (5): 1623–27. https://doi.org/DOI: 10.1017/RDC.2016.117.

Ritchie, Kenneth, Arild Folkvord, and Anne Karin Hufthammer. 2013. “Oxygen Isotope Ratios in Cod Otoliths Used to Reveal Seasonality of Fishing at Late Mesolithic Sites in Denmark.” Archaeofauna 22: 95–104.

Sakaguchi, Takashi. 2007a. “Refuse Patterning and Behavioral Analysis in a Pinniped Hunting Camp in the Late Jomon Period: A Case Study in Layer V at the Hamanaka 2 Site, Rebun Island, Hokkaido, Japan.” Journal of Anthropological Archaeology 26 (1): 28–46. https://doi.org/10.1016/j.jaa.2006.07.001.

———. 2007b. “Site Formation Processes and Long-Term Changes in Land Use among Maritime Hunter-Gatherers: A Case Study at the Hamanaka-2 Site, Rebun Island, Hokkaido.” Arctic Anthropology 44 (2): 31–50. https://doi.org/10.1353/arc.2011.0031.

Sakaguchi, Y. 1976. “Characteristics of Ozegahara Deposits and Climatic Changes since Late Glacial in Central Japan.” Bull. Dept. Geology, Univ. Tokyo 15: 1–24.

———. 1983. “Warm and Cold Stages in the Past 7600 Years in Japan and Their Global Correlation - Especially on Climatic Impacts to the Global Sea Level Changes and the Ancient Japanese History.” Bulletin of the Department of Geography, University of Tokyo 15: 1–31.

Sakurai, Izumi, Masabumi Seto, and Shigeru Nakao. 1996. “Effects of Water Temperature, Salinity and Substrata on Burrowing Behaviors of the Three Bivalves, Pseudocardium Sachalinensis, Mactra Chinensis, and Ruditapes Philipinarum.” Nippon Suisan Gakkaishi 62 (6): 878–85.

Sasaki, Koichi. 1981. “Growth of the Sakhalin Surf Clam, Spisula Sachalinensis (SCHRENCK), in Sendai Bay.” Tohoku Journal of Agricultural Research 32 (4): 168–80.

———. 1989. “Characteristics of the Bottom Sediments Inhabited by the Surf Clam Spisula Sachalinensis in Sendai Bay.” Nippon Suisan Gakkaishi 55 (7): 1127–31.

Sasaki, Shigefumi, and Tomoki Ohta. 1999. “Seasonal Variation of Chemical Components in Surf Clam (Spisula Sachalinensis).” Food Sci.Technol.Res.

Sassaman, Kenneth E. 2004. “Complex Hunter-Gatherers in Evolution and History: A North American Perspective.” Journal of Archaeological Research 12 (3): 227–80. https://doi.org/10.1023/B:JARE.0000040231.67149.a8.

Sato, Takehiro, Tetsuya Amano, Hiroko Ono, Hajime Ishida, Haruto Kodera, Hirofumi Matsumura, Minoru Yoneda, and Ryuichi Masuda. 2007. “Origins and Genetic Features of the Okhotsk People, Revealed by Ancient Mitochondrial DNA Analysis.” Journal of Human Genetics 52 (7): 618–27. https://doi.org/10.1007/s10038-007-0164-z.

———. 2009. “Mitochondrial DNA Haplogrouping of the Okhotsk People Based on Analysis of Ancient DNA: An Intermediate of Gene Flow from the Continental Sakhalin People to the Ainu.” Anthropological Science 117 (3): 171–80. https://doi.org/10.1537/ase.081202.

Sato, Takehiro, Hisako Kazuta, Tetsuya Amano, Hiroko Ono, Hajime Ishida, Haruto Kodera, Hirofumi Matsumura, Minoru Yoneda, Yukio Dodo, and Ryuichi Masuda. 2010. “Polymorphisms and Allele Frequencies of the ABO Blood Group Gene among the Jomon, Epi-Jomon and Okhotsk People in Hokkaido, Northern Japan, Revealed by Ancient DNA Analysis.” Journal of Human Genetics 55 (10): 691–96. https://doi.org/10.1038/jhg.2010.90.

Sato, Yo-Ichiro, Shinsuke Yamanaka, and Mitsuko Takahashi. 2003. “Evidence for Jomon Plant Cultivation Based on DNA Analysis of Chestnut Remains.” In Hunter-Gatherers of the North Pacific Rim, edited by J. Habu, J. M. Savelle, S. Koyama, and H. Hongo. National Museum of Ethnology, Osaka.

Savin, A. B. 2008. “Seasonal Distribution and Migrations of Pacific Cod Gadus Macrocephalus (Gadidae) in Anadyr Bay and Adjacent Waters.” Journal of Ichthyology 48 (8): 610–21.

Savin, A. B., and P. V. Kalchugin. 2011. “Seasonal Distribution and Migrations of Pacific Cod Gadus Macrocephalus (Gadidae) in the Northwestern Part of the Sea of Japan and Adjacent Water Areas.” Journal of Ichthyology 51 (4): 291–305. https://doi.org/10.1134/S0032945211020093.

Schmidt, Mareike, Christian Leipe, Fabian Becker, Tomasz Goslar, Philipp Hoelzmann, Jens Mingram, Stefanie Müller, Rik Tjallingii, Mayke Wagner, and Pavel E. Tarasov. 2019. “A Multi-Proxy Palaeolimnological Record of the Last 16,600 Years from Coastal Lake Kushu in Northern Japan.” Palaeogeography, Palaeoclimatology, Palaeoecology 514: 613–26. https://doi.org/10.1016/j.palaeo.2018.11.010.

Schmidt, Mareike, Pavel E. Tarasov, Philipp Hoelzmann, Hanno Meyer, and Christian Leipe. 2016. “Diatoms from Lake Kushu: A Pilot Study to Test the Potential of a Late Quaternary Palaeoenvironmental Archive from Rebun Island (Hokkaido Region, Japan).” Journal of Asian Earth Sciences 122: 106–22. https://doi.org/10.1016/j.jseaes.2016.03.005.

Schöne, Bernd R. 2008. “The Curse of Physiology - Challenges and Opportunities in the Interpretation of Geochemical Data from Mollusk Shells.” Geo-Marine Letters 28 (5–6): 269–85. https://doi.org/10.1007/s00367-008-0114-6.

Schöne, Bernd R, Katharina Schmitt, and Michael Maus. 2017. “Effects of Sample Pretreatment and

External Contamination on Bivalve Shell and Carrara Marble Δ18O and Δ13C Signatures." Palaeogeography, Palaeoclimatology, Palaeoecology 484: 22–32. https://doi.org/https://doi.org/10.1016/j.palaeo.2016.10.026.

Schrenk, L.I. 1862. "Vorläufige Diagnosen Einiger Neuer Molluskenarten Aus Der Meerenge Der Tartarei Und Dem Nord-Japanischen Meere." Bulletin de l'Académie Impériale Des Sciences de St. Pétersbourg 4.

Seaton, Philip. 2017. "Japanese Empire in Hokkaido." Oxford Research Encyclopedia of Asian History. Oxford Unversity Press. https://doi.org/10.1093/acrefore/9780190277727.013.76.

Self, A.E., Klimaschewski, A., Solovieva, N., Jones, V.J., Andrén, E., Andreev, A.A., Hammarlund, D., Brooks, S.J. 2015. "The relative influences of climate and volcanic activity on Holocene lake development inferred from a mountain lake in central Kamchatka." Glob. Planet. Chang. 134, 67–81.

Seo, Hyodae, Young-Oh Kwon, and Jong-Jin Park. 2013. "On the Effect of the East/Japan Sea SST Variability on the North Pacific Atmospheric Circulation in a Regional Climate Model." Journal of Geophysical Research 119 (2): 418–44. https://doi.org/10.1038/175238c0.

Shackleton, N J. 1973. "Oxygen Isotope Analysis as a Means of Determining Season of Occupation of Prehistoric Midden Sites." Archaeometry 15 (1): 133–41. https://doi.org/10.1111/j.1475-4754.1973.tb00082.x.

Shinya, Shoda, and Junho Son. 2017. "일본의 발굴조사와 보고서 작성 , 배포 , 활용 *." 야외고고학 30: 143–64.

Smale, Joran. 2014. "End of Okhotsk? A Peer Polity Interaction Approach to the Interaction, Exchange and Decline of a Northeast-Asian Maritime Culture on Hokkaido, Japan." Leiden University.

Smalley, P C, C N Maile, M L Coleman, and J E Rouse. 1992. "LASSIE (Laser Ablation Sampler for Stable Isotope Extraction) Applied to Carbonate Minerals." Chemical Geology: Isotope Geoscience Section 101 (1): 43–52. https://doi.org/https://doi.org/10.1016/0009-2541(92)90201-F.

Solovieva, N., Klimaschewski, A., Self, A.E., Jones, V.J., Andrén, E., Andreev, A.A., Hammarlund, D., Lepskaya, E.V., Nazarova, L. 2015. "Holocene environmental history of a small coastal lake from north-eastern Kamchatka Peninsula." Glob. Planet. Chang. 134, 55–66.

Spies, Robert B., and Thomas Weingartner. 2007. "Long-Term Change." In Long-Term Ecological Change in the Northern Gulf of Alaska, edited by Robert B. Spies, Second Edi. Elsevier Science. https://doi.org/10.1533/9781845692087.3.460.

Spötl, Christoph, and David Mattey. 2006. "Stable Isotope Microsampling of Speleothems for Palaeoenvironmental Studies: A Comparison of Microdrill, Micromill and Laser Ablation Techniques." Chemical Geology 235 (1–2): 48–58. https://doi.org/10.1016/j.chemgeo.2006.06.003.

Steinke, Stephan, Cornelia Glatz, Jeroen Groeneveld, Qiang Li, and Zhimin Jian. 2011. "Past Dynamics of the East Asian Monsoon: No Inverse Behaviour between the Summer and Winter Monsoon during the Holocene." Global and Planetary Change 78 (August). https://doi.org/10.1016/j.gloplacha.2011.06.006.

Stuiver, M, G W Pearson, and Tom Braziunas. 1986. "Radiocarbon Age Calibration of Marine Samples BAck to 9000 Cal Yr BP." Radiocarbon 28 (2B): 980–1021.

Stuiver, M, and Henry A. Polach. 1977. “Reporting of 14C Data.” Radiocarbon 19 (3): 355–63.

Stuiver, M, Paula J Reimer, and Ron W Reimer. 2022. “CALIB 8.2 [WWW Program].” http://calib.org.

Suzuki, Michio, and Hiromichi Nagasawa. 2013. “Mollusk Shell Structures and Their Formation Mechanism.” Canadian Journal of Zoology 91 (6): 349–66. https://doi.org/10.1139/cjz-2012-0333.

Tajima, Atsushi, Masanori Hayami, Katsushi Tokunaga, Takeo Juji, Masafumi Matsuo, Sangkot Marzuki, Keiichi Omoto, and Satoshi Horai. 2004. “Genetic Origins of the Ainu Inferred from Combined DNA Analyses of Maternal and Paternal Lineages.” Journal of Human Genetics 49 (4): 187–93. https://doi.org/10.1007/s10038-004-0131-x.

Takahara, Hikaru, Shinya Sugita, Sandy P. Harrison, Norio Miyoshi, Yoshimune Morita, and Takashi Uchiyama. 2000. “Pollen-Based Reconstructions of Japanese Biomes at 0, 6000 and 18,000 14Cyr BP.” Journal of Biogeography 27 (3): 665–83. https://doi.org/10.1046/j.1365-2699.2000.00432.x.

Takano, Yohei, Yoshihiro Tachibana, and Katsushi Iwamoto. 2008. “Influences of Large-Scale Atmospheric Circulation and Local Sea Surface Temperature on Convective Activity over the Sea of Japan in December.” Scientific Online Letters on the Atmosphere 4 (1): 113–16. https://doi.org/10.2151/sola.2008-029.

Takarabe, Kae. 2017. “The Smithsonian Meteorological Project and Hokkaido , Japan Kae Takarabe Introduction The History of Meteorology in Japan , Especially after the Meiji Restoration , Has Tended to Be Described in Terms of Knowledge Diffusion from Central Tokyo Outwards To ” 3775 (3775): 1–23.

Takeshi, Ishikawa. 2014. “Social Complexity in the Late Jomon Period: The Constitution of the Shimo’ota Shell Mound Cemetery of the Boso Peninsula , Eastern Kanto, Japan.” Japanese Journal of Archaeology 2 (May): 3–33.

Tatewaki, Misao. 1973. “The Geobotanical Relationship between Beringia and Northern Japan, with Special Reference to the Arctic-Alpine Flora of the Latter.” Journal of the Faculty of Agriculture, Hokkaido University 57 (3): 340–48. http://eprints2008.lib.hokudai.ac.jp/dspace/handle/2115/12884.

Tatewaki, Misao, and Mikio Tohyama. 1975. “Atlas of the Distribution of Alpine Plants in Hokkaido.” Journal of the Faculty of Agriculture 58: 57–100.

Thode, H G, R L Graham, and J A Ziegler. 1945. “A Mass Spectrometer and the Measurement of Isotope Exchange Factors.” Canadian Journal of Research 23b (1): 40–47. https://doi.org/10.1139/cjr45b-006.

Thomson, J.J. 1912. “XIX. Further Experiments on Positive Rays.” The London, Edinburgh, and Dublin Philosophical Magazine and Journal of Science 24 (140): 209–53. https://doi.org/10.1080/14786440808637325.

Thorrold, Simon R, Steven E Campana, Cynthia M Jones, and Peter K Swart. 1997. “Factors Determining Δ13C and Δ18O Fractionation in Aragonitic Otoliths of Marine Fish.” Geochimica et Cosmochimica Acta 61 (14): 2909–19. https://doi.org/https://doi.org/10.1016/S0016-7037(97)00141-5.

Toba, Yoshiaki, Kazumi Tomizawa, Yoshikazu Kurasawa, and Kimio Hanawa. 1982. “Seasonal and Year-to-Year Variability of the Tsushima-Tsugaru Warm Current System with Its Possible Cause.” Société Franco-Japonaise d’océanographie, Tokyo 20: 41–51.

Toland, Harry, Bill Perkins, Nick Pearce, Fergus Keenan, and Melanie J. Leng. 2000. “Study of Sclerochronology by Laser Ablation ICP-MS.” Journal of Analytical Atomic Spectrometry 15 (9): 1143–48. https://doi.org/10.1039/b002014l.

Tomii, Makoto. 2014. “Periodization in Japanese Prehistoric Archaeology.” Encyclopedia of Global Archaeology. Springer.

Tsutaya, Takumi, Tomonari Takahashi, Takayuki Omori, Kohei Yamazaki, Takao Sato, Minoru Yoneda, Rick J Schulting, Hirofumi Kato, and Andrzej W Weber. 2021. “Reconstruction of Diachronic Changes in Human Fishing Activity and Marine Ecosystems from Carbon and Nitrogen Stable Isotope Ratios of Archaeological Fish Remains.” Quaternary International. https://doi.org/https://doi.org/10.1016/j.quaint.2021.12.005.

Twaddle, Robin W., Sean Ulm, Jane Hinton, Christopher M. Wurster, and Michael I. Bird. 2016. “Sclerochronological Analysis of Archaeological Mollusc Assemblages: Methods, Applications and Future Prospects.” Archaeological and Anthropological Sciences 8 (2): 359–79. https://doi.org/10.1007/s12520-015-0228-5.

Urey, H.C. 1947. “The Thermodynamic Properties of Isotopic Substances.” Journal of the Chemical Society (Resumed), no. 582: 562. https://doi.org/10.1039/jr9470000562.

Urey, H.C., S. Epstein, H.A. Lowenstam, and C. Emiliani. 1954. “Final Report, Task Order XXVIII, Contract N6or1-02028, NR 081-096.”

Urey, H.C., H.A. Lowenstam, S. Epstein, and C.R. McKinney. 1951. “Measurement of Paleotemperatures and Temperatures and the Southeastern United States.” Bulletin of the Geological Society of America 62 (April): 399–416.

Uzawa, Kazuhiro. 1992. “Fish Otoliths as Indicator of Cod Fishing Seasonality in a Jomon Shell Midden (Usu-LO Site).” Journal of the Anthropological Society of Nippon 100 (3): 331–39. https://doi.org/10.1537/ase1911.100.331.

Valley, J, and Noriko Kita. 2009. “In Situ Oxygen Isotope Geochemistry by Ion Microprobe.” Kendall & McDonnell Criss Ambrose & Katzenberg 41 (April): 19–63.

Vieira, Ana Rita, Sandra Dores, Manuela Azevedo, and Susanne E Tanner. 2020. “Otolith Increment Width-Based Chronologies Disclose Temperature and Density-Dependent Effects on Demersal Fish Growth.” ICES Journal of Marine Science 77 (2): 633–44. https://doi.org/10.1093/icesjms/fsz243.

Vladimir, A. Rakov, and S.V. Gorbunov. 2004. “The Development of Malacofauna and Reconstruction Paleoenvironmental Changes in Coastal Areas of Sakhalin during the Holocene.” In Proceedings of the Third Workshop on the Okhotsk Sea and Adjacent Areas, edited by Skip McKinnell. North Pacific Marine Science Organization (PICES).

Vonhof, Hubert B, Stefan de Graaf, Howard J Spero, Ralf Schiebel, Suzan J A Verdegaal, Brett Metcalfe, and Gerald H Haug. 2020. “High-Precision Stable Isotope Analysis of <5 Mg CaCO3 Samples by Continuous-Flow Mass Spectrometry.” Rapid Communications in Mass Spectrometry 34 (19): e8878. https://doi.org/https://doi.org/10.1002/rcm.8878.

Wanamaker, Alan D, and David P Gillikin. 2019. “Strontium, Magnesium, and Barium Incorporation in Aragonitic Shells of Juvenile Arctica Islandica: Insights from Temperature Controlled Experiments.” Chemical Geology 526: 117–29. https://doi.org/https://doi.org/10.1016/j.chemgeo.2018.02.012.

Weber, Andrzej W., Peter Jordan, and Hirofumi Kato. 2013. “Environmental Change and Cultural Dynamics of Holocene Hunter-Gatherers in Northeast Asia: Comparative Analyses and Research

Potentials in Cis-Baikal (Siberia, Russia) and Hokkaido (Japan).” Quaternary International 290–291: 3–20. https://doi.org/10.1016/j.quaint.2012.07.021.

West, Catherine F., Stephen Wischniowski, and Christopher Johnston. 2012. “Pacific Cod (Gadus Macrocephalus) as a Paleothermometer: Otolith Oxygen Isotope Reconstruction.” Journal of Archaeological Science 39 (10): 3277–83. https://doi.org/10.1016/j.jas.2012.05.009.

Wick, Gary A. 2002. “Infrared and Microwave Remote Sensing of Sea Surface Temperature.” Seminar at the University of Colorado at Boulder “Remote Sensing Seminar” Graduate Course.

Williams, Peter. 1985. “Secondary Ion Mass Spectrometry.” Analytical Chemistry 15: 517–48. https://doi.org/10.1021/ac00292a600.

Winter, N J de, J Vellekoop, R Vorsselmans, A Golreihan, J Soete, S V Petersen, K W Meyer, S Casadio, R P Speijer, and P Claeys. 2018. “An Assessment of Latest Cretaceous \textit{Pycnodonte Vesicularis} (Lamarck, 1806) Shells as Records for Palaeoseasonality: A Multi-Proxy Investigation.” Climate of the Past 14 (6): 725–49. https://doi.org/10.5194/cp-14-725-2018.

Wood, R Seth, Bryan C Chakoumakos, Allison M Fortner, Kat Gillies-Rector, Matthias D Frontzek, Ilia N Ivanov, Linda C Kah, Brian Kennedy, and Brenda M Pracheil. 2022. “Quantifying Fish Otolith Mineralogy for Trace-Element Chemistry Studies.” Scientific Reports 12 (1): 2727. https://doi.org/10.1038/s41598-022-06721-7.

Yamaki, Kazushige. 2015. “Network Governance of Endangered Species Conservation: A Case Study of Rebun Lady’s-Slipper.” Journal for Nature Conservation 24: 83–92. https://doi.org/https://doi.org/10.1016/j.jnc.2014.10.004.

Yamamoto, K. 1947. Sapporo Nōrin-Gakkin-Hō. Sapporo Nōrin-Gakkin-Hō (Journal of the Sapporo Society of Agriculture and Forestry). Vol. 37.

Yamamura, Orio, Kazutoshi Watanabe, and Kenji Shimazaki. 1993. “Feeding Habits of Pacific Cod, Gadus Macrocephalus, off Eastern Hokkaido, North Japan.” Proc. NIPR Symp. Polar Biol 6: 44–54.

Yamaura, Kiyoshi. 1998. “The Sea Mammal Hunting Cultures of the Okhotsk Sea with Special Reference to Hokkaido Prehistory.” Arctic Anthropology 35 (1): 321–34.

Yang, Qing, Xiaoping Xia, Wanfeng Zhang, Yanqiang Zhang, Boqin Xiong, Yigang Xu, Qiang Wang, and Gangjian Wei. 2018. “An Evaluation of Precision and Accuracy of SIMS Oxygen Isotope Analysis.” Solid Earth Sciences 3 (3): 81–86. https://doi.org/https://doi.org/10.1016/j.sesci.2018.05.001.

Zaiki, Masumi, MJ Grossman, and T Mikami. 2012. “Document-Based Reconstruction of Past Climate in Japan.” PAGES News 20 (2): 82–83. https://doi.org/10.22498/pages.20.2.82.

Zhang, Haiwei, Yanjun Cai, Liangcheng Tan, Shijiang Qin, and Zhisheng An. 2014. “Stable Isotope Composition Alteration Produced by the Aragonite-to-Calcite Transformation in Speleothems and Implications for Paleoclimate Reconstructions.” Sedimentary Geology 309: 1–14. https://doi.org/10.1016/j.sedgeo.2014.05.007.

Appendix 1: Successful external grant applications

Application for NEIFSC Isotope Geoscience Support, October 2019, begins on page 157.

Application for NEIFSC Radiocarbon Support, March 2020, begins on page 160.

Introduction: This project applies high resolution $\delta^{18}O$ sampling of aragonitic marine carbonates to obtain information about palaeoceanographic conditions and season of capture from two taxa found in the stratified coastal archaeological site of Hamanaka II, Rebun Island in northwest Hokkaido, Japan. Remains of the large surf clam, *Spisula sachalinensisis,* and the Pacific cod, *Gadus macrocephalus,* in the site are considered evidence of human subsistence, and remain popular in modern Japanese cuisine. These taxa occupy distinct niches in the marine environment, the former in near-shore waters and the latter in deeper waters, in a region situated at the boundary of two prevailing currents in the Sea of Japan. The site, excavated in the 1990s by a team from the National Museum of Japanese History, and since 2011 as part of Hokkaido University's international field school, shows occupation from the Epi-Jomon (ca. 2700-1500 cal BP), Okhotsk (ca. 1500-500 cal BP) and Ainu (ca. 500-80 cal BP). It provides a dense record of late Holocene coastal hunter-gatherers, distinct from the development of Japanese agriculture and feudalism in the south. The longevity of hunter-gatherer lifeways in Hokkaido makes possible the study of behavioural adaptations and flexibility, especially in the context of a changing environment and ocean conditions. Oxygen isotope ($\delta^{18}O$) analysis of the two taxa to assess seasonal climate and resource scheduling allows human behaviour to be directly linked to palaeoclimatic reconstructions via estimation of past sea surface temperature (SST). Dual analysis of bivalves and otoliths provides a means to compare results for the two taxa, and a more holistic view of oceanic conditions that in turn influenced the island's climate and environment.

Background: The use of marine carbonate $\delta^{18}O$ as a record of SST is well attested in both modern and archaeological contexts, and examples can be seen using both the species targeted in the proposed project (e.g. Kastelle et al., 2017; Khim, Woo, & Je, 2000; West, Wischniowski, & Johnston, 2012; Yavnov & Ignat'ev, 1979). Both *S. sachalinensis* shells and *G. macrocephalus* otoliths are composed of aragonitic $CaCO_3$. In marine environments, aragonite precipitates in isotopic equilibrium with surrounding water, and $\delta^{18}O$ is inversely correlated to water temperature using the empirically determined equation of Grossman and Ku (1986). The equation requires an estimation of past $\delta^{18}O_{seawater}$, which is influenced by a combination of salinity, precipitation and sea level change (Ravelo & Hillaire-Marcel, 2007). Estimations in this project will be based on global and regional foraminifera records (Oba et al., 1991; Waelbroeck et al., 2002), but in any case, relatively $\delta^{18}O_{seawater}$ is unlikely to differ significantly from modern values accessible in the Schmidt et al. (1999) database due to stable late Holocene sea levels in the region (Müller et al., 2016).

The climate of northern Japan is strongly influenced by a number of atmospheric and oceanographic factors. Hokkaido's winters are influenced by the East Asian Winter Monsoon air currents, bringing cold air from the north/northwest (Abe et al., 2016). The most important oceanographic influences on Rebun are the Tsushima and Oyashio currents (Figure 1). Tsushima is a warm current, which flows from the East China Sea into the Sea of Japan around the west coast of Japan, while Oyashio is a cold-water current that flows down the northeast coast of Japan. In combination, these create a gradient in sea temperature (and in turn terrestrial temperature) from the warmer west to the cooler east (Abe et al., 2016). The Tsushima current prevents the formation of sea ice around western Hokkaido (Nikolaeva & Schebakova, 1990), but also encourages evaporation during winter monsoon winds resulting in high snowfall in the region (Abe et al., 2016; Kuroyanagi et al., 2006; Müller et al., 2016).

Broadly, the Hokkaido climate can be classified as cool, with a warm summer and no dry season (Peel, Finlayson, & McMahon, 2007). On Rebun Island specifically, temperature and precipitation both show significant seasonality, with an average interannual temperature range of c. 26°C (Schmidt et al., 2016). As atmospheric temperature and SST are strongly linked (e.g. Cayan, 1980), marine carbonates from Rebun should show strong seasonal patterning. Therefore, oxygen isotope analysis of marine carbonates can be used not only to provide intra-annual records of past SST, but also to show patterns of human resource use through the interpretation of growth-edge $\delta^{18}O$ as season of collection.

According to Oba et al. (1991), the Tsushima current has remained broadly at its modern volume since 8000 cal BP, but during the late Holocene several warm 'pulses' have been noted from diatom and pollen analysis from marine and lake cores (Igarashi, 2013; Koizumi, 1987). These warmer periods have been inferred using these indirect proxies, but evidence from carbonate $\delta^{18}O$ would indicate their effect on local SSTs and seasonal climatic variation. The subannual SST record resulting from this study will also be much higher resolution than can be produced from marine cores, which can typically at best be interpreted down to multi-decadal scale. Furthermore, wider climatic trends such as the Little Ice Age and Medieval Warm

Period have been identified in Japan but are rarely discussed with reference to Hokkaido. The addition of local subannual reconstructions will help assess the significance of these climatic patterns on Hokkaido and its prehistoric residents.

The archaeological context of Rebun Island is well-suited to the investigation of seasonal resource use. Unlike the rest of Japan, northern Hokkaido remains occupied by coastally adapted hunter-gatherer groups well beyond the Jomon up until the Meiji Restoration (1868). Because of this especially long hunter-gatherer history, the region provides a good case study to show development and resilience in foraging lifeways. As part of the Baikal-Hokkaido Archaeology Project (2011-2018) and IRIS (International Research Networks for Indigenous Studies and Cultural Diversity) Core-to-Core project, there is active archaeological investigation at Hamanaka II, including studies of the faunal collections by colleagues at Keio University, Tokyo. Pollen cores from nearby Lake Kushu (Figure 1) provide an additional local palaeoenvironmental record (e.g. Harris, 2014; Müller et al., 2016).

Materials & Methods: The samples in hand come from excavations at Hamanaka II (1994-1997, 2011-2019). Chronological attributions at the site have been made using ceramic typology and radiocarbon dating. The main radiocarbon sequence is as yet unpublished, but work has been done to assess the local marine reservoir effect (Miyata et al., 2016). *S. sachalinensis* valves are available across three major periods of archaeological occupation at Hamanaka II: Epi-Jomon (2700-1500 cal BP), Okhotsk (1500-1000 cal BP) and Ainu (1000-80 cal BP) (Figure 2), while *G. macrocephalus* otoliths are available from the Okhotsk levels (where there is a dense accumulation of marine faunal remains). The Okhotsk and Ainu periods coincide with the Medieval Warm Period and Little Ice Age, respectively, meaning that Hamanaka II provides appropriate material for the investigation of these climatic anomalies.

The sampling strategy is illustrated in Table 1. As *S. sachalinensis* shells are present in all archaeological periods, the species will be used to form the primary SST record. Sectioning of *S. sachalinensis* shells has confirmed the presence of subannual growth increments suited to SST reconstruction (Figure 3), as has the previous work of Khim et al. (2000). A small number of shells will be selected per layer (3), but with a large number of samples per shell (c. 60). The shells are long lived (30-40 years), but this sampling will target a c. 3 year growth period in the earlier and faster period of growth in order to obtain longer multiannual sequences. Therefore the total number of years reconstructed per layer will be 9, sufficient to draw conclusions on average seasonal climatic conditions. By contrast, a larger number of *G. macrocephalus* otoliths will be used to reconstruct Okhotsk seasonal fishing practices, analysing only the last period of growth. Suitable otolith material is not available for comparison to the Jomon and Ainu. Based on the literature (e.g. West et al. 2012), a year of growth for *G. macrocephalus* ranges from c. 0.8-1.2mm aragonitic growth depending on specimen age. Pilot studies will help determine the number of samples needed, but using 100µm micromilling spots we estimate c. 8-12 samples from the final year of growth.

Methodology will follow previous modern and archaeological studies of the same species which have shown good results from $\delta^{18}O$ analysis (Kastelle et al., 2017; Khim et al., 2000; West et al., 2012). Valves and otoliths will be half-sectioned, and high-resolution sampling will be done across the axis of maximum growth using a micromill drilling system. As per Loftus (2015), attenuated reflectance Fourier transform infrared spectroscopy (FTIR-ATR) will be used to check for the possibility of recrystallisation of aragonite into calcite. Due to the good preservational environment of the site, and the relatively recent age of specimens, it is not anticipated that recrystallisation will be a problem.

References: **Abe, C.**, *et al.* 2016. Holocene, 26(10), 1627–1645. **Batten, B.** Occ. Papers in Japanese Studies, No. 2009-01. **Cayan, D. R**. 1980. Monthly Weather Rev., 108, 1293-1301. **Grossman, E. L., & Ku, T. L.** 1986. Chem. Geol.: Isotope Geosci. Section, 59, 59–74. **Harris, S.** 2014. Cambridge Archaeological Journal, 24, 37–56. **Igarashi, Y.** 2013. Quat. Int., 290–291, 139–150. **Kastelle, C. R.,** *et al.* 2017. Fisheries Research, 185, 43–53. **Khim, B. K.,** *et al.* 2000. Continental Shelf Research, 20(8), 843–861. **Koizumi, I.** 1987. 第四紀研 (The Quaternary Research), 26(1), 13–25. **Kuroyanagi, A.,** *et al.* 2006. Global & Planetary Change, 53(1–2), 92–107. **Loftus, E.,** *et al.* 2015. J. Quat. Sci., 30(8), 731–735. **Müller, S.,** *et al.* 2016. Holocene, 26(10), 1646–1660. **Miyata, Y.,** et al. 2016. Radiocarbon, 58(4), 755-770. **Nikolaeva, A. S., & Schebakova, V. I.** 1990. In A. S. Nikolaeva & V. I. Schebakova (Eds.), Geograficheskii Atlas SSSR, 10–11. Moscow: GUGK. **Oba, T.,** *et al.* 1991. Paleoceanography, 6(4), 499–518. **Peel, M. C.,** *et al.* 2007. Hydrology & Earth System Sciences, 11(5), 1633–1644. **Ravelo, A. C., & Hillaire-Marcel, C.** 2007. Developments in Marine Geol., 1(07), 735–764. **Schmidt, G.A**., *et al.* 1999. https://data.giss.nasa.gov/o18data/. **Schmidt, M.,** *et al.* 2016. J. Asian Earth Sci., 122, 106–122. **Waelbroeck, C.,** *et al.* 2002. Quat. Sci. Reviews, 21, 295–305. **West, C. F.,** *et al.* 2012. J. Archaeol. Sci., 39(10), 3277–3283. **Yavnov, S. V., & Ignat'ev, A. V.** 1979. Soviet J. Marine Biol., 5, 409–414.

	Ainu (layer II)		Okhotsk (Layer III)		Epi-Jomon (Layer VIII)		
	Individuals	*Samples*	*Individuals*	*Samples*	*Individuals*	*Samples*	**Total**
S. sachalinensis	3	180	3	180	3	180	540
G. macrocephalus	-	-	10	100	-	-	100
							640

Table 1: Sampling strategy for material up to 2018. Layer references refer to Figure 2.

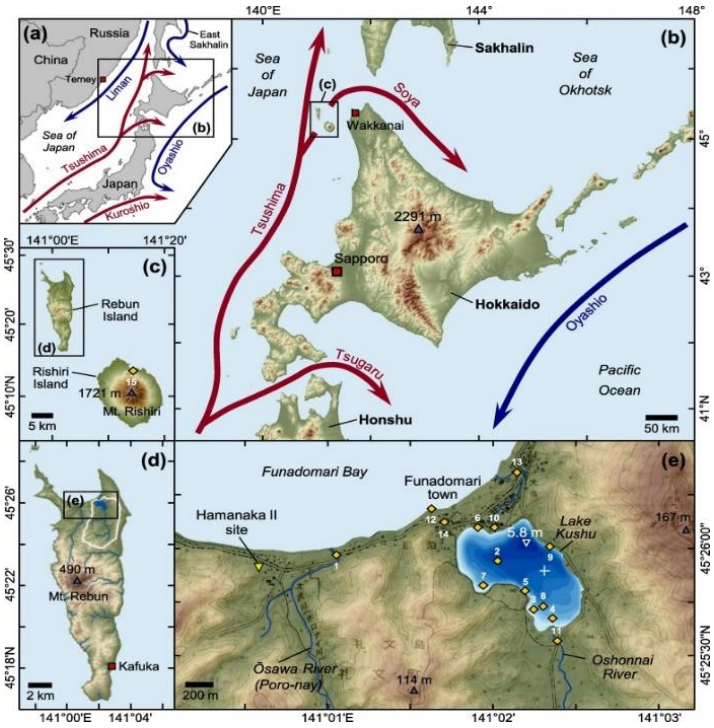


Figure 1: Map of Hokkaido showing the location of Hamanaka II, lake Kushu, and the major oceanographic currents influencing the region Image reproduced from Muller et al. 2016.

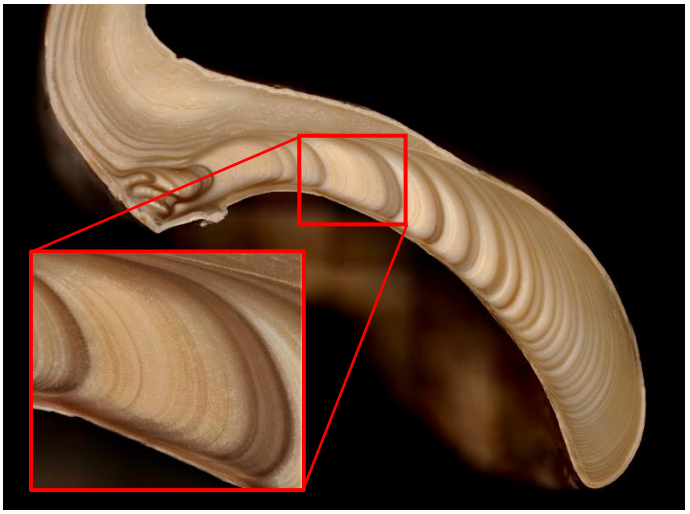


Figure 3: Section of S. sachalinensis umbo showing annual (darker bands) and subannual (in enlarged box) growth increments.

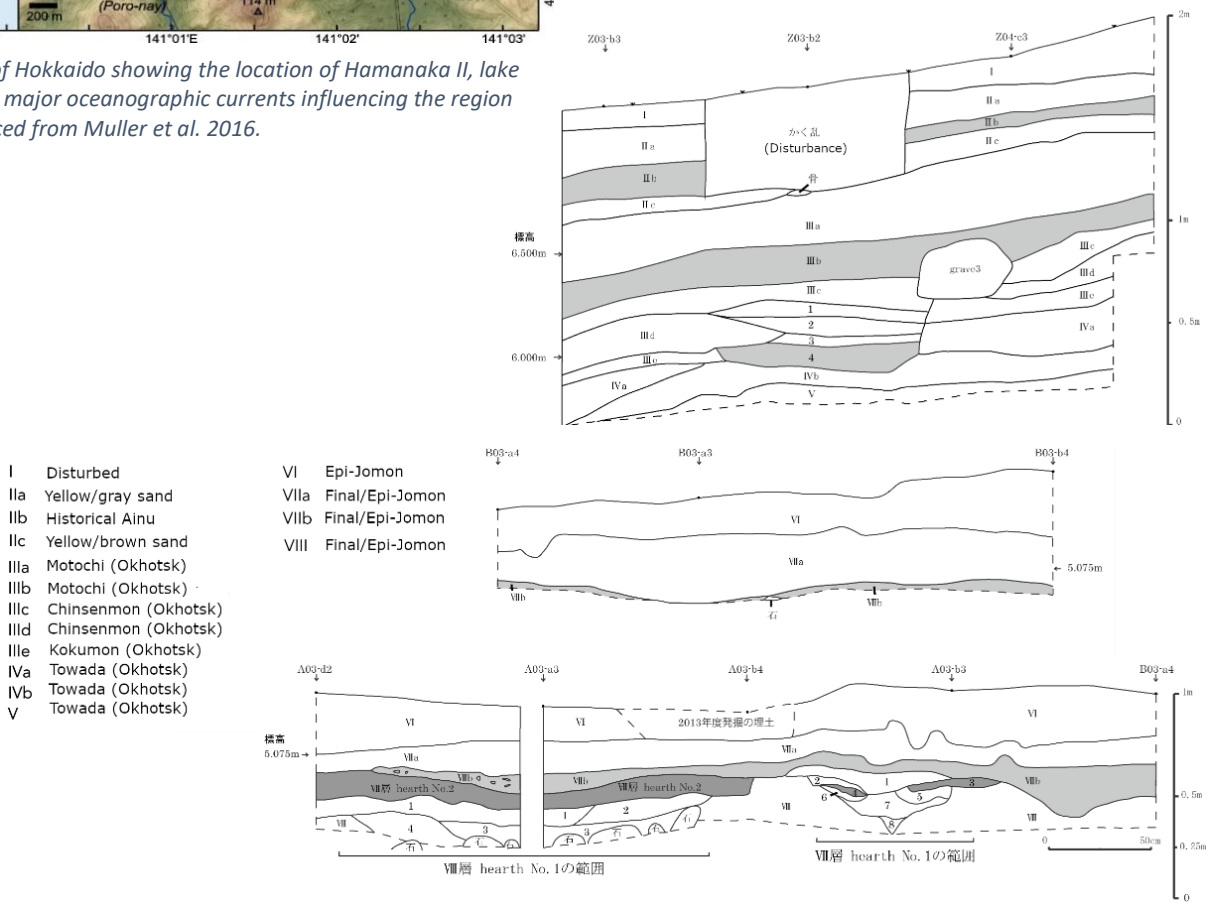


Figure 2: Stratigraphic profile from Hamanaka II (W wall). Samples from this proposal come from layers II, III and VIII.

14C dating of shells and otoliths from prehistoric N Japan

(Schulting et al.)

Introduction

We request funding for 22 AMS radiocarbon dates in support of a high-resolution stable oxygen isotope ($\delta^{18}O$) project to detect oceanographic shifts in the Sea of Japan during late prehistory that exert, in turn, influences on local climate. Using marine shells and otoliths, we aim to better understand oceanographic and climatic conditions at the coastal Japanese site of Hamanaka II, Rebun Island (Figure 1). Hamanaka II provides a long record of late Holocene hunter-gatherers from the Late Jomon to historical Ainu periods (~4000-80 cal BP). The site's faunal assemblage includes shells from the surf clam, *Spisula sachalinensis*, and otoliths from the Pacific cod, *Gadus macrocephalus* (Figure 2). *S. sachalinensis* was collected by coastal foragers/fishers from the near-shore subtidal, while *G. macrocephalus* was fished from deeper waters. We employ high-resolution subannual $\delta^{18}O$ analyses of these two taxa to estimate past sea surface temperatures (SST) in order to detect local oceanographic and climatic shifts. The site's stratigraphy, however, has only general chronology based on cultural periods, each apparently spanning multiple centuries. This is at odds with the three- to four-year resolution for $\delta^{18}O$, significantly hindering interpretation of oceanographic and climate shifts. We propose to directly date the specimens sampled for $\delta^{18}O$. These new dates will strengthen our temporal framework, and will also allow us to test how paired dates from the same incrementally-grown marine carbonates can inform Bayesian modelling to improve radiocarbon chronology.

Aims

The project aims to:

- provide a chronological framework for $\delta^{18}O$-based SST estimations, by dating molluscs and otoliths which have been subjected to sequential $\delta^{18}O$ analysis
- obtain a series of dates pertaining to the Final-/Epi-Jomon, Okhotsk and protohistoric Ainu deposits at Hamanaka II, in order to produce a combined Bayesian age model comprising all new and existing dates for the site
- conduct a pilot study on the utility of paired dates, combining sclerochronology, radiocarbon dating and Bayesian statistical modelling to obtain improved chronologies for individual shells/otoliths

Background

<u>Site location, climate and oceanography</u>

Hamanaka II is located on the northern shores of Rebun Island, northwest Hokkaido, and has a maritime climate strongly influenced by atmospheric and oceanographic variability. Hokkaido's climate is cool, with warm summers and no dry season. On Rebun, temperature and precipitation both show significant seasonality, with an average interannual temperature range of ~26°C. Winters are influenced by East Asian Winter Monsoon winds, bringing cold air from the north/northwest (Abe et al., 2016). The most important oceanographic influences are the Soya and Oyashio currents (Figure 1). The warm-water Soya current branches from the Tsushima current and flows around Hokkaido's north coast, primarily influencing shallow waters (Matsuyama et al., 2006). The cold-water Oyashio current flows down Japan's northeast coast. Combined, they create a temperature gradient in northern Japan from the warmer west to cooler east (Abe et al., 2016).

Seasonality in ocean temperature is primarily influenced by waxing and waning ocean currents. For the Tsushima and Soya currents, minimum transport volume occurs in the winter (Ebuchi et al., 2006; Toba et al., 1982) and maximum in the summer, perhaps due to additional input

from the southern warm Kuroshio current (Isobe, 1999). Seasonal currents and SST are strongly interconnected with atmospheric climate. Atmospheric conditions are a primary driver of SST (Imada et al., 2017), while higher (lower) SSTs in the Sea of Japan increase (decrease) windspeed and evaporation, driving regional precipitation especially during the winter monsoon season (Abe et al., 2016; Hirose and Fukudome, 2006; Seo et al., 2013; Takano et al., 2008). In other regions wide-scale climatic events such as the Little Ice Age (LIA) or Medieval Warm Period (MWP) have been observed in SST proxies (e.g. Corrège et al., 2001; Yan et al., 2015), including correlation between cooler climate and increased seasonal SST amplitude (Yan et al., 2015).

The Tsushima current reached modern volume by ~8,000 cal BP, notwithstanding several late Holocene warm 'pulses' identified from marine/lake cores (Igarashi, 2013; Koizumi, 1987; Oba et al., 1991). Research from the Sea of Okhotsk shows that relevant 'pulses' occuring at 2800-2400 and 1700-400 cal BP (Figure 3; Kawahata et al., 2003). Evidence from archaeological carbonate $\delta^{18}O$ will produce a higher-resolution proxy than marine/lake cores (typically only interpretable to multi-decadal scales) and will more directly indicate the effect of warm pulses on local SST and seasonal climate. Furthermore, wider climatic trends such as the LIA (~450-100 cal BP) and MWP (~1250-650 cal BP) have been identified in Japan (Batten, 2008) but are rarely discussed with reference to Hokkaido. The MWP is likely to be reflected in Ainu and Okhotsk samples in this study (Figure 3), but more precise dating is required to confirm this. Local reconstructions will help assess the significance of these climatic patterns on prehistoric Hokkaido.

Archaeology

Unlike central/southern Japan, Hokkaido remained occupied by coastally-adapted hunter-gatherers into the late 19th century. Consequently, the region provides a good case study for hunter-gatherer development and resilience. However, this unique development, combined with Hokkaido's colonial history within Japan, means that the island's recent hunter-gatherer past is often overlooked. Hamanaka II has been excavated by the National Museum of Japanese History (1994-1997), the Baikal-Hokkaido Archaeology Project (2011-2017) and Hokkaido University (2018-present). It has produced occupation evidence from the Final-/Epi-Jomon (~3000-1500 cal BP), Okhotsk (~1500-1000 cal BP) and historical Ainu (~1000-80 cal BP) periods.

Sediment cores from nearby Lake Kushu (Figure 1) provide a local palaeoenvironmental record covering the study period (e.g. Schmidt et al., 2019). The palynological record is especially useful, as it can be interpreted both in terms of terrestrial climate and human-environment interaction. For the Okhotsk period, Leipe et al. (2018) record changes corresponding to deforestation, indicating particularly intensive and possibly year-round settlement at Hamanaka II, compared with earlier, seasonal exploitation. However, precise dating of such sediment cores difficult, as dates from bulk soil samples do not equate to direct dates of the pollen record (Brown et al., 1989). A directly-dated seasonal climate record across this event will help gauge the potential role of climate change in both its onset and end.

At Hamanaka II, ceramic typology provides a relative chronological sequence, giving a cultural attribution for each stratigraphic layer (Figure 3). However, due to the duration of these time-units and the potentially rapid accumulation of midden material, the relative chronology of our samples within each layer is unknown. The typological chronology is supported by a series of existing radiocarbon dates, provided in Table 1, but are not available for each stratigraphic unit. The most relevant dating projects to the current study focus on Okhotsk and Ainu charred plant macrofossils (Leipe et al., 2017; Müller et al., 2016) and one Okhotsk burial (Okamoto et al., 2016). While the project's main aim is to improve temporal precision for $\delta^{18}O$ data beyond current multi-centennial

estimates, we will also fill existing gaps in the site's chronology by adding radiocarbon dates for layers II, IV and VIII (Figure 3). By combining the new and existing dates, we will be able to produce a new Bayesian model for the chronology of Hamanaka II.

Samples

Funding is requested for 22 dates. Proposed samples come from six bivalves (*S. sachalinensis*), three each from the Final-/Epi-Jomon (2700-1500 cal BP) and Ainu (1000-80 cal BP), and five otoliths (*G. macrocephalus*) from the intervening Okhotsk (1500-1000 cal BP), which lacked suitable shell material. All material is from the 2011-2018 excavations at Hamanaka II. Table 2 provides more detailed information on each sample's stratigraphic unit and cultural attribution, and Figure 3 shows relevant stratigraphy. Shells were collected by Tansy Branscombe during the 2018 excavations, while otoliths were sent to Oxford from Keio university in the same year. All material is stored in Oxford, and no further fieldwork is required.

The radiocarbon sampling strategy targets the bivalves and otoliths currently being undergoing $\delta^{18}O$ analysis at the British Geological Survey under the supervision of Professor Melanie Leng (NERC Facilities Grant IP-1944-1119. Results from a Final-/Epi-Jomon shell are provided in Figure 4, showing an inter- and intra-annual signal indicating a temperature range of ~17.5℃ when converted into SST using Grossman and Ku's (1986) equation. This provides a close match for the modern average SST range of 17.3℃. Otoliths are currently being prepared for sampling.

Two dates are proposed for each shell and otolith. This strategy utilises incremental carbonate deposition to provide 'stratigraphic' information for Bayesian modelling. Similar paired dating has been used to good effect on wooden artefacts (Brock et al., 2012), but is novel in marine carbonates although they are clearly incremental. In this pilot, one date will be produced from the earliest period of growth (umbo in shells, core in otoliths) and one from the edge representing last growth. This allows maximal temporal gap between the dates, as simulated dates in OxCal (Figure 5) have shown that a gap of 10-15 years can significantly reduce uncertainty, especially in the 95% confidence range.

For each shell/otolith it will be possible to reach an estimate of the temporal gap represented by each individual prior to sampling. For *S. sachalinensis* specimens are expected to have lived at least eight-nine years (up to maximum ~15 years), and each specimen can be aged microscopically using a thick section. *G. macrocephalus* can live up to 20 years, but aging is more difficult but will be possible by microscopic analysis of thin sections combined with confirmation of seasonal cycles through $\delta^{18}O$ results (Kastelle et al., 2017).

Anticipated Problems

<u>Marine reservoir effect</u>

As all our samples come from a marine environment, the main anticipated problem is adjusting for the local marine reservoir offset, ΔR. Fortunately, previous work has been done on Late Jomon (~3000 cal BP) material from Hamanaka II, producing a marine reservoir correction for the Soya current of ΔR = 172 ± 39 ^{14}C yr (Miyata et al., 2016). An alternative comes from a *Glycymeris* shell collected at Otaru Bay in 1899, producing a ΔR of 94 ± 43 ^{14}C yr (Yoneda et al., 2007). For this study we consider the Miyata et al. (2016) correction more suitable, as it is: **i)** averaged across multiple shells (including *S. sachalinensis*); **ii)** from the same site as our samples; and **iii)** because the shell used by Yoneda et al. (2007) likely precipitated under oceanographic conditions specific to the LIA cold period (Figure 3).

A further problem is providing reservoir corrections unique to the marine niches occupied by clams and cod. Again, the work of Miyata et al. (2016) is useful here. For shallow water *S. sachalinensis*, the Soya current correction of ΔR = 172 ± 39 ^{14}C yr is appropriate, especially given

the use of *S. sachalinensis* shells in its creation. Pacific cod, however, live largely offshore in deeper waters, out of the Soya current's direct influence. Consequently, the remains of Japanese sea lions from Hamanaka II may provide a more appropriate reservoir correction: ΔR = 389 ± 45 ^{14}C yr (Miyata et al., 2016). Sea lions feed on deep water species, including cod, so this larger correction better reflects the deep water 'older' carbon environment (Miyata et al., 2016).

Anticipated Outcomes & Summary

The proposed radiocarbon dating of marine carbonates will pinpoint the timing of $\delta^{18}O$ sequences produced from the same specimens. This will allow seasonal climatic conditions – as indicated by SST – to be compared to the history of cultural change from Hamanaka II, to identify the impact of changing climate and oceanography on Hokkaido's hunter-gatherers. Higher SST is expected to correlate to warmer, wetter and windier terrestrial conditions. Radiocarbon dates on the Okhotsk material should help assess the role of climate in intensified settlement at Hamanaka II, leading to the palynologically identified deforestation. Secondly, this study will act as a pilot assessment of the utility of Bayesian modelling using samples with inherent and fine-scale incremental chronology. The inclusion of paired samples per specimen allows us to exploit the chronological information available from annual growth bands to constrain dates, providing prior knowledge of the sequence to include in Bayesian statistical modelling. Our pilot will test this novel approach for marine carbonates, with potential to expand the technique to other incremental biological tissues.

Appendix

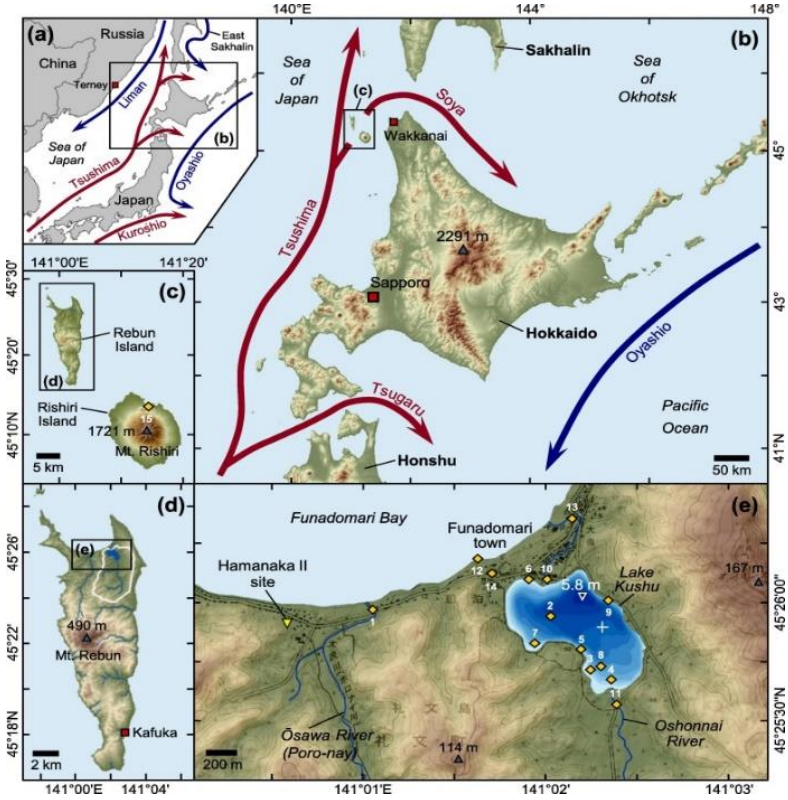


Figure 2: Map of Hokkaido showing the location of Hamanaka II, and the major oceanographic currents influencing the region. Image reproduced from Müller et al. 2016.

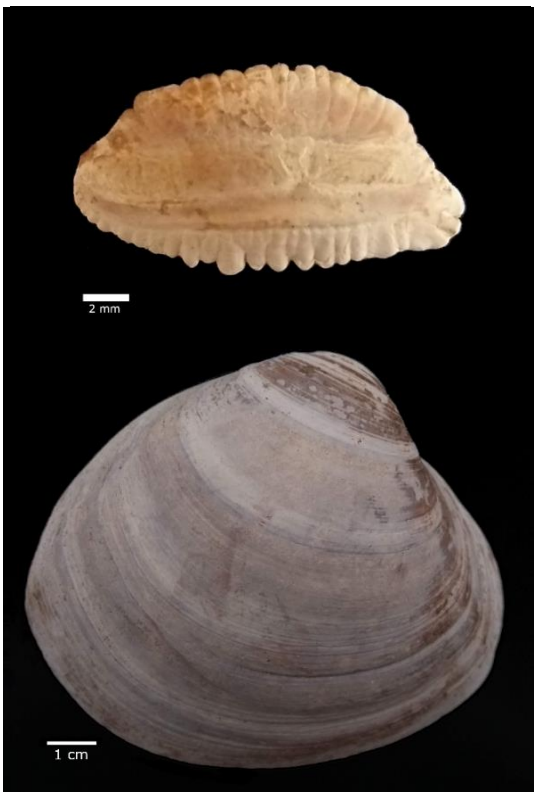


Figure 1: Photograph of archaeological G. macrocephalus otolith (top) and S. sachalinensis shell (ri).

*Table 1: Published radiocarbon dates for Hamanaka 2. *This material comes from earlier excavations at Hamanaka II, so layer V does not refer to the same layer as indicated in Figure 3.*

Layer	Lab No.	Date (^{14}C yr)	+/-	Calendar Date (cal BP)	Material	Cultural Attribution	Reference
I	Poz-60760	165	30	288-1	Seed	Historical Ainu	Müller et al. 2016
I	Poz-60761	115	30	270-11	Seed	Historical Ainu	Müller et al. 2016
I	Poz-60762	210	30	304-1	Wood	Historical Ainu	Müller et al. 2016
IIIa	Poz-84277	1215	30	694-889	Seed	Okhotsk	Leipe et al. 2017
IIIa	Poz-84278	1170	30	771-965	Seed	Okhotsk	Leipe et al. 2017
IIIb	Poz-81340	1220	30	692-887	Seed	Okhotsk	Leipe et al. 2017
IIIb	Poz-81341	1215	30	694-889	Seed	Okhotsk	Leipe et al. 2017
IIIb	Poz-81342	1180	30	730-951	Seed	Okhotsk	Leipe et al. 2017
IIIb	Poz-60766	1305	30	1292-1181	Seed	Okhotsk	Müller et al. 2016
IIIb	Poz-60767	1265	30	1284-1087	Seed	Okhotsk	Müller et al. 2016
IIIb	Poz-60768	1215	30	1256-1061	Seed	Okhotsk	Müller et al. 2016
IIIc	Poz-84280	1285	30	665-771	Seed	Okhotsk	Leipe et al. 2017
IIIc	Poz-84281	1275	30	661-800	Seed	Okhotsk	Leipe et al. 2017
IIId	Poz-84282	1295	30	662-770	Seed	Okhotsk	Leipe et al. 2017
IIId	Poz-84283	1335	30	646-766	Seed	Okhotsk	Leipe et al. 2017
IIId	Poz-84284	1475	30	542-644	Seed	Okhotsk	Leipe et al. 2017
IIId	Poz-84285	1275	30	661-800	Seed	Okhotsk	Leipe et al. 2017
IIIe	Poz-84286	1350	30	636-765	Seed	Okhotsk	Leipe et al. 2017
IIIe	Poz-84287	1520	30	428-609	Seed	Okhotsk	Leipe et al. 2017
-	Tka-16063	1689	20	890-795	Human bone	Okhotsk	Okamoto et al. 2016
V*	PLD-6305	3805	20	3361 ± 55	Charred food	Late Jomon	Miyata et al. 2009
V*	PLD-6306	3815	20	3371 ± 55	Charred food	Late Jomon	Miyata et al. 2009
V*	PLD-6453	3730	35	3286 ± 55	Charred food	Late Jomon	Miyata et al. 2009
V*	PLD-6454	3715	35	3271 ± 55	Charred food	Late Jomon	Miyata et al. 2009
V*	PLD-6455	3840	35	3396 ± 55	Charred food	Late Jomon	Miyata et al. 2009
V*	PLD-6456	2980	35	3324-3008	Wood	Late Jomon	Miyata et al. 2009
V*	PLD-6457	3035	35	3356-3085	Wood	Late Jomon	Miyata et al. 2009
V*	PLD-8847	3550	25	3378 ± 42	Marine shell	Late Jomon	Miyata et al. 2016
V*	PLD-8848	3550	25	3378 ± 42	Marine shell	Late Jomon	Miyata et al. 2016
V*	PLD-8849	3715	25	3542 ± 42	Marine shell	Late Jomon	Miyata et al. 2016
V*	PLD-8850	3470	25	3298 ± 42	Marine shell	Late Jomon	Miyata et al. 2016
V*	PLD-8851	3500	25	3328 ± 42	Marine shell	Late Jomon	Miyata et al. 2016
V*	PLD-10582	3735	30	3346 ± 42	Sea lion	Late Jomon	Miyata et al. 2016
V*	PLD-10583	3635	30	3346 ± 42	Alcidae	Late Jomon	Miyata et al. 2016

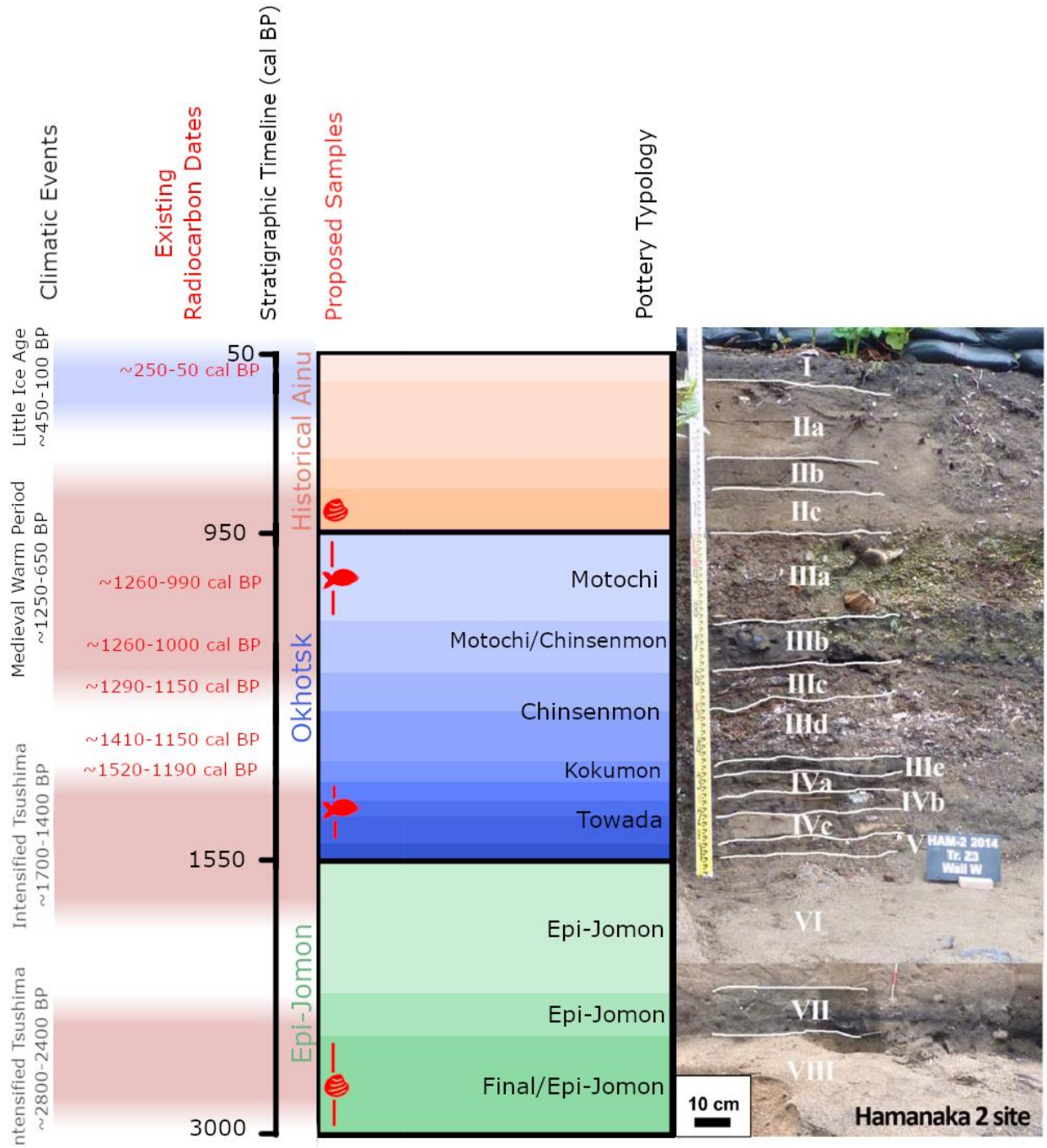


Figure 3: Stratigraphic profile for Hamanaka II (modified from Müller et al. 2016), showing locations of proposed samples, existing chronology and key climatic events. Towada (layer IV) samples did not have stratigraphic information to identify a sublayer

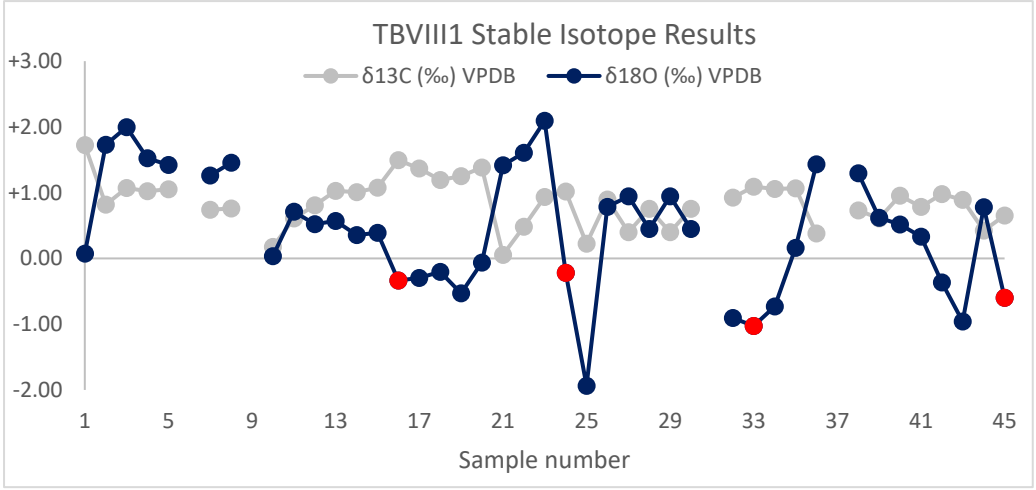
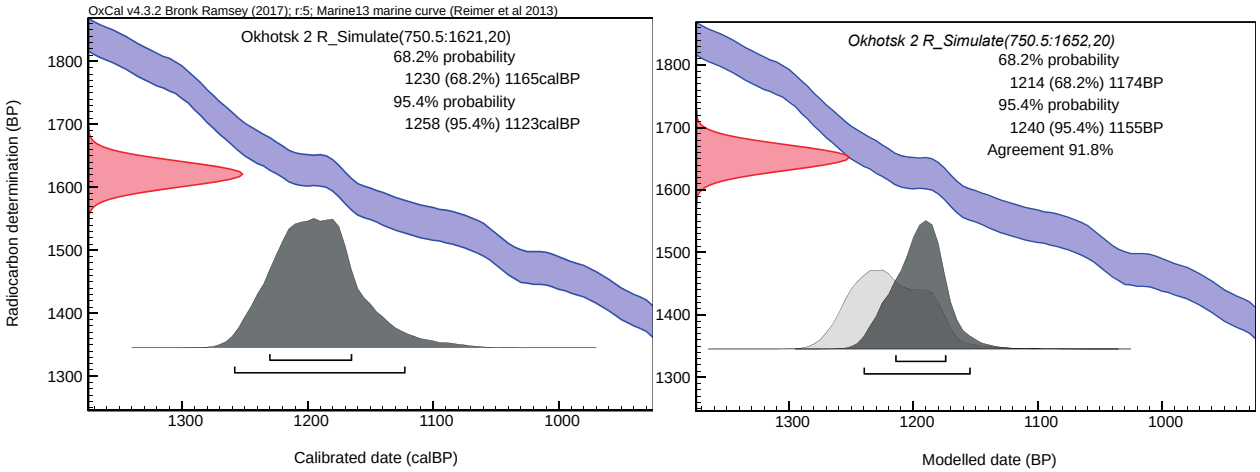


Figure 4: Graph showing stable oxygen and carbon isotope results from shell TBVIII1. Red markers show the final sample of each growth increment. Sample number starts towards the umbo at 1, and moves towards growth edge at 45



Calibrated single simulated date of 1200 cal BP, unmodelled. The range is 65 yr at 68% confidence and 135 yr at 95% confidence.

Simulated date of 1200 cal BP, preceded by 1210 cal BP (modelled with a 15 yr gap). The range is 40 yr at 68% confidence and 85 yr at 95% confidence.

Figure 5: Simulated radiocarbon dates showing how paired dates with a 15 year time gap can constrain calibration.

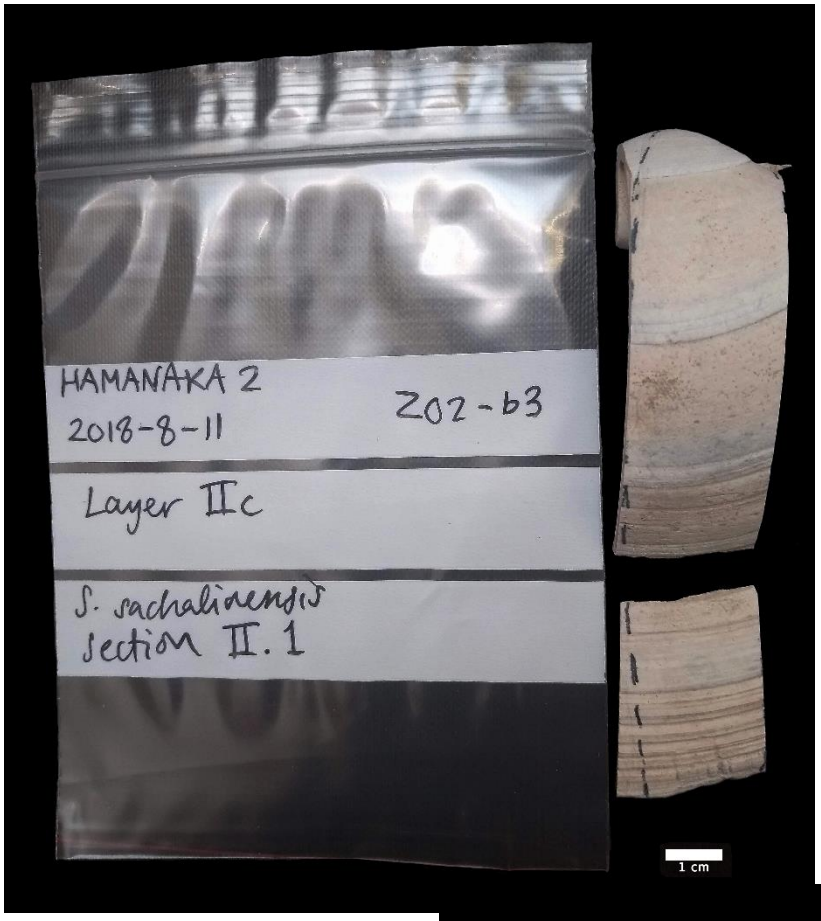
Table 2: Proposed radiocarbon samples and relevant contextual information. All samples are composed of aragonite ($CaCO_3$).

Sample no.	Sample ID	Species	Stratigraphic Unit	Archaeological context	Estimated Date Range (cal BP)
1	TBVIII1.1	*S. sachalinensis*	VIII	Final-/Epi-Jomon	~3000-2000
2	TBVIII1.2	*S. sachalinensis*	VIII	Final-/Epi-Jomon	
3	TBVIII2.1	*S. sachalinensis*	VIII	Final-/Epi-Jomon	
4	TBVIII2.2	*S. sachalinensis*	VIII	Final-/Epi-Jomon	
5	TBVIII4.1	*S. sachalinensis*	VIII	Final-/Epi-Jomon	
6	TBVIII4.2	*S. sachalinensis*	VIII	Final-/Epi-Jomon	
7	TBII1.1	*S. sachalinensis*	IIc	Historical Ainu	~990-250
8	TBII1.2	*S. sachalinensis*	IIc	Historical Ainu	
9	TBII2.1	*S. sachalinensis*	IIc	Historical Ainu	
10	TBII2.2	*S. sachalinensis*	IIc	Historical Ainu	
11	TBII3.1	*S. sachalinensis*	IIc	Historical Ainu	
12	TBII3.2	*S. sachalinensis*	IIc	Historical Ainu	
13	TBIII1.1	*G. macrocephalus*	IIIa	Late Okhotsk	~1260-990
14	TBIII1.2	*G. macrocephalus*	IIIa	Late Okhotsk	
15	TBIII2.1	*G. macrocephalus*	IIIa	Late Okhotsk	
16	TBIII2.2	*G. macrocephalus*	IIIa	Late Okhotsk	
17	TBIV1.1	*G. macrocephalus*	IV	Early Okhotsk	~1550-1200
18	TBVI1.2	*G. macrocephalus*	IV	Early Okhotsk	
19	TBIV2.1	*G. macrocephalus*	IV	Early Okhotsk	
20	TBIV2.2	*G. macrocephalus*	IV	Early Okhotsk	
21	TBIV3.1	*G. macrocephalus*	IV	Early Okhotsk	
22	TBIV3.2	*G. macrocephalus*	IV	Early Okhotsk	

References

Abe, C*. et al.* 2016. Spatio-temporal distribution of hunter–gatherer archaeological sites in the Hokkaido region (northern Japan): An overview. Holocene 26, 1627–1645. **Batten**, B. L. 2008. Climate Change in Japanese History and Prehistory: A Comparative Overview. 5th Annual Michael P. Malone Memorial Conference. Big Sky, Montana, 2008. **Brock**, F*. et al.* 2012. Paired Dating of Pith and Outer Edge (Terminus) Samples from Pre-Hispanic Caribbean Wooden Sculptures. Radiocarbon 54 (3-4). **Brown**, T. A*. et al.* 1989. Radiocarbon Dating of Pollen by Accelerator Mass Spectrometry. Quat. Res 32 (2), 205-212. **Corrège**, T*. et al.* 2001. Little Ice Age Sea Surface Temperature Variability in the Southwest Tropical Pacific. Geophys. Res. Letters 28 (18), 3477-3480. **Ebuchi**, N*. et al.* 2006. Observation of the Soya Warm Current Using HF Ocean Radar. Journal of Oceanography 62, 47-61. **Grossman**, E. L., and Ku, T. L. 1986. Oxygen and Carbon Isotope Fractionation in Biogenic Aragonite: Temperature Effects. Chemical Geology: Isotope Geoscience Section 59 (C): 59–74. **Hirose**, N., and Ken-ichi F. 2006. Monitoring the Tsushima Warm Current Improves Seasonal Prediction of the Regional Snowfall. Scientific Online Letters on the Atmosphere 2, 61–63. **Igarashi**, Y. 2013. Holocene vegetation and climate on Hokkaido Island, northern Japan. Quat. Int. 290–291, 139–150. **Imada**, Y. *et al*. 2017. Recent Enhanced Seasonal Temperature Contrast in Japan from Large Ensemble High-Resolution Climate Simulations. Atmosphere 8 (3), 1–13. **Isobe**, A. 1999. On the Origin of the Tsushima Warm Current Water and Its Seasonality. Acta Oceanologica Sinica 19, 117–33. **Kastelle**, C. R., *et al*. 2017. Age Validation of Pacific Cod (Gadus Macrocephalus) Using High-Resolution Stable Oxygen Isotope (δ 18O) Chronologies in Otoliths. Fisheries Res. 185, 43-53. **Kawahata**, H*. et al.* 2003. Terrestrial-Oceanic Environmental Change in the Southern Okhotsk Sea during the Holocene. Quat. Int. 108 (1), 67–76. **Koizumi**, I. 1987. Pulses of Tsushima Current during the Holocene. 第四紀研究 26, 13–25. **Leipe**, C*. et al.* 2018. Vegetation change and human impacts on Rebun Island (Northwest Pacific) over the last 6000 years. Quat. Sci. Rev. 193, 129–144. **Leipe**, C*. et al.* 2017. Barley (Hordeum vulgare) in the Okhotsk culture (5th-10th century AD) of northern Japan and the role of cultivated plants in hunter-gatherer economies. PLoS One 12. **Matsuyama**, M*. et al.* 2006. Current Structure and Volume Transport of the Soya Warm Current in Summer. J. of Oceanography 62 (2), 197–205. **Miyata**, Y*. et al.* 2016. Marine reservoir effects deduced from 14C dates on pottery residues, bones, and Molluskan shells from the Hamanaka 2 archaeological site, Rebun Island, Hokkaido, Japan. Radiocarbon 58, 755–770. **Miyata**, Y*. et al.* 2009. Traces of sea mammals on pottery from the Hamanaka 2 archaeological site, Rebun Island, Japan: Implications from sterol analysis, stable isotopes, and radiocarbon dating. Res. Org. Geochem 25, 15–27. **Müller**, S*. et al.* 2016. Palaeobotanical records from Rebun Island and their potential for improving the chronological control and understanding human–environment interactions in the Hokkaido Region, Japan. Holocene 26, 1646–1660. **Oba**, T*. et al.* 1991. Palaeoenvironmental Changes in the Japan Sea During the Last 85,000 Years. Paleoceanography 6, 499–518. **Okamoto**, Y*. et al.* 2016. An Okhotsk Adult Female Human Skeleton (11th/12th Century Ad) with Possible Sapho Syndrome from Hamanaka 2 Site, Rebun Island, Northern Japan. Anth. Sci. 124 (2), 107–15. **Schmidt**, M*. et al.* 2019. A Multi-Proxy Palaeolimnological Record of the Last 16,600 Years from Coastal Lake Kushu in Northern Japan. Palaeogeography, Palaeoclimatology, Palaeoecology 514, 613–26. **Seo**, H*. et al.* 2013. "On the Effect of the East/Japan Sea SST Variability on the North Pacific Atmospheric Circulation in a Regional Climate Model." Journal of Geophysical Research 119 (2): 418–44. **Takano,** Y., Yoshihiro T., Katsushi I. 2008. Influences of Large-Scale Atmospheric Circulation and Local Sea Surface Temperature on Convective Activity over the Sea of Japan in December. Scientific Online Letters on the Atmos. 4 (1), 113–16. **Toba**, Y*. et al.* 1982. Seasonal and Year-to-Year Variability of the Tsushima-Tsugaru Warm Current System with Its Possible Cause. Société Franco-Japonaise d'océanographie, Tokyo 20, 41–51. **Yoneda**, M*. et al.* 2007. Radiocarbon marine reservoir ages in the western Pacific estimated by pre-bomb molluscan shells. Nucl. Instruments Methods Phys. Res. Sect. B Beam Interact. with Mater. Atoms 259 (1), 432-437.

Appendix 2: Photographs of sampled shells and otoliths



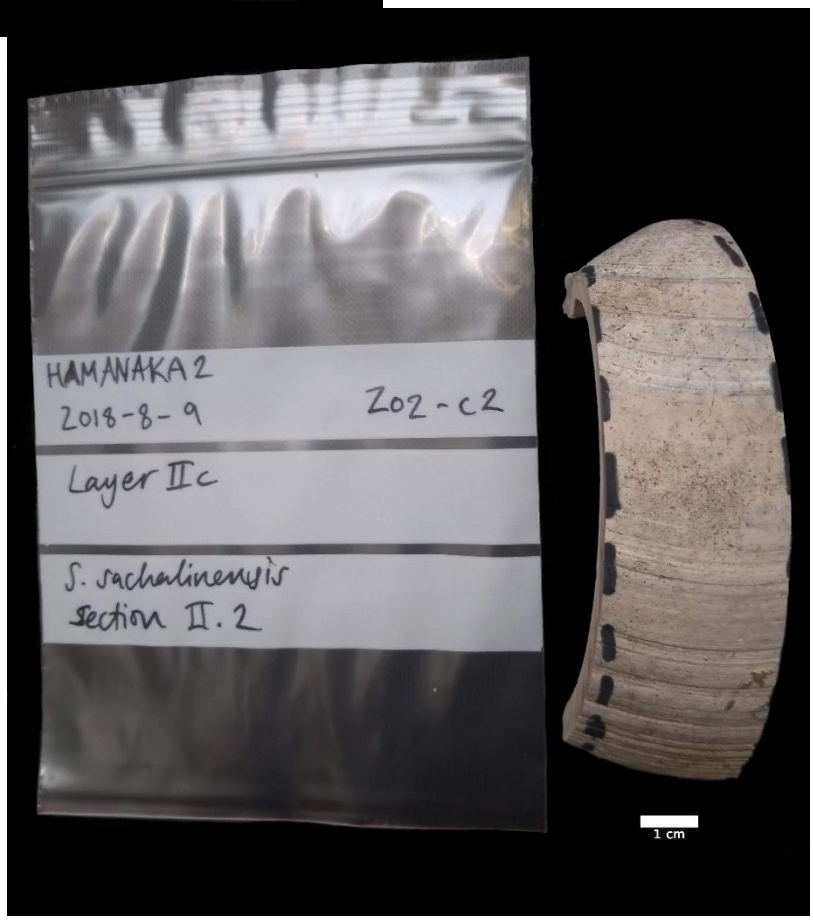
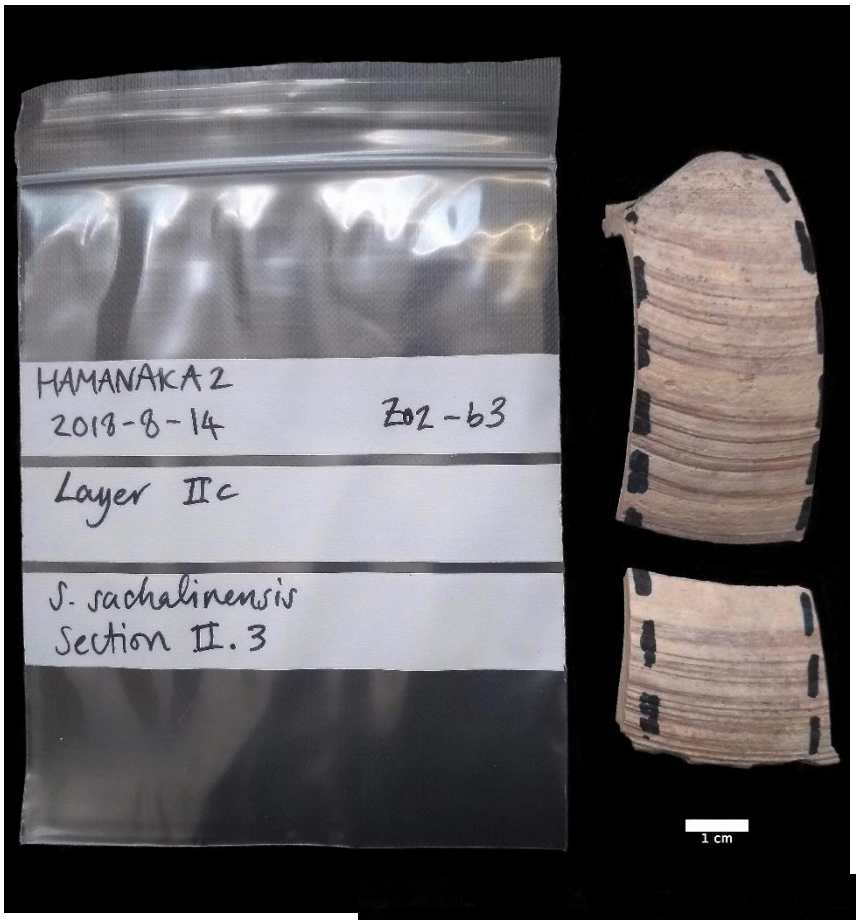


Figure 1: Left: Section of shell II1. Below: Section of shell II2



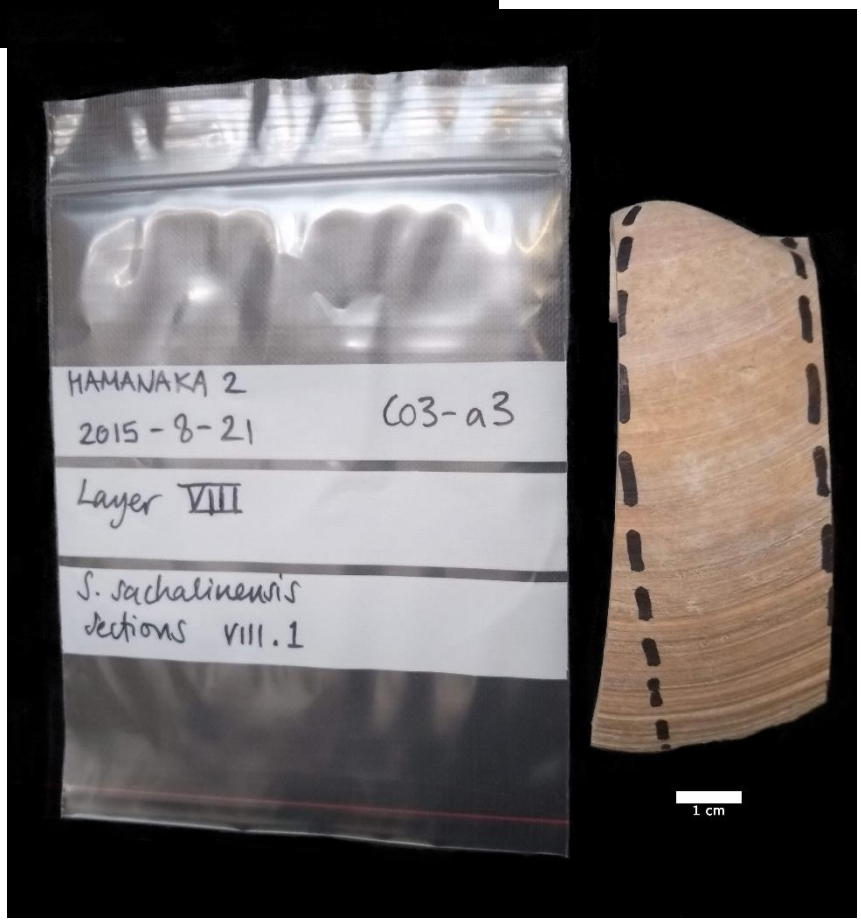


Figure 2: Left: Section of shell II3. Below: Section of shell VIII1

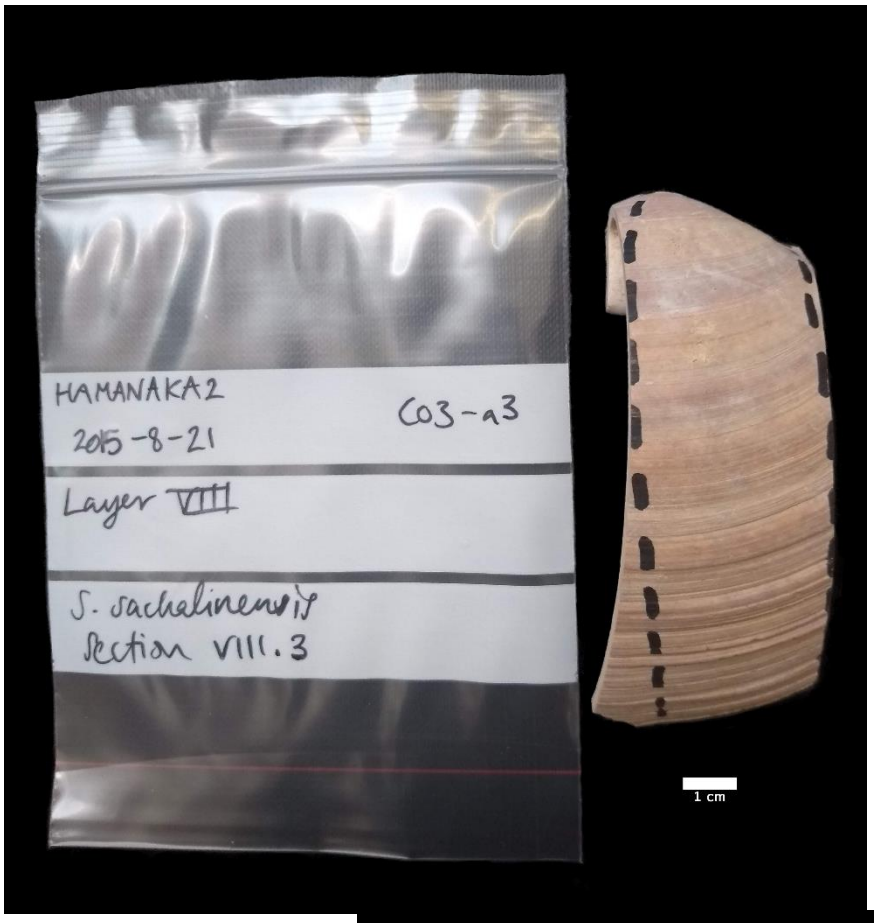
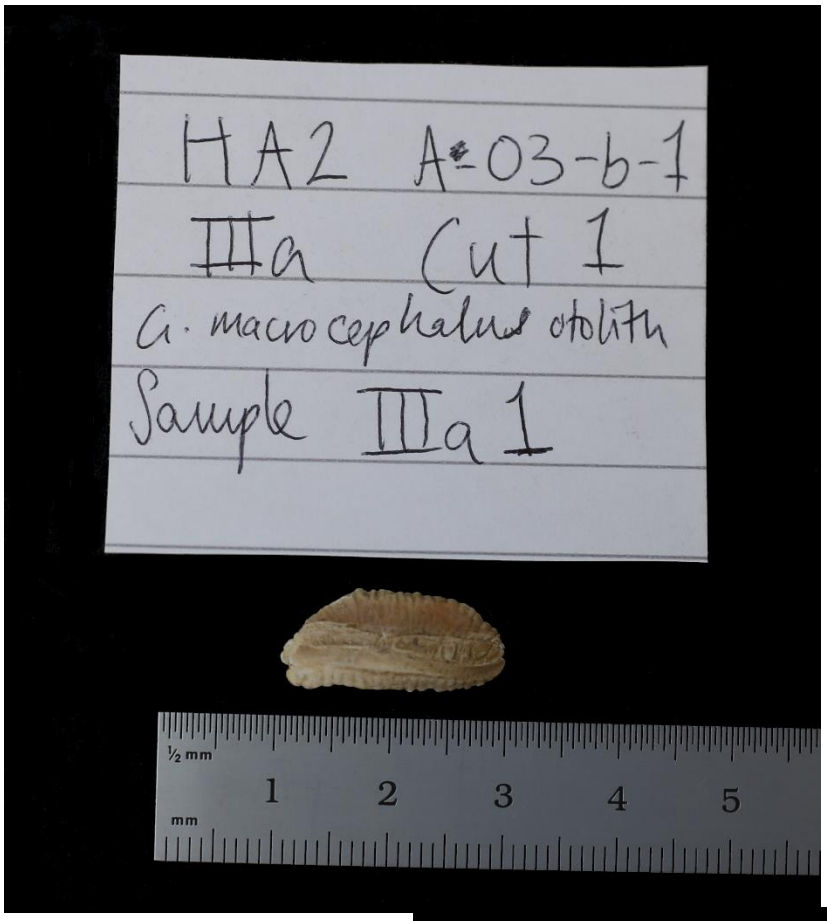


Figure 3: Left: Section of shell VIII3. Below: Section of shell VIII4





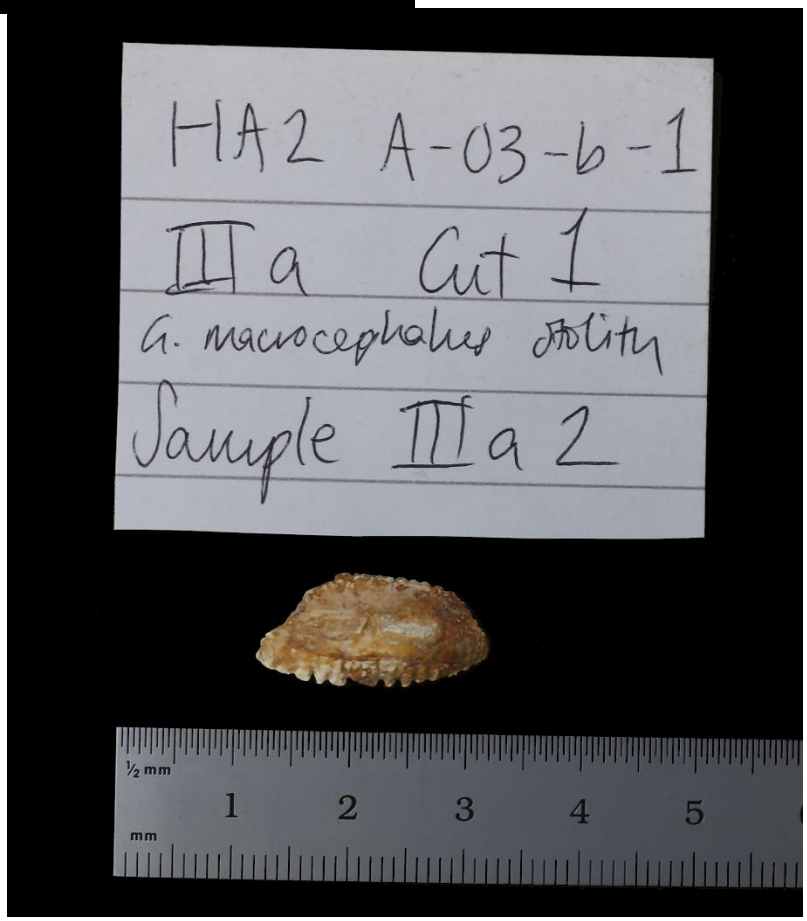


Figure 4: Left: Section of otolith IIIa1. Below: Section of otolith IIIa2



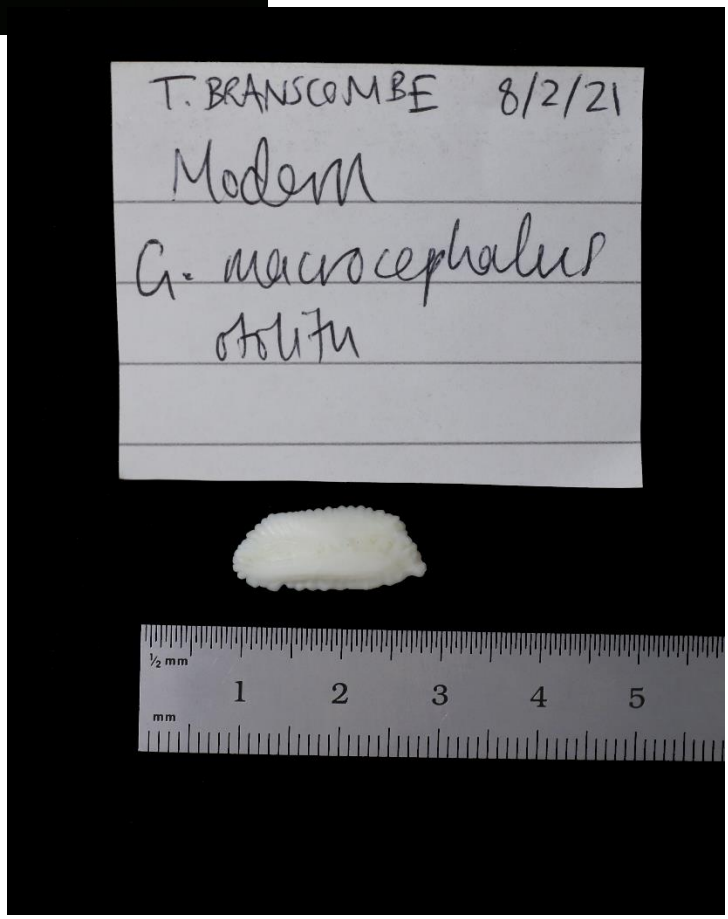


Figure 5: Left: Section of otolith IV2. Below: Section of modern otolith

Appendix 3: Full $\delta^{18}O$ and $\delta^{13}C$ results

Table 1: Full oxygen and carbon stable isotope results and SST calculations. Blank cells indicates no data produced.

Shell	Sample number	δ13C	δ18O	SST	Sampling method
II1	1	1.58	-1.37	21.68	Micromill
II1	2	1.15	-0.90	19.64	Micromill
II1	3				Micromill
II1	4				Micromill
II1	5	1.17	0.37	14.13	Micromill
II1	6				Micromill
II1	7				Micromill
II1	8	1.15	1.66	8.51	Micromill
II1	9	1.06	1.19	10.59	Micromill
II1	10	0.62	0.97	11.52	Micromill
II1	11	0.88	1.13	10.84	Micromill
II1	12	0.74	0.44	13.85	Micromill
II1	13	0.83	0.49	13.63	Micromill
II1	14	0.65	0.31	14.41	Micromill
II1	15	0.92	0.50	13.57	Micromill
II1	16	1.19	0.71	12.66	Micromill
II1	17	0.87	0.35	14.22	Micromill
II1	18	1.14	0.28	14.50	Micromill
II1	19				Micromill
II1	20	1.21	-0.23	16.75	Micromill
II1	21	1.27	-0.38	17.39	Micromill
II1	22	1.40	-0.29	16.99	Micromill
II1	23	1.44	-0.50	17.93	Micromill
II1	24	1.45	-0.50	17.91	Micromill
II1	25	1.56	-0.20	16.61	Micromill
II1	26	1.52	0.89	11.88	Micromill
II1	27	0.80	2.06	6.82	Micromill
II1	28	2.05	2.11	6.57	Micromill
II1	29				Micromill
II1	30	2.25	2.11	6.59	Micromill
II1	31	2.23	1.36	9.82	Micromill
II1	32	1.97	1.55	9.03	Micromill
II1	33	1.98	0.79	12.32	Micromill
II1	34	1.98	1.07	11.10	Micromill
II1	35	1.85	0.53	13.42	Micromill
II1	36	3.94	0.60	13.12	Micromill
II1	37	3.44	-0.20	16.59	Micromill
II1	38	1.32	0.34	14.28	Micromill
II1	39	3.96	-0.33	17.18	Micromill
II1	40	4.86	-0.21	16.64	Micromill
II1	41	2.41	-0.53	18.05	Micromill

II1	42	4.39	-0.79	19.15	Micromill
II1	43	1.44	-0.58	18.27	Micromill
II1	44	1.45	-0.35	17.26	Micromill
II1	45	1.40	1.20	10.55	Micromill
II1	46	1.75	1.98	7.14	Micromill
II1	47	1.37	2.11	6.60	Micromill
II1	48	2.01	0.95	11.63	Micromill
II1	49	2.08	0.34	14.25	Micromill
II1	50	1.53	-0.93	19.79	Micromill
II2	1	1.17	-0.60	18.36	Micromill
II2	2.5	0.92	-1.18	20.86	Micromill
II2	4	1.25	0.25	14.65	Micromill
II2	5	0.87	-1.44	21.98	Micromill
II2	6	1.09	-0.76	19.03	Micromill
II2	7	0.98	-0.85	19.41	Micromill
II2	8	1.19	-0.56	18.16	Micromill
II2	9	1.21	0.87	11.96	Micromill
II2	10	0.48	2.21	6.13	Micromill
II2	11	0.36	2.14	6.45	Micromill
II2	12	0.49	1.94	7.31	Micromill
II2	13	0.61	1.93	7.35	Micromill
II2	14	0.66	1.66	8.54	Micromill
II2	15	0.72	1.55	9.01	Micromill
II2	16	0.82	1.30	10.10	Micromill
II2	17	1.25	1.48	9.33	Micromill
II2	18	1.28	1.04	11.21	Micromill
II2	19				Micromill
II2	20	0.96	0.68	12.81	Micromill
II2	21	1.27	0.44	13.82	Micromill
II2	22	1.39	0.47	13.70	Micromill
II2					Micromill
II2	24	1.74	3.70	-0.33	Micromill
II2	25	0.36	2.80	3.57	Micromill
II2	26	-0.01	2.15	6.41	Micromill
II2	27				Micromill
II2	28	0.85	1.06	11.14	Micromill
II2	29				Micromill
II2	30	0.95	0.98	11.50	Micromill
II2	31	1.08	0.33	14.29	Micromill
II2	32	1.04	-0.09	16.15	Micromill
II2	33	0.78	-1.36	21.63	Micromill
II2	34	0.84	-1.12	20.59	Micromill
II2	35				Micromill
II2	36	0.20	2.39	5.36	Micromill
II2	37	0.22	2.22	6.10	Micromill
II2	38	0.34	1.64	8.62	Micromill
II2	39				Micromill

II2	40	0.63	0.91	11.78	Micromill
II3	1	1.39	0.81	12.23	Micromill
II3	2	1.33	-1.10	20.53	Micromill
II3	3	1.74	1.51	9.17	Micromill
II3	4	0.98	2.42	5.22	Micromill
II3	5	0.69	2.34	5.60	Micromill
II3	6	0.58	2.14	6.45	Micromill
II3	7				Micromill
II3	8	0.40	1.61	8.74	Micromill
II3	9				Micromill
II3	10	0.80	1.25	10.30	Micromill
II3	11				Micromill
II3	12				Micromill
II3	13	0.87	-1.15	20.75	Micromill
II3	14	1.66	-0.90	19.66	Micromill
II3	15	1.29	-0.44	17.63	Micromill
II3	16	1.57	1.52	9.16	Micromill
II3	17	1.40	2.14	6.44	Micromill
II3	18	2.52	2.31	5.69	Micromill
II3	19				Micromill
II3	20				Micromill
II3	21	0.52	1.57	8.93	Micromill
II3	22	0.88	1.10	10.95	Micromill
II3	23	1.03	1.18	10.61	Micromill
II3	24				Micromill
II3	25	0.36	0.58	13.20	Micromill
II3	26	0.53	0.48	13.66	Micromill
II3	27	0.41	0.06	15.49	Micromill
II3	28	1.30	-0.64	18.51	Micromill
II3	29	0.62	-0.34	17.23	Micromill
II3	30	1.07	0.44	13.82	Micromill
II3	31	2.46	1.44	9.50	Micromill
II3	32	0.19	2.28	5.82	Micromill
II3	33	1.05	2.05	6.85	Micromill
II3	34	0.86	1.68	8.47	Micromill
II3	35	0.73	0.23	14.75	Micromill
II3	36	1.23	-0.64	18.53	Micromill
II3	37	0.87	-0.62	18.43	Micromill
II3	38	0.83	1.66	8.53	Micromill
VIII1	1	1.72	0.07	15.43	Micromill
VIII1	2	0.82	1.73	8.23	Micromill
VIII1	3	1.07	2.00	7.07	Micromill
VIII1	4	1.02	1.52	9.13	Micromill
VIII1	5	1.05	1.42	9.56	Micromill
VIII1	6	0.58	1.28	10.20	Micromill
VIII1	7	0.74	1.26	10.27	Micromill
VIII1	8	0.76	1.46	9.41	Micromill

VIII1	9	0.50	1.11	10.92	Micromill
VIII1	10	0.17	0.04	15.59	Micromill
VIII1	11	0.61	0.71	12.66	Micromill
VIII1	12	0.81	0.52	13.47	Micromill
VIII1	13	1.03	0.57	13.27	Micromill
VIII1	14	1.01	0.36	14.19	Micromill
VIII1	15	1.08	0.39	14.04	Micromill
VIII1	16	1.49	-0.34	17.20	Micromill
VIII1	17	1.37	-0.30	17.02	Micromill
VIII1	18	1.19	-0.21	16.63	Micromill
VIII1	19	1.25	-0.53	18.04	Micromill
VIII1	20	1.38	-0.06	16.01	Micromill
VIII1	21	0.06	1.42	9.59	Micromill
VIII1	22	0.48	1.61	8.76	Micromill
VIII1	23	0.93	2.09	6.66	Micromill
VIII1	24	1.02	-0.22	16.69	Micromill
VIII1	25	1.17	-0.14	16.35	Micromill
VIII1	26	0.90	0.79	12.33	Micromill
VIII1	27	0.40	0.95	11.64	Micromill
VIII1	28	0.76	0.45	13.79	Micromill
VIII1	29	0.40	0.95	11.64	Micromill
VIII1	30	0.76	0.45	13.79	Micromill
VIII1	31	0.74	0.37	14.14	Micromill
VIII1	32	0.92	-0.91	19.67	Micromill
VIII1	33	1.09	-1.03	20.19	Micromill
VIII1	34	1.05	-0.73	18.91	Micromill
VIII1	35	1.07	0.16	15.04	Micromill
VIII1	36	0.38	1.43	9.52	Micromill
VIII1	37	0.78	1.23	10.41	Micromill
VIII1	38	0.73	1.29	10.12	Micromill
VIII1	39	0.61	0.62	13.05	Micromill
VIII1	40	0.96	0.52	13.50	Micromill
VIII1	41	0.78	0.33	14.30	Micromill
VIII1	42	0.98	-0.36	17.31	Micromill
VIII1	43	0.89	-0.96	19.90	Micromill
VIII1	44	0.42	0.78	12.36	Micromill
VIII1	45	0.65	-0.60	18.33	Micromill
VIII2	1	2.07	0.30	14.43	Micromill
VIII2	2	1.92	0.23	14.75	Micromill
VIII2	3	1.52	-0.06	15.98	Micromill
VIII2	4	1.48	0.59	13.19	Micromill
VIII2	5	0.65	1.67	8.51	Micromill
VIII2	6	0.80	1.59	8.82	Micromill
VIII2	7	1.02	1.54	9.03	Micromill
VIII2	8	1.37	1.84	7.76	Micromill
VIII2	9	0.87	1.07	11.09	Micromill
VIII2	10	0.89	1.12	10.88	Micromill

VIII2	11	1.01	0.58	13.24	Micromill
VIII2	12	1.26	0.78	12.33	Micromill
VIII2	13	1.30	0.27	14.57	Micromill
VIII2	14	1.34	0.08	15.41	Micromill
VIII2	15	1.26	-0.40	17.49	Micromill
VIII2	16	1.28	-0.36	17.32	Micromill
VIII2	17	1.10	-0.87	19.49	Micromill
VIII2	18				Micromill
VIII2	19	1.50	-0.85	19.44	Micromill
VIII2	20	1.64	-0.23	16.73	Micromill
VIII2	21	1.52	-0.39	17.45	Micromill
VIII2	22	0.88	1.86	7.66	Micromill
VIII2	23	0.62	1.19	10.59	Micromill
VIII2	24	0.81	1.22	10.44	Micromill
VIII2	25	0.55	1.20	10.55	Micromill
VIII2	26	0.69	1.15	10.74	Micromill
VIII2	27	0.61	0.89	11.86	Micromill
VIII2	28	0.48	0.14	15.14	Micromill
VIII2	29	0.77	-0.20	16.62	Micromill
VIII2	30	0.79	-0.44	17.63	Micromill
VIII2	31	0.89	-0.90	19.63	Micromill
VIII2	32	1.12	-1.14	20.69	Micromill
VIII2	33	1.10	-1.37	21.69	Micromill
VIII2	34	1.30	-0.90	19.65	Micromill
VIII2	35	0.69	1.76	8.12	Micromill
VIII2	36	0.23	1.48	9.30	Micromill
VIII2	37	0.83	1.97	7.18	Micromill
VIII2	38	1.13	2.22	6.09	Micromill
VIII2	39				Micromill
VIII2	40	1.21	2.06	6.78	Micromill
VIII2	41	1.11	-0.82	19.29	Micromill
VIII2	42	2.39	1.12	10.89	Micromill
VIII2	43	1.56	1.31	10.06	Micromill
VIII3	1	2.33	-0.42	17.55	Micromill
VIII3	2	2.59	0.16	15.06	Micromill
VIII3	3	2.44	0.20	14.88	Micromill
VIII3	4	1.73	1.63	8.67	Micromill
VIII3	5	0.69	0.90	11.84	Micromill
VIII3	6	1.36	0.97	11.54	Micromill
VIII3	7				Micromill
VIII3	8	0.40	0.82	12.19	Micromill
VIII3	9				Micromill
VIII3	10	0.14	-0.21	16.65	Micromill
VIII3	11	0.54	-0.23	16.75	Micromill
VIII3	12	0.67	0.25	14.66	Micromill
VIII3	13				Micromill
VIII3	14	0.69	-0.73	18.92	Micromill

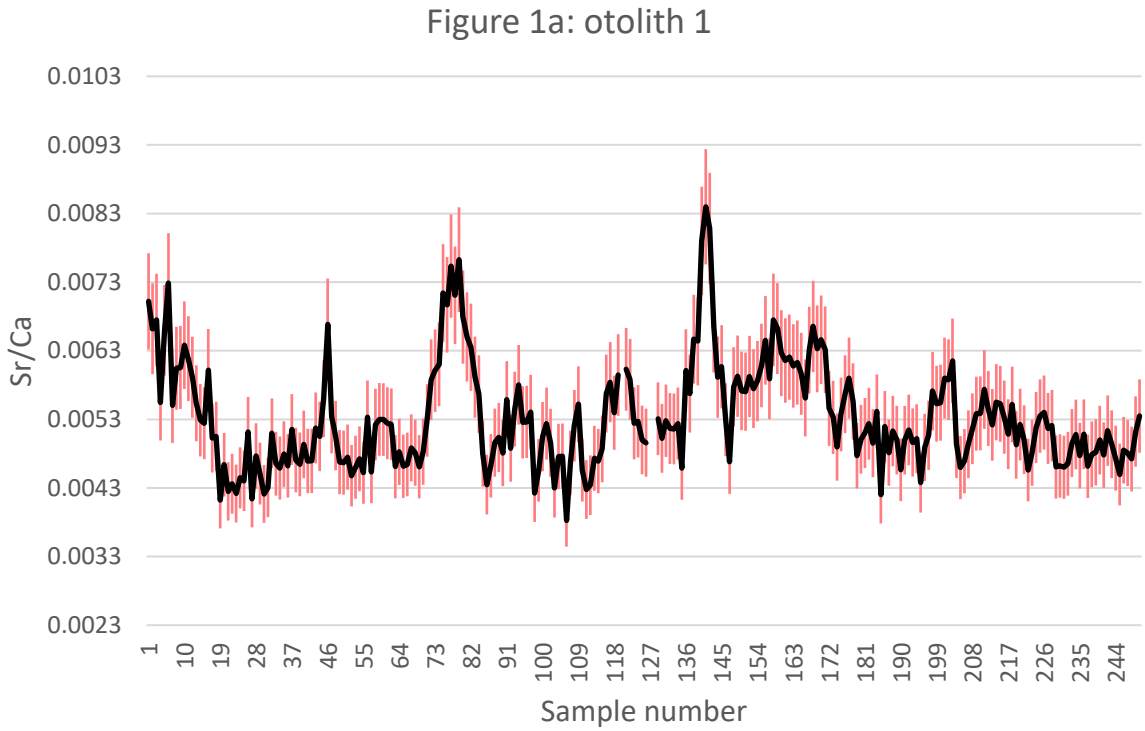
VIII3	15	0.63	-0.43	17.59	Micromill
VIII3	16	0.84	-0.78	19.11	Micromill
VIII3	17				Micromill
VIII3	18				Micromill
VIII3	19	1.00	-0.92	19.75	Micromill
VIII3	20	1.10	-1.13	20.64	Micromill
VIII3	21	1.11	-0.57	18.22	Micromill
VIII3	22	1.18	-0.35	17.27	Micromill
VIII3	23	1.05	-0.37	17.36	Micromill
VIII3	24				Micromill
VIII3	25	-0.03	1.13	10.83	Micromill
VIII3	26	0.38	1.23	10.39	Micromill
VIII3	27	0.44	0.96	11.58	Micromill
VIII3	28				Micromill
VIII3	29	0.72	0.83	12.12	Micromill
VIII3	30	0.55	0.71	12.65	Micromill
VIII3	31	0.44	0.39	14.03	Micromill
VIII3	32	0.51	0.01	15.70	Micromill
VIII3	33	0.65	-0.25	16.84	Micromill
VIII3	34				Micromill
VIII3	35				Micromill
VIII3	36				Micromill
VIII3	37				Micromill
VIII3	38				Micromill
VIII3	39				Micromill
VIII3	40				Micromill
VIII3	41				Micromill
VIII4	3	1.07	-0.86	19.48	Micromill
VIII4	4	1.20	-0.27	16.91	Micromill
VIII4	5	0.76	2.17	6.32	Micromill
VIII4	6	1.36	3.23	1.72	Micromill
VIII4	7	0.93	1.76	8.11	Micromill
VIII4	8				Micromill
VIII4	9	0.71	1.04	11.22	Micromill
VIII4	10	0.79	1.05	11.19	Micromill
VIII4	11				Micromill
VIII4	12	0.76	0.54	13.41	Micromill
VIII4	13	0.76	0.24	14.70	Micromill
VIII4	14	0.96	0.38	14.09	Micromill
VIII4	15	0.86	2.46	5.08	Micromill
VIII4	16	0.77	1.24	10.35	Micromill
VIII4	17	0.52	0.47	13.68	Micromill
VIII4	18	0.81	1.67	8.49	Micromill
VIII4	19	0.84	-1.04	20.24	Micromill
VIII4	20	0.92	2.43	5.19	Micromill
VIII4	21	0.75	1.78	7.99	Micromill
VIII4	22	0.68	1.21	10.51	Micromill

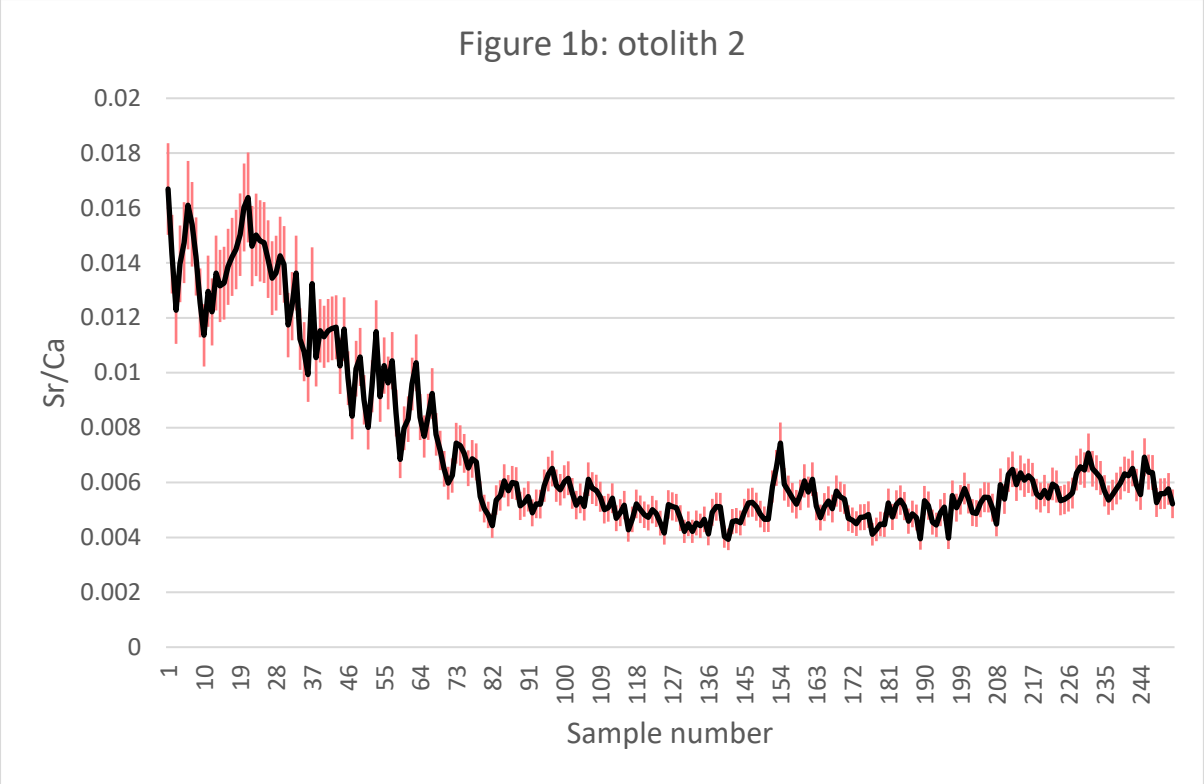
VIII4	23	0.95	1.77	8.06	Micromill
VIII4	24	0.85	0.97	11.53	Micromill
VIII4	25	0.76	0.62	13.05	Micromill
VIII4	26	0.79	0.73	12.56	Micromill
VIII4	27	0.89	0.49	13.59	Micromill
VIII4	28				Micromill
VIII4	29	1.06	-1.05	20.30	Micromill
VIII4	30	0.95	0.17	15.01	Micromill
VIII4	31	0.37	1.38	9.77	Micromill
VIII4	32	0.50	1.31	10.05	Micromill
VIII4	33	0.79	1.57	8.91	Micromill
VIII4	34	0.81	1.84	7.76	Micromill
VIII4	35	-0.60	-0.98	20.01	Micromill
VIII4	36	0.56	1.18	10.60	Micromill
VIII4	37	0.61	1.21	10.48	Micromill
VIII4	38	1.19	2.13	6.49	Micromill
VIII4	39	0.65	1.04	11.21	Micromill
VIII4	40	0.83	0.33	14.31	Micromill
VIII4	41	1.16	-1.07	20.38	Micromill
VIII4	42	1.16	-0.85	19.44	Micromill
II1	1	0.49	-0.92	-1.33	Hand drill
II1	2	1.12	0.88	0.46	Hand drill
II1	3	1.08	1.87	1.45	Hand drill
II1	4	1.22	1.28	0.87	Hand drill
II1	5	1.00	1.11	0.69	Hand drill
II1	6	1.17	0.81	0.39	Hand drill
II1	7	1.19	0.80	0.38	Hand drill
II1	8	1.15	-0.04	-0.46	Hand drill
II1	9	1.36	-0.18	-0.60	Hand drill
II1	10	1.25	-0.71	-1.13	Hand drill
II1	11	0.97	1.22	0.80	Hand drill
II1	12	1.06	2.06	1.65	Hand drill
II1	13	1.08	1.45	1.04	Hand drill
II1	14	1.38	0.74	0.33	Hand drill
II1	15	1.04	0.14	-0.28	Hand drill
II1	16	1.01	-0.42	-0.84	Hand drill
II1	17	1.26	-0.52	-0.94	Hand drill
II1	18	1.01	-0.03	-0.44	Hand drill
II1	19	0.58	1.72	1.31	Hand drill
II1	20	0.93	0.16	-0.26	Hand drill
VIII3	1	1.62	0.80	0.38	Hand drill
VIII3	2	0.75	1.32	0.90	Hand drill
VIII3	3	0.42	1.42	1.01	Hand drill
VIII3	4	0.54	1.22	0.80	Hand drill
VIII3	5	0.67	0.82	0.40	Hand drill
VIII3	6	0.85	-0.13	-0.55	Hand drill
VIII3	7	0.83	-0.75	-1.16	Hand drill

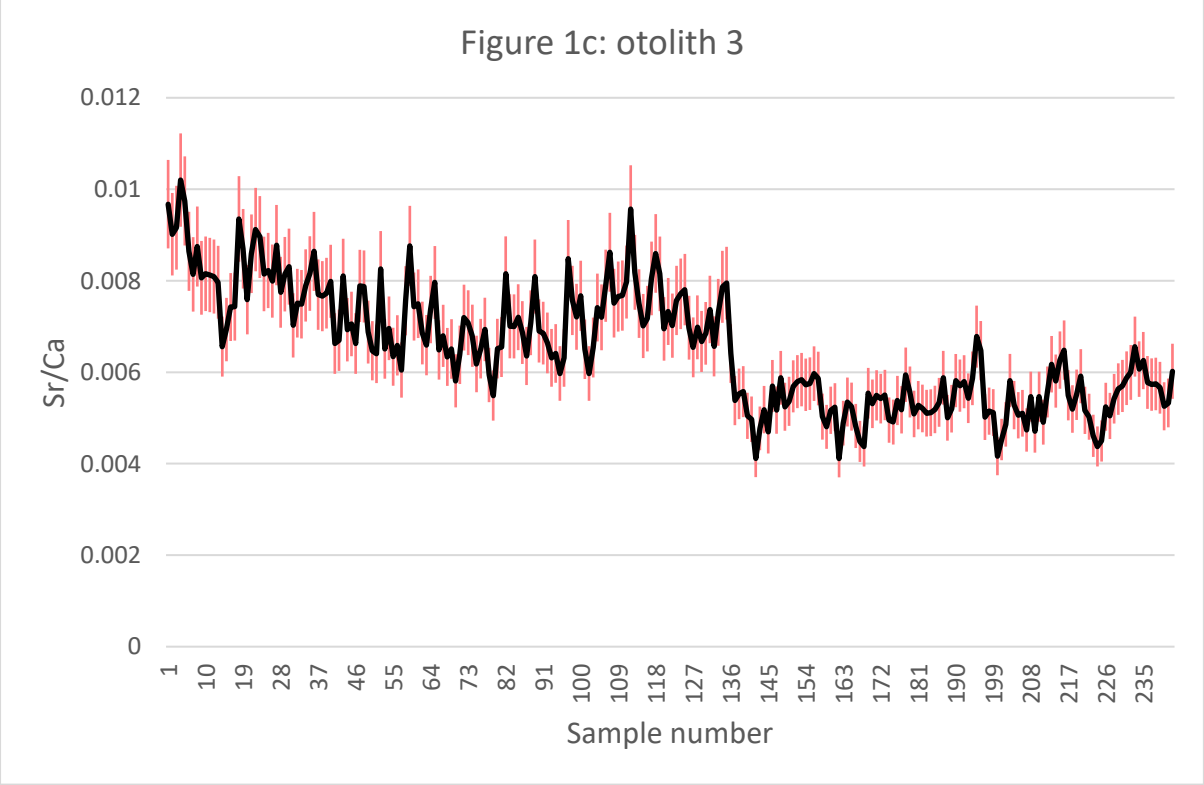
VIII3	8	1.06	-0.77	-1.19	Hand drill
VIII3	9	0.77	0.16	-0.26	Hand drill
VIII3	10	0.34	0.95	0.54	Hand drill
VIII3	11	0.31	0.84	0.42	Hand drill
VIII3	12	0.22	0.12	-0.29	Hand drill
VIII3	13	0.46	-0.33	-0.75	Hand drill
VIII3	14	0.81	-0.85	-1.27	Hand drill
VIII3	15	0.81	0.10	-0.32	Hand drill
VIII3	16	0.07	1.27	0.85	Hand drill

Appendix 4: Electron microprobe analysis

Figure 1: Results of trace element analysis on three Sebastes sp. *otoliths*




Figure 1b: otolith 2
Sr/Ca
0.02
0.018
0.016
0.014
0.012
0.01
0.008
0.006
0.004
0.002
0
1
10
19
28
37
46
55
64
73
82
91
100
109
118
127
136
145
154
163
172
181
190
199
208
217
226
235
244
Sample number


Figure 1c: otolith 3
Sr/Ca
0.012
0.01
0.008
0.006
0.004
0.002
0
1
10
19
28
37
46
55
64
73
82
91
100
109
118
127
136
145
154
163
172
181
190
199
208
217
226
235
Sample number

Appendix 5: Bayesian models for paired shell radiocarbon dates

Figure 1: Plot showing calibrated radiocarbon result for II1. Left: modelled edge date based on an 11-year age gap between umbo and edge, right: unmodelled edge date

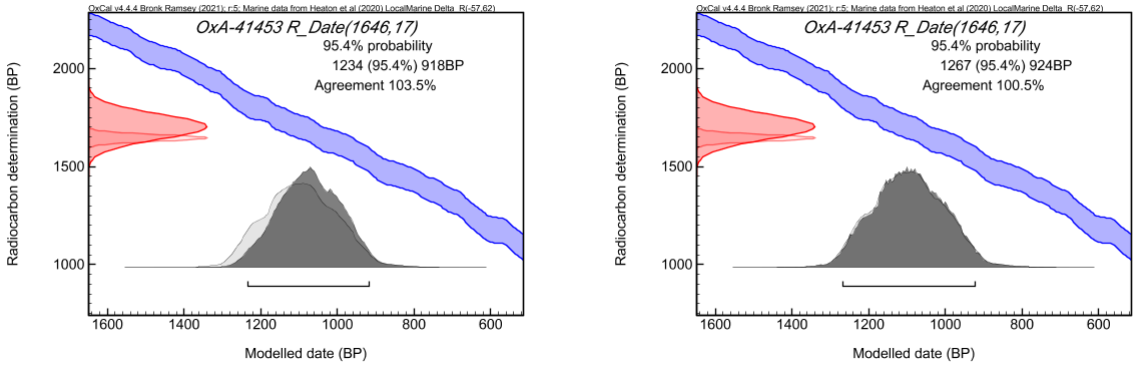


Figure 2: Plot showing calibrated radiocarbon result for II3. Left: modelled edge date based on a 20-year age gap between umbo and edge, right: unmodelled edge date

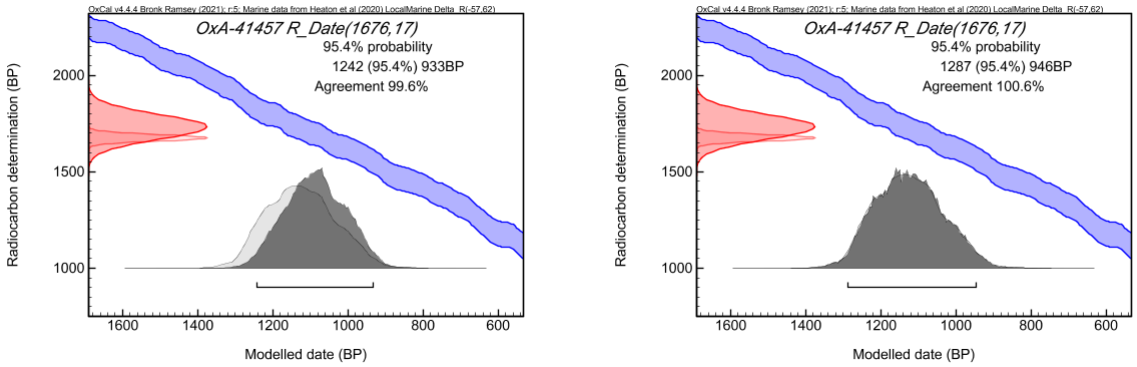


Figure 3: Plot showing calibrated radiocarbon result for VIII1. Left: modelled edge date based on a 24-year age gap between umbo and edge, right: unmodelled edge date

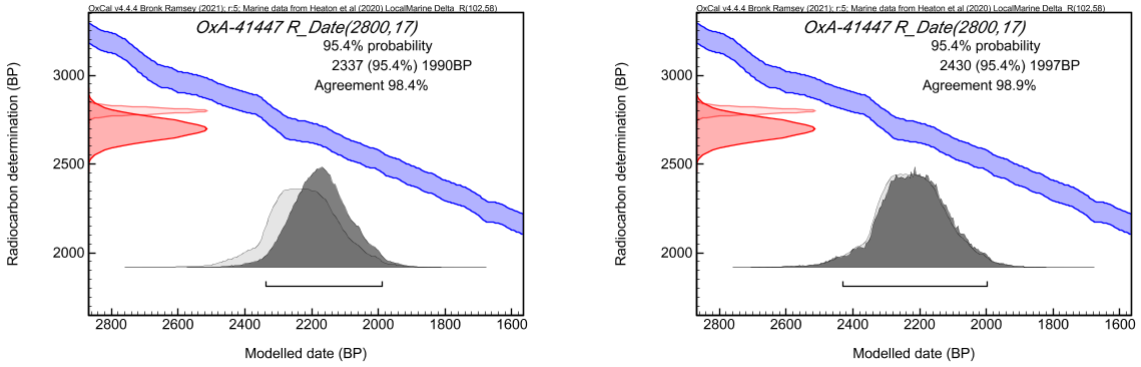


Figure 4: Plot showing calibrated radiocarbon result for VIII2. Left: modelled edge date based on a 12-year age gap between umbo and edge, right: unmodelled edge date

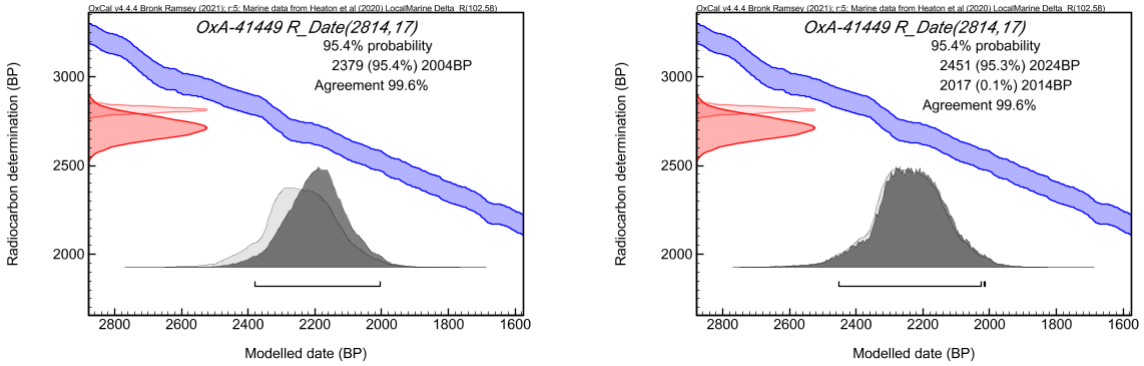


Figure 5: Plot showing calibrated radiocarbon result for VIII4. Left: modelled edge date based on a 18-year age gap between umbo and edge, right: unmodelled edge date

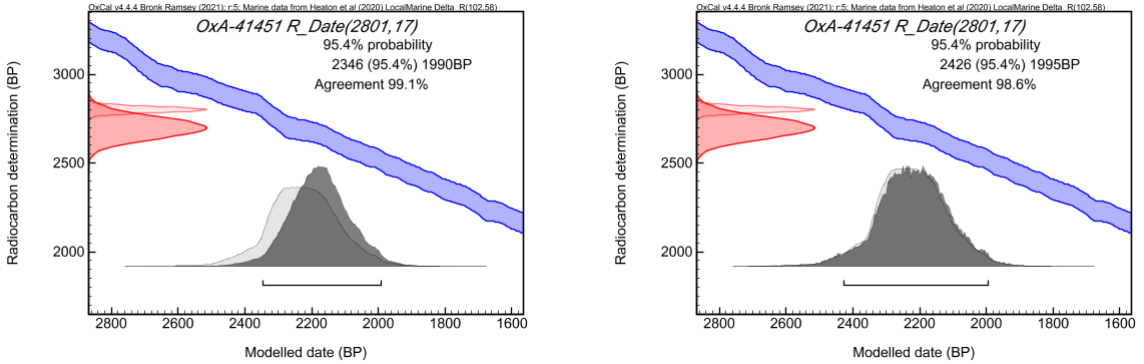
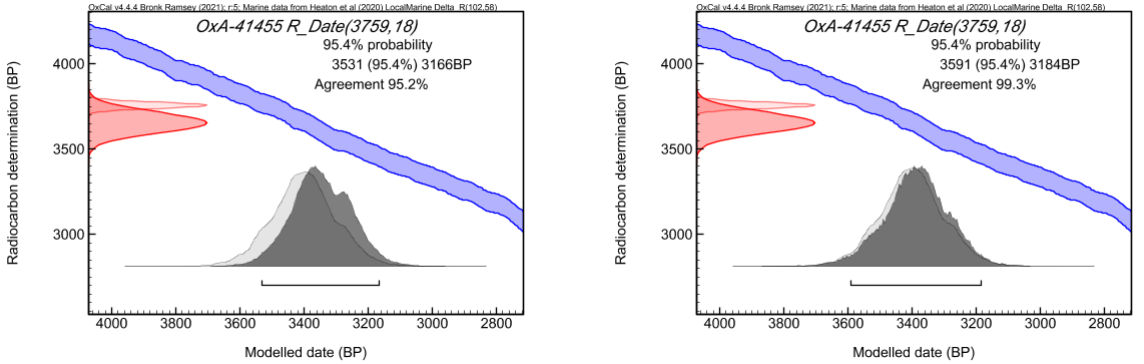


Figure 6: Plot showing calibrated radiocarbon result for II2. Left: modelled edge date based on a 17-year age gap between umbo and edge, right: unmodelled edge date



Co-authorship Statement

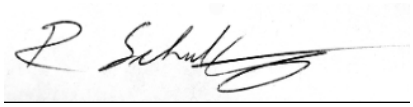
Paper 1: The potential of marine bivalve Spisula sachalinensis as a marine temperature record

Tansy Branscombe was the lead author and was responsible for the writing the NERC facilities grant application to fund stable isotope analysis, sampling the specimens, data analysis and writing the paper. Julia Lee-Thorp was the PI of the NERC facilities grant awarded for this research, along with the other authors as co-investigators. Melanie Leng oversaw the mass spectrometry, which was undertaken at her lab in the British Geological Survey, Keyworth. Rick Schulting, Julia-Lee-Thorp and Melanie Leng all contributed to data analysis through discussions with Tansy Branscombe, and all authors read and commented on the manuscript before it was submitted for review, as well as a revised version pre-acceptance.

Signed:



Tansy Branscombe



Rick Schulting



Julia Lee-Thorp



Melanie Leng

Co-authorship Statement

Paper 2: Micromilling Vs Hand Drilling in Stable Isotope Analyses of Incremental Carbonates: the Potential for $\delta^{13}C$ Contamination by Embedding Resin

Tansy Branscombe was the lead author and was responsible for the writing the NERC facilities grant application to fund stable isotope analysis, sampling the specimens, data analysis and writing the paper. Julia Lee-Thorp was the PI of the NERC facilities grant awarded for this research, along with the other authors as co-investigators. Melanie Leng oversaw the mass spectrometry, which was undertaken at her lab in the British Geological Survey, Keyworth. Rick Schulting, Julia-Lee-Thorp and Melanie Leng all contributed to data analysis through discussions with Tansy Branscombe, and all authors read and commented on the manuscript before it was submitted for review, as well as a revised version pre-acceptance.

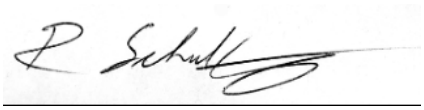
Signed:



Tansy Branscombe



Julia Lee-Thorp



Rick Schulting



Melanie Leng

Co-authorship Statement

Paper 3: Stable Isotope Palaeothermometry and Radiocarbon Chronology of Marine Carbonates from Hamanaka 2, Rebun Island (Japan)

Tansy Branscombe was the lead author and was responsible for the writing the NEIFSC radiocarbon funding application and NERC isotope facilities application, sampling the specimens, data analysis and writing the paper. Rick Schulting was the PI of the NEIFSC grant awarded for this research, and Julia Lee-Thorp was the PI of the NERC isotope facilities grant. Rick Schulting and Julia Lee-Thorp contributed to data analysis through supervisory discussions with Tansy Branscombe. Takao Sato provided otolith specimens from the zooarchaeological collection from Hamanaka 2 held at Keio University. Hirofumi Kato facilitated the field trips to Hokkaido in order to use the Hamanaka 2 collection stored at Hokkaido University, and to participate in the Hamanaka 2 excavation seasons in 2018 and 2019. All authors read and commented on the manuscript.

Signed:

Tansy Branscombe

Julia Lee-Thorp

Rick Schulting

Takao Sato

Hirofumi Kato